FINAL REPORT

ACOUSTIC AND STRUCTURAL DYNAMIC DIAGNOSTIC EVALUATION OF RIPRAP

Submitted to the Florida Department of Transportation

April, 2007

Project #S70005740000005 (108895)
FDOT Contract #PR231460 (DO80779)

Investigators:

Dr. Christopher Niezrecki (PI), Peter Avitabile (Co-PI), Mr. Peter Tavilla, and Dr. Paulin Buaka

Department of Mechanical Engineering
University of Massachusetts Lowell
One University Avenue
Lowell, MA 01854
E-mail: Christopher_Niezrecki@uml.edu
Phone: 978-934-2963, Fax: (978) 934-3048

Technical Report Documentation Page

1. Report No.	2. Government Accession No.	3. Recipient's Catalog No.
4. Title and Subtitle Acoustic and Structural Dynamic Diagnostic Evaluation of RIPRAP		5. Report Date April 2007
		6. Performing Organization Code
7. Author(s) Dr. Christopher Niezrecki (PI), Peter Avitabile (Co-PI), Mr. Peter Tavilla, and Dr. Paulin Buaka		8. Performing Organization Report No.
9. Performing Organization Name and Address		10. Work Unit No. (TRAIS)
		11. Contract or Grant No. PR231460 (DO80779)
12. Sponsoring Agency Name and Address Florida Department of Transportation 605 Suwannee Street, MS 30 Tallahassee FL 32399		13. Type of Report and Period Covered Final Report
		14. Sponsoring Agency Code

15. Supplementary Notes

16. Abstract

Acoustic impact-emission tests, Windsor Pin System® tests and impact frequency response functions are performed on Florida rock samples to identify causal relationships existing between measured responses and samples' petrographic characteristics. Regression analysis is used to relate measured responses with aggregate properties strongly affected by chemical and physical weathering. Aggregate properties such as mineralogy, porosity, and grain size are identified in thin section analyses performed by consultant geologists. The identification of causal relationships is necessary to satisfy a transfer function model of a durability test for aggregate used in civil engineering applications, namely bank and shore protection. Strong relationships are shown to exist between Windsor Pin System® measurements, impact frequency response functions and some aggregate properties for samples originating from the same quarry. Similarities & differences in the relationships are used to evaluate the feasibility of the applied methods as durability assessments and present considerations for future research of aggregate performance. Petrographic weighting factors are examined in the report to compare previously attempted methods of evaluating aggregate durability with those studied by researchers at UMass Lowell. These weighting factors are formulated by a consultant hired for the purposes of reporting sample petrography and are assigned based on his observations and experiences with Florida aggregates. These formulations are provided in Appendix B of the report, for reference. Inconsistencies observed between petrographic number determinations and the results of currently employed durability evaluations for the samples studied in this investigation suggest that factor weights be re-evaluated in general for Florida aggregates. However there is insufficient data to make specific recommendations on how to best improve the petrographic number technique and the assignment of factor weights to the various mineralogical and textural components of the samples.

17. Key Word	18. Distribution Statement
Rip Rap, Acoustic, Petrographic, Aggregate	No restrictions.

19. Security Classif. (of this report)	20. Security Classif. (of this page)	21. No. of Pages	22. Price
Unclassified.	Unclassified.	306	

Disclaimer

The opinions, findings, and conclusions expressed in this publication are those of the authors and not necessarily those of the State of Florida Department of Transportation.

ABSTRACT

Acoustic impact-emission tests, Windsor Pin System® tests and impact frequency response functions are performed on Florida rock samples to identify causal relationships existing between measured responses and samples' petrographic characteristics. Regression analysis is used to relate measured responses with aggregate properties strongly affected by chemical and physical weathering. Aggregate properties such as mineralogy, porosity, and grain size are identified in thin section analyses performed by consultant geologists.

The identification of causal relationships is necessary to satisfy a transfer function model of a durability test for aggregate used in civil engineering applications, namely bank and shore protection.

Strong relationships are shown to exist between Windsor Pin System® measurements, impact frequency response functions and some aggregate properties for samples originating from the same quarry. Similarities & differences in the relationships are used to evaluate the feasibility of the applied methods as durability assessments and present considerations for future research of aggregate performance.

Petrographic weighting factors are examined in the report to compare previously attempted methods of evaluating aggregate durability with those studied by researchers at UMass Lowell. These weighting factors are formulated by a consultant hired for the purposes of reporting sample petrography and are assigned based on his observations and experiences with Florida aggregates. These formulations are provided in Appendix B of the report, for reference. Inconsistencies observed between petrographic number determinations and the results of currently employed durability evaluations for the samples studied in this investigation suggest that factor weights be re-evaluated in general for Florida aggregates. However there is insufficient data to make specific recommendations on how to best improve the petrographic number technique and the assignment of factor weights to the various mineralogical and textural components of the samples.

TABLE OF CONTENTS

LIST OF TABLES

LIST OF FIGURES

NOMENCLATURE

Acronyms, Abbreviations, and Symbols

% Crit	Percent of Critical
AASHTO	American Association of State Highway and Transportation Officials
ASNT	American Society for Nondestructive Testing
ASR	Alkali Silica Reactivity
ASTM	American Standards for Testing Materials
AU	Acousto Ultrasonics
cm	Centimeters
Damp	Damping
dB	Decibels
E	Young's Modulus
FDOT	Florida Department of Transportation
Freq	Frequency
FRF	Frequency Response Function
g	Grams
Hz	Hertz
in	Inches
IR	Impulse Response
kHz	kilohertz
L.A.	Los Angeles
L.A. Abra	Los Angeles Abrasion
lbs	pounds force
LISA	Local Interaction Simulation Approach
m	Meters
mm	Millimeters
MPa	Mega Pascals
N	Newton
NDE	Nondestructive Evaluation
NDT	Nondestructive Testing
NEWS	Nonlinear elastic wave spectroscopy
No	Number
NRCS	Natural Resources Conservation Service
P	Precision Cut Core
PN	Petrographic Number
psi	pounds per square inch
QU	Quantitative Ultrasonics
SE	Seismic Echo
SNCGI	Scott Nagel Consultant Geologist, Inc.
Sound	Sodium Sulfate Soundness
SPRG	Specific Gravity
TRA	Time Reversed-Acoustic
TRE	Time Reversed Elastic
TYP	Typical
UPE	Ultrasonic Pulse Echo
UPV	Ultrasonic Pulse Velocity
USDA	United States Department of Agriculture
μ	Micro

Mathematical Variables

A	Mass of oven-dried test sample in air or used as a constant
B	Mass of saturated surface-dry tests sample in air
C	Mass of saturated test sample in water
C	Damping Coefficient
F	Function
F(U, G(x))	Functional relationship between response, input and system
f_n	Natural frequency
G	System
G(x)	System having properties x
I	Area Moment of Inertia
K	Stiffness
L	Length
M	Mass
U	Input
x	Properties
μ	Mass per unit length

INTRODUCTION

1.1 STATEMENT OF PROBLEM

The driving force for this investigation is the need to develop an accurate and efficient method of evaluating the durability and soundness of aggregate material used in Florida. Coarse aggregate materials studied consist of rock samples typically used in erosion control applications such as riprap, armor stone or bank and shore protection. This study attempts to fulfill the need for an improved testing protocol through a series of nondestructive tests consisting of both physical and structural dynamic testing techniques. Examination of linear regression coefficients corresponding to relationships between aggregate performance factors and data from the methods implemented will form the basis for evaluating the potential of the applied test methods to determine aggregate quality, i.e. durability. This is accomplished through the application of a transfer function approach. The knowledge gained from this study is intended to be used to develop a set of certification specifications which will either supplement or replace current certification testing methods used by the Florida Department of Transportation (FDOT) and other municipal authorities. The techniques investigated include impact frequency response function (FRF) measurements, acoustic impact-emission measurements, Windsor Pin System® tests, and petrographic analysis. The methods are chosen for their potential to reduce the cost and lead time on material certification by

eliminating the need to perform tests in the laboratory as well as their anticipated dependence on the various performance factors.

1.2 GENERAL REMARKS

The focus of this study is the identification of strong causal relationships between the measured responses of the applied methods and the mineralogical and textural characteristics of the aggregates studied. This is accomplished using a transfer function approach. Significant efforts are also made to understand the variables affecting the measured responses with respect to each of the physical tests performed.

The materials studied in this investigation consist of rock samples from several quarry locations in Florida and neighboring states, and were provided by the FDOT to investigate their properties for use in riprap. Concrete and bituminous applications are not considered. While the focus of this study is not directed toward these and other civil engineering applications, it should be noted that a significant amount of the information pertaining to aggregate quality, the tests used to evaluate it, and the various service conditions and failure modes affecting its performance come from studies on concrete and roadway structures (Saeed, 2001; Roy, 2002; Folliard, 2003). The concepts that are developed throughout this work may be applicable to a variety of different applications beyond the civil, mechanical & geotechnical disciplines.

The motivation for this investigation is partly to eliminate the need for test methods that are time and labor intensive. The effectiveness of the current methods, i.e. absorption, specific gravity, sodium sulfate soundness, and Los Angeles abrasion test, is questioned by several researchers (Eades *et al.*, 1997, Wu *et al.*, 1998, Meininger, 2002) so it is also of particular importance to identify methods which are more accurate.

"Riprap is a permanent, erosion-resistant ground cover constructed of large, loose, angular or sub-angular (rounded) stone" (Maine Erosion And Sediment Control BMP, 2003). An example of stone used on an embankment as riprap is shown in Figure 0-1.

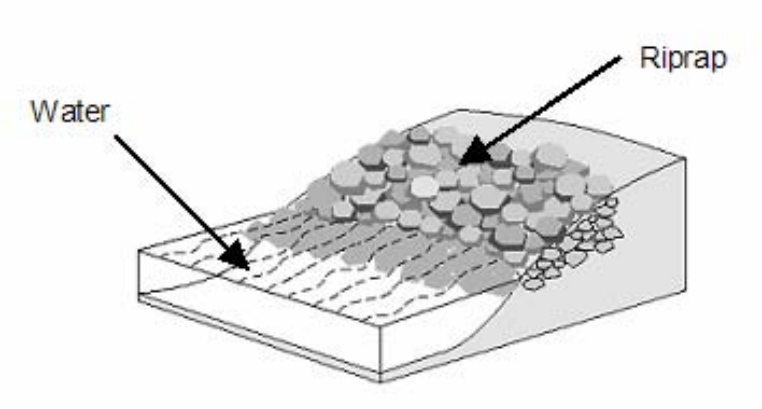

Figure 0-1 Basic use of Riprap (USDA, NRCS)

Riprap can be seen along canals, beach fronts, and culverts and is meant to protect the surrounding grade from being washed away by flowing water. The size and complexity of the riprap used in a particular location is dependent on such things as depth of flow, current velocity, entrained sediment and other factors. Typical engineering design parameters for this system can be estimated from any of the large number of design guides found in the literature. The failure modes of the material that are considered in this study will not include hydraulic design issues, i.e., instances where aggregate was washed away. Only the degradation of the material itself is considered.

In a given climate, riprap can experience a variety of service conditions which may or may not be deleterious. Such conditions include, but are not limited to: abrasive loads, cyclic wetting and drying, cyclic temperature fluctuations, and various chemical attacks. Many of the current testing methods used by the FDOT and other transportation

agencies have been developed by attempting to simulate one or more of these conditions. The failure modes of the material are discussed in considerable depth in Chapter 0.

Parameters measured from the applied methods are compared with the aggregates' properties that are most likely to affect the durability of the material in its intended application. The possible sources of degradation, service conditions, and knowledge of geological weathering mechanisms are used to identify properties that are expected to affect the performance of the aggregates. These properties form the basis for forming a transfer function relationship between the response characteristics of the applied tests and the material's mineralogy and texture. Examination of the relationships between grain size, mineral content, and porosity and the measured physical responses provides a foundation for future work.

1.3 CONCLUDING REMARKS

The development of a new evaluation method for aggregate material is truly multidisciplinary in nature. This task presents many challenges to the major disciplines which must be brought together in collaborative fashion. Transportation officials must contribute the appropriate political and financial support, geologists and geotechnical engineers must work together to develop the necessary fundamental understanding of the aggregate in its intended uses, and engineers from many disciplines must contribute the appropriate technical expertise and problem solving skills to compliment the knowledge and support of the other two parties. This having been said, this study addresses many critical issues that need to be addressed with respect to the development of an aggregate quality test.

The chapters that follow provide the information necessary to understand the applied methodology and interpretation of the results. An attempt has been made to unify the different discussions that are presented so that the work is more meaningful to the reader. The document can be broken down into three major sections.

The first section discusses the background behind aggregate quality testing and the challenges facing researchers wishing to develop new methods. In this section an overview of nondestructive testing is presented and with it the building blocks of the fundamental approach.

The second major section of the thesis develops the key points of the first section from a geological standpoint. It is evident from this discussion where the current evaluations find their roots. Geological concepts critical to this study are used to identify the petrographic characteristics of interest. These properties are used to explore the concept of a transfer function with respect to the development of new aggregate quality assessments. Reasons supporting the choice of applied test methods are discussed. After reading the first two sections the reader should have a firm understanding of the challenges facing the assessment of aggregate quality, the principles of geology upon which an assessment of quality should be made, and the steps to be taken in the final section to validate the chosen approach.

In the last section, data is presented from each of the applied test methods accompanied by discussions exploring important factors influencing the measurements. This is followed by discussion of the causal and/or non causal relationships that may exist between the applied tests and the properties identified in the supporting sections. Overall assessment of the results considers possible avenues of future work.

BACKGROUND

1.4 PREFACING REMARKS

The current methods and overview of the certification process used by the FDOT for evaluating aggregate durability is discussed in this chapter. In addition to detailed descriptions of the tests, additional information found in the literature is presented to assist the reader in understanding some of the challenges facing the development of an improved measure of quality.

1.5 CURRENT AGGREGATE APPROVAL PROCESS

The current FDOT certification process consists of four primary means of evaluating aggregate. These tests include: bulk specific gravity (AASHTO T 85-91 (2000), FM 1 T-085), absorption (AASHTO T 85-91 (2000), FM 1 T-085), sodium sulfate soundness (FM1-T104, AASHTO T 104-99), and the Los Angeles Abrasion test (ASTM C 535-01, FM 3-C 535). Each test is meant to quantify the material's durability either chemically, mechanically, or in combination. It is evident in the descriptions of some of the tests that their roots stem from attempts to simulate one or more of the service conditions the aggregate may see. The current tests are performed on groups of rocks collected from a particular quarry (Florida Construction Aggregates Manual, 2004).

Materials used in construction applications other than riprap are certified through many of the same and/or other similar methods. The FDOT currently approves materials based on the number of passing tests per lot size such that the probability of the whole lot meeting acceptance criterion adheres to the current specifications for aggregate materials (Construction Aggregates Manual, 2004). Approval of materials is performed on an ongoing basis for sources (quarries) which continually meet the FDOT's acceptance criterion. Materials are also approved on a conditional basis for suppliers who meet the department's specifications for periodic acceptance (Florida Construction Aggregates Manual, 2004). A flow chart of the current approval process has been provided by the FDOT and is shown in Figure 0-1.

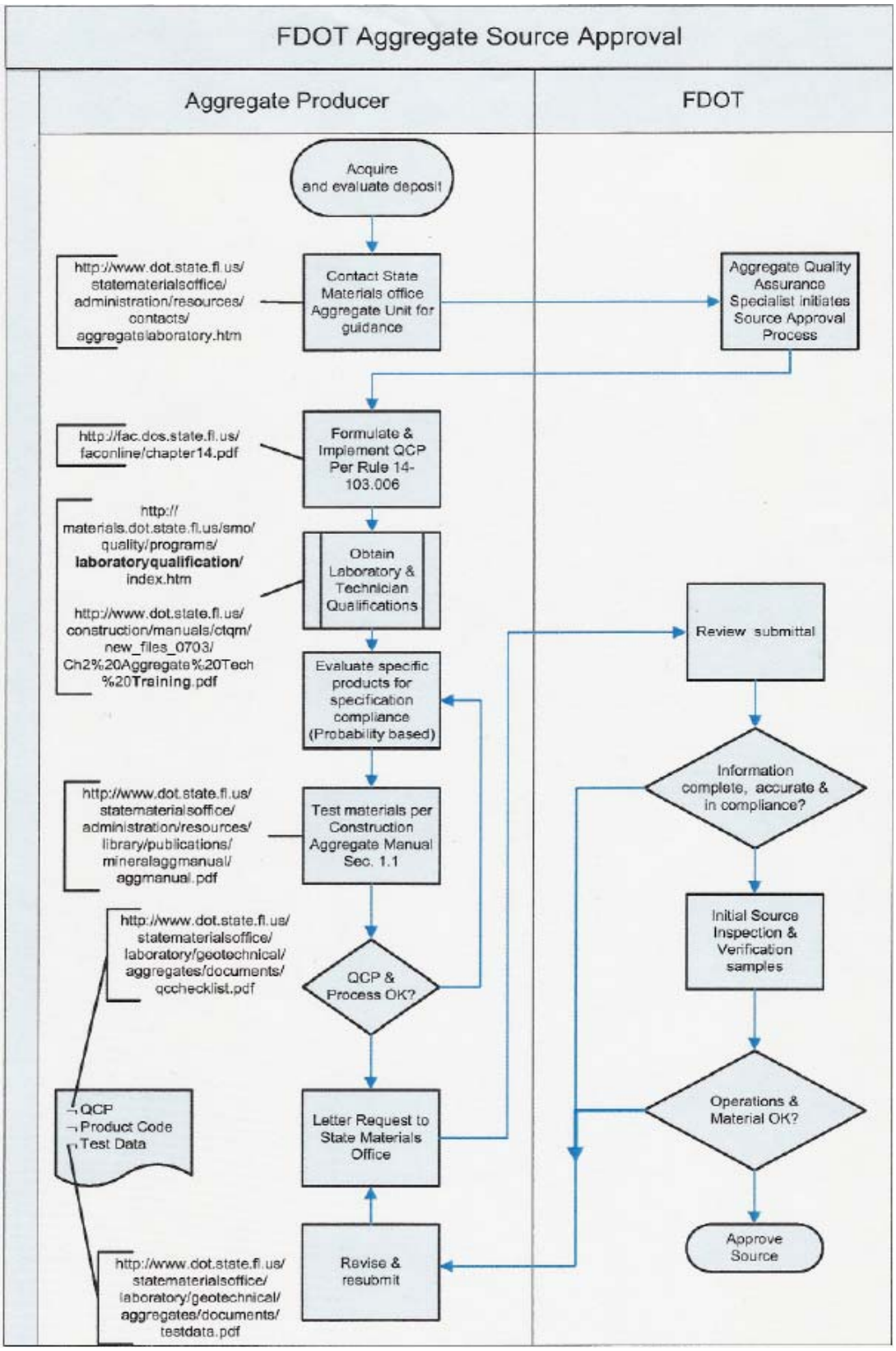

Figure 0-1 FDOT Source Approval Flow Chart (FDOT)

There is very little data available which describes the performance record of coarse aggregate materials (Eades *et al.*, 1997; Wu *et al.*, 1998, Gregory, 2004; McClellan, 2002). Observations of state highway and transportation agencies are typically the only means used to evaluate the effectiveness of tests currently in use. The FDOT in particular does not have a standard method of evaluating field performance, or other means of comparing actual durability with test data from durability and soundness testing. Many researchers have recognized a need to find more effective ways of predicting the performance of these construction materials (Meininger, 2002; Eades *et al.*, 1997; Wu *et al.*, 1998, Gregory, 2004; McClellan, 2002). Because there is no single test that researchers can agree upon which evaluates the material's performance as a function of all its service conditions, the methods for evaluating aggregate quality have evolved into a combination of both chemical and mechanical tests.

1.6 CURRENT FDOT TESTS

The current FDOT tests, mentioned in the previous section, have been adapted from tests developed over the past 100 years or so as a means to evaluate the durability and soundness of aggregate material for an intended use. For this investigation, the durability and soundness tests specific to Florida riprap approval are of primary importance and are described in detail. The tests used by the FDOT are the absorption, specific gravity, Los Angeles Abrasion Test, and the Sodium and Magnesium Sulfate Soundness test. To summarize the FDOT's specifications for acceptance, the required passing values for each test are provided in Table 0-1.

Table 0-1 FDOT Physical Requirements - Riprap

Test	***Requirement***
Absorption*	5% Maximum
Bulk Specific Gravity	2.30 Minimum
Los Angeles Abrasion (FM 1-T 096)*	45% Maximum Loss (Limestones)
	55% Maximum Loss (Granites)
Sodium Sulfate Soundness (AASHTO T 104)*	12% Maximum Loss

* Percent is in "by Mass" basis.
Reference: FDOT Standard Specifications For Road and Bridge Construction 530-2.2.3

1.6.1 SODIUM SULFATE SOUNDNESS TEST

The sodium sulfate or magnesium sulfate test is one of the primary tests that the FDOT uses to evaluate the quality of aggregate materials. Currently the FDOT follows their own standard for performing this test for riprap approval, FM1-T104, which is based on AASHTO T 104-99 Soundness of Aggregate by use of Sodium Sulfate or Magnesium Sulfate. According to the AASHTO standard:

"This method covers the procedure to be followed in testing aggregates to determine their resistance to disintegration by saturated solution of sodium sulfate or magnesium sulfate. This is accomplished by repeated immersion in saturated solutions of sodium or magnesium sulfate followed by oven drying to partially or completely dehydrate the salt precipitated in permeable pore spaces. The internal expansive force, derived from the rehydration of the salt upon re-immersion, simulates the expansion of water on freezing" (AASHTO T 104-99 (2003)).

The cyclic process of soaking and drying is repeated a total of five times. At the conclusion of the fifth cycle, the samples are sieved and weighed. The percent loss is on

a by-mass basis. Depending on the material, the loss as a result of the process can be quite high as the material can deteriorate significantly. The test can take up to a couple of weeks to perform. This test aims to bridge the gap between mechanical tests and chemical tests which attempt to simulate the working environment of the material during its service life, or "imitate the effects of extended natural weathering on aggregate materials" (Eades *et al.*, 1997).

The survivability of a material in the sulfate soundness tests varies depending on the material. As an example, Figure 0-2 shows the results of a typical igneous rock sample before and after the soundness test.

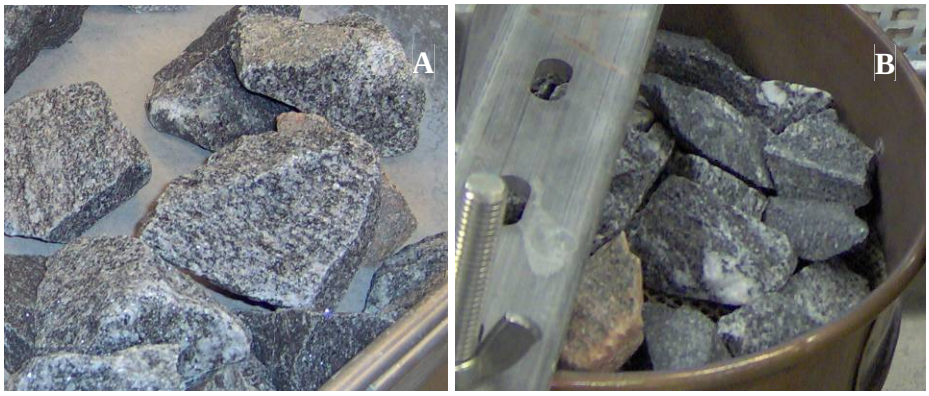

Figure 0-2 Sulfate Soundness Effect on an Igneous Rock Sample; A) Before; B) After

A careful examination of Figure 0-2 shows that there is little or no change in the aggregate from the sulfate soundness test. The igneous material shown in Figure 0-2 typically has a very low loss percentage for this test. Conversely, Florida limestone often does not fare as well. This is shown as a second example in Figure 0-3.

Figure 0-3 Sulfate Soundness Result for Limestone (TYP); A) Before; B) After

Figure 0-3B shows severe crumbling and deterioration of the aggregate after being exposed to the sodium sulfate solution as compared to Figure 0-3A. As a result of the deterioration from this test, many Florida aggregates are not approved for use as riprap or in other applications.

The FDOT performs the sodium sulfate soundness test as part of its approval process for many applications, and many states follow suit for concrete or road base material applications. In fact a total of 62% of states have requirements for either the sodium sulfate or magnesium sulfate test (Wu *et al.*, 1998). Because the effectiveness of this test as a performance indicator is based primarily on the observations of state highway and transportation agencies it has come under a great deal of scrutiny by researchers (Eades *et al.*, 1997; Wu *et al.*, 1998; Meininger, 2002; Gregory, 2004; McClellan, 2002).

Aside from a deficiency of field data and its relationship to other physical tests (Eades *et al.)*, the Sulfate Soundness test presents a few other problems when used to test Florida aggregates. There has been concern over the solubility of Florida aggregates in the sulfate solution (Eades *et al.*, 1997). The potentially high solubility of certain

aggregates could significantly increase the percent loss from the test. In addition, the test was originally designed to simulate the effects of repeated freezing and thawing which may not be appropriate for most of Florida's climate. There is also the problem of repeatability. Some researchers have commented on the lack of consistency in the way the test is performed (Meininger, 2002; Wu *et al.*, 1998). Meininger reports that the coefficient of variation for sodium sulfate tests performed in different labs averages over 40%, and can reach values of over 100% between any two labs (Meininger 2002). In general, the literature is consistent about the insufficiencies of the test, but also reports fair to marginal success in correlating field reports with the effectiveness of this test (Wu *et al.*, 1998; Eades *et al.*, 1997).

1.6.2 BULK SPECIFIC GRAVITY & ABSORPTION TESTS

The specific gravity and absorption tests currently followed by the FDOT can be referenced by either ASTM C127-88 or by AASHTO T 85-91 with slight modifications in accordance to Florida Method of Test FM 1 T-085. The standard specifies that the sample be weighed three times: once after it has soaked in water for 15 hours and then surface dried, again while it is fully submerged in water and a third time after it has been oven dried for several more hours. Using the equations provided in the standard, the different specific gravity and absorption quantities can be calculated as (AASHTO T 85-91):

$$Bulk\_specific\_gravity = \frac{A}{B-C} \quad (2\text{-}1)$$

$$Absorption = \frac{B-A}{A} \times 100 \quad (2\text{-}2)$$

Where:

A = mass of oven-dry test sample in air measured in grams

B = mass of saturated-surface-dry test sample in air in grams

C = mass of saturated test sample in water measured in grams

Currently the FDOT specifies that aggregates used for riprap have an absorption value not exceeding 5% by mass or a bulk specific gravity of less than 2.3 (FDOT Specification 530) as shown in Table 0-1. Other specific gravity values may be calculated using the formulas provided in the standard such as apparent specific gravity, saturated-surface-dry bulk specific gravity, average specific gravity, and average absorption values (AASHTO T85-91).

Specific gravity and absorption measures the extent to which water can enter the structure of the material and to some extent can be considered a measure of its permeability and/or its porosity. Some evidence suggests that the absorption test may be inaccurate for Florida aggregates due to their extensive pore structure (Gregory, 2004). In Chapter 0, the effects of porosity on the durability of aggregates are discussed from a geological standpoint.

1.6.3 LOS ANGELES ABRASION TEST

The Los Angeles Abrasion Test is a mechanical degradation test in which the aggregate's strength and resistance to crushing and abrasion is measured. The FDOT currently follows ASTM C 535 – 01 with slight modification in accordance with Florida Method of Test FM 3-C 535. Aggregate samples are weighed before being placed in a steel drum, similar to the one shown in Figure 0-4, with a single shelf protruding toward the center of the drum and 12 loose steel balls.

Figure 0-4 Typical L. A. Abrasion Tumbler (SuperPave)

The compliment of steel balls and aggregate samples are rotated in the device for a prescribed number of revolutions. The contents are then sieved and weighed to obtain the percent degradation (ASTM C 535 – 01). Harder material will generally survive the test with a small amount of rounding of the sharp edges while softer material will not survive the test. An example of the effects of the test is shown in Figure 0-5.

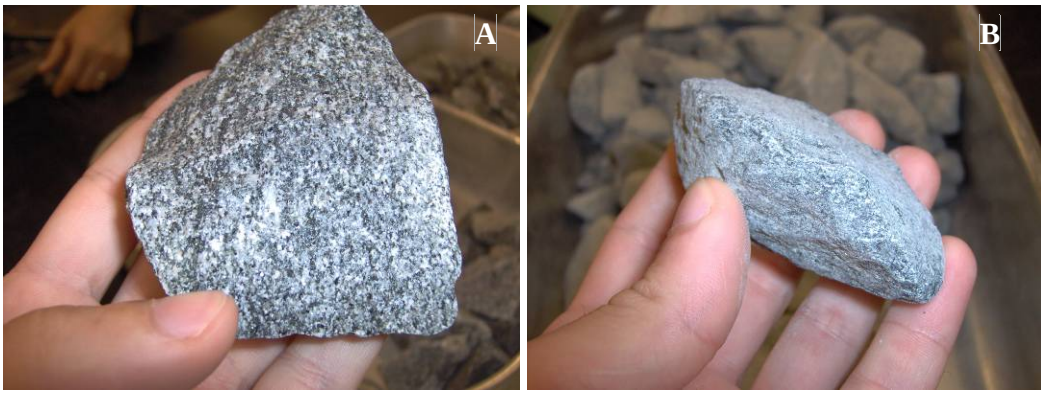

Figure 0-5 Result of L.A. Abrasion Test on Material Having Strong Abrasive resistance: A) Before; B) After

As with the other tests used by the FDOT, there is no abundance of field performance data to support the test's validity as an indicator of quality. Tests of this sort are merely a measure of performance under known conditions. The FDOT's requirements for material approval with respect to this test are included in Table 0-1.

1.6.4 SAMPLE POOL & FDOT TEST RESULTS

The FDOT provided the aggregate samples used in this study. In accordance with typical sampling practices, rocks were collected at seven quarries, six in Florida, and one in Georgia. The rocks collected are on average the size of a basketball and range in weight from approximately 10 to 50 pounds. Ten rocks from each source were provided for testing and a comparable number were processed by the FDOT using the durability and soundness tests described.

Each quarry, or source, is identified by a 5-digit alphanumeric code, e.g. 08-534, and individual samples are numbered 1 through 10 for each source using permanent marker. Samples are identified in this study using the FDOT source code and the sample number assigned. For example a rock labeled 12-521-2 indicates the sample is rock

number 2 from the source 12-521. The source locations are paired with their 5-digit codes in Table 0-2.

Table 0-2 Rock Sources, Identification Numbers & Descriptions (McClellan, 2006)

Source/Quarry No.	Location/Description
08-534	Brooksville, FL. Case hardened Suwannee Limestone
12-521	Bonita Springs, FL. Fossiliferous Tamiami Limestone
18-607	Center Hill, FL. Chert on top of Ocala Limestone
34-106	Gulf Hammock, FL. Mix of tan and grey dolomite
38-228	Perry, FL. Soft tan calcareous limestone & hard dense grey limestone
87-339	Hialeah, FL. Oolitic limestone
GA-178	Macon, GA. Metamorphosed granite.

For some of the test methods used in this study, i.e., the petrographic analyses (to be discussed in Chapter 0) and the impact frequency response tests (to be discussed in Chapter 0), several core samples were cut from a selection of rocks from each source. The cores retain the identification scheme used for the original rocks from which they were cut. In many cases, multiple core samples were cut from a single rock. Multiple cores are designated by a letter following the sample identification number previously described. For the other tests the samples were not cut into special shapes.

The descriptions of the samples in Table 0-2 are provided as part of the petrographic analyses performed by Dr. Guerry McClellan (McClellan, 2006) a consultant geologist who is experienced in working with FDOT aggregates and who also performed several petrographic analyses of the samples. The petrographic descriptions of the aggregates are discussed in detail in Chapter 0. Dr. McClellan's (2006) final report is included in Appendix B.3 for reference.

The aggregate sources are distributed throughout the state of Florida and one source originates from Georgia. Figure 0-6 shows the locations of the Florida sources in Table 0-2 in relation to major geologic formations in the state.

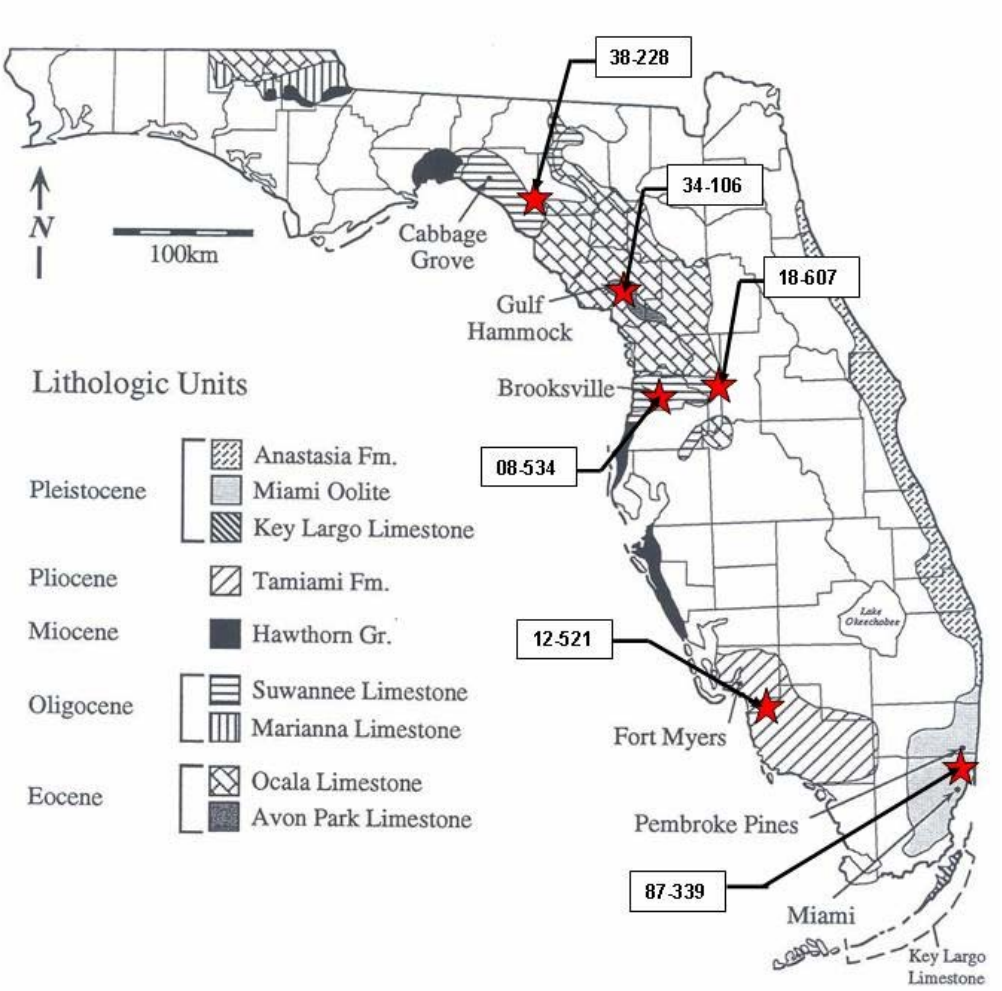

Figure 0-6 – Aggregate Sources & Florida Geologic Formations (Map & Quarry Locations Courtesy of FDOT)

The location of aggregate source quarries shown in Figure 0-6 are approximated based on the FDOT's daily materials/producer listings which can be accessed from the FDOT's website online. The map showing the geologic formations in Figure 0-6 has been provided by the FDOT and used in past studies, i.e. Eades *et al.* (1997) and Oyen *et al* (1998).

The FDOT used a portion of the collected samples to perform the tests listed in Table 0-1. The results of the tests were provided by the FDOT and listed in Table 0-3.

Table 0-3 Results of FDOT Testing on Aggregate Samples

	Test Results			
Source	**SPGR (Bulk)**	**Absorption (% dry mass)**	**Sound (% Loss)**	**L.A. Abra (Grade 2) (% Loss)**
08-534	2.401	2.00%	1.00%	19.00%
12-521	2.125	4.75%	17.00%	39.00%
18-607	2.410	2.44%	2.00%	16.00%
34-106	2.299	4.34%	19.00%	41.00%
38-228	2.536	1.40%	0.70%	41.00%
87-339	2.165	4.20%	9.00%	34.00%
GA-178	2.739	0.20%	0.00%	18.00%

	*Conclusions (Based on FDOT Specifications)***				
Source	**SPGR Pass (>2.3)**	**Absorption Pass (<5%)**	**Sound Pass (<12%)**	**L.A. Abra Pass (<45% Limestn, <55% Granit)**	**Rating (1-4)**
08-534	Yes	Yes	Yes	Yes	4
12-521	No	Yes	No	Yes	2
18-607	Yes	Yes	Yes	Yes	4
34-106	No	Yes	No	Yes	2
38-228	Yes	Yes	Yes	Yes	4
87-339	No	Yes	Yes	Yes	3
GA-178	Yes	Yes	Yes	Yes	4

** Reference: FDOT Standard Specifications For Road and Bridge Construction 530-2.2.3

Based on the physical requirements listed in Table 0-1, and the provided results in Table 0-3, each test was evaluated as either passing or failing. The rating listed in Table 0-3 is based on the number of passing tests, i.e. a rating of 4 indicates the aggregate passed all four of the FDOT's required tests. The results and ratings in Table 0-3 will be used in some of the analyses in Chapter 0. It should be noted that the information provided by the FDOT is representative of the collected samples for this study. It may not be representative of results typical for each source. The FDOT only provided test

results for the aggregates collected for this study so no statistical significance of the data can be inferred from the results displayed in Table 0-3 for any of the sources.

1.7 OVERALL EVALUATION OF CURRENT FDOT TESTS

The literature's findings on the current test methods show that a great deal of work is needed to understand their actual effectiveness. Years of research have gone into the development of testing procedures and specifications for coarse aggregate in Florida and other states; yet, there does not seem to be any database relating the results of these durability and soundness tests with any measure of performance for these materials, especially for use in riprap. Standards evaluating the field performance of aggregate used in riprap are also not well documented. This presents a significant challenge for the development of a physical testing program that is meant to accurately predict the performance of aggregate materials, especially for use as riprap. There are minimal amounts of data available for aggregate used in concrete or in bituminous applications, but even this information is based largely on observation (Wu *et al.*, 1998). Bayne *et al.* (1955) worked to establish a petrographic analysis technique (which will be discussed in further detail in Chapter 4) in which performance data and aggregate properties were closely studied. Bayne *et al.* (1955) reported that the magnesium sulfate and absorption tests only showed some relationship to performance, while the other tests, i.e. abrasion and specific gravity, did not show any relationship to performance.

It should not go overlooked that the collection of tests currently in use does represent an intuitively "good" attempt at estimating the effects of weathering on these materials. The absorption based tests, like the sulfate soundness tests, absorption, and specific gravity, intuitively seem like obvious choices of tests because they measure the

exposure to potentially corrosive chemicals. It makes sense that the higher the absorption, the more surface area that is potentially exposed to chemical agents that could be detrimental to the aggregate's performance. Even the Los Angeles Abrasion Test is an intuitively good test since it subjects the material to harsh conditions and attempts to estimate how well the material will withstand mechanical wear. Another intuitive reason for the sulfate soundness test is that the salt not only subjects the material to a chemically damaging substance, but also subjects it to mechanical wear. Though these tests have come under a great deal of scrutiny, their use is not completely unjustified. It is clear from the literature however that an alternate approach may be needed to quantify the effects of service conditions on performance.

From the descriptions of the various tests, it should be clear that many of the current methods used to evaluate aggregate quality have been developed from an attempt to simulate many of the various service conditions that the material may see. It should also be clear that only a few key properties of aggregates are examined in the tests, especially tenacity and porosity. These properties are examined in greater detail in Chapter 0 from a geological standpoint.

1.8 ADDITIONAL AGGREGATE QUALITY TESTS

There are other aggregate quality tests in use throughout the United States and abroad which deserve recognition. These methods include the Micro-Deval, freeze-thaw tests, Iowa Pore Index, petrographic analysis and several others. While these tests are not necessarily used extensively by the FDOT, they have gained popularity among other transportation authorities for aggregates used in various applications.

The Micro-Deval test is similar to the L.A. Abrasion or Lovegrove Attrition test (Eades *et al.*, 1997) and consists of aggregate samples, water and a collection of steel balls placed in a jar mill and rotated for prescribed period of time (Wu *et al.*, 1998). As with the L.A. Abrasion test, the results are expressed in percent loss of the original sample's mass.

There are several freeze-thaw tests used. Some actually involve the rapid freezing and thawing of aggregate in either water or air such as ASTM C 666 (Eades *et al.*, 1997), and others involve salt solutions and are similar to the sodium and magnesium sulfate test previously described (Wu *et al.*, 1998).

The Iowa Pore Index test is a measure of permeability and porosity. Water is forced into an oven dried sample under pressure for a short period of time. The test has shown to be effective in identifying aggregates with extensive pore structures (Eades *et al.*, 1997).

Petrographic analysis is a method of visually evaluating rock samples. The techniques vary from macroscopic to microscopic depending on the features of interest. The details of this method of analysis are examined in greater detail in Chapter 0. It is important to understand that in petrographic analysis for determining quality, geologists use their knowledge and experience of the chemical and physical properties observed in the sample to make educated forecasts of the rock's durability. While this method may seem somewhat subjective, it is the only single method of evaluating aggregates where both mechanical and chemical degradation are effectively considered at the same time.

1.9 PREVIOUS WORK TO IMPROVE EVALUATION OF AGGREGATE QUALITY

There is a wealth of information pertaining to the development of new and possibly more accurate test methods to determine the quality of concrete and roadway materials. Recently, however, there have been a few studies done to either improve upon the current test methods employed by the FDOT, or to apply new techniques to the problem. Improvements to current methods (Gregory, 2004; McClellan *et al.*, 2002) include modifications to the sodium sulfate soundness and absorption tests. Additional tests range from physical destructive tests to chemical degradation tests.

A study published by Eades *et al.* (1997) attempted to evaluate the current testing protocols through cross correlation studies. Ultimately, the researchers concluded that many of the tests may be inadequate to determine aggregate quality and that a multi parameter approach was necessary. Most notable of the cross correlation study's results was that the sodium sulfate soundness tests often had poor correlations with the other quality tests. Though still poor, the correlation of sodium sulfate soundness with absorption and specific gravity, often cross correlated parameters, was much better overall. The lack of correlation of the sulfate soundness test with other tests should not immediately be interpreted as an indication of a poor test method. It could simply mean that the tests compared are affected by different properties. Among the additional techniques that were applied to determine aggregate quality, Eades *et al.* (1997) used the Iowa Pore Index test, modified petrographic number (to be discussed later), and X-ray analysis.

Additional studies, making minor changes to the current FDOT test methods, and implementing a different approach that integrates multiple parameters or aggregate

performance specific to riprap have also been undertaken (McClellan *et al.*, 2002; Gregory, 2004). Modification to the absorption test involved covering core samples with distilled water and placing them in a dessicator for several hours to remove any entrained air. The intent is to obtain maximum absorption values, assuming that maximum absorption is a better indicator of aggregate quality for riprap than the standard absorption test. Absorption values were also studied as a function of different solutions. Modification to the sodium sulfate soundness test consisted of changing the cyclic nature of the test to one of more frequent cycling without the need to control temperature or sulfate saturation. The solution was replaced with synthetic sea water and additional salt crystals were used to maintain the solution's saturation. Core samples were placed on a Ferris wheel so that the samples could be submerged and dried in an automated fashion. Heat lamps were used to rapidly dry the samples once removed from the solution. The effect was that an increased number of rehydration cycles could be achieved during the normal time it would have taken to conduct the test (Gregory, 2004; McClellan *et al.*, 2002).

In the studies performed by Gregory (2004), and McClellan *et al.* (2002), additional tests were applied to the task of developing a more accurate method of evaluation. Perhaps the most interesting of the methods applied in these related studies is that of a riprap rating system. The system is based on a set of cause-and-effect relationships that are related through an interaction matrix. The interaction matrix attempts to quantify the interactions between factors such as service conditions, petrography, strength, density, and durability properties. Using this matrix, the authors applied a cause-and-effect relationship between different features and developed a scaling

system by which various physical and chemical test results could be normalized to determine the overall quality of the aggregate. This method is important because it not only attempts to identify important factors affecting performance while also taking into account the service conditions, but it also utilizes a multi parameter approach.

Ultimately, the studies previously discussed only succeeded in doing one or both of the following: making the current tests more consistent or more efficient, perpetuating the forward march of the development of new methods of evaluating aggregate quality without validation with field performance information. The techniques attempted in each study are interesting to point out, since it is apparent that meaningful work is being done to better assess aggregate quality. The steady integration of multi parameter methods is an indicator of this.

1.10 CONCLUDING REMARKS

The techniques presented in this chapter are supported by some researchers and unsupported by others as adequate indicators of aggregate quality. While the effectiveness of the methods has been downplayed due to the lack of substantial data, the personnel of transportation authorities are generally well experienced when it comes to working with aggregates. The studies examined as part of this research show the need for substantial data correlating tests with performance, but they also indicate that transportation authorities have a reasonable sense of the behavior of materials used in their jurisdictions. While their observations are very helpful, and possibly quite accurate, the lack of a unified approach for observing and quantifying performance makes the validation of any newly developed method challenging. In the study performed by Eades *et al.* (1997) it is often stressed that field performance is the only true measure of the

effectiveness of the many tests being used today. "A question that remains is what property of the aggregate is being measured by each of these tests and what, if anything, does that have to do with performance…" (Eades *et al.*, 1997). This question is addressed throughout the thesis.

NONDESTRUCTIVE TESTING TECHNIQUES

1.11 PREFACING REMARKS

Non-destructive testing or evaluation (NDT or NDE respectively) has been an important research topic for more than 50 years. Advancements in material science, mathematics, engineering, and measuring equipment have helped work in this area progress. The average person employs several, though less sophisticated, techniques on a daily basis. Some of these methods are as basic as noticing a change in sound of a machine when a part needs to be changed to knowing that a turkey is fully cooked by the way it looks and smells.

The push to develop non-destructive testing methods stems from a variety of sources. Governments push designers and manufacturers to produce goods at higher levels of quality to insure safety. At the same time the producers of these goods must utilize inexpensive testing methods which insure a high level of quality. Destructive tests are potentially more expensive due to the loss of product, and they are not always as accurate as current NDT methods.

1.12 OVERVIEW OF NONDESTRUCTIVE TESTING METHODS

There are several professional organizations which have greatly helped to organize and expand many of today's NDT's. Organizations such as the American

Society for Nondestructive Testing (ASNT) and others have divided the realm of NDT into several categories. These categories are based on the excitation and measurement techniques used in the tests. The basic classes of NDT as developed by ASNT are: mechanical, optical, penetrating radiation, electromagnetic and electrical, sonic and ultrasonic, thermal and infrared, chemical and analytical, image generation, and signal image analysis (ASNT – Classification of NDT Methods, 2006). Within each of these classes exists many different tests for various applications. Reviews of NDT applications and ideas have been published by Doebling *et al.,* (1996) and others in an attempt to expand the field and help researchers find techniques for various applications. Researchers affiliated with Los Alamos National Laboratory have made tremendous strides in the NDT and material classification fields which have relevance to this work (see works by Johnson, Guyer, Abeele, & Delsanto).

The basic principle behind many nondestructive testing methods is to relate some change in an input-output relationship of the test to a defect in the structure. The input-output relationship may be formed for any type of energy that may be imparted on the structure whether it is optical, electrical, acoustic, mechanical, or thermal. Usually NDT methods are concerned with a change in response from a known good or undamaged condition (Doebling *et al.,* 1996). Figure 0-1 shows the basic methodology of NDT.

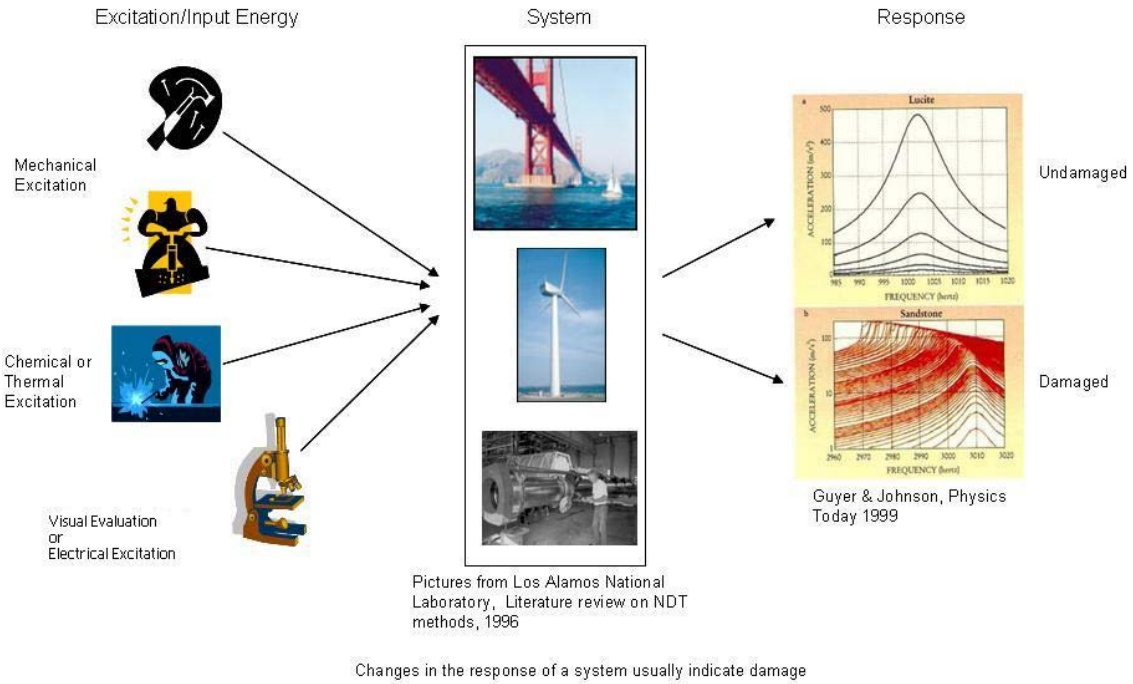

Figure 0-1 Input Output Relationship for General NDT Applications

The input-output concept of many nondestructive tests, as shown in Figure 0-1 is very important to this work and is revisited continuously throughout the development of the applied method. The concept is one of a transfer function, and is adapted to the investigation at hand in Chapter 0. The difficulty in applying most of the NDT methods that are discussed in the following sections is that aggregates are heterogeneous, and many of the features causing responses indicative of damage in other structures are inherent to the material. Without a means to compare and contrast "good" and "bad" samples, one must proceed with care when attempting to apply any of the NDT methods that are described. In Chapter 0, methods for overcoming this challenge are discussed.

1.12.1 MECHANICAL NDT METHODS

The mechanical methods that are described here encompass all the seismic, acoustic and ultrasonic NDT methods. This is done because in each case it is mechanical energy that is propagated through the material and that energy, in each case, is measured in a similar manner.

Typical mechanical tests include modal hammer tests, shaker tests, Schmidt hammer, and other hammer tests. In each case the material of interest is impacted or excited in some physical manner. Typically, an accelerometer is used to measure acceleration, or frequency response functions. Some of the simpler tests, including the rebound hammer, measure the amount of energy dissipated by the material instead of its vibration characteristics. Often it is important that a force hammer be used to measure the amount of energy imparted on the structure being tested. These tests are typically local or small scale tests. The same basic principles are applied to seismic tests to detect global, and in some cases local damages. Damage in a material, in the case of these tests, is typically characterized by a shift in the structure's natural frequency. This shift has been observed by many to behave in a nonlinear fashion (Abeele *et al.*, 2001, Doebling *et al.,* 1996, Guyer *et al.*, 1999, Johnson, 1999) as shown in the bottom plot on the response side of Figure 0-1 or in Figure 0-2.

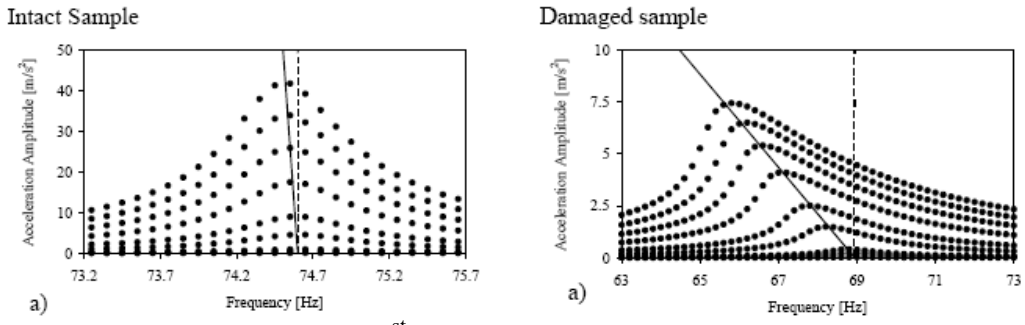

Figure 0-2 Results Obtained on 1st Bending Mode of an Intact Slate Beam for Different Drive Levels Showing Response of Intact & Damaged Samples (Abeele, 2001)

The observed shift in frequency may not be restricted to damaged materials. Guyer *et al.* (1999) and Johnson *et al.* (2007) have found that many materials, including geomaterials, belong to a class of materials which exhibit a slow hysteretic behavior. This behavior has similar characteristics to those shown in Figure 0-2, and indicates that standard non-destructive testing techniques may not be appropriate for use on aggregates.

Today's current applications of mechanical NDT methods focus on detecting damage in existing structures. Damage is defined in a variety of ways and depends on the structure. Often damage is considered a crack or imperfection in the structure or material.

There are as many variations of sonic NDT methods as there are on other physical mechanical tests. Many involve the propagation and reflection characteristics of mechanical or acoustic waves in a structure and attempt to identify voids, cracks, or other 'flaws' and include nonlinear elastic wave spectroscopy (NEWS) (Abeele *et al.*, 2001), local interaction simulation approach (LISA) (Delsanto *et al.*, 2002), modal testing, ultrasonic pulse velocity (Bodare, 2006,), and several others. Another sonic NDT method is acoustic emission analysis (EMPA Materials Science & Technology, 2007), where the

growth of cracks and other processes are measured by recording elastic waves in the structure.

Seismic methods include various reflection and refraction detection tests which are similar in nature to the mechanical tests described previously. Excitations are often imparted on the ground by explosives or large vibrators (Bodare, 2006, Essenreiter *et al.*, 1998). Similar to smaller scale mechanical tests, transducers are used to detect mechanical wave propagations through the medium, usually the earth, being tested. Subsurface features can be detected based on reflective or refractive behavior of the mechanical waves.

1.12.2 ADDITIONAL NDT METHODS

Electrical tests, chemical tests, optical, analytical, and even nuclear tests comprise additional classes of NDT. Tests in these areas are not as applicable to this investigation and will only be discussed briefly so that the overview of available methods is more encompassing. Much of this information has been referenced from the many NDT societies and testing agencies that employ these methods. Additional references are included following the works cited section and may guide the reader in further study, if necessary. A list of many more NDT methods is provided in Appendix A.

Optical methods are employed in a variety of fields and measure such properties as stress, strain, displacement, and chemical composition. Some optical methods currently in use are photoelastic stress analysis and holographic interferometry.

Electrical methods are used to observe inhomogenities, and other changes in structural conditions through a variety of means. Some electrical tests involve eddy

current imaging and magneto-inductive testing (EMPA Materials Science & Technology, 2007), and resistivity testing.

Chemical NDT is used in alloy identification, composition, cracks, elemental analysis and distribution, grain size, inclusions, mactrostructure, porosity, segregation, and detection of surface anomalies. Thermal NDT is used to observe heat contours, plating thickness, conductivity, and stress for a variety of applications. Nuclear nondestructive tests are used in borehole exploration to detect porosity and saturation of surrounding soil conditions. Nuclear proctor density tests are used in compaction testing in geotechnical applications and are widely accepted in industry.

1.13 NONDESTRUCTIVE METHODS FOR TESTING CONCRETE

Some of the test methods applied in this study find their roots in NDT of concrete. Concrete is similar to the aggregates studied. Typically concrete is poured as a viscous liquid mix of cement and pieces of aggregate of various sizes. Like the aggregates being studied in this investigation, concrete is largely a heterogeneous material. Many of the tests applied to concrete are mechanical in nature and may have similarities to those discussed in the previous section on mechanical NDT methods. It should also be noted that petrographic analysis, mentioned previously, also has a role in the nondestructive evaluation of concrete. There are many publications on the NDT methods of concrete alone. The various methods are used to test concrete strength and condition, but often the location of embedded reinforcement or other structural features are also of interest. The primary tests consist of penetration tests, pull-out tests, rebound, and dynamic tests (Pascale *et al.*, 2000, Feldman, 1977, Hurst, 1966, Neville, 1973, Malhotra, 1976). Additional tests include electrical resistance, chemical, and sonic techniques. James

Instruments Inc. is one of the industry's leading suppliers and developers of several NDT methods for concrete testing, including devices for locating rebar, identifying Alkali Silica reactions, and the Windsor Pin System®. A common dynamic test which has been mentioned already is the ultrasonic pulse velocity test. Electrodynamic Determination of the Modulus of Elasticity, or the resonance method, is another dynamic test which is similar in practice to a modal hammer impact frequency response function. It involves clamping a test cylinder to a fixture and using electro-magnetic exciter and pickup, the specimen is excited at varying frequencies until the first resonance is found. The frequency has been correlated with the elastic modulus of the specimen (Neville, 1973). Ultrasonic testing is also used to detect embedded rebar in concrete structures.

The rebound and penetration tests are very similar in that they both approximate the strength of concrete. The rebound hammer test correlates strength with the rebound number, while penetration tests correlate the depth of penetration with strength. Of particular interest in this group of NDT for concrete are the Windsor Pin or Windsor Probe tests (NDT James Inc., Neville, 1973). The Windsor Probe test uses a shot-gun charge to embed a steel pin into the concrete's finished surface. The exposed length of the pin is measured once embedded in the material. The Windsor Pin System® is non-explosive and uses a steel pin to make an indentation in the material's surface (NDT James Inc.). The depth of penetration is measured and correlated with concrete strength. Both Windsor penetration tests are essentially the same in practice, embedding a hardened steel pin into the material, and are similar in practice to hardness tests. Penetration tests are more susceptible to surface inconsistencies than rebound or other dynamic tests. Penetration through soft grains or voids often can cause inconsistent

measurements. These tests are however easy to perform and can be done in the field. The Windsor Pin System® is discussed in further detail in Chapter 0.

Perhaps the most relevant aspect of NDT methods for concrete is that the effectiveness of these tests to measure the properties of the structure of interest is well documented and some of these tests have been shown to be very useful. There is considerable published information about the performance of concrete, its failure modes, and the means of determining its quality, far more than seems to exist for riprap.

1.14 CONCLUDING REMARKS

The overview of NDT methods shows the vastness of the field and the numerous tests available for a variety of applications. Special attention was given to mechanical NDT methods and those used to test concrete. Most of the tests that are used in this study are of a mechanical nature, i.e., impact FRF, Windsor Pin System® measurements, and acoustic impact-emission tests.

GEOLOGICAL CONSIDERATIONS AND PETROGRAPHIC DESCRIPTIONS OF AGGREGATE SAMPLES

1.15 PREFACING REMARKS

In the previous chapters the current FDOT durability tests consisting of density, absorption, abrasion, and chemical tests were explained in depth. In addition to the current tests used by the FDOT, other tests were also examined that are being used to describe aggregate quality. From this background, the factors important to durability are somewhat clear. In more than 100 years of investigating aggregate quality, researchers have more or less deduced that porosity, material binding forces, and chemical reactivity are very important. What may not be clear at this point is where these factors come from, and if they are truly appropriate to measure when evaluating aggregate quality. To better understand the factors affecting aggregate performance, the basic concepts of geology are explored, especially those expressed in works by Boggs (2001), Berner *et al.* (1996), Skinner (1992), Kemp (1929), Tyrrell (1929), and Moorhouse (1959).

In the sections that follow, an overview of the fundamental concepts governing the formation and chemical makeup of rocks is given with particular interest to the properties and compositions that were encountered in this study. The purpose of the discussion is to develop a foundation for the analyses, and the terminology that is used. By examining the composition of geomaterials and certain aspects of the rock cycle, a

group of key factors affecting material performance across many rock types are identified. By examining the weathering processes that contribute to the break down and disintegration of rocks, a better sense of the features that determine quality can be realized. Many of these factors are in-line with those examined by current test methods, others are not. The overview of geologic concepts is followed by a discussion of the various petrographic analyses performed by consulting geologists for this study.

1.16 OVERVIEW OF ROCKS & MINERALS

For the purposes of this study, the three major rock classes, igneous, sedimentary, and metamorphic rocks are considered. Other classes of rocks, i.e., plutonic rocks, ores etc, are often grouped within the appropriate class and will not be considered separately. Most of the samples used in this investigation were identified as limestone, a sedimentary rock, but there were also granite samples, igneous rocks, within the sample pool. For this reason much of the attention is paid to both igneous and sedimentary materials. For completeness, however, metamorphic rocks are discussed briefly.

1.16.1 MINERALS

Minerals are the principle components of rocks and must meet four basic criteria. A mineral must be naturally formed, must be an inorganic solid, have a specific chemical composition, and must also have a characteristic crystal structure (Allaby, 2003; Skinner, 1992). Chemical composition of minerals depends on the ratio of anions and cations. Mineral groups are formed through extensive ionic substitution without changing this ratio (Skinner, 1992). Minerals are typically described using physical properties such as

hardness, cleavage, color, crystal structure, luster, and streak, (Chesterman, 1979; Skinner, 1992). In most cases these properties are well documented and serve as the basis for identifying and classifying minerals. Hardness is defined as a mineral's resistance to scratching, while cleavage is defined as the tendency of the material to break along plains of weakness. Two excellent examples of cleavage are taken from Skinner (1992) and are shown in Figure 0-1.

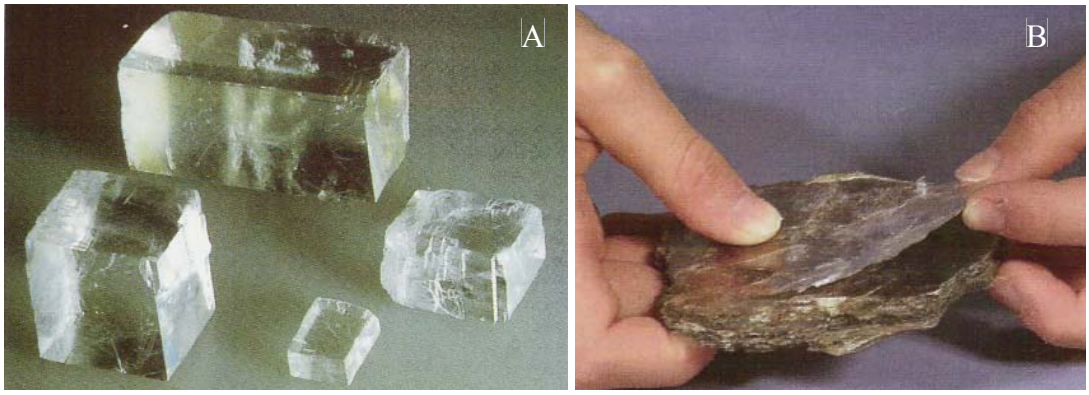

Figure 0-1 Examples of Excellent Cleavage Planes in A) Halite (NaCl) & B) Muscovite, Taken from Skinner, 1992

Streak, though less important for the purposes of this study, is the color of a mineral when ground into a powder (Chesterman, 1979). Rocks are composed of various combinations of minerals, the concentration and consistency of which is very specific. The specific mineralogical and textural characteristics of rocks are the basis of their classifications.

There are several common mineral groups. Some of these include: silicates, comprised of strong complex ion $(SiO_4)^{-4}$, carbonates containing $(CO_3)^{-2}$, phosphates containing $(PO_4)^{3-}$, and sulfates $(SO_4)^{2-}$ (Skinner, 1992). Quartz is an important silicate mineral composed only of SiO_2. Carbonates are common among the samples studied and form such compounds as calcite, aragonite and dolomite. Sulfates are common among

compounds such as anhydrite and gypsum and are formed from evaporated seawater (Skinner, 1992). The chemical nature of the minerals found in rocks is very important since the types of bonds, crystal structure, and other properties will have an effect on the rock's solubility, chemical reactivity to its environment, and its mechanical properties.

1.16.2 IGNEOUS ROCKS

Igneous rocks are by far the most abundant of the rocks found in the earth's crust. Igneous rocks comprise 95% of the earth's crust, though most of the rocks found on the earth's surface are sedimentary (Skinner, 1992). Igneous rocks are formed from the cooling and consolidating of liquid magma, a very hot fluid found deep beneath the earth's surface (Kemp, 1926). Magma is composed of silicates, oxides, and sulfides (Kemp, 1926).

The various texture types, crystalline arrangements, and mineralologies of igneous rocks will not be discussed in detail for since the majority of the samples studied were not of igneous nature. Igneous rocks are most often found where there are mountains or were mountains at one time (Skinner, 1992).

Granite is a typical igneous rock. One group of samples studied in this investigation was identified as granite. Rocks from source GA-178, Macon, Georgia, were composed mainly of biotite (3-37%), orthoclase (3-38%), plagioclase (12-24%), and quartz (19-48%) with small amounts of other compounds including carbonate, hornblende and microline. A picture of a typical granite sample encountered in this study is shown in Figure 0-2.

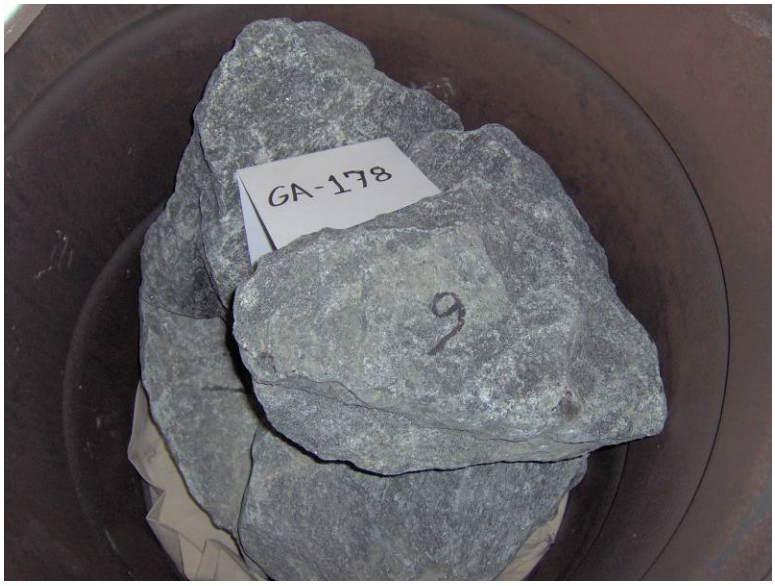

Figure 0-2 Typical Granite Sample Encountered in Study

The ways in which igneous rocks form prevent them from having many voids. Igneous rocks are usually hard and dense with few voids, properties often shared with metamorphic rocks (Skinner, 1992). In Chapter 0 the effects of some of the current durability and soundness tests on igneous rocks were shown in Figure 0-2 and Figure 0-5. The igneous rocks in these figures have excellent resistance to abrasion and chemical attack. Petrographic descriptions for the granite samples can be found in Appendix B.

1.16.3 SEDIMENTARY ROCKS

Sedimentary rocks are those formed from the depositing of sediment through a variety of processes. These processes include flowing water, wind, glaciers, the physiological processes of organisms (Allaby, 2003; Skinner 1992; Tyrrell, 1926; and Kemp, 1926), and chemical precipitation. Sedimentation usually occurs in layers called strata (Skinner, 1992).

Sediment is formed through the denudation of older rock material (Tyrrell, 1929; Skinner, 1992; & Kemp, 1929). Denudation comes from the Latin word meaning to strip bare and typically refers to the general processes by which rocks break down (Allaby, 2003). Sediments are deposited in various ways, some of which were previously mentioned, and are compressed to form sedimentary rocks. The process by which the various unconsolidated sediments are made into rocks is known as lithification (Allaby, 2003). Lithification takes place through the process of diagenesis (Skinner, 1992), or the changes that take place at low temperature and pressure on sediments after deposition (Allaby, 2003). As more and more sediment accumulates, the underlying layers are compressed. Water that existed in the various spaces between sedimentary deposits is squeezed out and the grains become cemented together. These processes are known as compaction and cementation (Skinner, 1992; Allaby, 2003). There are other processes which can affect the formation of sedimentary rock given the presence of different minerals, chemically suitable conditions, and pressure. They are left to the reader to investigate further.

There are many different types of sediment namely clastic, chemical, and biogenic sediment. Clastic particles consist of mineral grains, rock fragments, and in some cases, shells or skeletal mater of organisms (Skinner, 1992). Sedimentary rocks formed from clastic sediment may in many ways resemble concrete. Clastic sediments form conglomerates like breccia, as well as sandstone, siltstone, and shale (Skinner, 1992).

Chemical sediments are formed by the precipitation of soluble compounds as a result of biochemical and inorganic chemical reactions (Skinner, 1992). Ionic

compounds and minerals, such as rock salt or halite (NaCl), are typically soluble in water. Chemical precipitates can also occur when sea or lake water evaporates and leaves behind various compounds in suspension (Kemp, 1926). Another common rock formed from chemical precipitation is gypsum, a compound used to make drywall.

Biogenic sediments contain shells, skeletons, plant remains, and often fossils (Kemp, 1926; Skinner, 1992). These sediments occur wherever organisms are found, especially in marine environments.

Six of the seven sample lots studied in this investigation were identified as limestone. Limestone and dolomite rocks makeup the primary members of the carbonate family of chemical/biochemical sedimentary rocks (Boggs, 2001) and are discussed in further detail in Section 1.18. The primary mineral composition of limestone is calcium carbonate ($CaCO_3$) of which calcite is the most common (Kemp, 1926; Moorhouse, 1959; Skinner, 1992), but magnesium calcium carbonate, or dolomite ($MgCO_3$), is also common.

The sediments in limestone are primarily marine in nature and are composed of algae, foraminifera, corals, and mollusks (Kemp, 1926). Common organic constituents of limestone's sediment are calcareous deposits, remains of microscopic marine organisms forming an ooze on the sea floor (Skinner, 1992), ooliths, organic sub-spherical sand-sized carbonate particles (Allaby, 2003), and bryozoans, small aquatic colonial animals (Allaby, 2003). Limestone may also contain clastic or chemical precipitates.

1.16.4 METAMORPHIC ROCKS

Metamorphic rock is formed when existing igneous or sedimentary rock is altered by changes in pressure, temperature and or volatile content (Allaby, 2003). The changes take place in the solid state (Skinner, 1992) and include re-crystalization and partial melting and remixing of the mineral grains so long as the original rock's identity is retained (Tyrrell, 1929).

The changes to the rock's solid state are driven by elevated temperatures (greater than 200^{o} C) and pressures (greater than 300 MPa) (Skinner, 1992). The changes occur as a result of instability under these new conditions and may take thousands of years or perhaps longer to take place (Skinner, 1992). The formation of new minerals and the re-crystallization of the existing rock is toward a more stable equilibrium (Tyrrell, 1929). Intergranular fluid plays an important role in promoting chemical reactions to take place which foster the growth of new crystals as metamorphism takes place (Skinner, 1992; Kemp, 1929).

1.17 WEATHERING OF ROCKS

Weathering, or the process of denudation discussed earlier, is the process affecting rocks that is perhaps the most important to this study. It is through examination of these phenomena that the factors most likely to affect the aggregates' field performance are to be revealed. In the previous sections the various rock types and their different structures were discussed. While most of the samples examined in this study consist of limestones, it will eventually be important to consider other rock types as well. For this reason weathering is addressed in this section from a general view point. From

this discussion, mineralogy, grain size, and porosity will emerge as the most important physical attributes of the aggregates that affect their durability in various applications.

Weathering consists of a combination of physical, chemical, and biological processes which break down and disintegrate rocks (Boggs, 2001). This process produces solid fragments and secondary minerals as well as dissolved byproducts which can either be left at the weathering site or transported through a variety of processes (Boggs, 2001). The processes that move weathered material from one place to another consist of mass transport in slumps, debris flows, and mud flows, or in fluid flow processes such as moving water, glaciers, and wind (Boggs, 2001).

Weathering is an important part of the rock cycle shown in Figure 0-3 (http://rst.gsfc.nasa.gov, 2006).

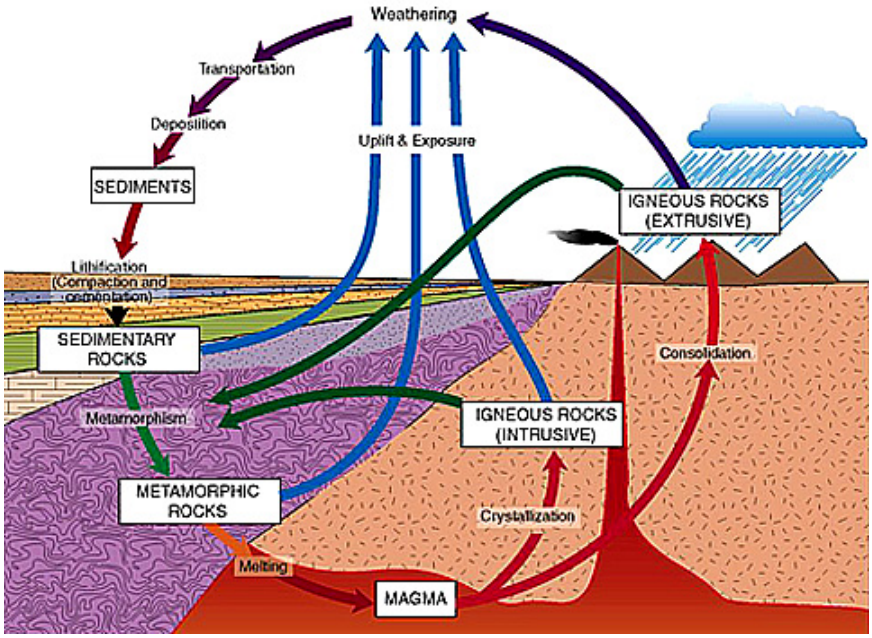

Figure 0-3 Graphical Representation of the Rock Cycle (http://rst.gsfc.nasa.gov/)

The rock cycle represents the process by which rocks, and the earth's crust, are continually recycled. It is often broken to two segments, one for the continental crust,

and the other for the oceanic crust (Skinner, 1992). Many of the processes shown in Figure 0-3 should be familiar from the previous discussion about rocks and minerals. From the discussion of sedimentary rock in Section 1.16.3, sediment was created due to the effects of weathering of older rock (Tyrrell, 1929; Skinner, 1992; Boggs, 2001; & Kemp, 1929).

As previously discussed in Section 1.2, only the degradation of the materials investigated are being considered. Ruling out the effects of erosion on the engineered structure consisting of aggregate due to poor hydraulic design leaves only the fundamental mechanical and chemical weathering failure types to consider. Only the break down and disintegration of the pieces forming the engineered structure whether its rip rap, pavement, or other system is considered for this study. The discussion in the next two sections is shaped around the two classes of weathering processes: physical weathering and chemical weathering processes. The aggregate features most affected by these processes are used to develop a fundamental component of the transfer function approach discussed in Chapter 0.

1.17.1 MECHANICAL WEATHERING

Mechanical weathering, or physical weathering, is a process by which rocks are physically broken down by mechanical processes. These processes include: crystal growth (Boggs, 2001), pressure release (Allaby, 2003), frost wedging, and thermal weathering (Skinner, 1992; Boggs, 2001). Erosion of rocks may also take place by means of sediment suspended in air or water flowing around the rock, abrading away the surface (Kemp, 1926; Tyrrell, 1926). Physical weathering is often difficult to distinguish

from chemical weathering except in cold or very dry climates. It is also interesting to note that physical weathering does not change the chemical or mineralogical makeup of the rock being weathered (Boggs, 2001), but does serve to increase the surface area of a weathering rock so that chemical weathering can take place more efficiently.

Plant roots and other organic processes can also have an effect on rocks in much the same way as frost wedging (Skinner, 1992; Kemp, 1926; Tyrell, 1926; & Boggs, 2001). Plant roots that grow in the cracks of rocks can, over time, widen a crack and split the rock. Frost wedging has a similar effect but is caused by the expansion of water in voids upon freezing. The effects of frost wedging are common where temperature fluctuations around the freezing point occur (Skinner, 1992).

Crystal growth is another mechanical weathering mechanism that works to expand void spaces. As water flowing though voids and cracks evaporates sediments are deposited within the voids and crystals begin to grow. This is also known as salt weathering and has a similar function as the formation or hydration of clay minerals that may work themselves into voids or cracks (Boggs, 2001). The force of the growth often causes splitting and cracking (Skinner, 1992; Kemp, 1926; Tyrrell, 1926). From Chapter 0, the sodium sulfate soundness test performed by the FDOT attempts to simulate this weathering mechanism at an accelerated rate.

Heat is thought to be yet another mechanism of mechanical weathering causing exfoliation. Exfoliation is the flaking of plate like pieces of rock and is caused more notably by forest fires, but cyclic heating and cooling cycles are also thought to have a long term impact on weathering (Skinner, 1992; Kemp, 1926; Tyrrell, 1926; & Boggs, 2001). When heated or cooled, different rates of expansion and contraction of the rock's

structure can cause cracks to form. These cracks allow other weathering processes to further deteriorate the rock.

1.17.2 CHEMICAL WEATHERING

All minerals are subject to chemical attack. Chemical weathering takes place by dissolving rock minerals into solution and depositing new ones (Kemp, 1926). The chief reagent is water or water solutions acting as weak acids, resulting from organic decay and dissolution of carbon dioxide to form carbonic acid (Trryell, 1926, Skinner, 1992), or water rich in alkaline carbonates (Skinner, 1992). Chemical weathering generally takes place where the conditions are most favorable, in warm, wet climates (Skinner, 1992). Chemical weathering is the most important process which breaks down rocks, and therefore the aggregate materials studied here. The chemical weathering processes of particular interest are hydrolysis, hydration and dehydration, oxidation/reduction, solution, and ion exchange processes. These processes are summarized in Table 0-1, taken from Boggs (2001).

Hydrolysis consists of reactions of acidic ions in solution with silicate minerals (Boggs, 2001). These reactions can result in soluble cations (Boggs, 2001) or insoluble clays (Skinner, 1992). The dissolution of certain clay minerals, the biologic processes of plant life, and dissolution of carbon dioxide (CO_2) in water creates the acidic solutions that drive the reactions (Boggs, 2001).

Hydration and dehydration is a chemical process by which minerals either gain or loose electrons to form new minerals respectively (Boggs, 2001). Gypsum, for instance, is the hydrated form of anhydrite ($CaSO_4$). Typically rocks altered in this way suffer

from some change in volume, usually an increase in volume with hydration and the opposite with dehydration. These volume changes result in the disruption of the rock (Boggs, 2001) and allow other weathering processes to work more efficiently.

Table 0-1 Principle Processes of Chemical Weathering, Taken from Boggs (2001)

Name of process	Nature of process	Examples	Principal types of rock materials affected
Hydrolysis	Reaction between H^+ and OH^- ions of water and the ions of silicate minerals, yielding soluble cations, silicic acid and clay minerals (if Al present)	$2KAlSi_3O_8 + 2H^+ + 9H_2O \rightarrow H_4Al_2Si_2O_9 + 4H_4SiO_4 + 2K^+$ (orthoclase) aq (kaolinite) (silicic acid) aq $2NaAlSi_3O_8 + 2H^+ + 9H_2O \rightarrow H_4Al_2Si_2O_9 + 4H_4SiO_4 + 2Na^+$ (albite) aq (kaolinite) (silicic acid)	Silicate minerals
Hydration and dehydration	Gain or loss of water molecules from a mineral, resulting in formation of a new mineral	$CaSO_4 \cdot 2H_2O \leftrightarrow CaSO_4 + 2H_2O$ (Dehydration) (gypsum) (anhydrite) $Fe_2O_3 + H_2O \leftrightarrow 2FeOOH$ (Hydration) (hematite) (goethite)	Evaporites Ferric oxides
Oxidation	Loss of an electron from an element (commonly Fe or Mn) in a mineral, resulting in the formation of oxides or, if water is present, hydroxides	$4FeSiO_3 + O_2 \rightarrow 2Fe_2O_3 + 4SiO_2$ (pyroxene) (hematite) (quartz) $MnSiO_3 + 1/2\,O_2 + 2H_2O \rightarrow MnO_2 + H_4SiO_4$ (rhodonite) $2FeS_2 + 15/2\,O_2 + 4H_2O \rightarrow Fe_2O_3 + 4SO_4^{2-} + 8H^+$ (pyrite) (hematite)	Iron and manganese-bearing silicate minerals, sulfur
Solution	Dissolution of soluble minerals, commonly in the presence of CO_2, to yield cations and anions in solution	$H_2O + CO_2 + CaCO_3 \leftrightarrow Ca^{2+} + 2HCO_3^-$ (carbonation) (calcite) (bicarbonate) $CaSO_4 \cdot 2H_2O \rightarrow Ca^{2+} + SO_4^{2-} + 2H_2O$ (direct solution) (gypsum)	Carbonate rocks Evaporites
Ion exchange	Exchange of ions, principally cations, between solutions and minerals	$Na\text{-clay} + H^+ \rightarrow H\text{-clay} + Na^+$	Clay minerals
Chelation	Bonding of metal ions to organic molecules having ring structures	Metal ions (cations) + chelating agent [excreted by lichens] $\rightarrow H^+$ ions + chelate [in solution]	Silicate minerals

Oxidation and reduction reactions comprise yet another important chemical weathering process. Oxidation and reduction reactions are characterized by the loss of electrons through oxidation, or the gaining of electrons through reduction. These reactions take place during the weathering processes of silicate minerals where iron or manganese is present (Boggs, 2001). The gain or loss of electrons in these reactions creates chemical and electrical instability in the material, making it more susceptible to other forms of attack (Boggs, 2001).

Solution weathering takes place when certain minerals are exposed to rain or ground water, particularly calcite, dolomite, gypsum, and halite (salt) (Boggs, 2001). These minerals can potentially be highly soluble, especially if atmospheric CO_2 is dissolved in rain water (Boggs, 2001). Solution weathering is an important weathering process in climates where carbonates are exposed to wet conditions at or near the water table, which is the case for many of the materials studied in this investigation when used for bank and shore protection.

The final chemical weathering process discussed here is the chemical process through which ions in solution are exchanged with ions in minerals. Ion exchange typically occurs in clay minerals and is an important process allowing clays to change from one clay type to another (Boggs, 2001). Typical ions which are exchanged in this manner include sodium and calcium (Boggs, 2001).

1.17.3 ADDITIONAL REMARKS ON WEATHERING

In the previous two sections physical and chemical weathering were discussed with the intent of exploring which properties of the aggregates are most important to

study in an effort to develop a quality test. While physical weathering most often takes place in cold or arid climates (Boggs, 2001) chemical weathering takes place to some extent in almost every climate. From this discussion is apparent that the most important aspect of aggregate quality is its mineralogy. Knowing an aggregates mineral content is critical in understanding what weathering processes it will be most susceptible to. One cannot also rule out that that many of the chemical weathering processes have the same effect on rocks as the physical process; they break the rock into smaller pieces, increasing the surface area over which further chemical weathering process proceed to disintegrate and recycle the rock more efficiently. This implies that grain size and porosity are also critical features to a rock's durability as each can significantly increase or decrease a samples weathering potential.

Florida aggregates are comprised mostly of carbonate materials such as limestone. From the previous discussion on weathering processes, it is also apparent that many of the aggregates quarried in Florida may be placed in service conditions which are ideal for weathering to take place causing eventual breakdown and possible failure of systems comprised of aggregate, i.e. roadway, embankment, etc. This observation is important for future evaluations of the quality of these materials. A closer examination of the rates at which rocks weather may provide a foundation for future aggregate quality standards.

The rate at which a rock is weathered is dependent on climate, mineralogy, and grain size (Boggs, 2001). While expressed in much of the literature, Kemp (1929) perhaps explains in a broad sense what promotes the fastest weathering rates across a variety of materials:

"Rocks are most weathered above the water table, in warm moist climates, where the topography favors considerable circulation of water. The rocks most rapidly weathered are the porous, fine-grained rocks containing soluble minerals, notably the carbonates, basic silicates, pyrite or volcanic ash. The porosity may be primary, as in a fragmental rock…" (Kemp, 1926).

The ideas expressed by Kemp are generally consistent with much of the other literature describing the factors affecting the weathering of rocks (Oyen *et al.*, 1998; Berubé 2001; Skinner, 1992). While Kemp (1926) concisely supports the idea that mineral composition, grain size and porosity are very important to consider when evaluating the durability of aggregate material, Boggs (2001) also points out that weathering of certain materials may be heavily dependent upon site-specific conditions and further states that there are no set rules which can be applied to sedimentary rocks for determining their susceptibility to weathering (Boggs, 2001). For these rocks, their durability is dependent on the type and amount of cement, mineralogy and climate (Boggs, 2001).

In rock types other than sedimentary rocks, the degree of stability is often in reverse of Bowen's reaction series for petrogenisis (Kemp, 1926; Skinner, 1992; Boggs, 2001). The series is reproduced from Skinner (1992) in Table 0-2, showing the most stable minerals with respect to chemical weathering at the top, and those least stable at the bottom (Kemp, 1926; Skinner, 1992) and is similar to those provided by other authors including Boggs (2001).

Table 0-2 Reverse Bowen Reaction Series for Chemical Weathering Stability, Taken from Skinner, 1992

Stability	***Mineral***
<-- Decreasing Chemical Stability (susceptibility to chemical weathering)	Iron oxides & hydroxides
	Aluminum oxides & hydroxides
	Quartz
	Clay minerals
	Muscovite
	Potassium Feldspar
	Biotite
	Sodium Feldspar
	Amphibole
	Pyroxine
	Calcium Feldspar
	Olivine

It is interesting to point out that Quartz is often regarded as one of the most resistant mineral to weathering (Kemp, 1926; Tyrell, 1926; Skinner, 1992) but many authors have commented on its susceptibility to alkali-silica reactions, especially when quartz containing aggregate is used in concrete (Oyen *et al.,* 1998; Berubé 2001).

1.18 CARBONATE SEDIMENTARY ROCKS

As an important pre-cursor to the petrographic analyses in the next section there are three aspects of carbonate rocks, and limestones in particular, that are important to discuss. They are mineralogy, texture, and classification of carbonates. Structure is another important aspect of these materials, however the other three aspects will play a more important role in understanding the petrographic descriptions discussed in Section 1.19. Mineralogy has already been discussed in Section 1.16.3. With the exception of trace amounts of other minerals, the most important for this study being

quartz, limestone consists predominately of calcium carbonate grains, or magnesium carbonate grains.

Texture describes the granular composition of particles in a rock, i.e. their size and shape (Allaby, 2003). Carbonates have three distinct textural forms: carbonate grains, microcrystalline calcite, and sparry calcite (Boggs, 2001). Carbonate grains are often called allochems and consist of pieces of aggregate precipitated out of solution (Boggs, 2001). Particles generally range in size from 0.02 mm up to 2.0 mm but may also consist of shells, fossils and other clastic or biogenic particles (Boggs, 2001). Typical grains observed in carbonates include clasts, skeletal particles, ooids (coated carbonate grains surrounded by thin coatings of aragonite or calcite), peloids (mostly fecal pellets or calcite grains without definitive structure), and aggregates (Boggs, 2001).

Microcrystalline calcite, or micrite, often serves as the binding structure or cement for carbonates. It's comprised of very fine-grained calcite crystals on the order of 1-5 microns (0.001 – 0.005 mm) in size (Boggs, 2001). On the petrographic descriptions micrite is described as matrix, and is the most highly concentrated feature observed across many of the carbonate slides examined.

Sparry calcite shows up in the petrographic descriptions as the second most concentrated feature in the carbonate samples. It consists of larger calcite crystal grains which lack internal structure. Crystals are generally 0.02 mm to 0.1 mm in size (Boggs, 2001), though particles as large as 0.50 mm to 1.90 mm were observed in some samples studied.

Other textural features that are important for interpretation of the petrographic analyses include amorphous calcite, and some porosity types. Amorphous calcite is

defined by one of the consultant geologists (Nagel, 2006) as calcite which is larger in size than micrite, but too small for its grain structure to be identified with an optical microscope. For a majority of the petrographic slides examined the voids are merely identified as voids. Some petrographers choose to distinguish between moldic, interparticle, or intragranular pores in a sample. More information is provided with descriptions of the petrographic analyses in Section 1.19 and in Appendix B.

Limestone is often considered very heterogeneous because of the multitude of constituents, and how they may be combined to form rock. As a result, several different classification schemes have been devised over the last 100 years. Boggs (2001) makes reference to a classification scheme developed by Folk in 1959 which is based on the types of carbonate grains and the grain to micrite ratio (Boggs, 2001). Mineralogy is used primarily to distinguish between limestone and dolomite since most carbonates are comprised of a single mineral form (Boggs, 2001). The classification of carbonates using Folk's system is based on determining the relative concentrations of allochems, micrite, and sparry calcite cement (different from the sparry calcite grains discussed previously) (Boggs, 2001). Further details on the classification of carbonates using this system are available in the literature.

1.19 PETROGRAPHIC ANALYSIS OF AGGREGATE SAMPLES

Petrographic analysis was briefly discussed in Section 1.8 as a visual inspection of rocks at the macroscopic scale, microscopic scale, or both. The technique has been developed over time but more recently with an aim at determining the quality of Florida aggregates (Eades *et al.*, 1997, Oyen *et al.*, 1998, McClellan, 2002, and Gregory, 2004).

This recent work has been in the application of a petrographic number technique pioneered by Bayne *et al*. (1955) which will be addressed shortly.

The data that is utilized in this study consists of microscopic evaluations of the rock samples provided by the FDOT. The analysis is performed on a thin section mounted to a microscope slide. The sample is thin enough to allow light to pass through. The slide is placed on a mechanical stage which moves in set increments under the lens. The microscope may be outfitted with several polarizing light filters and different eye pieces (Moorhouse, 1959) depending on the application. The geologist records the mineral or feature which is identified by a marker visible in the eye piece. This process is repeated over about 100 points and the percentages of the various components are calculated based on how many counts of each component were recorded. The concentrations of the different features are considered an average for the sample and are generally consistent for multiple slides analyzed from the same rock. Typical analyses report a list of features observed in the sample with concentrations and average size ranges for their particles.

Petrographic descriptions are furnished by two consultant geologists contracted independently for this project. Petrographic descriptions provided by Scott Nagel Consultant Geologist Incorporated (SNCGI) of Boston, Massachusetts (http://sncgi.com) (Nagel, 2006) and by Dr. Guerry McClellan, Consultant Geologist, of Gainesville, Florida (McClellan, 2006). The findings of petrographic studies furnished by each geologist are provided in Appendix B for reference. Depending on the geologist, and his or her experience with Florida aggregates, some features may have been treated

differently in the analyses, and for this reason data from the two geologists are not combined.

1.19.1 PETROGRAPHIC ANALYSES BY SNCGI

The analyses performed by SNCGI (Nagel, 2006) comprise the majority of the analyses and report mineralogy, porosity, grain sizes, and a description of the slide. Reports from SNCGI are accompanied by a photograph of the slide and can be viewed in Appendix B.2 (Nagel, 2006). Examples of several petrographic slides from SNCGI's reports are shown in Figure 0-4 and represent the array of textural features observed in the carbonates and the densely packed crystalline structure of the granites (Nagel, 2006).

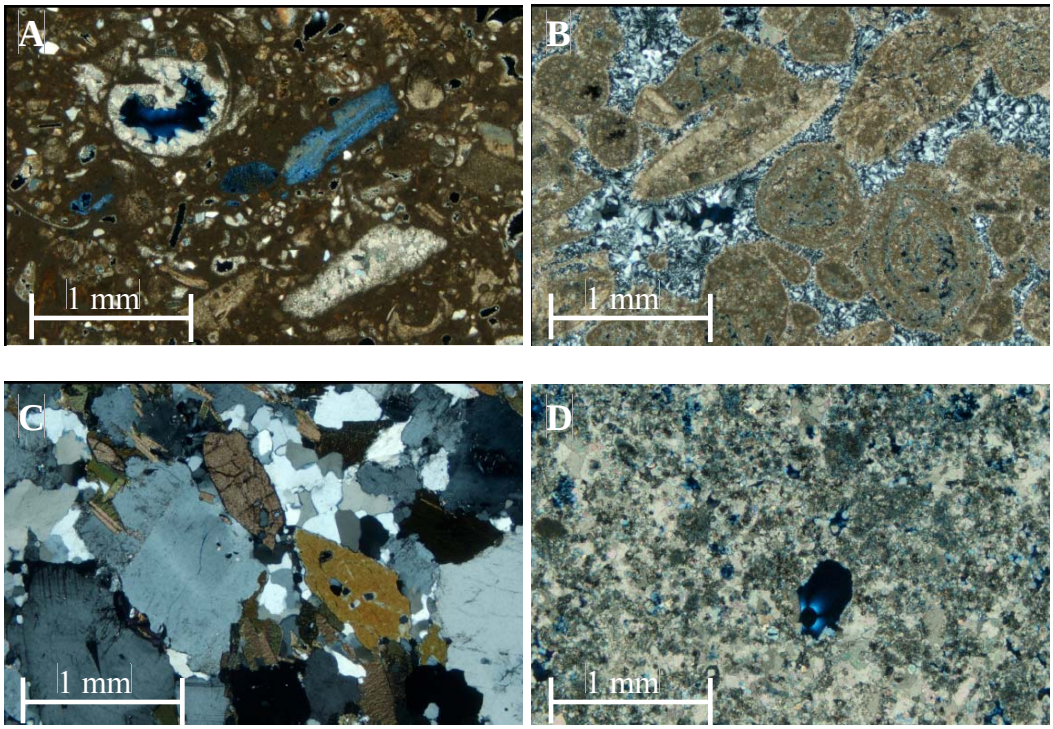

Figure 0-4 Typical Thin Sections, 40x Magnification A) 12-521-09 (Limestone); B) 18-607-10E (Limestone); C) GA-178-06 (Grainite); D) 34-106-09A (Limestone) (Nagel, 2006)

The data from SNCGI's analyses (Nagel, 2006) serve as the system properties that are used in the development of the transfer function approach in Chapter 0. The mineralogy, porosity, and grain size of the major petrographic features are compared with the measured responses from the physical tests on the corresponding rock sample or core. These features were identified in Section 1.17 to be most important to the weathering processes affecting the aggregates.

The concentrations of the petrographic properties have been tabulated in Table 0-3 for two of the aggregate sources. Additional tables summarizing the results of the point-count analyses and petrographic reports can be found in Appendix B.2. Slides are denoted in the same way as the core samples previously described. If multiple slides from a particular core sample were analyzed, an additional letter is added to the core-sample identification number. Later analyses will be performed on the average concentrations of the various features for each sample.

Table 0-3 Petrographic Features Sources 08-534 and 12-521 (Nagel, 2006)

Source			08-534			12-521				
Feature/slide No.			1	2B	7	1B	6	8AA	8BB	9
Calcite, Sparry	Percentage (%)		9%	1%	2%	2%	2%	2%	2%	2%
	Size (mm)	Min	0.12	0.04	0.12	0.02	0.08	0.03	0.03	0.03
		Median	1.01	0.17	0.25	0.03	0.18	0.06	0.05	0.11
		Max	1.90	0.30	0.38	0.04	0.28	0.08	0.07	0.18
Matrix	Percentage (%)		73%	91%	85%	73%	81%	84%	75%	79%
	Size (mm)	Min	0.00	0.00	0.00	0.00	0.00	0.00	0.00	0.00
		Median	0.01	0.01	0.01	0.01	0.01	0.02	0.02	0.01
		Max	0.01	0.01	0.01	0.01	0.01	0.03	0.03	0.01
Quartz	Percentage (%)		17%	3%	9%	1%	1%	3%	3%	1%
	Size (mm)	Min	0.07	0.03	0.04	0.05	0.04	0.08	0.05	0.05
		Median	0.11	0.07	0.10	0.14	0.11	0.13	0.18	0.20
		Max	0.15	0.10	0.15	0.23	0.17	0.18	0.30	0.35
Void	Percentage (%)		1%	5%	4%	24%	16%	11%	20%	18%
	Size (mm)	Min	0.03	0.10	0.07	0.07	0.02	0.05	0.02	0.12
		Median	0.42	0.49	0.28	1.25	1.61	1.14	4.19	2.60
		Max	0.80	0.87	0.48	2.42	3.20	2.23	8.35	5.07

The petrographic properties shown in Table 0-3 are common amongst the carbonate samples. Though none of the samples from the sources shown in Table 0-3 contained amorphous calcite, it too is identified as a major component of the carbonate samples examined. Amorphous calcite, sparry calcite, matrix (micrite), quartz and the porosity (voids) are the five major features that will be examined in the analysis discussed in Chapter 0. The average concentrations of these features computed for each carbonate source are shown in Figure 0-5. The granite samples will not be examined as closely as the carbonates. Only the quartz concentrations of the granite samples are used in the analysis in Chapter 9 to develop causal relationships with the applied tests. The granite petrographic descriptions are also included in Appendix B.2.7.

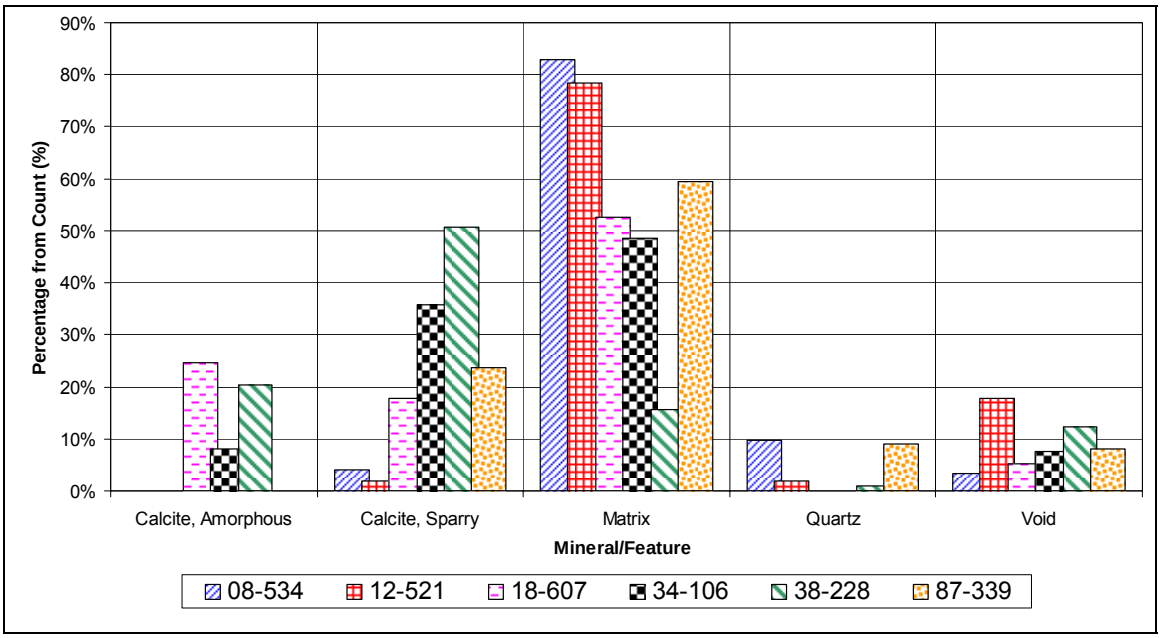

Figure 0-5 Concentration of Major Petrographic Features in Carbonate Samples Averaged by Source (Nagel, 2006)

The analyses performed by SNCGI (Nagel, 2006) represent a typical point-count analysis. While some variation was observed from one slide to another from the same

rock, the reported percentages should be accepted as reasonable representations of the samples.

1.19.2 PETROGRAPHIC ANALYSES BY G. MCCLELLAN

The petrographic analyses performed by Dr. McClellan (2006) serve to verify that the aggregate samples studied are typical of their reported sources and in most cases this was true. Additionally, Dr. McClellan's (2006) analyses are used to provide an alternate approach to the petrographic descriptions following the petrographic number technique first developed by Bayne *et al.* (1955) and later adjusted for use with carbonates typical of Florida geology by Eades *et al.* (1997) and Oyen *et al*, (1998).

In the petrographic number technique, typical features are expanded to include fossil and non fossil grains, different cement or matrix types, and different porosity types. Each feature is assigned some weighted value (factor weight) which is multiplied by the percentage of the constituent. The factor weights are based on earlier studies and experience with Florida aggregates and range from 1.0 for a durable component to 6.0 for a deleterious component (Eades *et al.*, 1997, Oyen *et al.* 1998). The weighted values are summed at the end of the analysis to generate a petrographic number which is analogous to a scoring system for the sample. Petrographic numbers of 100 (factor weights of 1 assigned to each feature observed in a 100 point-count analysis) are considered to be the most durable. Petrographic numbers between 100 and 140 are generally considered to predict good performance while petrographic numbers exceeding 140 are considered an indicator of potentially poor performance (Oyen *et al.,* 1998). A typical scoring sheet for this type of analysis is shown in Figure 0-6 taken from Oyen *et al,* (1998).

Petrographer: _____ Date: _____
Aggregate #: _____ Thin-Section #: _____
Locality: _____ Formation: _____
Point Count Total (N): _____

Rock Types	Description	% of Total	Factor Weight	Weighted Value
Sedimentary				
Limestone	- fossil grains		1.3	
	- non-fossil grains		1.0	
	- porosity types			
	moldic	_____	3.0	_____
	vuggy	_____	3.0	_____
	interparticle	_____	3.0	_____
	intraparticle	_____	2.0	_____
	intercrystalline	_____	2.0	_____
	Total Porosity			
	- cement/matrix			
	micrite	_____	1.5	_____
	microspar & spar	_____	1.0	_____
	Total Cement/Matrix			
Dolostone	- dolomitic cement & grains		1.5	
Other Mineral Grains				
	- quartz/chert		Var*	
	- opaques		6.0	
	- clays		6.0	
Igneous				
Granites			1.0	
Metamorphic				
Marble			1.5	
Quartzite			1.2	
	Total Percentage	_____	*PN Total*	

* Factor value based on the XRD crystallinity index method of Murata and Norman (1976) - (1, 3, 6)

Additional Comments _____

Figure 0-6 Sample Thin-Section Petrographic Data Form Taken From Oyen *et al.*, (1998)

The analyses in this study will make use of both the point-count and petrographic number data from Dr. McClellan's analyses (McClellan, 2006). The data from McClellan's report (McClellan, 2006) is far less statistically significant however, since only nine samples were examined in comparison to the 50 or so that were examined by SNCGI (Nagel, 2006). The complete details of the petrographic descriptions provided by

each geologist can be found in Appendix B. This technique has not been perfected as of yet. Correlations with field performance, as in any of the FDOT tests, must still be studied for this technique. Previous work by the developers of the technique suggests the strong possibility of the petrographic number technique to develop into a useful means of evaluating aggregate in the future and for this reason it is being utilized in this study.

1.20 CONCLUDING REMARKS

The discussions in this chapter are important for several reasons. The first reason is that the fundamental concepts of geology including minerals, rock types and how they are formed were described. It should be clear how the lithologies of limestone and granite differ. Additionally, the structure of carbonate rocks was examined in further detail to bring some meaning to the petrographic descriptions of the samples studied. Later parts of the discussion focused on the principle mechanisms of weathering, the process by which rock is broken down naturally. The various chemical and mechanical methods of weathering discussed should support the intent of the current tests used by the FDOT to mimic one or more of the weathering mechanisms that act on most rock species. Most importantly, weathering mechanisms are used to identify the principle features of aggregate expected to have the greatest impact on performance, i.e. porosity, grain size, and mineralogy. These factors are the system parameters of interest in the transfer function approach that is described in the next chapter.

It is important to mention that while physical weathering plays a role in the performance of aggregate, the primary mechanism of failure for these materials is of a chemical nature. The tests used in this study, i.e. Windsor Pin System®, acoustic impact-emission, and impact frequency response function test, are all physical tests that are

assumed to be strongly affected by the mechanical properties of the constituents which affect durability.

The petrographic analyses, as a whole, merely provide a measure of the various textural and mineralogical components of the samples with little regard for how they may work together to affect field performance. This is true with the exception of the petrographic number technique which has not been well established as an accurate rating system. The analysis in Chapter 0 only takes into account the concentrations and the median sizes of the features identified in the petrographic analyses. The effect of different combinations of the petrographic properties on the measured responses from the applied tests is addressed throughout the remainder of the thesis.

Because a complete understanding of the samples' durability cannot be obtained from the petrographic descriptions alone, additional cooperation with geologists is critical for future research efforts concerning aggregate quality to be successful. Geologists and researchers can collectively work together to best understand how certain combinations of minerals in the various rock types affect aggregate performance for a particular application. This is addressed further in Chapter 0.

OUTLINE OF EXPERIMENTAL APPROACH

1.21 PREFACING REMARKS

This chapter recapitulates many of the important points of the previous chapters, outlines the general methodology for the analyses and serves as a building block for the experimental results. A great deal of effort has been spent, up to this point, developing the background and fundamental concepts governing this investigation. It is important that the appropriate ideas are summarized and combined here.

1.22 REVIEW OF KEY CONCEPTS

In Chapters 0 and 0, the current FDOT durability and soundness tests were discussed along with additional quality tests and nondestructive evaluation methods. Recall that the four primary tests used by the FDOT, bulk specific gravity, absorption, L.A. Abrasion, and the Sodium Sulfate Soundness test have been developed from the culmination of more than 100 years of experience working with aggregate by various researchers. Even long after their development, research continues to improve the accuracy of the tests, and possibly replace them with better methods, as in the case of this investigation. There is no standard by which the effectiveness of these tests is measured, yet transportation officials have observed fair to moderate correlation between these tests and aggregate performance.

The current tests used by the FDOT, and other methods recently developed to determine aggregate quality, seem to be concerned with the same core group of properties. Chapter 0 showed that these properties are primarily the material binding forces, porosity, and chemical durability. These factors coincide with many highlighted in the discussion in Chapter 0 where some fundamental concepts of geology were explored. By ruling out hydraulic design issues, concrete and bituminous applications (i.e. pavements) the failure modes that are left for consideration are those caused by physical and chemical attack as discussed in Section 1.17. From the principles of weathering discussed in Chapter 0 grain size, porosity, and mineral content were determined to be the most significant factors affecting the durability of rocks and their corresponding aggregate. It is clear that they coincide with the important factors examined by current tests.

While the tests employed by the FDOT examine many of the same factors that geologists have determined are significant, there is no direct relationship between the various combinations of these properties and actual performance. The specifications of transportation agencies are not written in terms of allowable porosity, grain size, or mineral contents. The specifications are written in terms of indirect measurements of these properties. Without a uniform system of quantifying aggregate performance to provide an understanding of the key performance factors and their interactions for various materials, it is nearly impossible to develop an accurate quality test at this time. Instead of determining a measure of quality, this investigation is focused on determining the relationship between the factors of interest and the test methods employed. Establishing these relationships provides a foundation for understanding a new method of aggregate

property characterization which is vital to the problem at hand if future research is to be successful.

1.23 DEVELOPMENT OF THE TRANSFER FUNCTION APPROACH

In Chapter 0 the development of transfer function relationships between the applied tests and factors affecting aggregate performance was mentioned. Transfer functions have been the topic of discussion throughout much of the work thus far and it should be pointed out that virtually any test can be represented as a transfer function relationship. To illustrate the versatility of a transfer function approach, a simple block diagram is presented in Figure 0-1.

Figure 0-1 Simple Transfer Function Block Diagram

In any test, or means of evaluation, there is typically some system being evaluated, represented by *G(x)* in Figure 0-1. This could be anything from a student, structure, physical or logic based system. The system is usually taxed by some stimulus in the form of a certain type of energy, question, or other input which is meant to cause a response. The response is typically related in some way to a system property of interest and so the input used is a way of measuring the property that affected the response. This is the very basic foundation of any test from a transfer function point of view. If the output is not the result of the system properties' change on the input, then the applied input to the system does not represent a valid test of those properties.

A similar relationship was described for many nondestructive test methods in Chapter 0 with the concepts of a transfer function shown in Figure 0-1 which has a similar resemblance to Figure 0-1. The nondestructive test methods described in Chapter 0 were only able to relate the system's response to the damage or property of interest by comparing the responses of both damaged and undamaged specimens, i.e., they examine changes in response with the introduction of a flaw. Through careful investigating, researchers have been able to learn the behavior of many nondestructive tests' responses for systems with varying degrees of damage or presence of other properties of interest.

Clearly the typical nondestructive testing approach will not work for the determination of aggregate quality unless the true meaning of quality is adequately defined by transportation agencies. The basis for developing a quality standard based on known durable and non-durable samples does not exhibit a high level of confidence. The system properties that are important, according to the fundamentals of weathering, are indirectly related to the response of the aggregate with respect to the currently used tests. In this investigation, the direct relationships between the petrographic factors, grain size, porosity, and mineral content, and the measured responses are studied. No effort is made to investigate various combinations of these characteristics with respect to the measured responses. The bearing this has on future work is addressed in Chapters 0 and 0.

Petrographic analyses by two independent geologists, discussed in Chapter 0, provide the direct measurements of the weathering factors. The analyses serve as the definition of the system properties to be measured. The responses from the various inputs used, i.e. Windsor Pin System®, acoustic impact-emission, and impact FRF measurements are compared against the measured system properties. Through linear

regression, the dependency of the measured responses on the system properties is evaluated. Those relationships with strong correlations represent transfer functions with the possibility of being used to discern aggregate quality.

The details of each test are presented in the following chapters including efforts to analyze the data independent of the system properties and verify that the measured response consistently depends on the material properties. In cases where the responses are found to be significantly affected by factors other than the material properties, the data is identified and excluded from further analysis.

From experience, it is well established that inertial and elastic properties will have a direct effect on the measured frequencies of the system under impact FRF and acoustic impact-emission tests. It seems reasonable then to assume that mineral content, and perhaps porosity, will have a significant impact on the measured frequencies from these tests. Likewise, material compressive strength is also directly related to mineral content, grain size, and porosity. The Windsor Pin System® has been tested and calibrated by the manufacturer to be an indicator of compressive strength in concrete. Concrete has a similar structure to many of the aggregates studied. To summarize, it is expected that the variation in certain properties will have a profound affect on the measurements made in each line of tests. The analysis of the relationships that exist between the petrographic properties and the other methods is discussed in Chapter 0.

Other researchers have had moderate success in comparing the petrographic properties with physical properties of materials similar to those investigated in this study. One such study reported fair correlations of quartz-feldspar ratios of Turkish granites with physical properties including, uniaxial compressive strength, tensile strength, and

modulus of elasticity (Tuğrul *et al.*, 1999). Tuğrul *et al.* (1999) also compared other petrographic characteristics with engineering properties mentioned with similar results, indicating the possibility of obtaining reasonable correlations in this study.

The physical tests applied in this study have well established dependencies on some of the same engineering properties when used in their typical applications that Tuğrul *et al.* (1999) correlated with granites. The Windsor Pin System® has been correlated with the compressive strength of concrete, whereas the acoustic impact-emission tests and impact frequency response function test have direct dependencies on the ratio of stiffness and mass in the sample. In many cases engineering properties can be estimated by examining the response characteristics of these tests.

1.24 CONCLUDING REMARKS

The direct measurement of system properties is accomplished through petrographic analysis. The properties important to material durability, i.e. grain size, porosity, and mineral content, are compared against the measured responses from Windsor Pin System®, impact FRF, and acoustic impact-emission responses. Regression analysis is used to determine if strong relationships exist between the tests' response, and the properties of interest. Previous studies like the one performed by Tuğrul *et al.* (1999) have indicated that it is possible to obtain reasonable correlations between the petrographic properties of geomaterials and engineering properties. Several of these engineering properties are directly related to the response characteristics of the applied tests methods in this study. In the chapters that follow, the response measurements from each test will be discussed. Regression analyses follow these discussions in Chapter 0.

WINDSOR PIN SYSTEM® TESTS

1.25 PREFACING REMARKS

The Windsor Pin System® and data collected on the various samples is described in this chapter. Additionally, any pertinent observations about the test are discussed and recommendations for future tests using the Windsor Pin System® are made.

1.26 EXPERIMENTAL DESCRIPTION

The Windsor Pin System® is similar in practice to Rockwell or Brinell hardness tests performed on other materials for engineering purposes. In typical hardness tests, the size and depth of the indentation made by the test is used to develop a hardness number which can then be equated with the tensile strength or other properties of the material (Callister, 2003). In the case of the Windsor Pin System®, a steel pin is driven into the surface of concrete or masonry mortar by a spring loaded device. The depth of the hole created by the pin is inversely proportional to the compressive strength of the concrete or mortar (NDT James, 2006). The test is considered mildly nondestructive since the surface of the material being tested is often spawled. NDT James Instruments Inc. is the supplier who developed and provided the test equipment used and is shown in Figure 0-1.

Figure 0-1 Windsor Pin System® & Additional Equipment

The test conforms to the requirements of ASTM-C803 (NDT James, 2006) and is sister to the company's Windsor Probe Test® which imbeds a steel probe into the material with a powdered charge.

The Windsor Pin System® device consists of two handles, a chuck where the pin is inserted, and a high strength spring released by a triggering mechanism. The spring is retracted by turning a bolt with a wrench and held in place by the triggering mechanism. After locking the spring in the retracted position, the loading bolt must be backed off for the device to fire properly as a safety measure. The device is capable of testing concrete with compressive strengths as high as 5300 psi. The stored potential energy of the spring is 91 lbs*in (108 Nm) (NDT James, 2006). The Windsor Pin System® was selected over the Windsor Probe® since the chuck does not allow the pin to be released from the chuck when fired into the air. The explosive nature of the Windsor Probe® and the potential for injury lead to the selection of the Windsor Pin System® as a safer alternative. Both systems rely on the same principles in practice.

The pin used by the Windsor Pin System® is made of high strength steel (NDT James, 2006) and is initially about 1.2 inches long. Reportedly the pin can be used up to seven times before it must be replaced. To continuously monitor the acceptability of the pin, a go/no-go gage is included with the kit shown in Figure 0-2B (NDT James, 2006).

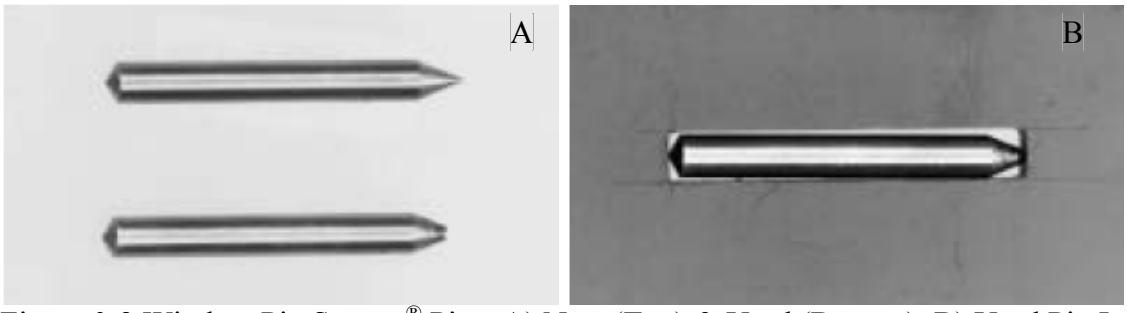

Figure 0-2 Windsor Pin System® Pins: A) New (Top) & Used (Bottom); B) Used Pin In Go/No-Go Gage (NDT James, 2006)

The depth of pin penetration is measured with a needle micrometer supplied with the equipment. The device needs a flat surface on which to perform the test so that penetration measurements are made accurately. To prepare the surface of the rock, grinding stones were used to grind away minor surface imperfections. In some cases a flat area was ground; in others, a rounded groove resembling that of a mortar joint was made, whichever proved easiest. For some of the materials, grinding of the surface was ineffective or created a less adequate surface on which to perform the test. For this reason the device was used without the flat-surface spacer chuck installed, shown in Figure 0-3.

Figure 0-3 Windsor Pin System® Without Spacer Chuck Installed (NDT James, 2006)

The device is typically used to measure mortar joints in this configuration since the v-shaped groove conveniently fits between masonry stone and abuts the surface of the mortar being tested. For the tests in this investigation, this configuration was used to assure that the penetration depth could be accurately measured by eliminating any question of the contacting surface that existed before the test for surfaces that could not be adequately prepared by grinding. The needle micrometer, shown in Figure 0-4, could be similarly configured and so the measurement could be made relative to the original positioning of the device on the sample.

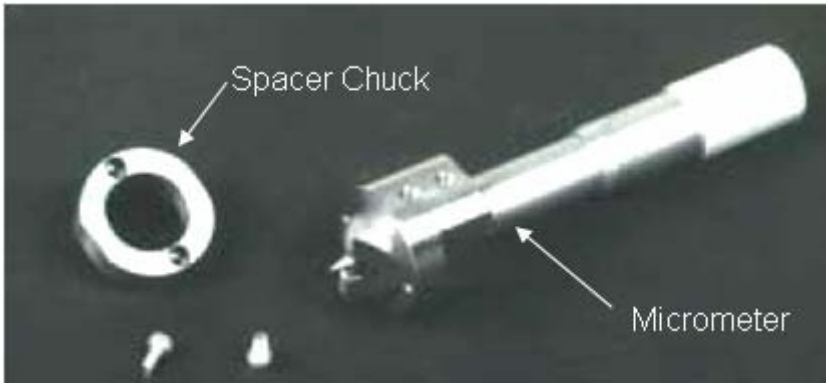

Figure 0-4 Needle Micrometer & Spacer Chuck (NDT James, 2006)

So long as the micrometer's groove is oriented in the same way on the sample as the test device, measurements can be made from the same reference elevation on the surface.

The test can be performed by firmly holding the Windsor Pin System® device against the sample after compressing the spring, as shown in Figure 0-5, and pulling the trigger. The rock sample being tested was supported on a double layer of cardboard placed on the lab's tile floor. The device has a small amount of recoil depending on the material tested. The pin creates a small hole in the material's surface which is cleaned with a blower. The penetration depth is measured with the micrometer.

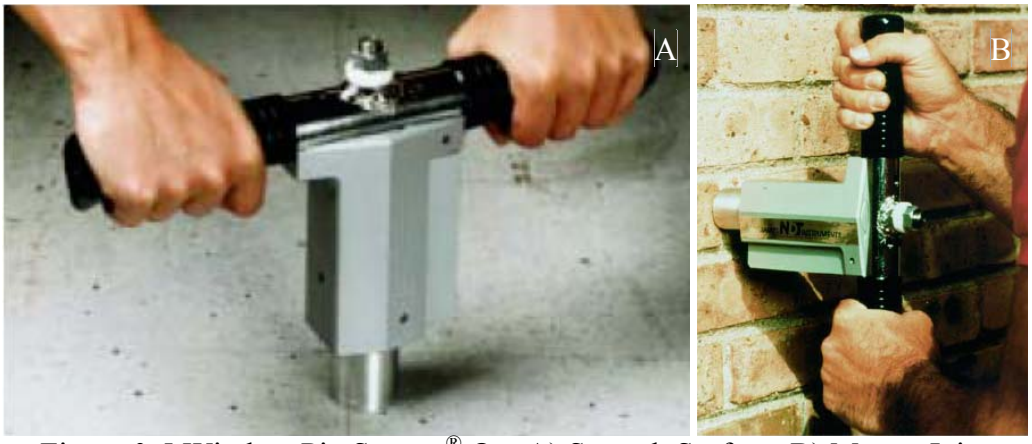

Figure 0-5 Windsor Pin System® On: A) Smooth Surface; B) Mortar Joint (NDT James, 2006)

Because of the micrometer's configuration, the micrometer reading of the hole's depth is subtracted from 1 inch to represent the actual depth of penetration. For different types of concrete and mortar, charts are provided to equate the measurements to compressive strength. Because these charts are based on extensive testing and calibrating with concrete, and not the aggregate itself, the charts were not used to extract mechanical

properties. No compressive tests were conducted due to the limited number of samples to correlate with the Windsor Pin System® data. Instead, the measurements are compared with the petrographic properties in Chapter 0. Had the compressive strength of the sample been of particular interest, the device would have been calibrated through multiple compressive break tests.

1.26.1 EXPERIMENTAL RESULTS

The rocks tested with the Windsor Pin System® are the same rocks from which cores were cut for the frequency response function tests and petrographic analysis. Three or four samples from each source were tested. For each sample, the pin was driven three times in different locations. Depending on the quality of the measurements determined by the investigator at the time of the test, an additional measurement was conducted. Typical reasons of collecting a 4^{th} measurement include extreme spawling, broken pin, or skipping across the sample from the recoil action. The measurements obtained from the performed tests are tabulated in Table 0-1.

Table 0-1 Windsor Pin System® Test Measurements

No.	Source	Sample Number	Micrometer readings / Measurement Number (inches)				Average (in)	Average Depth (inches)
			No. 1	No. 2	No. 3	No 4 (if required)		
1	08-534	1	0.892	0.911	0.904		0.902	0.098
2	08-534	2	0.905	0.913	0.935	0.913	0.917	0.083
3	08-534	7	0.944	0.915	0.907	0.918	0.921	0.079
4	12-521	1	0.879	0.866	0.875		0.873	0.127
5	12-521	6	0.816	0.782	0.876	0.801	0.819	0.181
6	12-521	8	0.871	0.883	0.885		0.880	0.120
7	12-521	9	0.878	0.869	0.875		0.874	0.126
8	GA-178	3	0.895	0.918	0.937	0.924	0.919	0.082
9	GA-178	4	0.913	0.918	0.919	0.925	0.919	0.081
10	GA-178	6	0.891	0.897	0.893		0.894	0.106
11	GA-178	9	0.868	0.911	0.905	0.892	0.894	0.106
12	18-607	5	0.952	0.953	0.927	0.937	0.942	0.058
13	18-607	8	0.905	0.905	0.910		0.907	0.093
14	18-607	9	0.880	0.891	0.909	0.913	0.898	0.102
15	18-607	10	0.895	0.877	0.916		0.896	0.104
16	34-106	2	0.847	0.850	0.871	0.861	0.857	0.143
17	34-106	6	0.797	0.660	0.822	0.791	0.768	0.233
18	34-106	9	0.847	0.831	0.782	0.847	0.827	0.173
19	34-106	10	0.849	0.862	0.858	0.831	0.850	0.150
20	38-228	1	0.885	0.896	0.897		0.893	0.107
21	38-228	3	0.862	0.864	0.870		0.865	0.135
22	38-228	4	0.851	0.883	0.899	0.924	0.889	0.111
23	87-339	5	0.567	0.731	0.792		0.697	0.303
24	87-339	6	0.848	0.845	0.852		0.848	0.152
25	87-339	8	0.881	0.874	0.879		0.878	0.122
26	87-339	10	0.812	0.554	0.673	0.873	0.728	0.272

For each sample, the first measurement was performed with a fresh pin. Subsequent measurements on the same sample were performed after measuring the pin length with the go/no-go gage. If the pin was sufficiently blunted by the previous test, it was discarded and a new one was used for the remaining measurements. In most cases, the pin survived 3 or 4 successive measurements on the same sample. In some cases, however, the pin only survived one or two measurements. With successive tests using

the same pin, the general trend for many of the samples tested is that the micrometer readings indicated progressively shallower measurements. The micrometer reading is subtracted from 1 inch to obtain the depth of penetration. The trend of decreasing penetration with respect to measurement number for a particular pin is illustrated for two sets of samples in Figure 0-6 and Figure 0-7 using the data from Table 0-1.

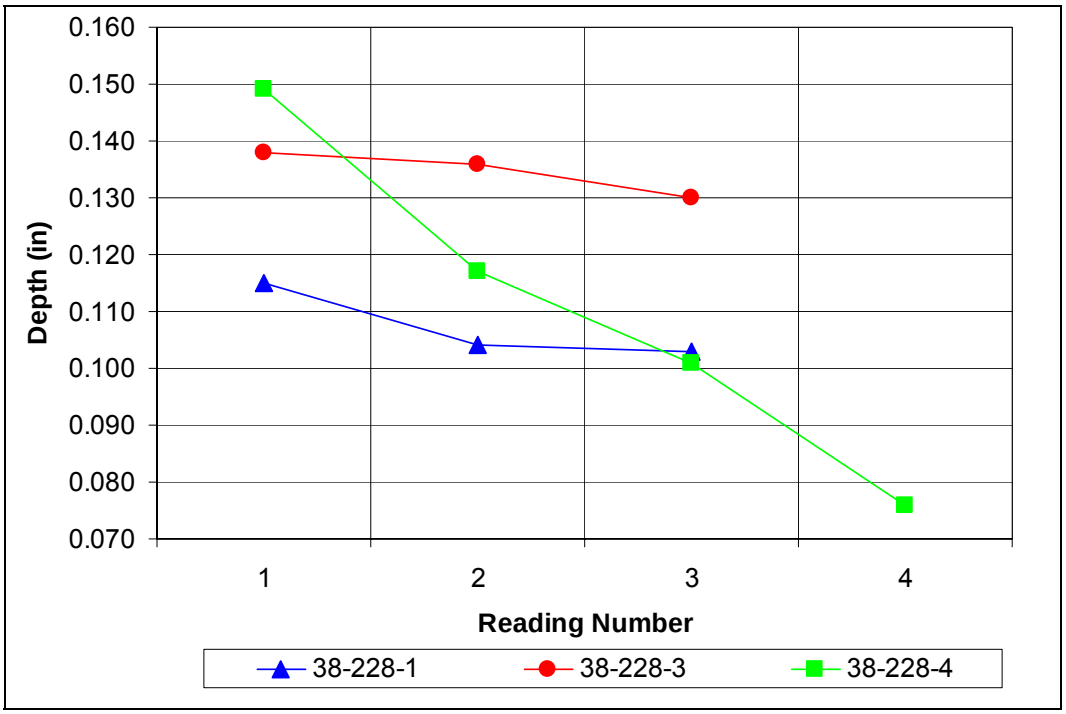

Figure 0-6 Depth of Penetration with Respect to Measurement Number for 38-228

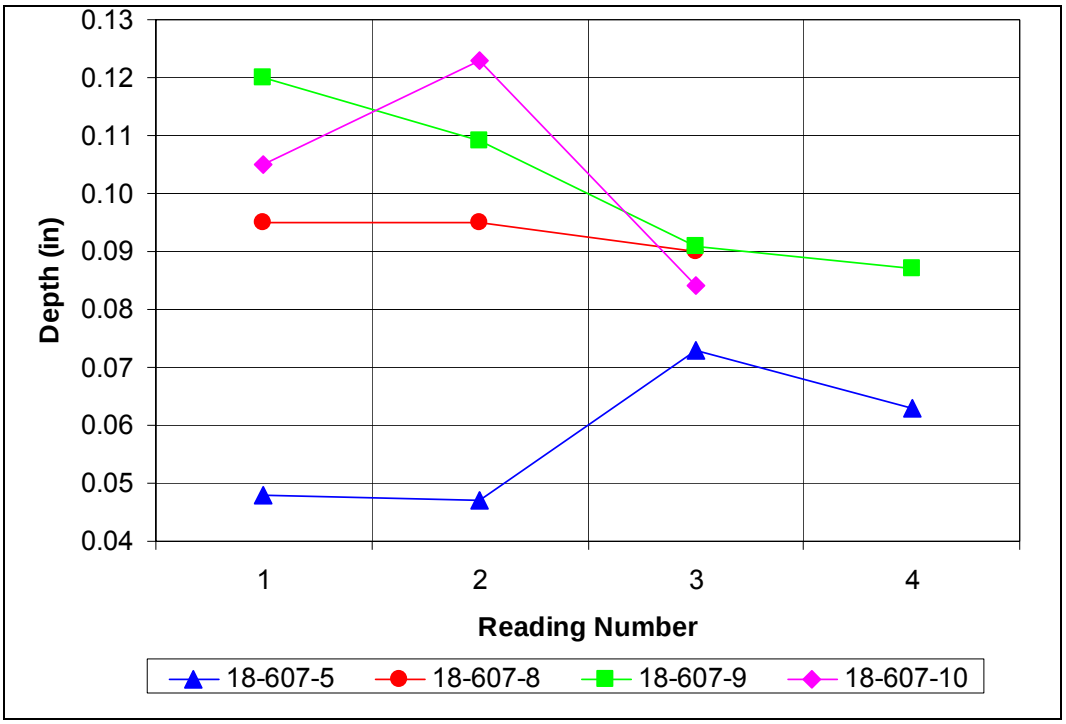

Figure 0-7 Depth of Penetration with Respect to Measurement Number for 18-607

The trend shown in Figure 0-6, is without much of the scatter typical in some of the measurements. The trend of decreased penetration with successive use of the same pin is expected since the pin is blunted with each use. Figure 0-7 is more representative of the general behavior of the data for a majority of the sources. Two of the samples shown in Figure 0-7, 18-607-5 and 18-607-10, did not follow the general trend of progressively shallower penetration. Several of the samples exhibited a similar behavior. The variation in measurements is most likely the contribution of many factors, including surface preparation, material grain or void impacted, and the quality of the hole left by the pin. Additional data plots similar to those shown in Figure 0-6 and Figure 0-7 can be found in Appendix C.

To provide a quantitative sense of the aggregates' response to the Windsor Pin® Tests for samples from each source, the average of the measurements were taken across

all the samples from a particular source, i.e. all the measurements in the first measurement column from source 08-534 were averaged and so on for the other sources. These average depths are shown in Figure 0-8.

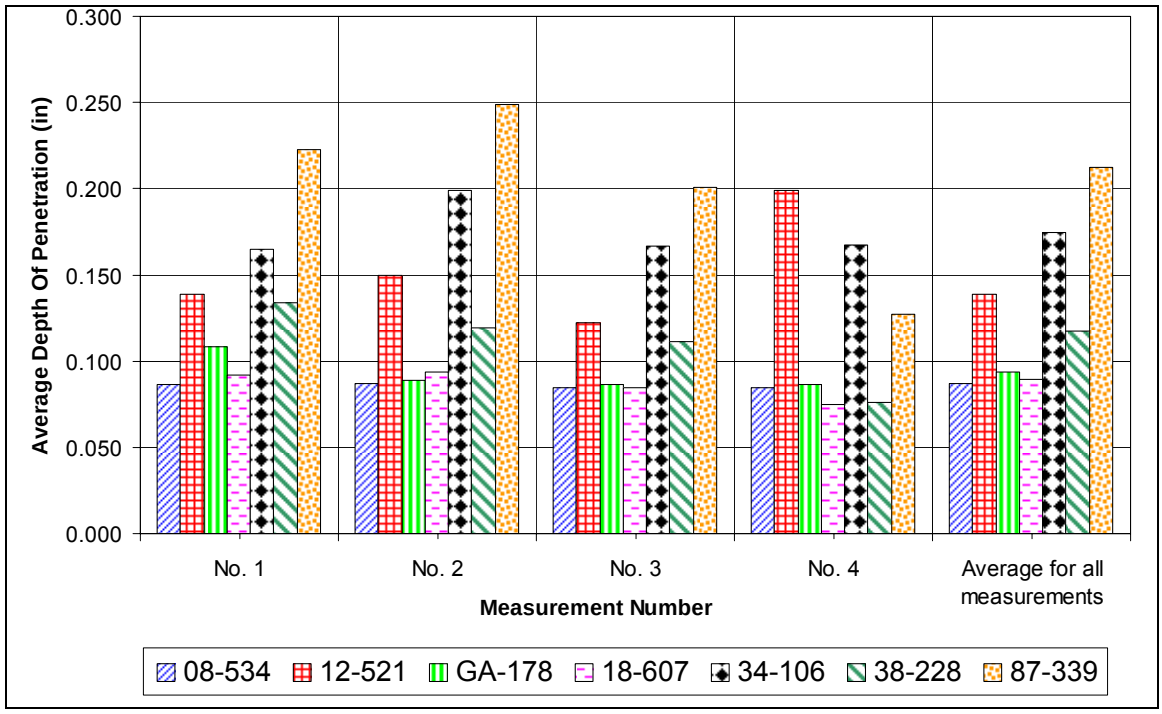

Figure 0-8 Average Depth for Each Source with Respect to Measurement Number for Windsor Pin System® Tests

The data in Figure 0-8 indicates that some sources were more consistent than others across the samples tested and that the average of all the measurements is consistent with the average of the individual measurements for each source.

1.27 OBSERVATIONS

Overall, the Windsor Pin System® was easy to use; however, there is a learning curve associated with its use. There were frequent times when a test or measurement had to be discarded because the device's recoil on the uneven surface would cause it bounce off the sample or fracture the surface so badly that an accurate measurement was

impossible or without confidence relative to the device's original orientation. In these cases the test was repeated. Preparation of the sample's surface was often labor intensive and difficult. The difficulty encountered in preparing the sample is in part because more appropriate tools were not readily available at the time the test was performed and also because of the nature of some of the material.

The penetration of the pin seemed to be highly affected by the material structure in the localized area where the test was performed. Driving the pin in an area where the rock was very porous often led to deeper penetrations than solid areas. Conversely, areas that were solid may not have been as hard as material in porous areas and so the pin penetrated the surface as if it were going through chalk or highly compressed dry powder. These situations left an almost perfect hole and the pin was often wedged in the material by friction. The pin on the other hand was barely blunted at all in these situations. The sample's inconsistencies, both surface preparation and material structure issues, may explain much of the variance observed for samples similar to 18-607-5 and 18-607-10 shown in Figure 0-7. The device manufacturer recommended performing between 3 and 7 measurements, depending on the material, to reduce the variability caused by these factors. In this investigation only 3 or 4 measurements were taken in the interest of efficiency and cost, since there were many test specimens and the pins are costly. In every instance possible, test locations were selected to best represent the sample's characteristics.

In addition to the inconsistencies associated with the test specimens, bent pins were a frequent occurrence. In no case did the pin bend so much that is was deemed rejected by the go/no-go gage but the deformation was noticeable. Bent pins may be

attributable to the force applied to the device to press it against the sample during the test. The minimum passing length measured by the go/no-go gage is 1.159 inches, allowing a total shortening of 0.046 inches from an original length of 1.205 inches +/- .001 inches. The allowable deformation of the pin seems to be adequate as used pins which still pass the go/no-go gage test are still pointed.

1.28 CONCLUDING REMARKS

The Windsor Pin System® bears a similar resemblance in concept to typical hardness tests performed in the engineering disciplines. The device is easy to use, portable, and well suited for in-situ strength testing for concrete and mortar as it was designed. The data indicates an expected behavior of decreasing penetration depth with multiple uses of the same pin.

Applying the Windsor Pin System® for use on individual rock samples required preparation of the sample's surface. This task would have been more easily accomplished with more appropriate tools. Local properties of the sample reduce confidence in the data's consistency in some cases. Confidence in the data can easily be improved with additional testing performed on rock specimens cut in half. The flat surface left by this process would eliminate the need to prepare the surface further and would also allow use of the flat surface chuck and the ability to select three or more test locations representative of the sample's composition.

Initial assessment of the Windsor Pin System® for use as a measure of aggregate is that additional work should be done to increase the confidence level in its operation and the factors affecting the measurements before it can be ruled out. The benefits of easy use and portability make it an attractive method to investigate further. Correlation

of penetration measurements to concrete and mortar compressive strength suggests that with the reduction of the mentioned inconsistencies, the Windsor Pin System® may lead to an additional quality test. The most immediate benefit that the Windsor Pin System® poses for transportation officials is its potential as an initial screening tool for selecting aggregate test specimens at the quarry.

The data presented in Table 0-1 is compared with the data obtained from petrographic analysis in Chapter 0. Further analysis of the use of the Windsor Pin System® in relation to its feasibility as a means to measure aggregate's weathering characteristics is discussed.

ACOUSTIC IMPACT-EMISSION TESTING

1.29 PREFACING REMARKS

The acoustic impact-emission test is described in this chapter. The data collected are presented in time and frequency domain plots of the measured responses. Following the presentation of representative data, the details of additional tests performed are discussed in an effort to determine the feasibility of the acoustic impact-emission testing as a measure of aggregate quality.

1.30 EXPERIMENTAL DESCRIPTION

The acoustic impact-emission test consists of a two-inch stainless steel ball bearing suspended from a wooden jig configured to double as a microphone stand. The bottom of the jig was lined with 1 inch yellow packing foam sheets. The rock sample is suspended from an aluminum ladder using fishing net and bungee chords such that the ball would impact the same location with each swing. Clothes line tensioners are used to raise or lower the sample into position relative to the ball bearing. The ball bearing remains in a single configuration for all of the tests for consistency. The ball bearing is retracted to a position determined by a meter stick clamped to the end of the wooden jig ensuring that the potential energy released by each swing is roughly the same. The acoustic response from the impact of the ball bearing with the sample is measured using a

B&K model 4190, ½" free-field microphone head and B&K model 4229 preamplifier measuring to 20 kHz. The test configuration is shown in Figure 0-1.

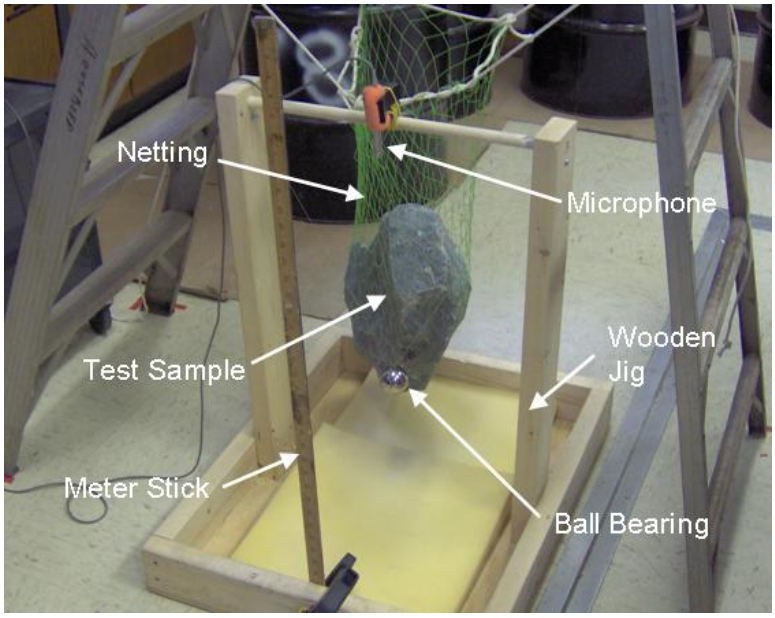

Figure 0-1 Acoustic Impact-Emission Test Setup

Tests were conducted in a large laboratory which had masonry walls and many objects of varying density that were not moved during the test. The test setup was marked on the floor with tape to insure that the room was configured in roughly the same way for each test. Tests were performed during times when roadway and hallway traffic would have the least impact on the measurements.

The rock samples used for the tests were not prepared in any way and so the geometry of the test samples was not consistent. The location of the impact was marked on each rock with permanent marker to facilitate additional testing for repeat measurements if necessary. Samples that were tested in a single orientation were marked with an asterisk. Samples tested in multiple orientations were marked differently for each orientation using a circle (direction 1), square (direction 2), or triangle (direction 3). This

method of notation was used to differentiate the sample identification numbers and the test points. An example of the impact point identification is shown in Figure 0-2.

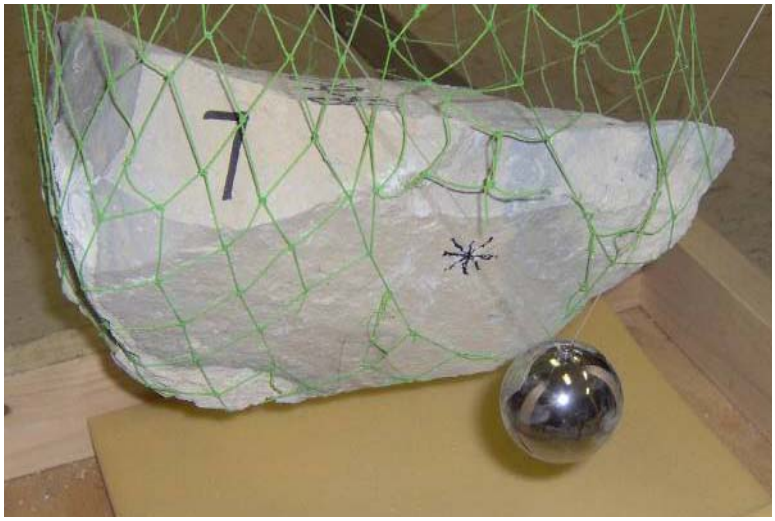

Figure 0-2 Example of Asterisk Denoting Impact Identification Point

In total, three samples from each source were tested using the acoustic impact-emission test.

The concept of the acoustic impact emission test comes from the idea that geologists can discern the quality of aggregate samples by listening to the sound that is made when the rock is struck by a hammer. While several of the geologists consulted during this research were familiar with the technique of listening to the sound emitted by a rock struck by a hammer, each seemed to have a different opinion as to its effectiveness and exactly what could be understood about the sample from it. The technique seems to be dependent on individual experience rather than an accepted technique as it is not discussed in any of the literature referenced.

1.31 EXPERIMENTAL RESULTS

Data collected consists of both time and frequency responses of the acoustic signal radiated by the impact of the ball bearing and the sample. Prior to testing, the microphone was calibrated so that the voltage signals measured by the microphone could be converted to sound pressures. Time data shows the sound pressure with respect to time measured during and after the impact. A representative time response measurement from each of the seven sources is shown in Figure 0-3. The traces in Figure 0-3 show the time response of the fifth (last) impact of the averaged measurements.

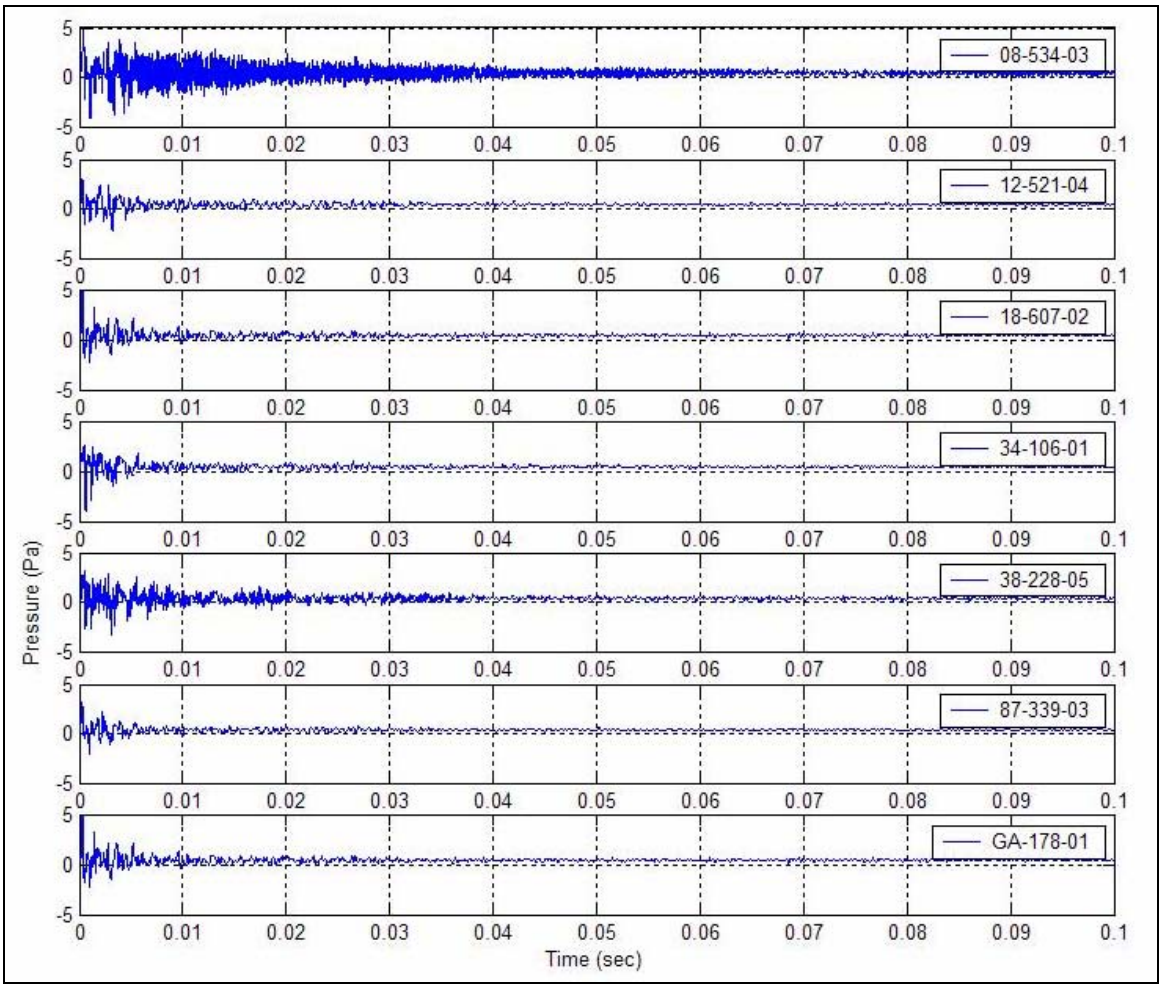

Figure 0-3 Sound Pressure With Respect to Time for Seven Rock Samples

Time response data is useful in comparing the relative amount of ringing the response exhibited. For example, the response of sample 08-534-03 from Figure 0-3 indicates that the impact caused a bell like response with the sample ringing for some time after the impact. The high amplitude of the response of sample 08-534-03 also indicates that the response was probably quite loud. Conversely, the other samples' responses in Figure 0-3 do not always indicate a very bell like response. Some samples, like 87-339-03, are quite dead, and the response quickly diminishes. Samples with similar responses typically sound dull in comparison to a bell. The relative ringing or deadening of a sample's response is perhaps an indication of the material damping, or degree of energy dispersion, in the sample when excited in this manner.

Complementing the time response data, the frequency content of the impact's acoustic response was also measured. The sensitivity of the microphone was used to compute the sound pressure level in decibels. Sound pressure level in decibels is a logarithmic representation of the signal's power relative to some reference pressure unlike the time response data which shows the measured sound pressure on a linear scale. Frequency response data is displayed as autospectra with frequency on the horizontal axis, and sound pressure level in decibels on the vertical axis. Figure 0-4 shows the autospectra for the average result of five impacts measured on the same samples shown in Figure 0-3.

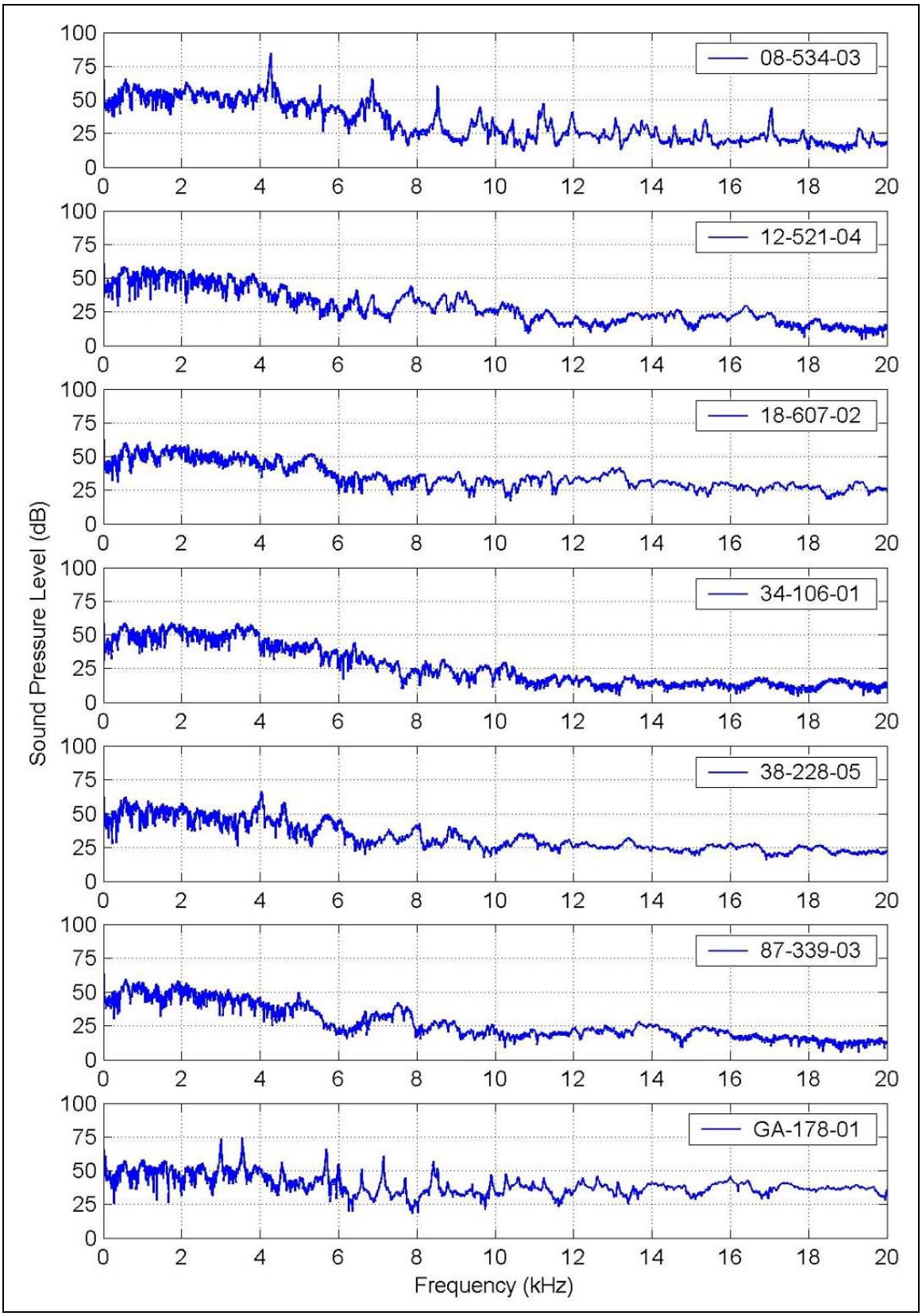

Figure 0-4 Sound Pressure Level in Decibels With Respect to Frequency for Seven Samples

Frequency responses provide information about the pitch of the response emitted from the impact of the ball bearing with the rock, information that could not easily be discerned from the time responses in Figure 0-3. For some of the samples, a peak appears at a frequency of high response. In some cases, sharp peaks are present in the frequency domain for samples with long time responses. Additional plots of the measured responses can be found in Appendix D.

The time and frequency information of the measured acoustic signal emitted from the impact of the ball bearing and the rock sample is useful for understanding qualitative information about the rock's response, i.e. whether the response rings or damps quickly, but it is not good for quantitative measurements. In Chapter 0 it is shown that impact FRF measurements typically produce clean responses showing definitive resonant frequencies of the sample. The acoustic data does not always reveal such information. Without being able to use any quantitative information from the test with consistency, it is difficult to compare the data with that collected from petrographic analysis.

An additional drawback to the acoustic impact-emission test lies in the sample preparation. The mechanical excitation invoked by the impact of the ball and the sample causes the sample to vibrate; this is similar to the excitation in the impact FRF tests. The geometry of the sample affects the distribution of both mass and stiffness and thus the frequency of response and the physical deformation pattern the sample undergoes when excited. Without uniformly prepared specimens it is likely that the deformation pattern of the sample and the frequency at which it resonates will not be the same for any two samples which would result in the emission of a different acoustic signal. To illustrate

the effect of geometry on the measured response, a sample was tested in three different orientations. The frequency spectra for each orientation tested is shown in Figure 0-5.

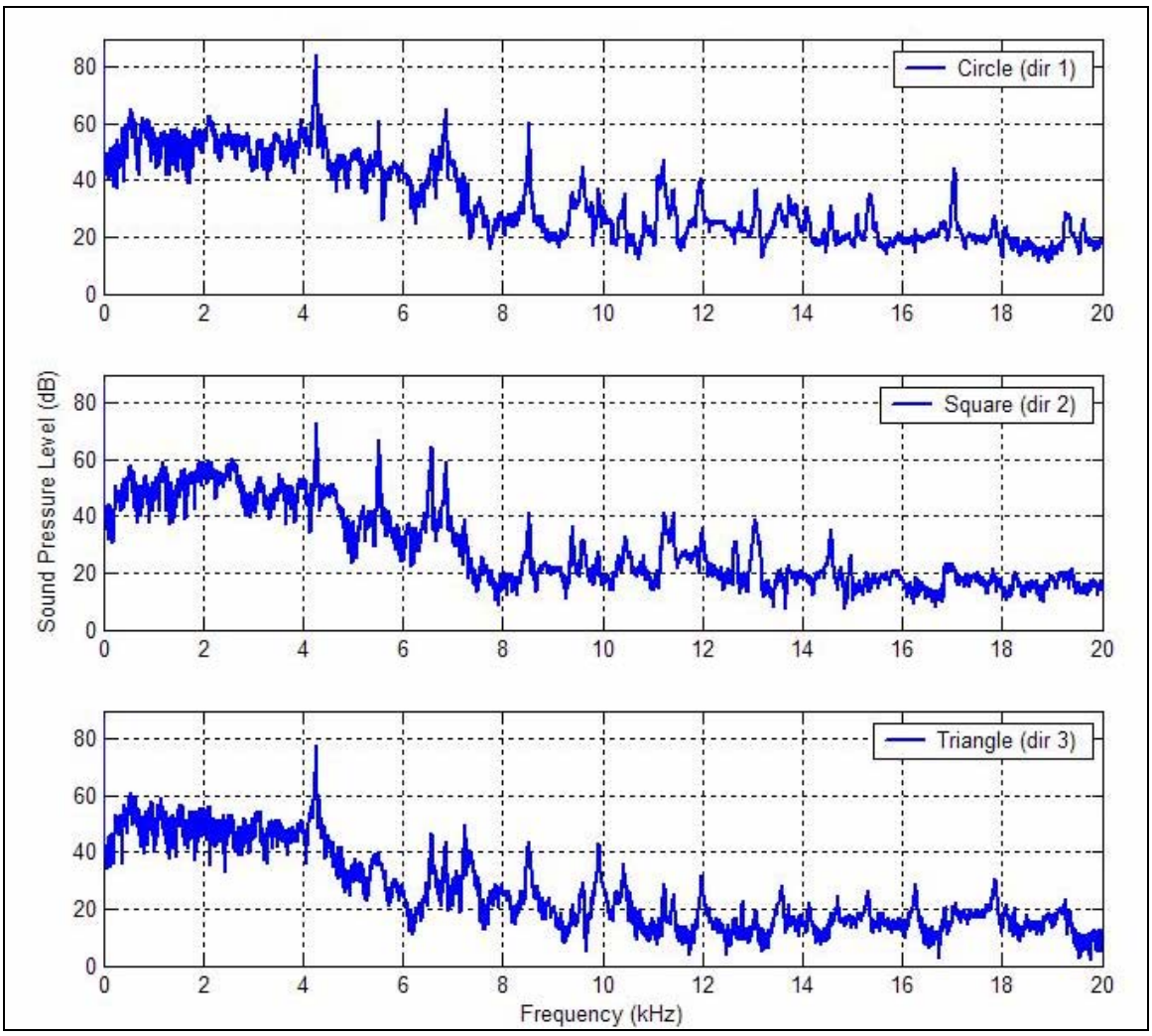

Figure 0-5 Sound Pressure Level with Respect to Frequency for a Single Sample in Three Different Orientations (08-534-03, Brooksville Limestone)

While there is a strong peak consistently around 4.25 kHz, subsequent portions of the responses vary considerably from one direction to the next. If geometry were not a factor in the measured response, the spectra would be more consistent than that shown in Figure 0-5. The variance in the response as a function of the sample's orientation shows the geometry's affect on the response and can be further supported by examining the time

response of the same sample in the same orientations as shown in Figure 0-5. The time responses are shown in Figure 0-6.

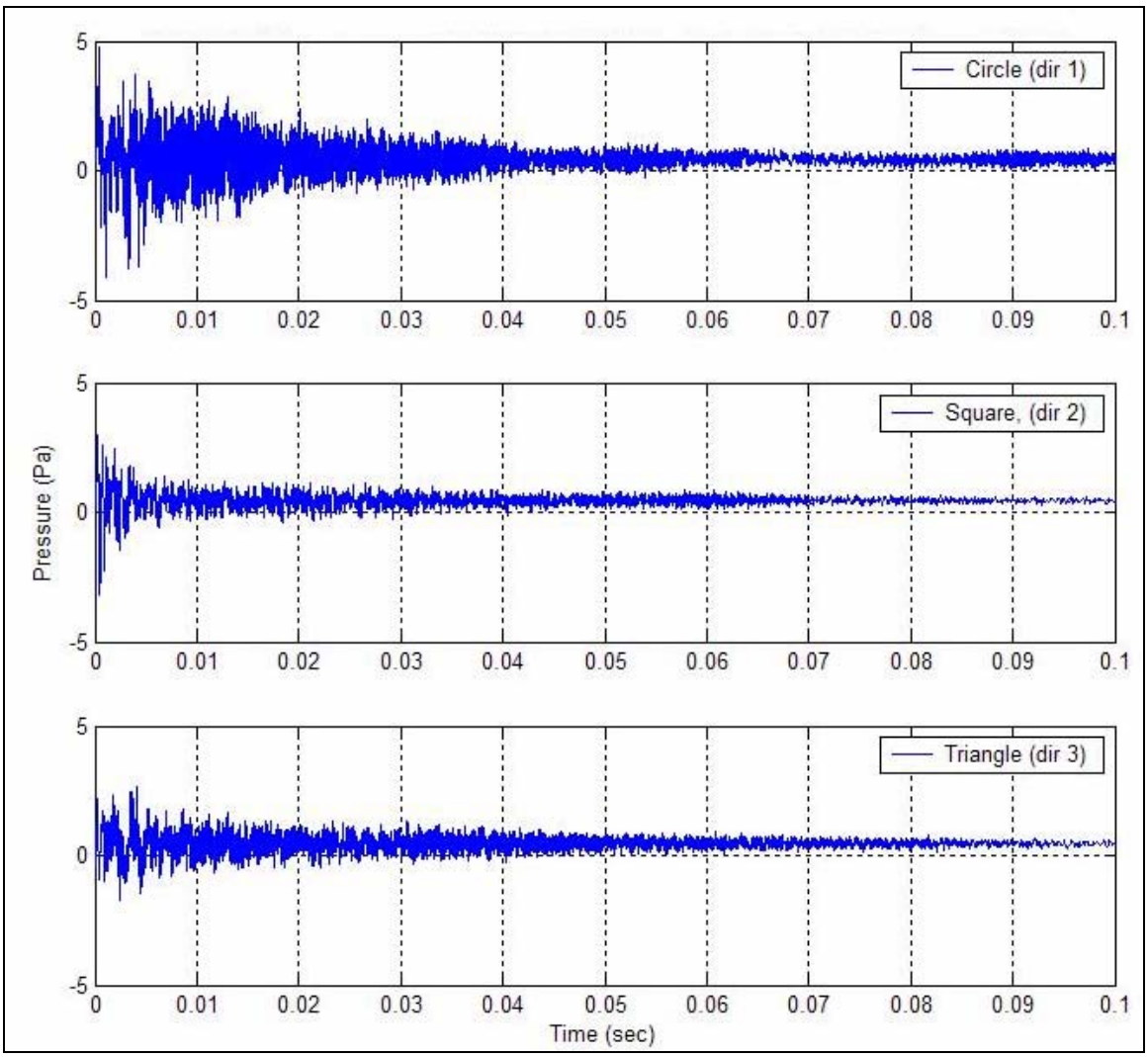

Figure 0-6 Sound Pressure with Respect to Time for a Single Sample in Three Different Orientations (08-534-03, Brooksville Limestone)

The time responses are considerably different for each orientation even though the test was performed on the same sample.

A closer examination of the time and frequency domain measurements in Figure 0-3 and Figure 0-4 compared with the measurements shown for 08-534-3 show that it is possible for samples from different sources to exhibit similar responses and also for the

same rock to exhibit different responses if impacted in different location. Similar observations are made when the measured time response is played back over an audio system. Samples from the same source often sound very different. Conversely, samples from several different sources were often indistinguishable from one another when listening to their response. While an auditory evaluation of the response is not as scientific as examining the differences in the measured response through time and frequency domain measurements, the observations provide a qualitative sense of the tests characteristics.

As an additional investigation, the acoustic impact-emission tests were repeated using a PCB Model 086C03 force gage mounted to a modally tuned hammer in place of the ball bearing. The set up was configured to maintain the microphone's relative positioning to the sample as in the previously discussed tests. A PCB model 303A02 accelerometer was also attached to the sample to measure the response of the rock when impacted by the hammer in addition to the acoustic response which was still measured by the microphone. Measuring the input force, the vibration response, and the acoustic response of the sample when impacted allowed three things to be done. The first is to compare the mechanical and acoustic responses and see how similar they are. Differences are possibly caused by acoustic excitation of the room, test setup, or acoustic noise in the room. Secondly, the input spectrum can be measured showing what frequency range the excitation is effective for. The third item that can be examined is the transfer function and coherence of the measured responses with respect to the input force. The tests were performed on the same sample tested in three different orientations as

previously shown. The sample was reconfigured to impact the same location as the previous tests.

The autospectra measured by the accelerometer and microphone are overlaid in Figure 0-7. In this case, the measured voltages of the response are shown so that both responses can be compared more easily.

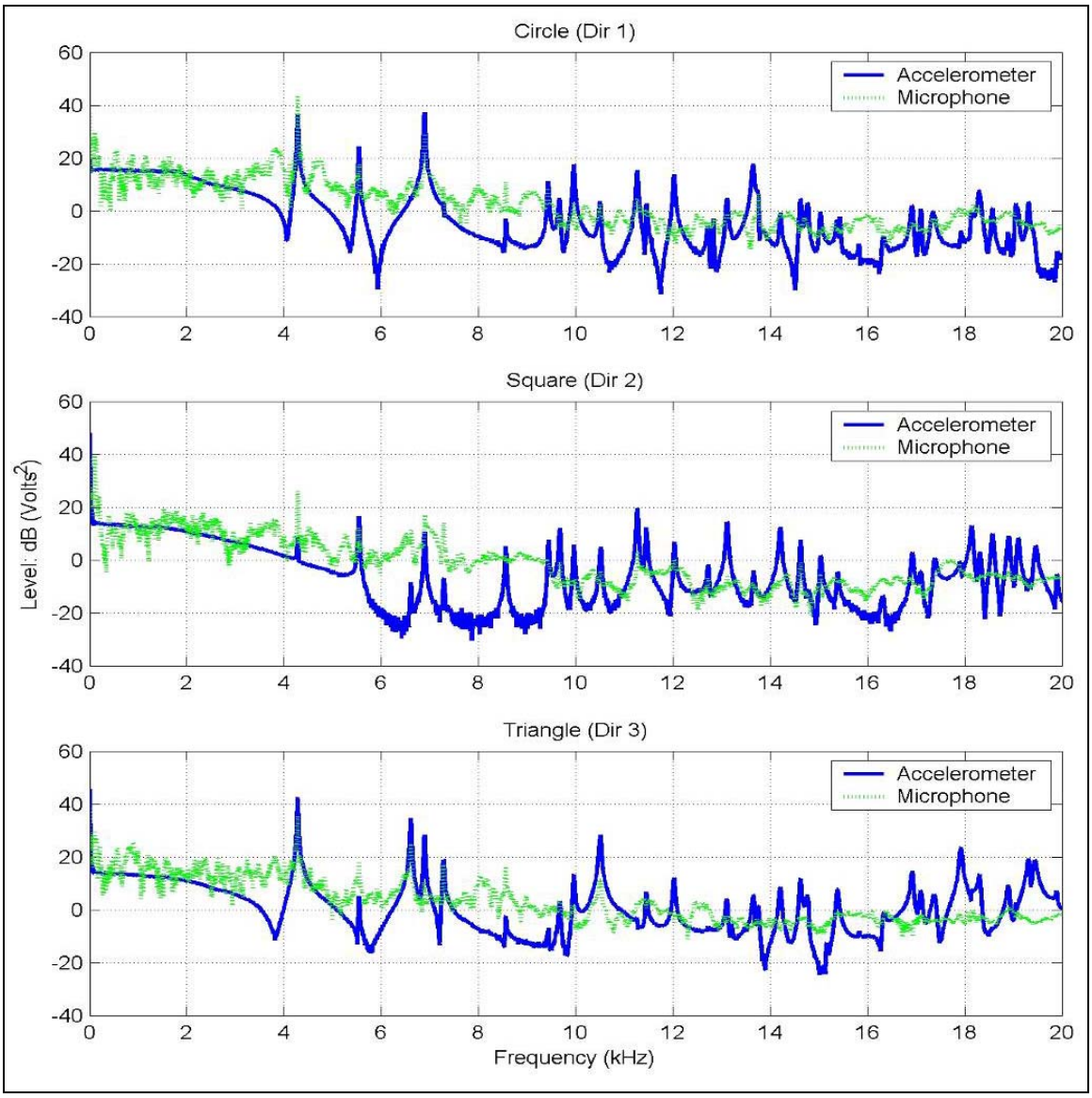

Figure 0-7 Mechanical & Acoustic Autospectra with Respect to Frequency for a Single Sample in Three Different Orientations (08-534-03, Brooksville Limestone)

Figure 0-7 shows the response measured by the accelerometer is considerably less noisy than the microphone's measurement. It is clear that the responses often line up showing that the acoustic response has some significant similarities to the mechanical response caused by the vibration of the sample, i.e. the mechanical response caused acoustic waves at the frequency of response. There are several instances where the acoustic response and mechanical response of the sample do not coincide. Instances when the responses do not agree could be caused by acoustic noise in the room also measured during the test. Sources of additional acoustic energy in the room may be attributed to roadway traffic, test equipment fans, or other structures responding to the acoustic waves generated during the test.

The measured voltage corresponding to the force input spectrum is also important to consider when examining the accelerometer measurements. The input spectrum shows the frequency range that is excited by the hammer when impacting the rock and is shown for the three orientations of sample 08-534-03 in Figure 0-8.

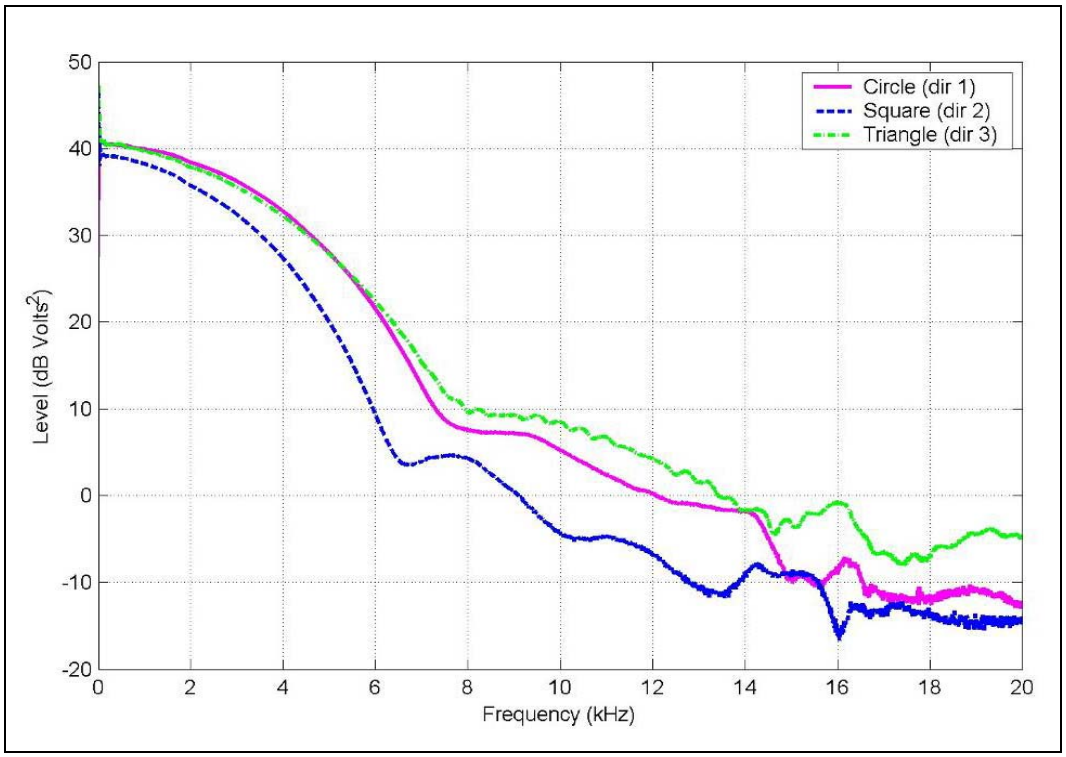

Figure 0-8 Input Spectrum with Respect to Frequency for Sample Excited in Three Different Orientations (08-534-03, Brooksville Limestone)

The input spectrum's power level is shown in decibels, a logarithmic scale. Three decibels is roughly a halving in amplitude and attenuation of more than 30 decibels is considered to have low energy. Figure 0-8 indicates that the input is not exciting the structure very well beyond 6 kHz as a significant amount of energy is attenuated in the lower portions of the frequency range measured. Because the hammer is less massive than the ball bearing used it is expected that even less energy was transmitted to the sample beyond 6 kHz for the other tests. Consequently, resonant frequencies of the sample beyond this frequency may not have been excited well, possibly explaining why many of the frequency responses measured had no areas of peak response indicated in Figure 0-4.

The additional acoustic energy in the room is also presumed to affect the measured acoustic response. To examine this, the transfer function between the hammer's input voltage and the voltage measured due to acoustic response are shown in Figure 0-9.

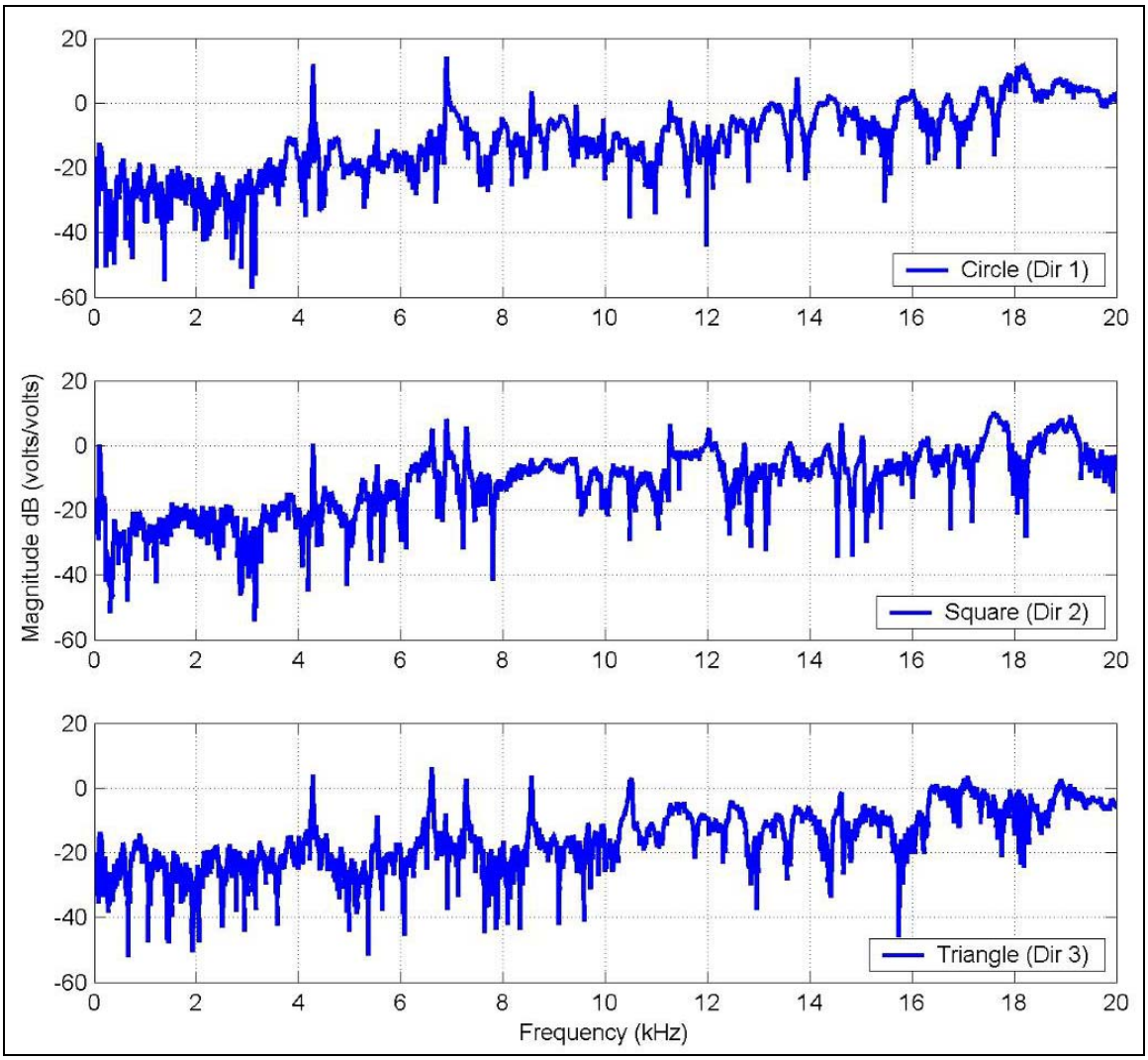

Figure 0-9 Transfer Function of Acoustic Response with Respect to Input for a Single Sample in Three Different Orientations (08-534-03, Brooksville Limestone)

The data shown in Figure 0-9 corresponds to the acoustic data shown in Figure 0-7. A useful tool that is often used to evaluate transfer function measurements is coherence. Coherence can be thought of a measure of how much of the measured output

is directly related to the measured input. Coherence is best when it has a value of one, indicating that measured response is caused solely by the input. The coherence of the transfer function measurements of the measured responses with respect to the input force are compared in Figure 0-10.

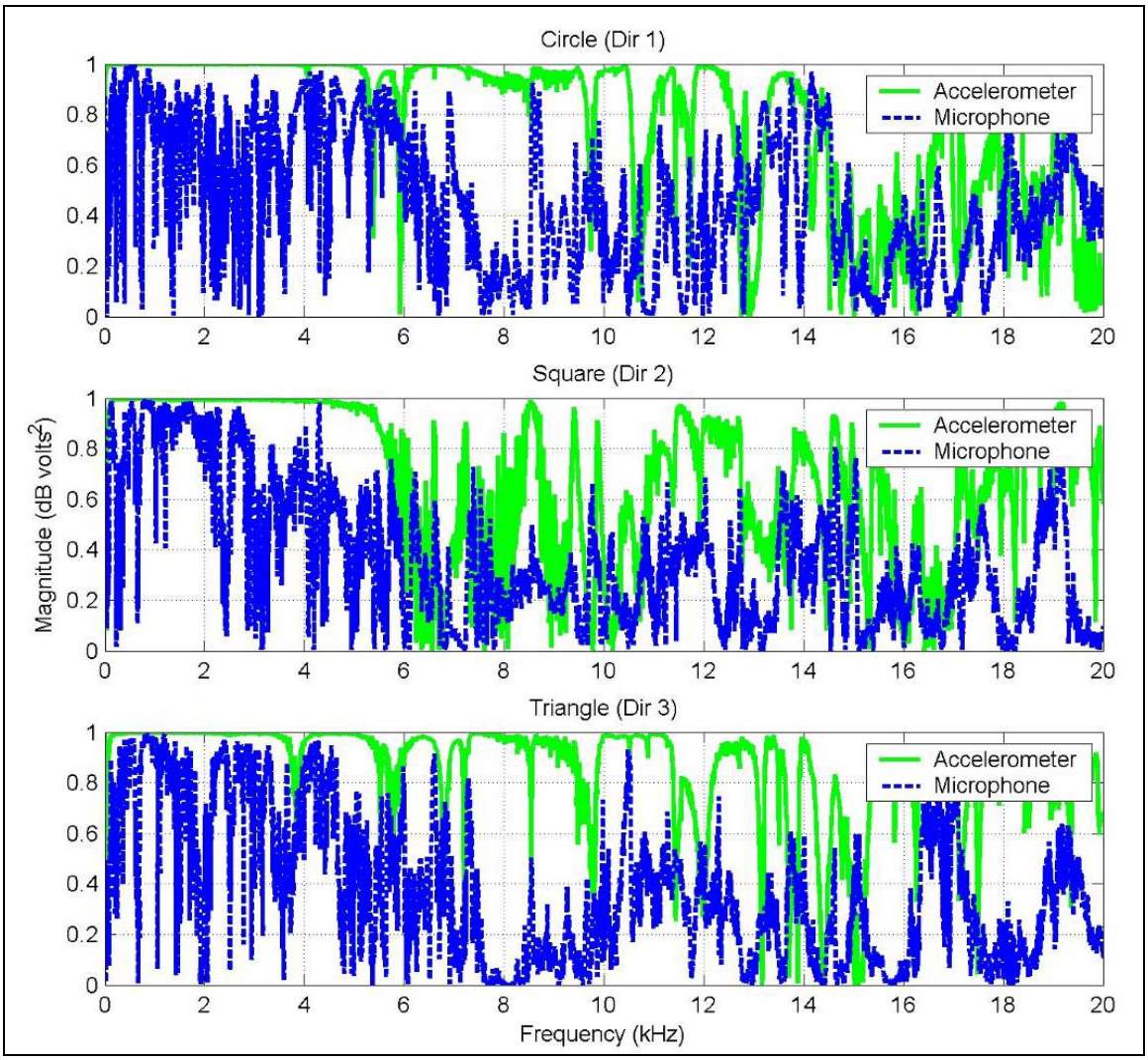

Figure 0-10 Comparison of Transfer Function Coherence Measurements for 08-534-03, Brooksville Limestone, in Three Different Orientations

From Figure 0-10 it is clear that the coherence is better for both the acoustic response and the mechanical response below 6 kHz, where the input to the system has the most energy. Additionally, it is clear that the coherence indicates that the direct

contacting measurement using the accelerometer is always better than the measured acoustic response. The coherence of the acoustic response indicates that the measured response is due to more than just the impact of the force hammer with the sample. To further support this, the measured acoustic response is compared with the ambient noise level measured in the room, shown in Figure 0-11.

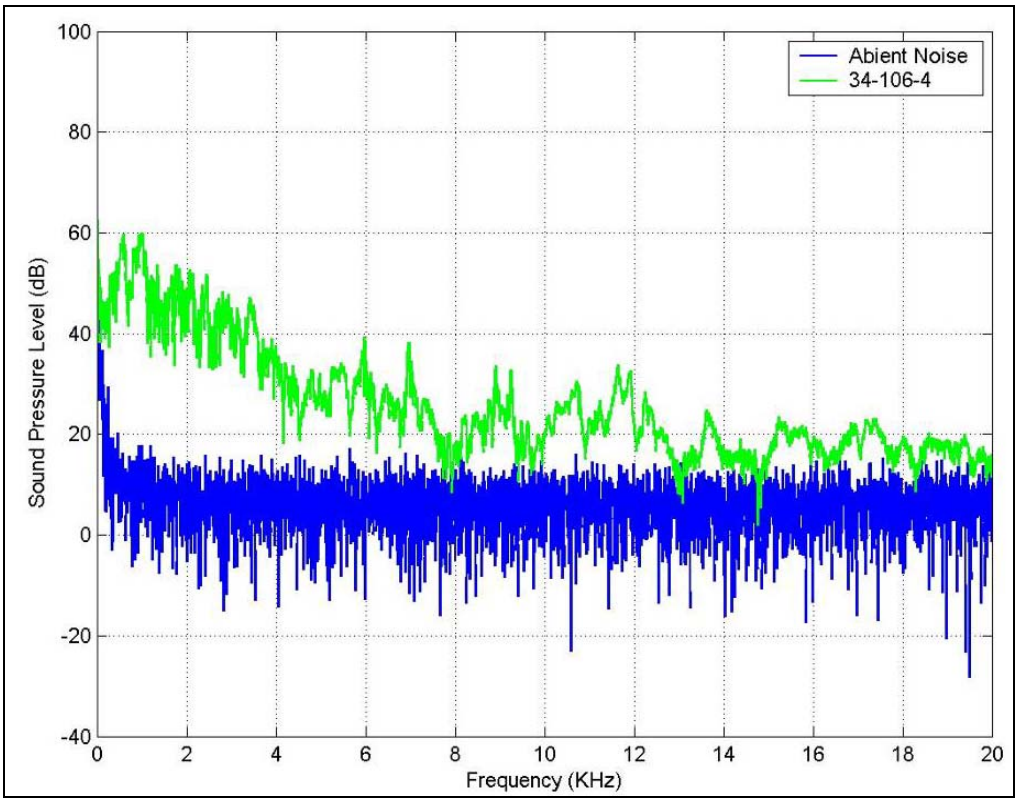

Figure 0-11 Autospectra of Ambient Noise & Measured Acoustic Response with Respect to Frequency

The measurements shown in Figure 0-11 indicate that beyond approximately 6 kHz the measured acoustic response begins to approach the same level as the ambient noise and at some frequencies drops below. The decrease in the signal-to-noise ratio at higher frequencies is consistent with the poor coherence in the transfer function of sound pressure with respect to input force shown in Figure 0-10.

1.32 OBSERVATIONS

There are several important observations evident from the results of the acoustic impact-emissions test. The most important observation is that in many cases the accelerometer and microphone responses provide the same information about the sample. Measured responses from the contacting measurements were less sensitive to the extraneous acoustic energy in the room indicating that contacting measurements can be made with higher confidence than non contacting acoustic measurements. Additionally, it has been shown that the sample geometry and impact location can have a significant affect on the sample's measured response.

There are some additional aspects of the test itself that warrant mention. The setup by nature is somewhat inconsistent. The use of rock samples that have not been cut into uniformly prepared specimens makes it difficult to determine the effects of the support conditions on the sample when suspended in the net. The irregular shape of the samples also made it difficult to insure that the position of the ball relative to the sample, when both were suspended statically, was consistent. The net used to support the samples during the test was not very durable. The repeated action of placing and removing the samples degraded the quality of the net over time resulting in holes larger than the original mesh. Preliminary tests on a granite tile indicated that certain parts of the test setup could have a substantial impact on the measured response if not set up in a consistent manner. The most significant aspect of the test setup is the positioning of the microphone relative to the impact and its orientation with respect to the impact direction. The test setup was designed to overcome any inconsistencies associated with microphone placement. The presence of larger holes in the netting did not appear to have a

significant effect on the data of these preliminary tests; however, the wear and tear of the net throughout the tests is mentioned for considerations in developing future tests.

1.33 CONCLUDING REMARKS

The results of the acoustic impact-emission test indicate that many variables exist which degrade its effectiveness as a quality test. Measurements on rough rock samples cannot be made with confidence because of the presence of background noise, poor excitation at higher frequencies, and the different and irregular geometries of the samples. These variables make it difficult to understand the true material differences of one sample compared to another from the data. Time and frequency data collected is useful for piecing together the impact's sound characteristics, but is unable to provide a quantitative measure of any property or groups of properties.

It is recommended that future tests be performed using uniformly prepared specimens with contacting measurement equipment to reduce as many of the variables encountered in this experimental procedure as possible. The lack of quantitative data makes the information acquired from this test method difficult to compare with the petrographic properties. The impact FRF tests discussed in the next chapter is identical in practice to the contacting measurements discussed in this chapter and will attempt to significantly improve the shortcomings of the acoustic impact-emission test.

IMPACT FREQUENCY RESPONSE FUNCTION TESTS

1.34 PREFACING REMARKS

This chapter discusses the impact frequency response function (FRF) test. Details of the test setup and data collected are presented along with the findings of supporting investigations performed to evaluate factors affecting the measured response. Impact FRF testing represents an improved method of test over the acoustic impact-emission test since many of the variables found to be significant in the previous discussion are significantly reduced or eliminated. Additional factors specific to impact FRF testing are identified for consideration in future work, namely the effect of boundary conditions and methods of adhering test equipment to a structure.

1.35 EXPERIMENTAL DESCRIPTION

Impact FRF testing is accomplished by exciting a structure using a force hammer (PCB Force Hammer model 086A80 with model 105M33 transducer) and measuring the vibration response with an accelerometer (PCB model 352A10) in a similar fashion to the contacting measurements collected for acoustic impact-emission testing described in Chapter 0.

Impact testing is performed on core specimens cut from rock samples originally the size of basketballs, the same size rocks that were tested using the Windsor Pin System® and acoustic impact-emission testing. Cores are nominally 2.54 cm (1 inch) in diameter by 9.525 cm (3.75 inches) long and weigh generally between 75 and 130 grams (2.5 and 4.5 ounces). Typical variations in geometry average between 0.5% and 2% from the mean in any dimension across all the cores prepared. Several core samples are shown in Figure 0-1.

Figure 0-1 Representative Core Samples

The cores were prepared by Geotesting Express of Boxborough, Massachusetts (www.geocomp.com). A wet coring bit manufactured by Blazer Diamond Products® (www.blazerdiamond.com) was used to core the rocks. The coring bit was installed on a heavy drill press fitted with a water swivel. While this system was part of a laboratory setup, portable wet and dry coring rigs are available from several commercial manufacturers. A rock saw was used to trim the ends of the cores at the specified length.

Using prepared specimens is important to this investigation for several reasons. First, the use of specimens which are all the same geometry increases confidence in the test's ability to measure material properties. Since the resonant frequencies of the sample are dependent largely on the ratio of mass and stiffness distributions within the sample, it should make sense that the variables affecting this distribution be minimized. By using cores, the geometry is simple, it's consistent, and there are analytical models available which may be used to identify Young's modulus, check the deformation patterns against

theory, or otherwise perform additional, standard engineering tests on the samples, though some of these tests may be destructive. Due to time and budgetary constraints, no destructive tests were performed on the cores for this study. The reason for minimizing the geometric differences in the samples is that the sample will most certainly have properties dependent upon the geometric distribution of both mass and stiffness. The effect of different mass and stiffness distributions in the sample is analogous to the bending strength of a typical 2x4 beam of standard length. The board is significantly stiffer about one axis than another.

Typically, one end-to-end and one drive point measurement are made along each of two longitudinal directions 90 degrees apart, shown as the Y and Z directions in Figure 0-2, for a total of 4 measurements per sample. Each frequency domain measurement is linearly averaged over five impacts. In some cases more measurements were made at incremental points along the length of the core, but a majority of the data consists of the four measurements described. The purpose of taking measurements in both directions is to identify if significant differences in response occur at different orientations, which may be an indicator of fabric or other directional dependencies of the material. A measurement set-up in the Y direction is depicted in Figure 0-2 and Figure 0-3.

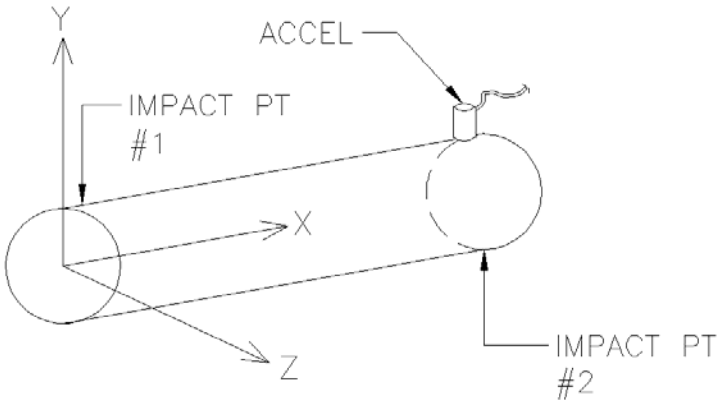

Figure 0-2 Typical Impact FRF Test Setup on Prepared Core Specimen

Figure 0-3 shows a photograph of the impact hammer, accelerometer, and a core sample in the same test configuration shown in Figure 0-2.

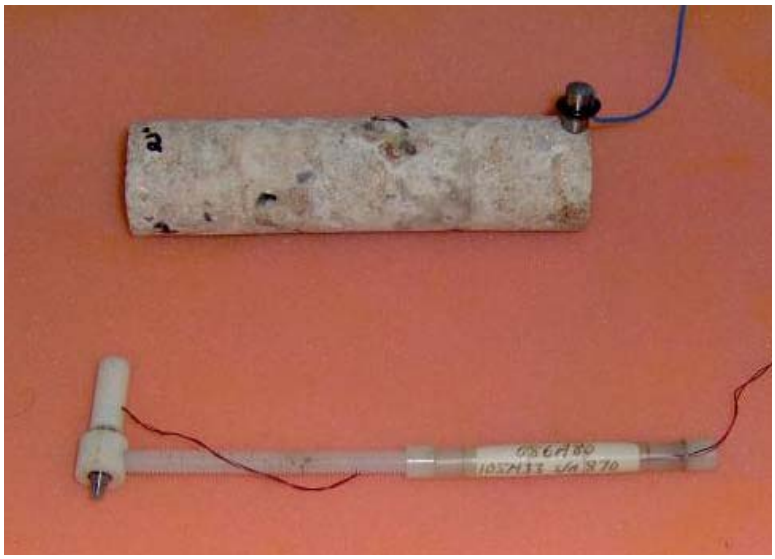

Figure 0-3 Core Specimen, Impact Hammer, and Accelerometer in Typical Test Configuration

Measurements are collected using a DSPT SigLab® Analyzer with a frequency bandwidth of 50 kHz. The high bandwidth is necessary to capture the first two major resonance groups which typically occur between 6 kHz and 30 kHz. Measurements with good coherence and input spectrums are typically obtained at frequencies as high as 25-30 kHz when affixing the accelerometer with wax and using a small lightweight force hammer with a metal tip as shown in Figure 0-3. Measurements are first evaluated based on the frequency range excited by the impact relative to the resonant frequencies, the noise on the response curve, and the coherence. The effect of the boundary conditions and adhesive used to affix the accelerometer are discussed as part of the analysis in the observations section of this chapter since they were found to have an effect on the

consistency of the measurements. The mass of the hammer and the hardness of the tip used have a significant effect on the bandwidth excited by the impact. Lightweight hammers and hard tips excite higher frequencies whereas more massive hammers with soft tips typically excite lower frequencies. The small size of the core specimens dictates the use of a very lightweight hammer not only to avoid damaging the specimen but to also excite at least the first major resonance group. The size of the hammer used for impact testing depends on the size and mass of the structure and the amount of energy required to excite the modes of interest.

Samples are evenly supported on one inch thick foam, or suspended using a rubber band as a sling. For most measurements the sample is supported on foam for consistency, assuring that the support conditions are the same for every test.

The transfer function of acceleration with respect to force is the frequency response function (FRF) of interest for this portion of the investigation. For each of the two orientations tested, the FRF is processed in ME'Scope® to estimate the modal characteristics of the sample, i.e. frequencies and percent of critical damping. The first resonant frequencies from impact measurements on core samples are compared with the features identified by petrographic analysis in Chapter 0. It will be shown in the following sections that damping estimates are strongly dependent on the boundary conditions of the test setup. Since the effects of the material properties on damping estimates cannot be easily separated from the effects of the boundary conditions, the damping estimates will not be used to identify relationships between impact FRF testing and the sample's petrography.

1.36 EXPERIMENTAL RESULTS

Core samples prepared from basketball sized rocks from the seven quarry locations listed in Table 0-2 were weighed and their dimensions measured. From these measurements the volume and bulk density were computed. The length and diameter of the samples were measured three times on each core. The average of the three measurements is shown in Table 0-1. The geometric volume is calculated based on the average length and diameter measurements. The mass was measured on a digital balance and the density is computed by simply dividing the measured mass by the computed volume for each sample. The core samples retain the identification scheme of the parent rocks from which they are cut. Multiple cores may have been cut from the same rock and in this case the sample identification number is followed by a letter beginning with the letter "A". Sample numbers followed by the letter "P", as in some of the 08-534 samples, indicates that the samples were cut to a more precise tolerance after being tested once in the same manner as the other samples. Initially, the core samples were prepared with a wet coring bit manufactured by Blazer Diamond Products®. The cores were then cut to the specified length using a rock saw. The samples are roughly within 1 percent of the mean length (+/- 0.097 cm at most) but the precise cutting using a lapping machine improved this to +/- 0.003 cm from the mean length.

Table 0-1 Bulk Properties of Prepared Core Samples

Source	Core Sample No	Mass (g)	Length (cm)	Diameter (cm)	Geometric Volume (cm^3)	Mass Density (g/cm^3)
08-534	1	115.4	9.553	2.494	46.679	2.472
08-534	2B	104.2	9.520	2.430	44.148	2.360
08-534	7	108.9	9.470	2.482	45.803	2.378
08-534	1P	113.4	9.355	2.494	45.710	2.481
08-534	2BP	102.7	9.352	2.430	43.371	2.368
08-534	7P	107.9	9.352	2.482	45.234	2.385
12-521	1C	100.0	9.517	2.457	45.126	2.216
12-521	6	95.5	9.483	2.477	45.708	2.089
12-521	8	101.6	9.487	2.457	44.982	2.259
12-521	9	113.3	9.497	2.484	46.028	2.462
GA-178	4A	122.1	9.538	2.482	46.162	2.645
GA-178	4B	120.7	9.495	2.473	45.613	2.646
GA-178	6	127.0	9.499	2.495	46.445	2.734
GA-178	9	129.1	9.527	2.488	46.298	2.788
18-607	5	106.5	9.514	2.487	46.205	2.305
18-607	8	111.8	9.476	2.494	46.302	2.413
18-607	9A	110.3	9.458	2.471	45.341	2.433
18-607	10C	107.2	9.460	2.491	46.098	2.325
34-106	2	98.8	9.538	2.474	45.848	2.155
34-106	6C	93.8	9.515	2.480	45.957	2.041
34-106	9	89.4	9.474	2.472	45.480	1.966
34-106	10	122.5	9.578	2.493	46.739	2.622
38-228	1A	114.8	9.467	2.432	43.966	2.611
38-228	3	116.2	9.478	2.472	45.501	2.554
38-228	4	104.4	9.487	2.460	45.106	2.315
87-339	5	90.4	9.486	2.471	45.475	1.987
87-339	6	110.8	9.601	2.486	46.596	2.378
87-339	8A	111.5	9.437	2.469	45.177	2.468
87-339	10A	93.8	9.597	2.439	44.847	2.092

Examination of Table 0-1 reveals that there is often considerable variability in the sample density for samples originating from the same source. The best agreement lies in two samples cut from the same rock, i.e., GA-178-4A and GA-178-4B. These cores were not only cut from the same rock, they are also cut from the same core as a long core was divided in two to make these samples. In most cases the samples were allowed to air dry

for at least 3 days before the measurements in Table 0-1 were made. The precision cut samples were measured only after air drying for 1 or 2 days after being received from the lab that prepared the samples before being measured and impact testing performed.

Typical tests are performed with the sample resting on flat 1" thick foam. The input autospectrum, transfer function of acceleration with respect to force (this is the frequency response function (FRF)), and the corresponding coherence are examined for each sample for measurements consisting of the average of five impacts. These are the same traces examined in the later parts of Chapter 0. The result of averaging five impacts is considered a single measurement. Figure 0-4 shows a set of typical response curves for three core specimens, each from a different aggregate source. Typically when displaying transfer functions, magnitude (in dB) and phase are shown together as in Figure 0-5. Additional phase plots are omitted here since the additional information contained in the phase plots is not necessary for this study.

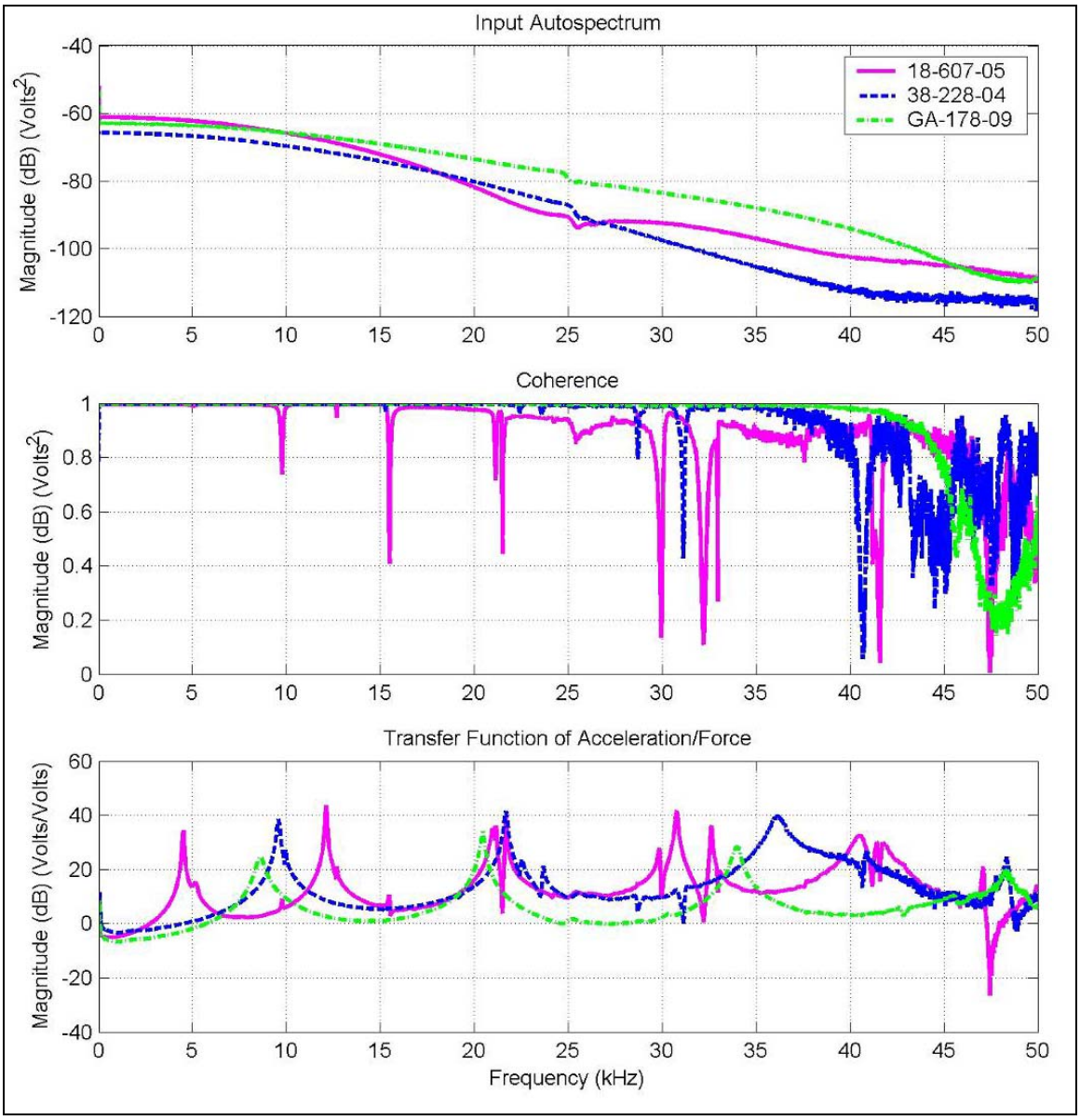

Figure 0-4 Typical Impact FRF Measurements for Three Samples

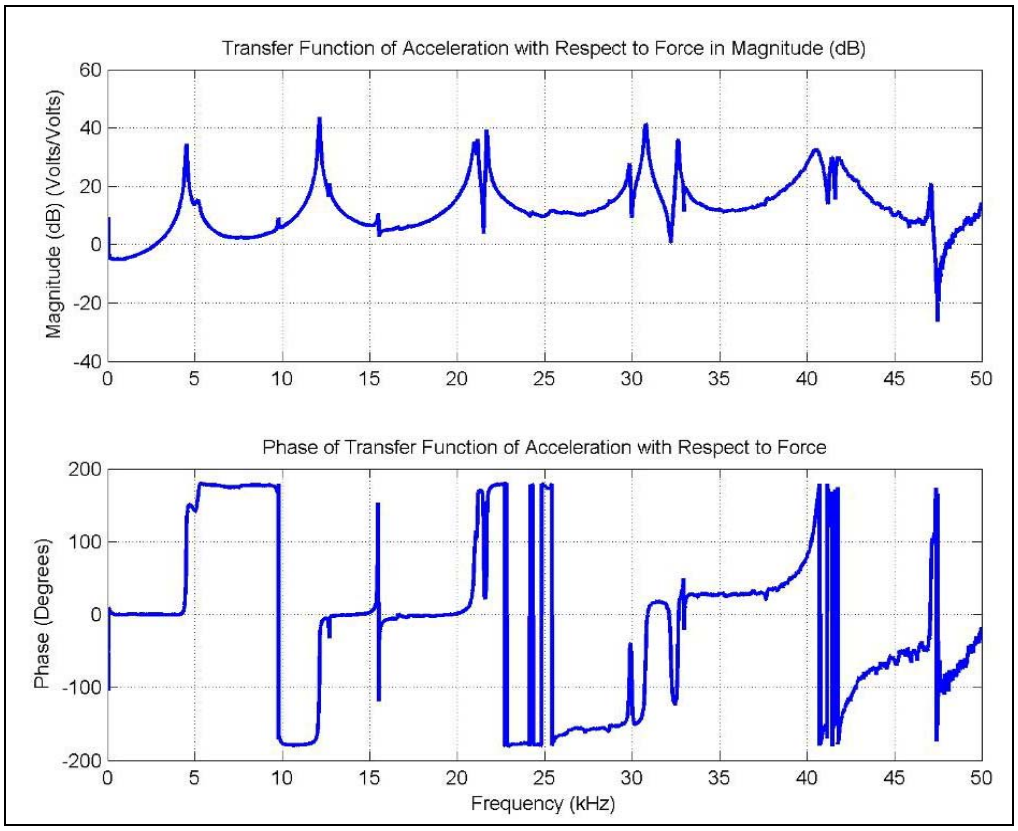

Figure 0-5 Magnitude and Phase of Transfer Function of Acceleration with Respect to Force (Both in Volts) for 18-607-5

The data shown in Figure 0-4 was collected by impacting one end of the core and measuring the acceleration at the other end, indicated by Impact Point #1 in Figure 0-2 (end-to-end). For each core, four measurements were made, one drive-point and one end-to-end measurement for each of the two orientations chosen. In general these measurements agree for a particular specimen when visually examining the traces. A comparison of a drive-point and an end-to-end measurement for one direction are shown in Figure 0-6 along with a comparison of end-to-end measurements for the two orientations tested for a core sample from 12-521, Bonita Springs, Florida.

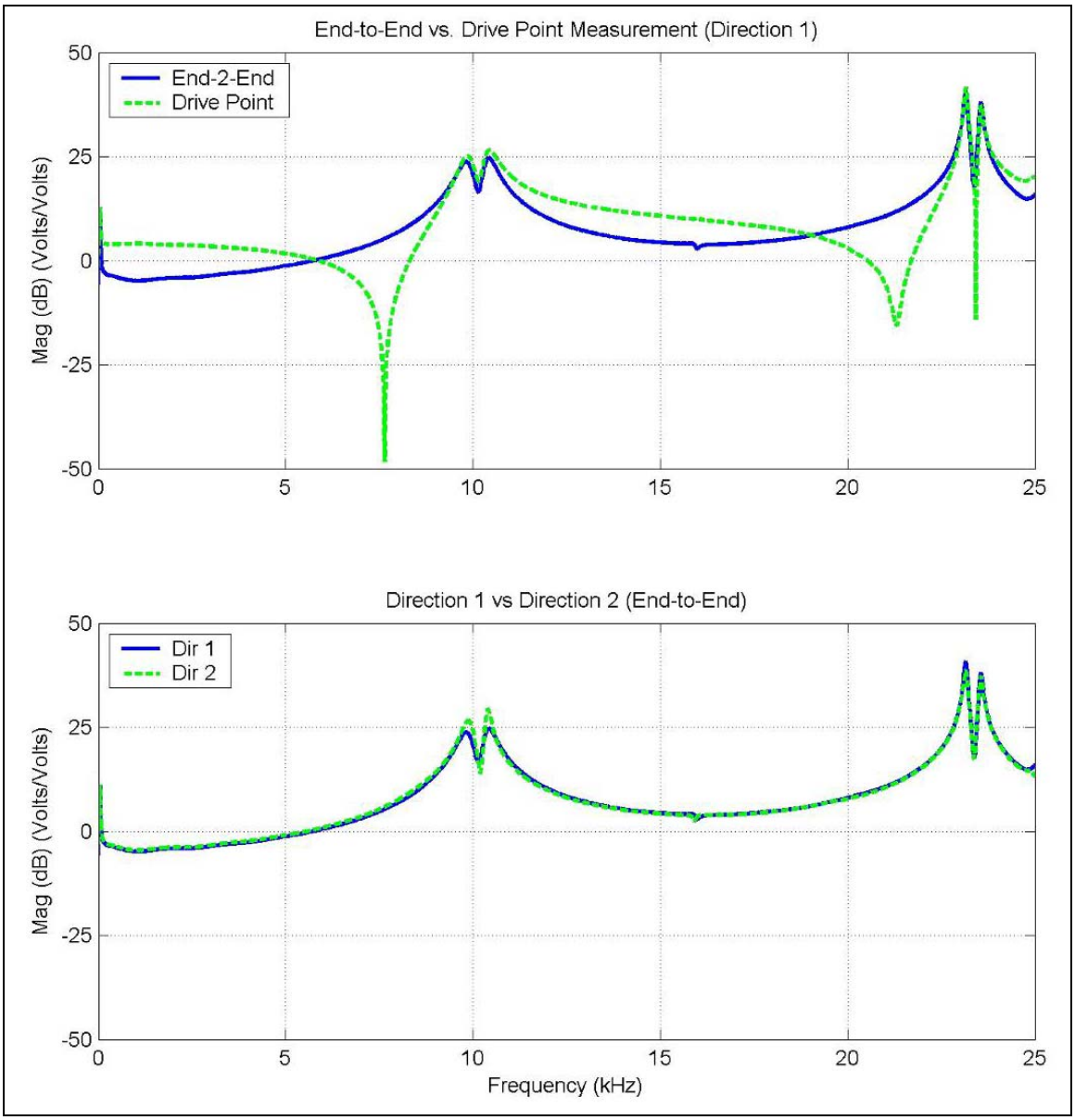

Figure 0-6 Comparison of FRF Measurements on a Single Core Sample (12-521-09)

As shown in Figure 0-6 the frequencies where resonant peaks occur are generally very consistent for the same specimen. Differences in the amplitudes of the peaks are common especially when comparing measurements from direction-1 and direction-2. The amplitude and sharpness of the resonant peaks are generally used to infer the amount

of damping for a particular resonance. A more detailed discussion of the damping estimates follows in the next section.

In Figure 0-6 the dip in the drive-point measurement represents an anti-resonance or a frequency where there is little or no response of the structure regardless of the input force. While anti-resonances are useful for understanding a structure's dynamic characteristics for many applications, only the resonant peaks are of interest to this study.

While responses for a single core were generally consistent, as shown in Figure 0-6, measurements on samples from the same source did not often compare as well with each other. Figure 0-7 compares end-to-end FRFs of all the samples from two sources. One source shows an example of samples with consistent responses for the first resonance group while the other source does not. It should also be noted that some of the samples respond very similarly though they are from different sources.

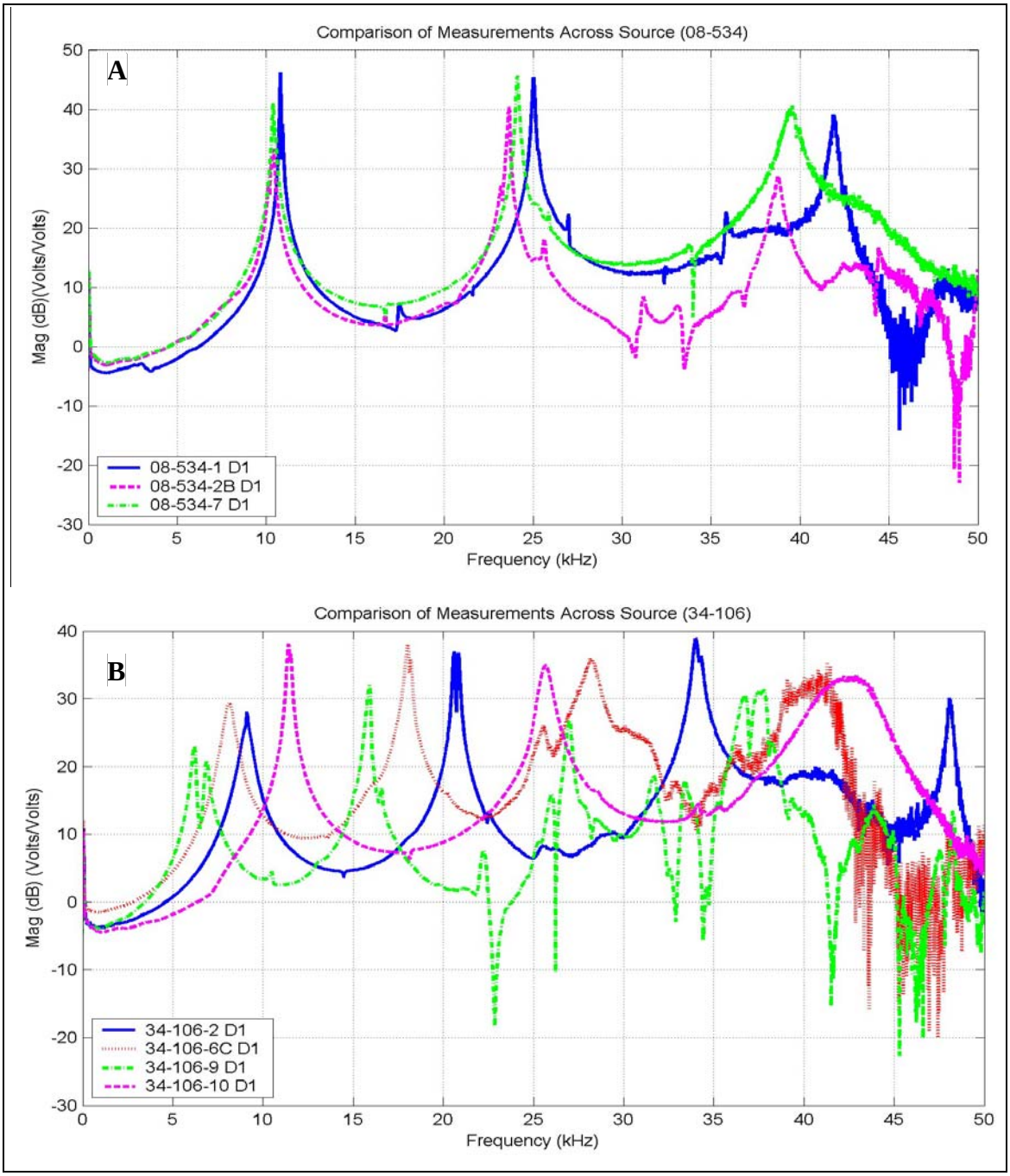

Figure 0-7 Comparison of FRFs For Core Specimens From Different Sources: A) 08-534; B) 34-106

The measured FRFs are exported to ME'Scope® and processed to estimate the frequencies and percent of critical damping for each resonant peak visible in the response up to approximately 30 kHz. The software allows this to be done for multiple curves at

once and allows the user to define the bandwidths in which to fit the function. Using multiple response curves to extract the modal parameters has the effect of finding a best-fit line to the data. The estimated frequencies for all of the 3.75" core samples are presented in Table 0-2 and will be compared with the petrographic properties in Chapter 0.

Table 0-2 Impact FRF Measured Responses for 3.75" Core Samples

Source	Core Sample No	Frequencies Estimated using ME'Scope		
		Mode 1 (kHz)	Mode 2 (kHz)	Mode 3 (kHz)
08-534	1	10.9	11.0	25.1
08-534	2B	10.3	10.3	23.4
08-534	7	10.3	10.4	24.1
08-534	1P	11.2	11.3	25.7
08-534	2BP	10.4	10.6	23.9
08-534	7P	10.6	24.4	24.6
12-521	1C	9.2	9.4	20.6
12-521	6	8.0	8.3	18.5
12-521	8	9.0	20.4	21.3
12-521	9	9.7	10.4	23.2
GA-178	4A	10.7	24.2	24.7
GA-178	4B	10.9	24.5	25.1
GA-178	6	9.5	22.5	0.0
GA-178	9	8.6	20.4	0.0
18-607	5	8.3	9.1	19.5
18-607	8	10.6	10.8	24.1
18-607	*9A*	9.1	9.7	22.0
18-607	10C	9.4	9.8	20.8
34-106	2	9.1	20.6	20.8
34-106	6C	8.1	18.0	18.0
34-106	9	6.2	6.8	15.1
34-106	10	11.5	25.8	0.0
38-228	1A	10.7	25.3	0.0
38-228	3	10.7	11.0	25.3
38-228	4	9.6	9.9	21.7
87-339	5	6.5	7.1	15.4
87-339	6	9.4	9.7	21.7
87-339	8A	11.2	24.2	24.8
87-339	10A	7.4	8.1	18.4

Response curves are fit using data from only one direction at a time, i.e. Y or Z directions, and only using one end-to-end and one drive-point measurement to extract the frequencies and damping of the system unless other measurements for that direction are available. In cases where more measurements were taken, all the measurements are used, and thus the best fit process is based on a larger data set. Each resonant peak was fit using a narrow bandwidth. The data in Table 0-2 represents the reduced data, i.e. the average measured frequencies for each sample.

Damping estimates are formulated by selectively curve fitting the response curves from both test directions for a particular resonant frequency and for a particular sample. The damping estimates are scrutinized by the investigator during the process to assure that the reported damping is representative of the corresponding resonant frequency. Details of the modal parameters estimated for each measurement and the formulation of the reported data are kept on file in the lab. The method of estimating damping is not very robust, especially since damping estimates vary significantly from one measurement to the next for the same sample and resonant peak. The observed variability in the damping estimates significantly reduces the confidence of the estimated damping values for the samples. In the next section several tests performed to determine the cause of the inconsistent damping estimates are discussed in detail. It will also be shown that the resonant frequencies can be estimated from the collected data with far better consistency and confidence than damping.

The frequencies in Table 0-2 represent the average for each mode only if the percent difference of the frequencies is less than five percent. If the percent difference exceeds five percent, each measurement is examined individually and the estimated

frequencies are grouped so that the reported frequency in Table 0-2 is an average of the response for a particular core at a particular frequency. Such estimates were not necessary very often.

Examination of Table 0-2 shows that for many of the samples, modes one and two have very closely estimated frequencies if not identical. This is due to the presence of closely spaced peaks. ME'Scope® will find two closely spaced resonances even if the trace does not indicate two peaks when viewing across a large bandwidth of frequencies. Zooming on a particular resonant peak often reveals multiple peaks. An example of closely spaced peaks is shown in Figure 0-8.

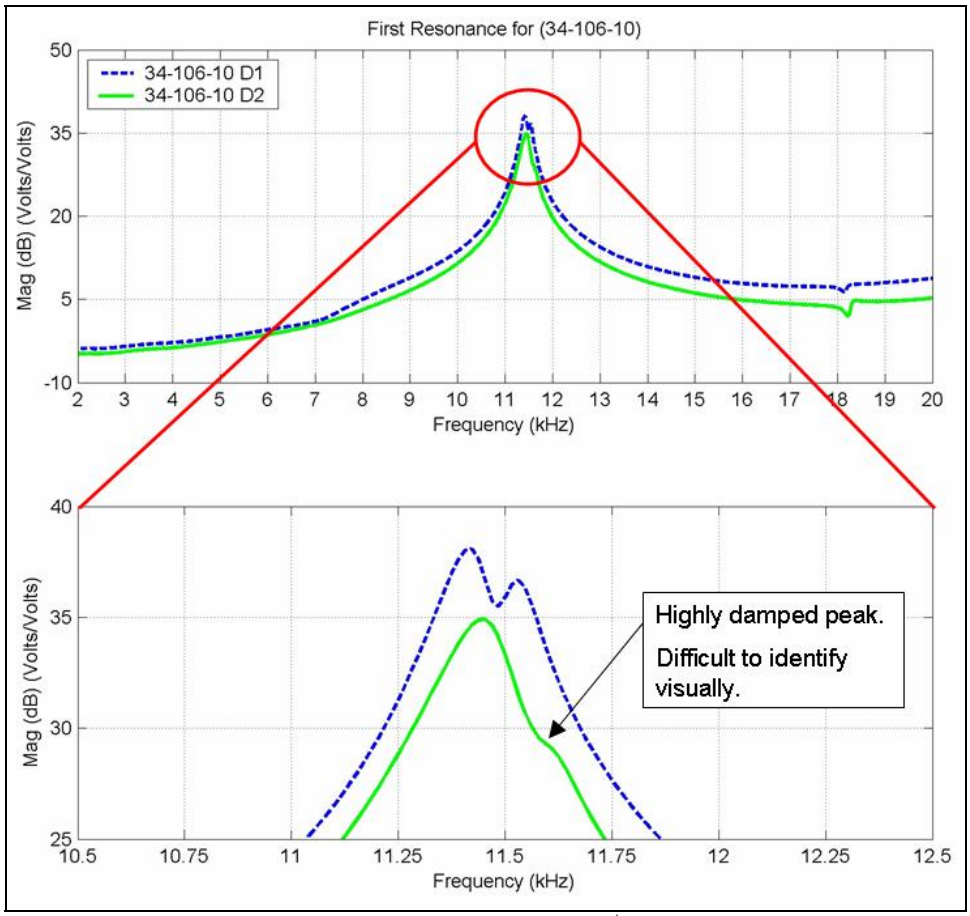

Figure 0-8 Closely Spaced Peaks Evident in 1st Resonance for 34-106-10

As a result of closely spaced peaks, modes one and two are often very close in frequency. The frequencies of the peaks are generally very consistent from one direction to the other (relative to the bandwidth and frequency of the measurement). In some cases, one peak may be more heavily damped, as shown in Figure 0-8, making it hard for the investigator to identify visually. If the quality of the measurement is good, the software will still be able to identify it as a mode during the curve fitting process. In instances where there may have been two peaks, each measurement is examined individually and the frequencies selected as previously described. In other cases, there is only one resonant peak at a resonant frequency regardless of the measurement and so the second mode is quite higher in frequency, explaining why some of the frequencies in Table 0-2 overlap from one mode to the next.

Clearly the presence of closely spaced peaks makes it cumbersome to compare resonant frequencies with petrographic properties. One cannot simply take all the estimated frequencies for the modes beyond mode 1 and compare them. All of the modes at or about 10 kHz must be compared separately from the modes that occur at or about 25 kHz. The need to hand select frequencies for modes beyond mode 1 makes it difficult to perform analyses as efficiently as examining mode 1 only. For ease of use and consistency only the first resonant frequencies are compared with the petrographic properties in Chapter 9. Mode 1 is also the easiest to measure and most often falls within the published frequency range of the test equipment. The energy transmitted to the structure, and the coherence of the response for mode 1 is generally much better than for the other measured modes and so a higher level of confidence is placed in these

parameters. Additional FRF's and detailed information pertaining to the estimation of the modal parameters is contained in Appendix E for reference.

1.37 OBSERVATIONS

There are many aspects of the impact FRF test that were examined during this study. The experimental results discussed in the previous section are the results used in Chapter 9 to determine the causal relationships between the sample's petrography and the modal parameters. Additional observations made from analysis of test data and secondary investigations using the impact FRF technique are discussed in this section. Most of these additional studies were performed to investigate the source of variations in frequency occurring across samples from a particular source, and reasons why damping estimates varied so widely among all the samples.

1.37.1 MODE SHAPES OF CORE SPECIMENS

Before discussing the attempts to understand the variability in the measured parameters it is most appropriate to mention some global observations pertaining to the samples studied. As mentioned previously, some cores were impacted at several incremental points along the length of the structure. When all of the measurements were imported to ME'Scope® the mode shapes were extracted from the data in addition to frequency and damping estimates. The mode shapes are the deformation patterns of the structure when it responds at a resonant frequency. Samples from 08-534 were impacted at nine equally spaced points along the core's length for each of the two orthogonal directions tested. The mode shapes of the core specimens tested in this manner are

typical bending modes for a free-free beam structure similar to those shown in Figure 0-9, which represent the analytical shapes for a free-free beam structure (Harris *et al.*, 2002).

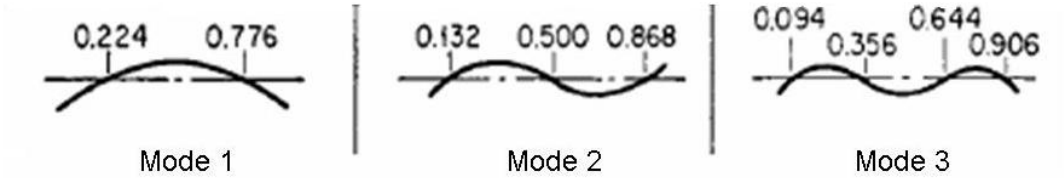

Figure 0-9 Typical Bending Modes, Free-Free Beam (Harris *et al.*, 2002)

The observed shapes were consistent among all the cores impacted at as many points. A select group of cores were tested in a similar manner some having lengths at 7.6 cm (3 inches), and others having lengths of 13 cm (5.125 inches), and their mode shapes were also consistent with the normal bending modes shown in Figure 0-9.

When the mode shapes of two closely spaced peaks were examined, like those shown in Figure 0-8, it was observed that the shapes were nearly identical for each of the peaks in the narrow band of interest. The mode shape of the structure at one frequency were generally smoother than the shape at the other frequency indicating that one of the measured frequencies corresponds to a mode shape that is slightly off set from the test axis. This behavior is representative of the 2x4 analogy used previously except instead of considering bending about either of its principle axes, the test is capturing portions of the response from each axis. The measurement is a combination of the response in multiple planes. In an ideal situation, a homogeneous material with a perfectly cylindrical shape would exhibit only one peak, regardless of the orientation of the y and z axes. The test setup, in-homogeneities, and directional stiffness planes in the structure bias the response

in certain directions. As a result of this bias, the deformation pattern of the structure will tend to lay along its principle axes at slightly different frequencies. The effect of this is double peaks in the frequency response function.

1.37.2 EFFECTS OF MASS & LENGTH ON FREQUENCY

Examination of the FRF's and the listed frequencies for mode 1 show that there is little consistency in the measured frequencies in terms of samples from the same source responding the same, and each source responding differently from the others. In other words, there doesn't appear to be any superficial pattern which emerges from the data collected, similar to the observations of the acoustic impact-emission test described in Chapter 0. Recall however, that each sample has slight variations of the various petrographic properties as reported in Chapter 0 so some variation in the modal parameters is expected. Even though the samples were all cut into cylindrical specimens having the same geometry, there is still some variability in the geometry that must be accounted for. The difference in length about the mean for the cores is roughly 1% and assuming that all other factors remain constant, the variability on the core's length translates to approximately a 2% variation in frequency. Additionally, there is as much variability in the mass of the samples as there is in the frequencies. The effect of small changes in mass and length on the measured frequencies can be approximated analytically using (Harris, *et al.*, 2002):

$$f_n = \frac{A}{2\pi}\sqrt{\frac{EI}{\mu L^4}} \qquad (8\text{-}1)$$

Where:

f_n = Natural Frequency (Hz)
A = Constant
E = Young's Modulus
I = Area Moment of Inertia
L = Length of Beam
μ = Mass per unit length of beam

To better visualize these observations, mass is plotted with respect to measured first resonant frequency for the core samples in Figure 0-10.

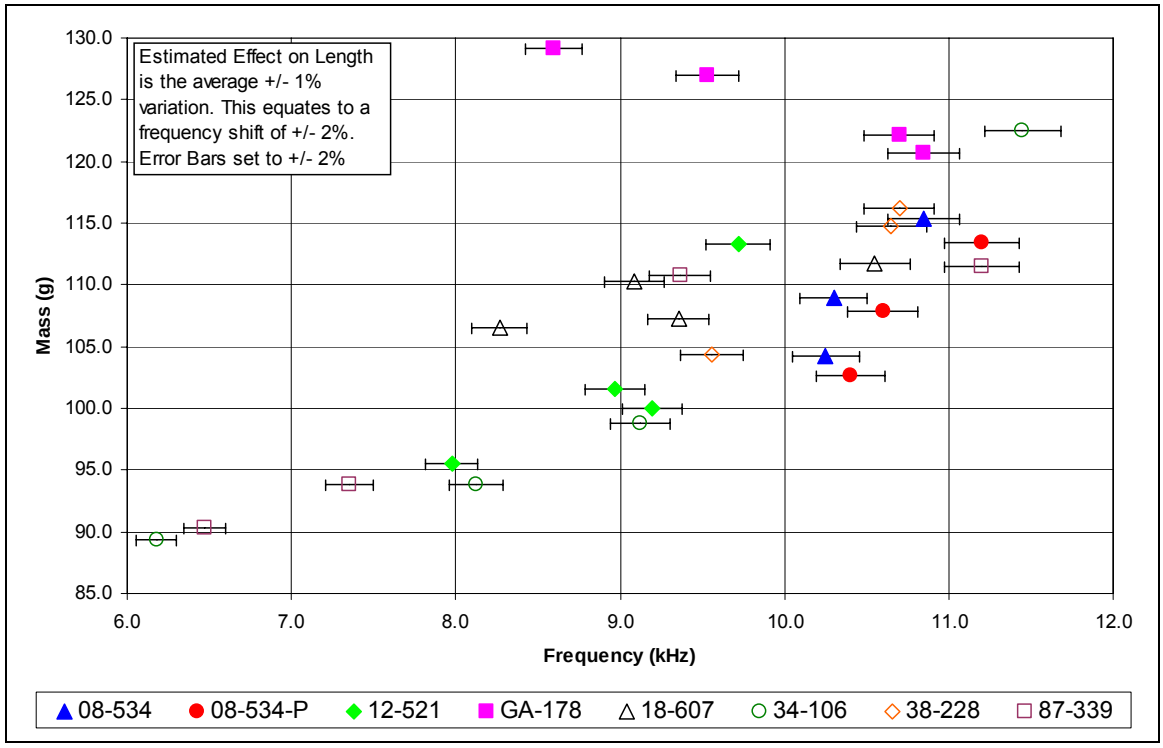

Figure 0-10 Mass with Respect to First Resonant Frequency for Core Samples

The x-error bars in Figure 0-10 are set at +/- 2% to account for the effect of the variation in length of the samples. In some cases, the variation in length indicated by the

x-error bars does account for the differences in frequency for some of the samples originating from the same source; however, this is not the case for most of the samples shown in Figure 0-10. Examining the effective change in length of the precision cut cores from the source 08-534 provides an excellent opportunity look at the length's effect on the first resonant frequency in more detail. The lengths and measured frequencies of the 08-534 cores both before and after precision cutting are shown in Table 0-3 along with the percent change in length and its estimated effect on the first resonant frequency.

Table 0-3 Core Data with Effect on First Resonant Frequency for 08-534, Brooksville Limestone; Before & After Precision Cutting (P)

Site	Sample No	Length (cm)	Mode 1 (kHz)	% Change in length	Estimated % Change in Frequency
08-534	1	9.553	10.850	-	-
08-534	2B	9.520	10.250	-	-
08-534	7	9.470	10.300	-	-
08-534	1P	9.355	11.200	-2.074%	3.194%
08-534	2BP	9.352	10.400	-1.761%	2.701%
08-534	7P	9.352	10.600	-1.243%	1.893%

The measured frequencies from Table 0-3 are plotted with respect to the measured length and the estimated effect on frequency in Figure 0-11 showing that while for 08-534-1 and 08-534-1P (precision cut core) the estimated effect on frequency due to the change in length was accurate, the estimates for the other two samples is not.

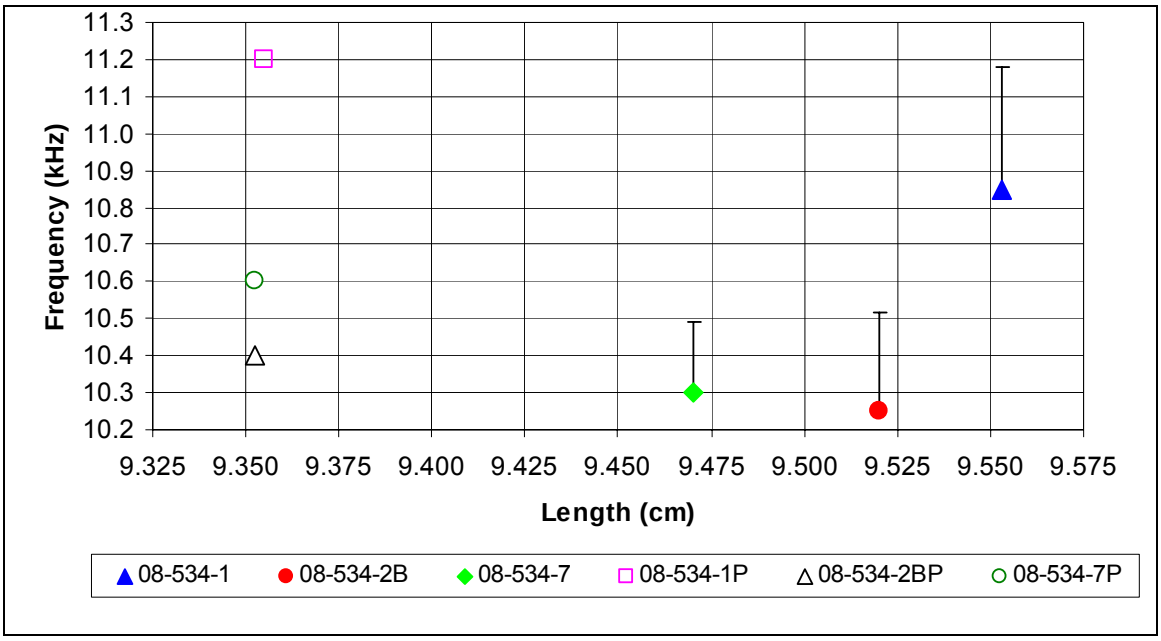

Figure 0-11 Measured & Estimated Frequencies with Respect to Length for Core Samples From 08-534, Brooksville, FL

The y-error bars shown in Figure 0-11 represent the estimated frequency of the original core due to the same change in length it experienced when precision cut. While Figure 0-11 shows that the precision cut cores have significantly reduced the variability in the length of the samples it is important to note that the measured frequencies have spread out considerably from their original measurements, likely because of differences in the petrographic properties of each sample. The relationship between the measured frequencies and these properties is examined in Chapter 0.

Assuming all else equal (including the length of each core), samples with similar masses should also respond at roughly the same frequency, but the data in Figure 0-10 shows only a few instances when samples of similar mass respond at the same frequency. Additionally Figure 0-10 also shows that for the limestone samples as the mass increases, the resonant frequency also increases indicating that the additional mass of these samples is contributing more to the stiffness of the structure than to its mass. The granite samples,

those from GA-178, show the expected trend of decreasing frequency with an increase in mass. The differences in the measured frequencies with respect to mass for the different lithologies indicates that porosity, one of the biggest differences between the two aside from mineral content, has a significant effect on the response. Additionally, the trend could also indicate that the sample size is such that the response is easily affected by small changes in certain properties since small amounts of material seem to greatly contribute to the structure's stiffness in the limestone samples. As the size of the samples increases, it's possible that these effects would be less pronounced and the frequencies would decrease with an increase in mass. Such an investigation may support this conjecture in future work.

1.37.3 FACTORS AFFECTING DAMPING ESTIMATES

A great deal of effort has been placed in discussing the measured frequencies of the core specimens and that frequency alone is to be used as an indicator of possible relationships between the test data and petrology. An examination of damping estimates during the curve fitting process showed that damping estimates are widely varied and inconsistent for the samples tested. This is especially true if the estimated damping is compared for the core samples from 08-534 before and after precision cutting. The significant variability in the damping estimates indicates that there are variables associated with the test setup that have a strong effect on the damping estimates, and that this effect is perhaps strong enough to distort the effect that the material properties have on these estimates.

In addition to noticeable differences in the estimated damping obtained during the curve fitting process, a sense of the different damping levels can be inferred from the FRF. Lightly damped resonant peaks are generally sharp while heavily damped peaks are often lower amplitude and less sharp or rounded. Figure 0-12 shows a comparison of a lightly damped response with a heavily damped response for two core samples.

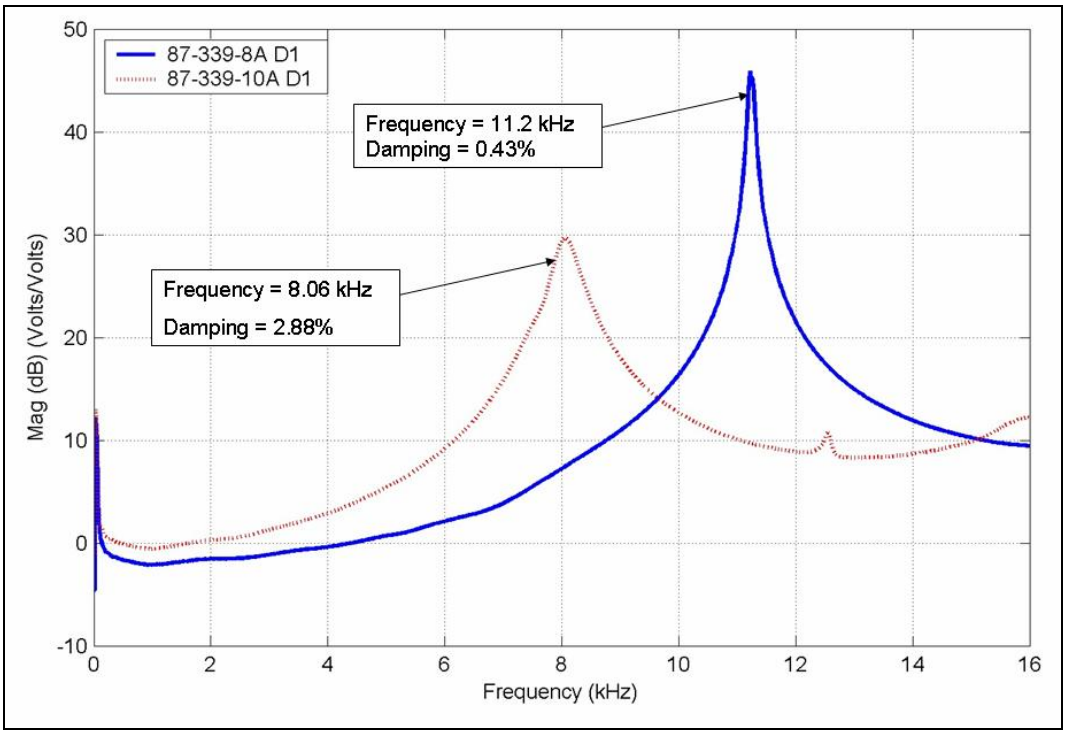

Figure 0-12 Comparison of Damping for Different Core Samples Response Curves

Examining the first resonance in the FRFs of several of the samples taken at different times indicates that tests performed on different days exhibited noticeable differences in the response. Typical differences observed in the responses are shown in Figure 0-13.

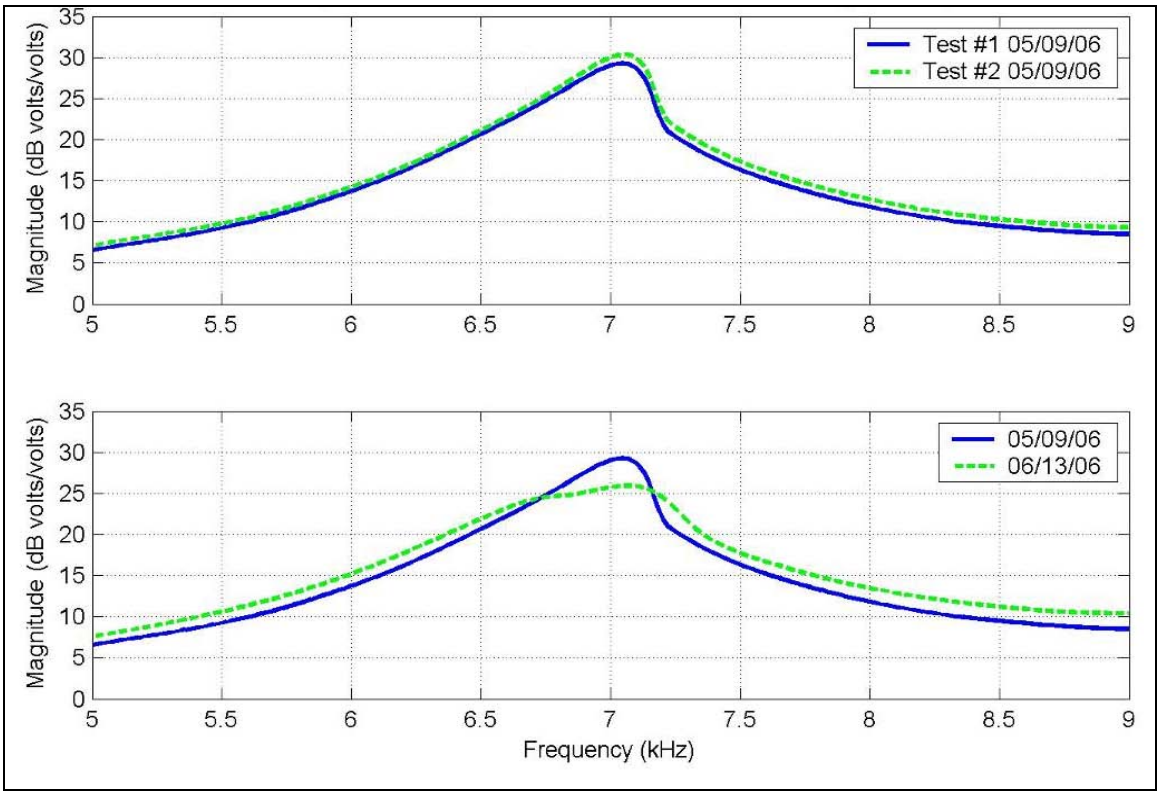

Figure 0-13 Frequency Response Functions Obtained at Different Times for 87-339-5

Figure 0-13 shows that measurements taken on the same day under the same test conditions are very consistent while measurements taken on different days can exhibit slightly different FRFs. This variability was common for many of the samples. It is extremely difficult to determine what aspect of the test setup would have changed over time to affect the measurements only observing the estimated parameters and the noticeable differences in the FRFs as shown in Figure 0-13.

In an attempt to determine the source of the inconsistencies associated with the damping estimates two important investigations were performed. The first examined the effects of the storage environment, and the second examined different methods of affixing the accelerometer to the structure and the effect of the boundary conditions on the response.

The effects of the storage conditions on the measured frequencies and damping is investigated because it was also observed that significant differences in temperature and humidity often could have existed in the lab on the different dates the tests were performed. To examine the effects of temperature and humidity, a series of tests were conducted on cores that were stored in environmentally controlled rooms for a few days. Initially the cores were stored at 70° F with a relative humidity of 50%. They were then put in another environment maintained at 104° F and 90% relative humidity. At periodic intervals the cores were impact tested and then returned to the room for storage. The data was curve fit in ME'Scope® to obtain frequency and damping estimates. A plot showing the recorded damping estimates on each day is shown in Figure 0-14.

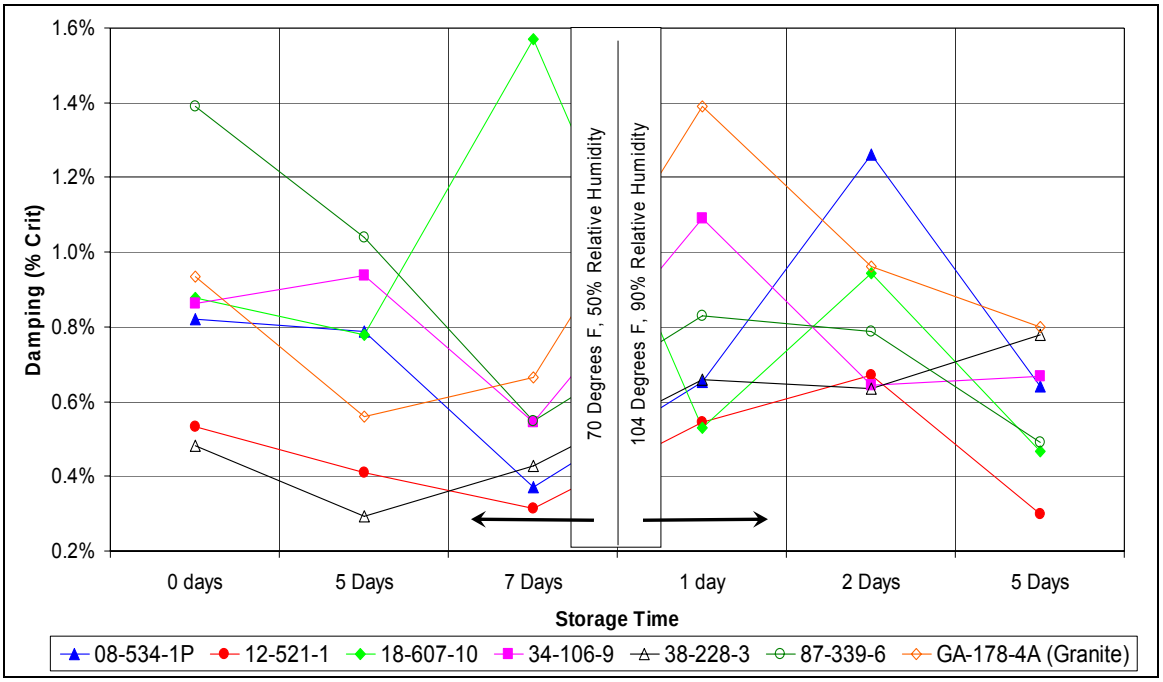

Figure 0-14 Damping Estimates with Respect to Storage Time in Environmentally Controlled Storage Conditions

Figure 0-14 shows considerable variation in the damping estimates even under the carefully controlled storage environments. For some of the samples examined, the

damping does appear to begin converging to a lower percent of critical damping after five to seven days, indicating that it may take a considerable amount of time for the samples to fully adjust to new environmental conditions. While this observation can be made from the data at hand, it is not a completely convincing source of the variations in the damping estimates. The measured frequencies of the samples stored under the environmentally controlled conditions are far more consistent as shown in Figure 0-15.

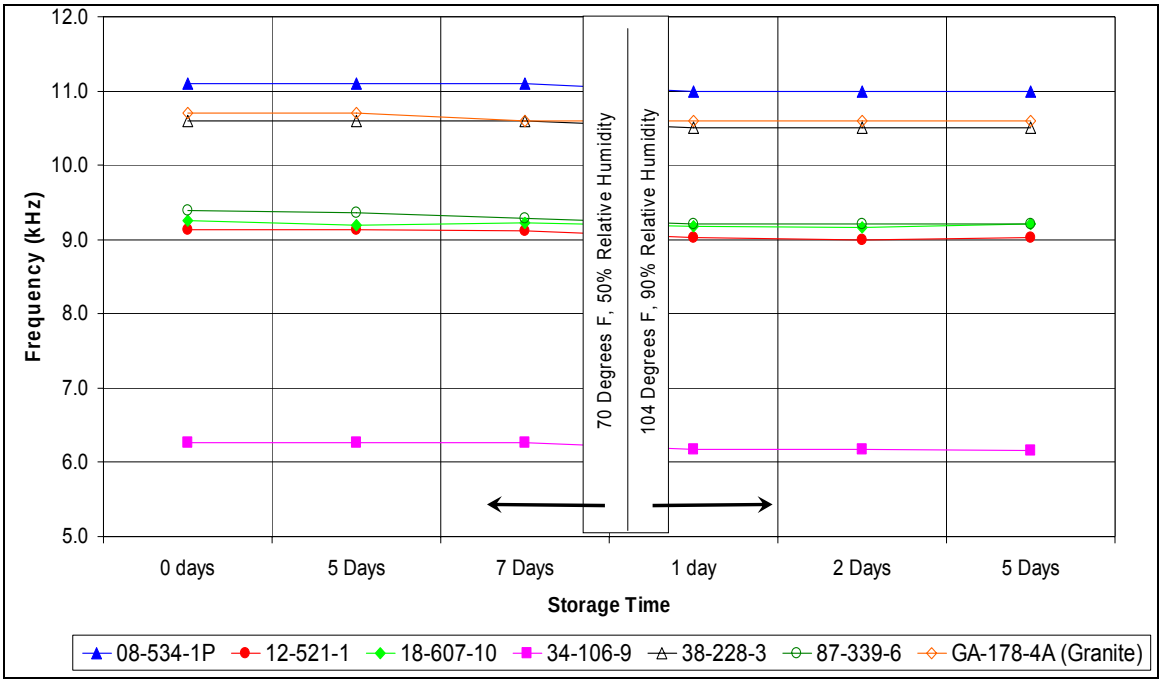

Figure 0-15 First Resonant Frequency with Respect to Storage Time in Environmentally Controlled Storage Conditions

The variation in frequency over time shown in Figure 0-15 does not appear to be significant. It should be noted however that several of the samples experienced small changes in mass between the time the sample was removed from its storage condition and the impact test was completed. The change in mass was approximately 0.1 grams at most (roughly 0.1%) and approximately corresponds to the small changes in frequency observed in Figure 0-15. The poor consistency in the damping estimates compared with

the measured frequencies is the most important reason for excluding the damping estimates from further analyses in Chapter 0. A much higher confidence level exists in impact FRF test's ability to measure resonant frequency than damping at resonance.

Because the environmentally controlled tests did not provide a definitive reason for the inconsistencies of the damping estimates, a boundary condition study was undertaken. This study began by performing impact tests on three aluminum cylinders which were machined to the same geometric dimensions as the core samples cut from the rocks. The tests were performed in the same manner also and frequency and damping estimates were compared. The results were consistent with the measurements taken on the rock cores. The frequencies were measured with consistency but the damping was not. This indicated that some variable associated with the test set up may be the source of the variability.

The method used to investigate the effect of the test's boundary conditions and methods of affixing the accelerometer to the structure is more involved than the previous investigation. In all, three structures are tested using three different adhesion methods, and two different boundary conditions to determine the effect each would have on the measured responses. FRF's are curve fit in ME'Scope® and the modal parameters extracted for several modes in the measured bandwidth.

The structures consist of an aluminum cylinder the same dimensions as the rock cores, a small granite tile having approximate dimensions of 15.24 cm square (6 inches square), by 1.9 cm (0.75 inches) thick, and a larger granite tile (different material than the first), having dimensions of 30.5 cm square (12 inches) by 1.27 cm thick (0.50 inches). The structures are denoted as AL Core 3, Tile #11, and Tile #12 respectively.

The boundary conditions consist of one expected to exhibit light damping, and one expected to exhibit moderate damping. In all cases the moderate damping condition consisted on one inch thick yellow packing foam, with the test specimen evenly supported by it. The light damping condition consists of either suspending the structure with flexible rubber bands or supporting it on a small air bag. The aluminum cylinder is suspended using a rubber band folded to act as a sling. Once suspended the instrumentation is configured in the same way as shown in Figure 0-2 (for impact point #1 only) but the impact point is rotated to be horizontal with respect to the ground. When supported on the foam, the aluminum cylinder is tested in exactly the same manner as the rock cores (impact point #1 only). Both tiles were laid flat supported by either the foam or the airbag depending on the boundary condition being tested. The accelerometer is affixed at one corner and the impact performed at an adjacent corner. The accelerometer is affixed using either a small amount of wax (just enough to cover the base of the sensor with a thin film), a large amount of wax (using a pea-sized glob), or with superglue which was allowed to set for 5-10 minutes before performing the test. The impact hammer, tip, and analyzer settings were selected independently for each structure tested based on the frequency range of the structure's first few resonant frequencies.

The modal parameters estimated from the impact tests on the three structures and the various test conditions are provided in Table 0-4. Perhaps the most readily discernable information in Table 0-4 is that in almost every case, the frequencies were very consistently measured with only minor variation regardless of the test set up. In most cases, the measured frequencies were lower for the test were the accelerometer was affixed with a large amount of wax, indicating that the additional mass of the wax had an

effect on the response. While the measured frequencies are not always exactly the same from one test configuration to the next, the variation in frequency is considerably smaller than that of the damping estimates for the same tests. These results further support the previous statement that a higher confidence level should exist in the frequencies estimated from the measurements than in the damping estimates.

Table 0-4 Estimated Modal Parameters For Boundary Condition Study

Mode 1

Structure	Boundary Condition	Frequencies Adhesion			Damping Adhesion		
		Superglue	*Sm Wax*	*Lg Wax*	*Superglue*	*Sm Wax*	*Lg Wax*
AL_Core_3	Foam	1.05E+04	1.05E+04	1.02E+04	0.620%	0.865%	2.490%
AL_Core_3	Suspended	1.05E+04	1.05E+04	1.02E+04	0.821%	0.758%	2.000%
Tile_11	Foam	2.96E+03	2.96E+03	2.96E+03	0.343%	0.434%	0.185%
Tile_11	Air Bag	2.95E+03	2.96E+03	2.96E+03	0.210%	0.276%	0.080%
Tile_12	Foam	314	315	314	0.884%	0.783%	0.944%
Tile_12	Air Bag	307	307	307	0.152%	0.159%	0.177%

Other Modes

Structure	Boundary Condition	Frequencies Adhesion			Damping Adhesion		
		Superglue	*Sm Wax*	*Lg Wax*	*Superglue*	*Sm Wax*	*Lg Wax*
Tile_11	Foam	2.96E+03	2.96E+03	2.96E+03	0.343%	0.434%	0.185%
		5.22E+03	5.21E+03	5.21E+03	0.153%	0.163%	0.160%
Tile_11	Air Bag	2.95E+03	2.96E+03	2.96E+03	0.210%	0.276%	0.080%
		5.21E+03	5.21E+03	5.21E+03	0.113%	0.134%	0.127%
Tile_12	Foam	314	315	314	0.884%	0.783%	0.944%
		440	439	440	1.100%	0.816%	0.740%
		497	497	497	0.882%	0.944%	0.876%
		755	755	756	0.739%	0.758%	0.661%
		782	782	782	0.560%	0.565%	0.531%
Tile_12	Air Bag	307	307	307	0.152%	0.159%	0.177%
		435	435	434	0.263%	0.248%	0.325%
		494	494	493	0.248%	0.263%	0.307%
		754	754	753	0.242%	0.251%	0.331%
		781	780	779	0.199%	0.214%	0.253%

Though it may be difficult to infer from the table, there is a general trend in the damping estimates with respect to both the chosen boundary conditions and also with respect to the adhesion method used to attach the accelerometer to the test structure. In

almost every case, the tests performed with the foam boundary condition exhibited a higher estimate of percent critical damping than did the tests performed on either the air bag or suspended with rubber bands. This is shown in Figure 0-16 for the samples tested for the first resonance.

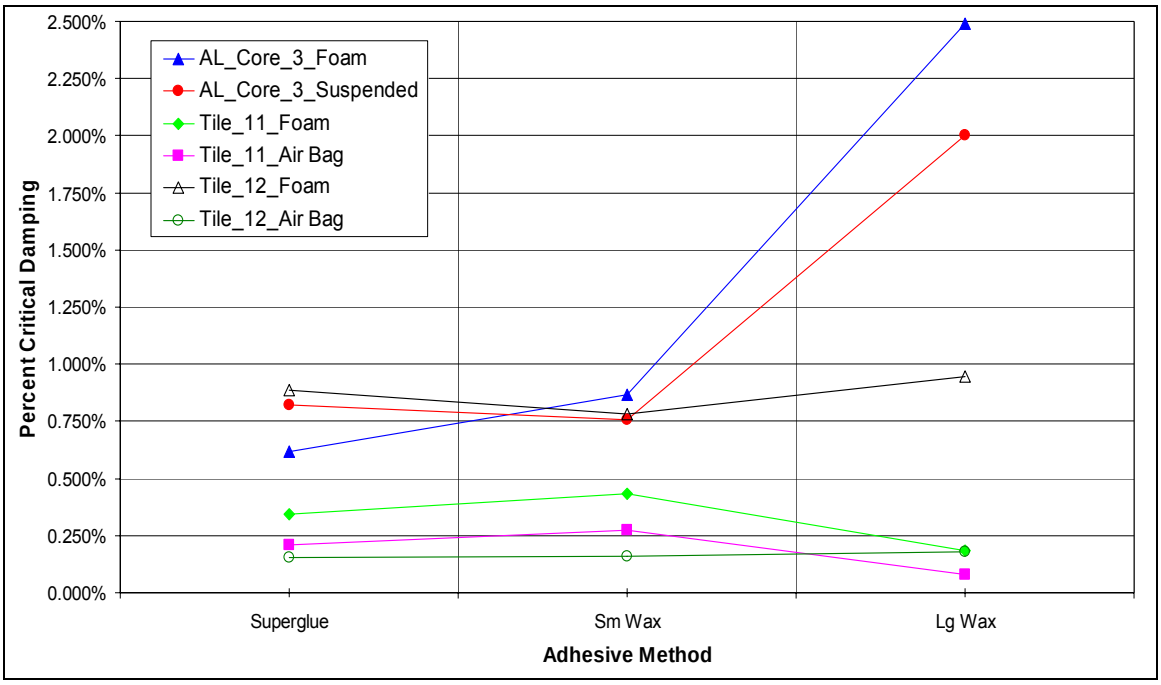

Figure 0-16 First Resonant Damping Estimates With Respect to Various Boundary Conditions

In addition to showing that the support conditions consistently affect the damping estimates for the first mode of each structure, Figure 0-16 also shows that for two of the structures the adhesion method also has a considerable affect on the damping. The use of excessive amounts of wax can lead to inconsistent damping estimates, especially in small, lightweight structures with high resonant frequencies as in the case of the aluminum cylinders. It is logical to also assume, based on these results, that the amount of wax used to affix the accelerometer to the rock cores is a significant variable that led to the

observed variation in damping estimates. Similar inferences can be made if the damping estimates for the five modes listed in Table 0-4 for Tile 12 as shown in Figure 0-17.

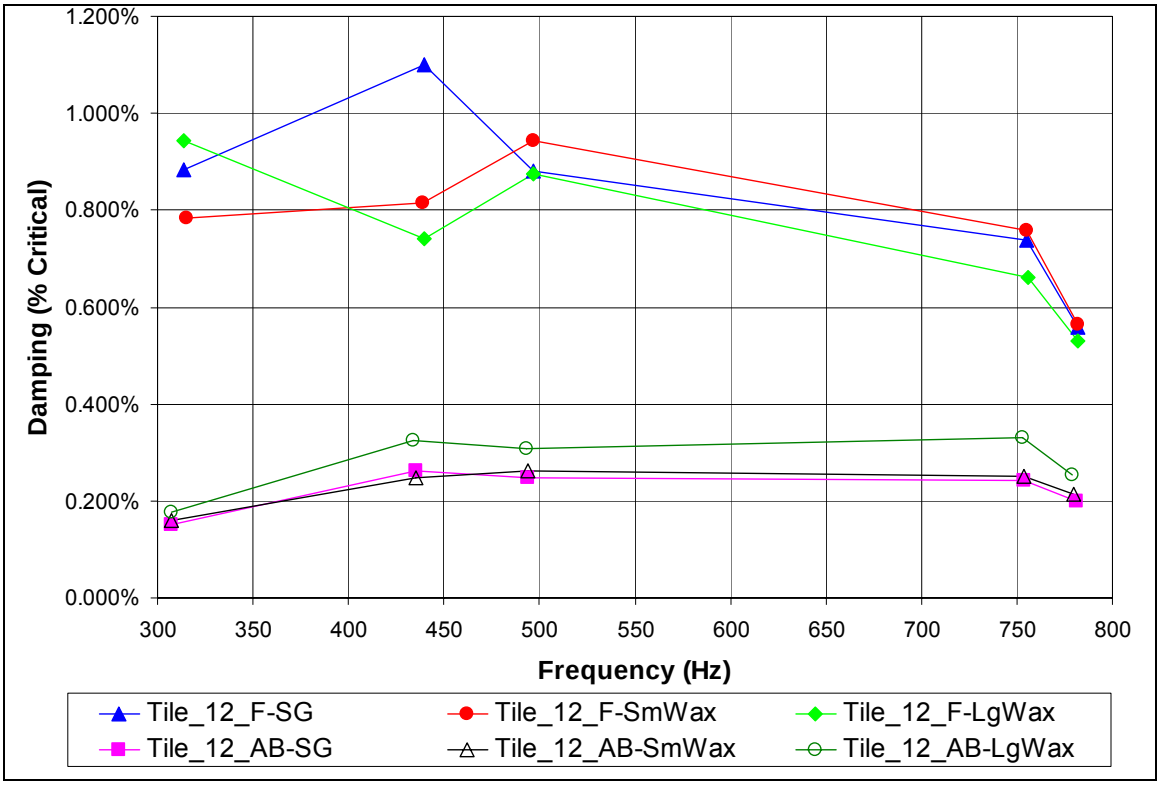

Figure 0-17 Damping Estimates for Various Test Configurations for Tile #12

Clearly from Figure 0-16 and Figure 0-17 the test setup, in particular the boundary conditions, play a substantial role in the damping estimates. Figure 0-17 further shows that the method of supporting the structure can have a significant impact on the damping estimates. In addition, the figure also shows that the adhesives tend to progress from superglue to small amounts of wax, to larger amounts of wax in terms of their affect on damping. To relate the findings of this study back to the impact tests on the rock cores, it is unlikely that the support condition would have a significant impact on the relative measurements since for all the tests, this aspect of the setup remained constant, as did the analyzer settings and equipment used. Based on the results shown, a

likely cause of the observed variability in damping estimates in the rock cores is the amount of wax used to affix the accelerometer to the structure. Not only does the wax and the foam seem to produce higher damping estimates overall, there is really no consistent way of keeping track of the amount of wax used on each core for every test. Future investigations should work to overcome this variable so that damping estimates can be later compared with the sample's petrographic properties.

1.38 CONCLUDING REMARKS

The impact frequency response test which focuses on estimating resonant frequencies and damping from transfer functions of acceleration with respect to force on cored rock specimens is a significant improvement over the acoustic impact-emission test described in Chapter 0. Resonant frequencies were easily estimated using commercial software providing data which can be used to establish causal relationships with the petrographic properties of the aggregates. While the support conditions, equipment, and the geometry of the samples are kept consistent throughout the testing, other variations in the test setup were evident from observed inconsistencies in damping estimates.

Analysis of the data revealed that differences in the core's mass and length may have had a minor affect on the estimated resonant frequencies. The test setup was further investigated indicating that storage environment, support conditions, and especially the manner in which sensors are mounted to test structures has a significant effect on damping estimates. Based on the observed effect of the boundary conditions on the test data, the amount of wax used to affix the accelerometer to the core samples is the primary cause of significant variation on the damping estimates for these samples. Future investigations should work to reduce the effect of this variable, and the other variables

mentioned, on the measurements before attempting to relate damping with aggregate petrography.

Throughout the analysis of the rock core's estimated modal parameters for the first resonance, it is clear that the frequencies can be measured with a higher confidence level than damping. Observed variations in the measured frequencies are not nearly as significant as those observed for damping. For this reason the damping estimates are excluded from analysis with the samples' petrographic properties. Future research efforts which are able to minimize the effects of the test setup and streamline the process of evaluating resonant frequencies may be able to include damping estimates as well as the modal parameters for higher order modes.

ANALYSIS FOR CAUSAL RELATIONSHIPS

1.39 PREFACING REMARKS

In this chapter the culmination of the analysis relating the systems' petrographic properties with the test data is discussed. Comparisons of data provided by the consulting geologists are made with useful data obtained from the performed tests, i.e. Windsor Pin System® and impact FRF testing using linear regression. Results of the acoustic impact-emission test are not used in this part of the analysis since it was shown that impact testing on rock cores would provide more meaningful data. Additionally damping estimates from the impact FRF tests showed that these estimates are heavily dependent on the boundary conditions of the test setup and are also excluded from this analysis. Data from the FDOT is also compared with the aggregate's petrographic properties for comparison against the tests used in this study.

Linear regression analysis is used as the means of correlating the system properties and the measured responses. Regression coefficients serve as indicators of causal relationships. Regression coefficients of $R^2 = 0$ indicate that no relationship exists between the compared variables, and R^2 values near 1.0 indicate a very strong correlation between the variables. Comparisons are made graphically, though the number of graphs generated is quite extensive. For this reason, the regression coefficients are presented in tabular format and supported when necessary by the appropriate graphs. In some cases

the slope of the regression lines will be examined to determine whether certain regression coefficients are meaningful.

Previous chapters discussed the current methods of aggregate quality used by the FDOT with the distinction that these methods, while backed by experience, do little to provide actual determinations of aggregate quality. Instead, the current tests are indirect measures of the properties affecting the aggregates' resistance to weathering. The use of the FDOT's provided test data in this chapter does little to establish the feasibility of the mechanical tests used; however, transportation agencies, including the FDOT, may be interested in correlations of the current quality tests with the measured system properties and how they compare with the primary methods used in this study.

Analysis of regression coefficients is done in a variety of different ways in this chapter. There are analyses referred to as local comparisons, or those regressions comparing the system properties and measured responses for each source individually. Data analyzed in these comparisons may be reduced in some way, i.e. multiple petrographic analyses for the same sample will be averaged so that the reduced data represents an average for that sample. The other comparisons are referred to as global comparisons, or comparisons which span samples from multiple sources. These analyses are performed to examine the relationships between the system properties and the measured responses. The analyses do not take into account the possible contributions that combinations of properties have with respect to the geologic formation from which the sample came or the measured response from the applied tests. It is hypothesized that different combinations of features will affect both field performance and the measured responses of aggregates from different sources; performing global analyses will be one

way of verifying this hypothesis. Global analyses may also be performed on data which is averaged by source so that the data point for each source is an average of the measurements for those samples. The methods of data reduction and comparison are described in each of the following sections as appropriate.

The petrographic analysis techniques used by the consultant geologists was discussed in Chapter 4. From these analyses both local and global comparisons will be made with the measured responses as appropriate. The petrographic data used here is more focused on the data provided by SNCGI (Nagel, 2006) since it contains both concentration and grain size information for each one of the samples used in both the Windsor Pin System® and impact FRF tests. Global analyses using the Data provided by McClellan (2006) are also included for some of the analyses. Analyses are also more heavily focused on the carbonate samples since the sample pool and available test data on the igneous samples is somewhat limited. The features of the carbonates that will be of primary interest are the concentrations and median grain sizes of amorphous calcite, sparry calcite, matrix, quartz and void concentration (porosity) observed in the samples.

1.40 PETROGRAPHY VERSUS WINDSOR PIN SYSTEM® DATA

Analysis for causal relationships existing between the measured depth of penetration from the Windsor Pin System® and petrographic properties for the carbonate samples begins with local comparisons. Linear regression analysis is performed in Microsoft® Excel. The average depth of penetration of the pin for each sample shown in Table 0-1 is plotted against the concentrations and median grain sizes (separately) of the properties identified in Chapter 4 from SNCGI's analysis (Nagel, 2006). While the plots are omitted from this section in the interest of conserving space, the regression

coefficients from the plots are shown in Table 0-1. Plots showing the depth of penetration for each sample with respect to the petrographic properties examined are provided in Appendix F. At least one sample from a particular source must contain a percentage of the property examined in order to perform the regression. The remaining samples in the source are padded with zeros in the case where not every sample contains the property. The use of only three of four data points for each source may not represent a robust sample pool but utilizes as much of the available data as possible from each source. Comparisons for which there was not the required amount of information are indicated in the table with the entry "N/A". The "All Samples" column is created using all the samples, even those for which no traces of the petrographic property exist.

Table 0-1 Regression Coefficients for Windsor Pin System® Penetration with Respect to Petrographic Features and Sizes (Nagel, 2006)

Concentrations of Petrographic Properties Compared to Depth Measurements - All Lithologies

Source/ Property Concentration	Local Comparisons							Global Comparisons	
	08-534	12-521	GA-178	18-607	34-106	38-228	87-339	Avg by Source	All Samples
Amorphous Calcite	N/A	N/A	N/A	0.2467	0.7813	0.1305	N/A	0.0789	0.0551
Sparry Calcite	0.8837	0.0000	N/A	0.9501	0.0155	0.0504	0.1379	0.1494	0.0242
Matrix	0.7119	0.2389	N/A	0.1051	0.0315	N/A	0.2132	0.0039	0.0001
Quartz	0.6101	0.1806	0.9771	N/A	N/A	0.1579	0.2750	0.0238	0.0036
Voids	0.7903	0.1103	N/A	0.9940	0.2001	0.3586	0.4091	0.1232	0.0329

Median Grain Size of Petrographic Properties Compared to Depth Measurements - All Lithologies

Source/ Property Median Size	Local Comparisons							Global Comparisons	
	08-534	12-521	GA-178	18-607	34-106	38-228	87-339	Avg by Source	All Samples
Amorphous Calcite	N/A	N/A	N/A	0.2588	0.2223	0.0000	N/A	0.0098	0.0002
Sparry Calcite	0.9014	0.7806	N/A	0.8915	0.8587	0.4965	0.7780	0.0213	0.0036
Matrix	0.0000	0.1806	N/A	0.0164	0.1769	N/A	0.0000	0.0041	0.0026
Quartz	0.3414	0.5395	0.8318	N/A	N/A	0.1579	0.3958	0.0440	0.0495
Voids	0.1687	0.1997	N/A	0.9753	0.7949	0.0433	0.7077	0.3031	0.0351

Regression coefficients of $R^2 = 0.70$ or higher are highlighted in Table 0-1 and it is assumed that these indicate a strong relationship between the property and the depth of

penetration for the given source shown. Table 0-1 indicates that for samples originating from 08-534, GA-178, and 18-607 the depth of penetration is strongly related to at least one of the properties and its median grain size.

Globally comparing the average depth of penetration by source with the corresponding averaged petrographic properties did not reveal any significant relationships in either property concentration or its median size. Furthermore, globally comparing all the samples (data that is not averaged by source but rather fully expanded) with the indicated properties often revealed less meaningful relationships than the data averaged by source. Eliminating samples from GA-178, which are of a different geologic makeup, from the analysis did not substantially increase the regression coefficients shown in Table 0-1.

While many of the comparisons tabulated in Table 0-1 did not reveal compelling evidence of strong relationships between the measured response and the system properties, a general trend exists if the data is examined for several of the sources. To illustrate this, the regression coefficients for each source are plotted with respect to the petrographic properties of interest in Figure 0-1.

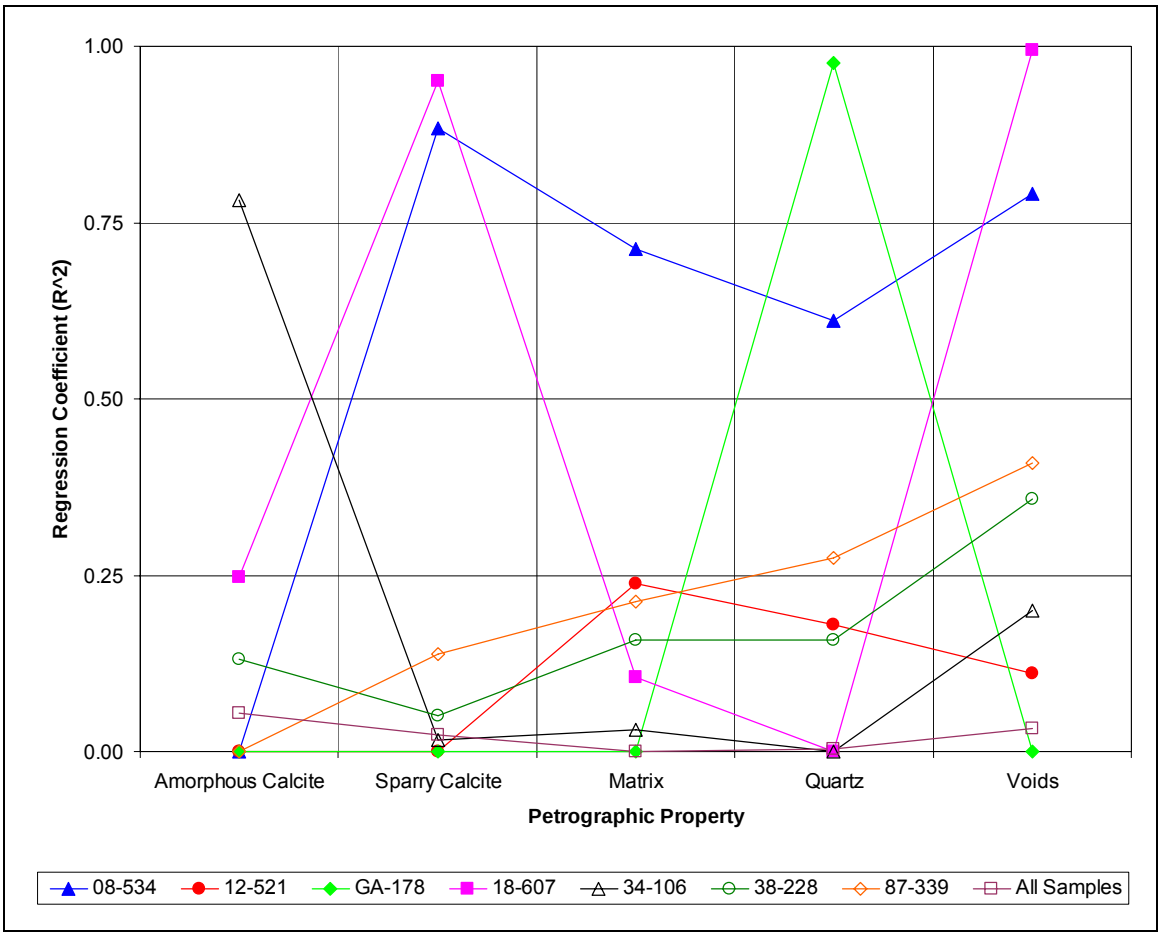

Figure 0-1 Regression Coefficients From Comparing Penetration Depth from Windsor Pin System® Tests and Concentrations of Select Petrographic Properties

Several of the traces in Figure 0-1 follow a similar pattern though the regression coefficients are not always indicative of causal relationships. For example, the regression coefficients are higher for concentration of voids than any other property in many cases. Sources 08-534 and 18-607 have very similar behaviors in terms of the relative level of correlation between the penetration depth and the properties examined. The similar behavior of their regression coefficients does not seem to translate to similarities in their properties however. The five petrographic properties of the two sources are compared side by side in Table 0-2.

Table 0-2 Select Petrographic Properties for 08-534, Brooksville, FL, and 18-607, Center Hill, FL Samples

Property		Slide						
		08-534			*18-607*			
		1	2	7	5	8	9	10
Calcite, Amorphous	Percentage (%)					76%		17%
	Median Size (mm)					0.02		0.02
Calcite, Sparry	Percentage (%)	9%	1%	2%	6%	19%	25%	21%
	Median Size (mm)	1.01	0.17	0.25	0.15	0.13	0.11	0.10
Matrix	Percentage (%)	73%	91%	85%	82%		73%	60%
	Median Size (mm)	0.01	0.01	0.01	0.02		0.02	0.02
Quartz	Percentage (%)	17%	3%	9%				
	Median Size (mm)	0.11	0.07	0.10				
Void	Percentage (%)	1%	5%	4%	13%	5%	2%	2%
	Median Size (mm)	0.42	0.49	0.28	3.54	1.77	1.18	0.71
Total $CaCO_3$	Percentage (%)	82%	92%	87%	87%	95%	98%	98%
	Average	87%			95%			

Among the biggest differences in aggregates from the two sources shown in Table 0-2 are that samples from 08-534 do not contain any amorphous calcite, while samples from 18-607 do not contain any quartz. In fact the only two things these samples seem to have in common are concentrations of porosity and matrix, both of which were correlated in vastly different amounts with the Windsor Pin® test. The sparry calcite and matrix grain sizes are relatively consistent between the two sources. While outwardly it would seem there is little consistency in the two sources one should keep in mind that the two calcites and matrix are more or less of the same chemical composition, calcium carbonate. If the total compositions of calcium carbonate are compared, i.e. summing the calcites and matrix concentrations, the two sources are not quite as dissimilar. This is expected since limestone is predominately calcium carbonate.

If this type of comparison is taken a step further and the compositions of the samples from 38-228 and 87-339 are examined similar conclusions can be made. These sources are compared side by side in Table 0-3.

Table 0-3 Select Petrographic Properties for 38-228, Perry, FL and 87-339, Hialeah, FL Samples

Property		Slide						
		38-228			*87-339*			
		1	3	4	5	6	8	10
Calcite, Amorphous	Percentage (%)	7%	25%	32%				
	Median Size (mm)	0.02	0.02	0.02				
Calcite, Sparry	Percentage (%)	85%	70%	7%	26%	22%	29%	20%
	Median Size (mm)	0.07	0.17	0.15	0.23	0.19	0.14	0.26
Matrix	Percentage (%)	0%	0%	39%	59%	52%	60%	63%
	Median Size (mm)			0.01	0.01	0.01	0.01	0.01
Quartz	Percentage (%)	0%	0%	3%	10%	23%	9%	2%
	Median Size (mm)			0.13	0.25	0.24	0.25	0.26
Void	Percentage (%)	9%	5%	20%	6%	3%	2%	16%
	Median Size (mm)	0.55	1.17	3.50	1.34	2.54	3.00	2.42
Total $CaCO_3$	Percentage (%)	92%	95%	78%	85%	74%	89%	83%
	Average	88%			83%			

Table 0-3 shows that while outwardly there are significant differences in the petrographic properties, the total concentrations of porosity and calcium carbonate are very similar when comparing the two sources. Overall, the samples in Table 0-3 seem to have a higher concentration of quartz and voids than the samples shown in Table 0-2.

Since it has been shown that sources with similar concentrations of calcium carbonate also seem to have similar correlations with the Windsor Pin System® measurements it makes sense to examine the regressions for this relationship as well. A plot comparing the total concentrations of calcium carbonate for the limestone samples with their corresponding Windsor Pin® measurements is shown in Figure 0-2.

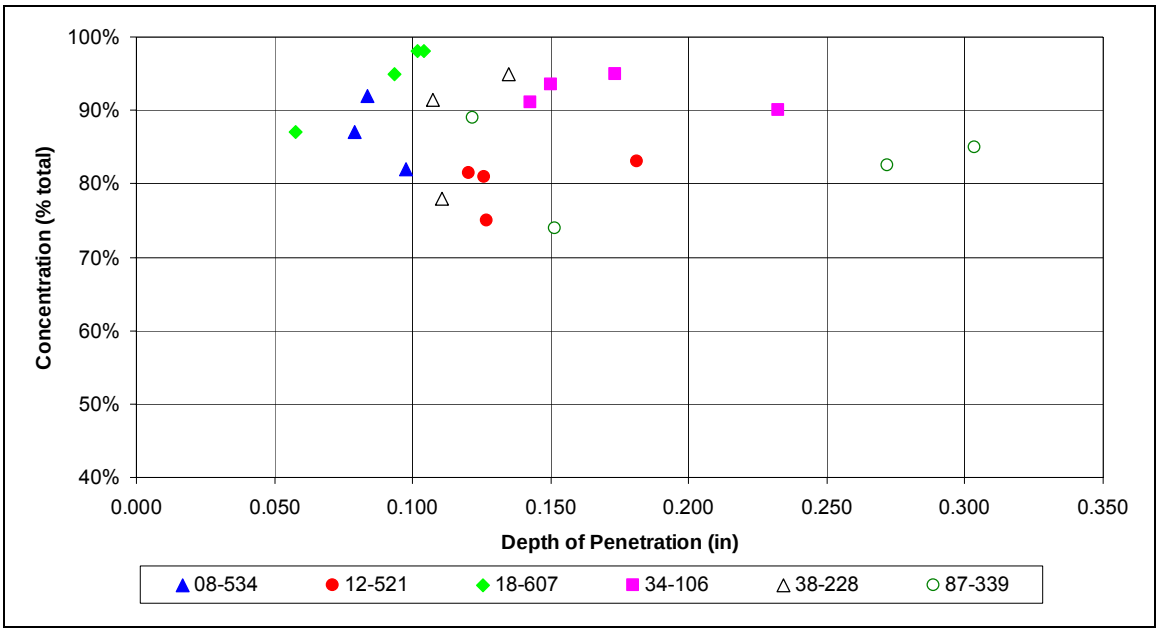

Figure 0-2 Total Concentration of $CaCO_3$ for Limestone Samples with Respect to Windsor Pin System® Measurements

Figure 0-2 shows that all of the samples have similar compositions of calcium carbonate which is expected. In most cases, there is not a strong relationship between the total concentration of calcium carbonate and the Windsor Pin® measurements. The regression coefficients between the two are given in Table 0-4.

Table 0-4 Regression Coefficients Comparing Windsor Pin® and Total Concentration of Calcium Carbonate

Source/ Property Concentration	Local Comparisons							Global Comparisons	
	08-534	12-521	GA-178	18-607	34-106	38-228	87-339	All Samples	Carbonates Only
Total CaCO3	0.5287	0.2389	N/A	0.9940	0.2140	0.3233	0.0085	0.0372	0.0260

The relatively low global relationship between the Windsor Pin System® and the total concentration of calcium carbonate is expected based on the data in Figure 0-2. Locally there is only one source which showed a strong correlation between the two variables.

The only clear determination which can be made from this discussion is that in general, some of the sources seem to show similar trends in the relative correlations between the Windsor Pin® System and the petrographic properties even though the regression coefficients do not always indicate strong relationships. Sources which seem to have very similar levels of correlation across the five properties examined do not necessarily have a similar petrographic makeup. It is apparent that while sources may possess similar concentrations of certain properties, their interaction with their other constituents may be the cause of differences in their level of correlation with the Windsor Pin® test.

The regression coefficients for the global analyses did not show a strong correlation between the Windsor Pin System® and the properties examined. In terms of a quality test, it may be possible to calibrate the Windsor Pin System® for the sources which showed some causal relationships. Further testing should be performed to identify whether these relationships can be used to provide accurate estimates of the properties which the test seems to be related to in order to generate a more statistically meaningful model.

It may be possible in future investigations to relate ratios of certain properties found in aggregate samples to the Windsor Pin System® with strong correlations in a global analysis. If such an analysis reveals a significant correlation with the Windsor Pin System® in a global sense, a better foundation for a quality test would exist. Clearly the presence of some strong relationships between the measured response of the Windsor Pin System® and the aggregate's properties warrants such investigation. Cooperation with

qualified geologists on an analysis of this type would be ideal in order to streamline the process of identifying the correct combination of petrographic factors for comparison.

1.41 PETROGRAPHY VERSUS FIRST RESONANT FREQUENCIES OF ROCK CORES

Like the Windsor Pin® data, the measured frequencies from the impact FRF tests are also compared with the major petrographic characteristics found in the limestone samples. These are the same properties examined for relationships with the Windsor Pin System®. Linear regression analysis is performed graphically using the trend line function in Microsoft® Excel. Recall that only the first resonant frequencies of the 3.75 inch core samples are used for the analysis.

The regression coefficients resulting from comparisons of both feature concentration and median grain size are shown in Table 0-5.

Table 0-5 Regression Coefficients Comparing First Resonant Frequency of Core Samples and Selected Petrographic Properties

Concentrations of Petrographic Properties Compared to First Resonant Frequencies - All Lithologies

Source/ Property	Local Comparisons								Global Comparison
	08-534	08-534(P)	12-521	GA-178	18-607	34-106	38-228	87-339	All Samples
Amorphous Calcite	N/A	N/A	N/A	N/A	0.8554	0.0030	0.4683	N/A	0.0384
Sparry Calcite	0.9984	0.9838	0.0000	N/A	0.2876	0.3802	0.9519	0.2304	0.0534
Matrix	0.9347	0.9918	0.1891	N/A	0.9115	0.3577	0.9985	0.0690	0.1489
Quartz	0.8718	0.9610	0.0000	0.4893	N/A	N/A	0.9985	0.1123	0.0679
Voids	0.9722	0.9999	0.1530	N/A	0.2841	0.0330	0.9626	0.3499	0.0890

Median Grain Size of Petrographic Properties Compared to First Resonant Frequencies - All Lithologies

Source/ Property Median Size	Local Comparisons								Global Comparison
	08-534	08-534(P)	12-521	GA-178	18-607	34-106	38-228	87-339	All Samples
Amorphous Calcite	N/A	N/A	N/A	N/A	0.6066	0.3169	0.0000	N/A	0.0848
Sparry Calcite	0.9999	0.9758	0.3944	N/A	0.0988	0.4456	0.1121	0.8386	0.0028
Matrix	0.0000	0.0000	0.0000	N/A	0.7588	0.1121	0.9985	0.0000	0.1491
Quartz	0.6447	0.7940	0.8626	0.2416	N/A	N/A	0.9985	0.2657	0.0004
Voids	0.0132	0.0027	0.1825	N/A	0.2521	0.0433	0.9445	0.7606	0.0506

Regression coefficients greater than $R^2 = 0.70$ are highlighted in Table 0-5 and represent strong relationships between the first resonant frequency of the core samples and the corresponding petrographic property for the source indicated. The regression coefficients for the core samples from source 08-534, Brooksville, Florida, are given in Table 0-5 for measurements made before and after precision cutting for comparison. It is interesting to note that in some cases precision cutting improved the correlation and in other cases it did not. This result further shows the importance of geometry as a factor in measuring the frequency response function of a given structure. In some cases, a very small improvement in the variability of the structure's geometry resulted in a significant change in the relative level of correlation between the structures natural frequency and the properties examined in Table 0-5.

While not clearly visible from the tabulated regression coefficients in Table 0-5, there are some trends in the regression coefficients with respect to the properties examined, shown graphically in Figure 0-3.

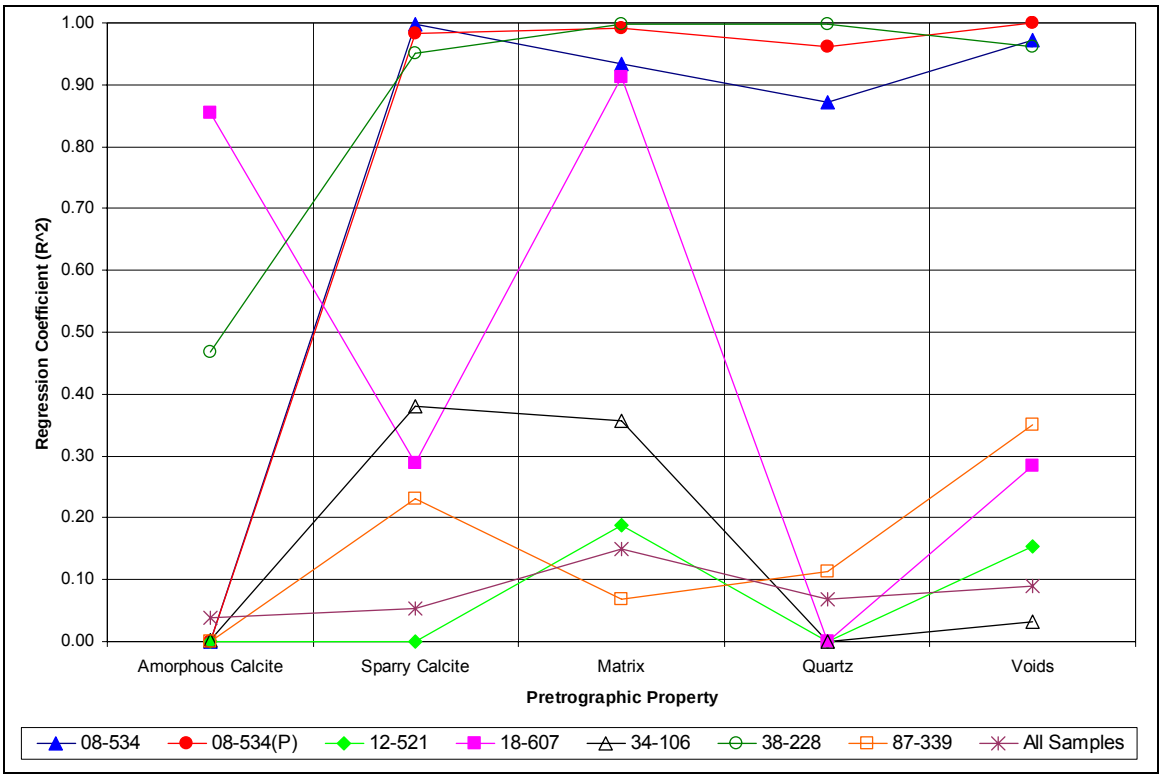

Figure 0-3 Regression Coefficients with Respect to Select Petrographic Properties for First Resonant Frequency of Rock Cores

As expected, the two traces corresponding to samples from 08-534 show very similar behaviors in Figure 0-3, with the precision cut cores having overall higher correlations to the aggregate's properties. As with the Windsor Pin® regressions in Figure 0-1, Figure 0-3 shows consistently better correlations with one of the calcium carbonate properties and the percent concentration of voids in the material for most of the sources. The previous analysis comparing similarities in petrography between sources with these behaviors did not reveal any significant findings for the Windsor Pin System® data. It is unlikely that much more can be learned from repeating that approach for this data. Figure 0-3 merely illustrates that while there are not always strong relationships between the measured response and the petrographic properties examined, the relative

levels of correlation of the data with the petrography are somewhat similar for the sources studied.

The data in Table 0-5 and Figure 0-3 show that there are some obvious relationships between the measured resonant frequency and one or more of the sample's petrographic properties when compared on a local or source-by-source basis, similar to what is observed for the Windsor Pin® data. Also in similar fashion to the Windsor Pin System® is the lack of a strong correlation between the measured first resonant frequencies and any of the petrographic properties examined across all the samples in a global sense. Again this result indicates that it may be possible to calibrate the impact FRF test to an individual source's petrography. Further testing should be performed to identify whether these relationships can be used to provide accurate estimates of the properties which the test seems to be related to.

Before continuing to examine the frequencies obtained from impact testing with additional petrographic data there is a need to discuss differences in the regressions from which the data in Table 0-5 is generated. First it is important to keep in mind that the frequencies estimated during the curve fitting process described in Chapter 0 represent an estimate of the ratio of stiffness to mass in the test structure, i.e. the rock core. Had the damping been measured more consistently, it would have provided an additional system property for comparison in this chapter. Knowing the ratio of stiffness to mass in the test structure is advantageous for this study since that information is directly related to the mechanical properties of the sample's petrography and how those features interact, but there are an infinite number of systems whose mass and stiffness can describe the same measured response. A more detailed understanding of the engineering properties of the

various minerals comprising the aggregates studied could theoretically produce very good global correlations with impact testing if a "frequency number" or other estimate of the aggregates' stiffness and mass could be developed from knowledge of the petrography alone and then compared with the measured responses. Such an analysis would also shed further light on the contribution that each petrographic feature makes on the measured frequency response and also perhaps the aggregates' durability in the field. This is an important analysis that needs to be addressed in future studies. If the combinations of petrographic properties that best correlate with the measured responses also correspond to combinations of petrographic properties important to durability, then the basis for an accurate and viable test method will be established with a high level of confidence.

Having spent a great deal of the discussion examining evidence of how different combinations of petrographic features may affect the measured frequency response, it is also important to consider, for the case of the impact FRF data, the slope of the best fit lines corresponding to the regression coefficients listed in Table 0-5. In section 1.37.2, the relationship between mass and resonant frequency was examined in Figure 0-10. Recall that the observed trend of increased frequency with increased mass is somewhat unexpected and is perhaps an indication that additional mass contributes more to the stiffness of the material than it does to the inertial effects of the mass itself. If the plots comparing the major petrographic properties with the first resonant frequency are examined, the effect of feature concentration on frequency can be examined more closely. If the slopes of the regression lines are the same (either all positive or all negative) then the effect of the feature on the aggregate's mass to stiffness ratio is probably the same for every property. If the trends do not have the same slope, the data

further supports the need to examine how combinations of petrographic features affect the measured frequencies and in turn the aggregates resistance to weathering in the field.

The petrographic concentrations are plotted with respect to the measured first resonant frequencies in Figure 0-4 through Figure 0-8 with the regression lines used to generate the data in Table 0-5. The similarities or differences in the slopes of the regression lines is are of particular interest in the graphs. The "linear (XX-XXX)" series correspond to the regression lines for the source indicated.

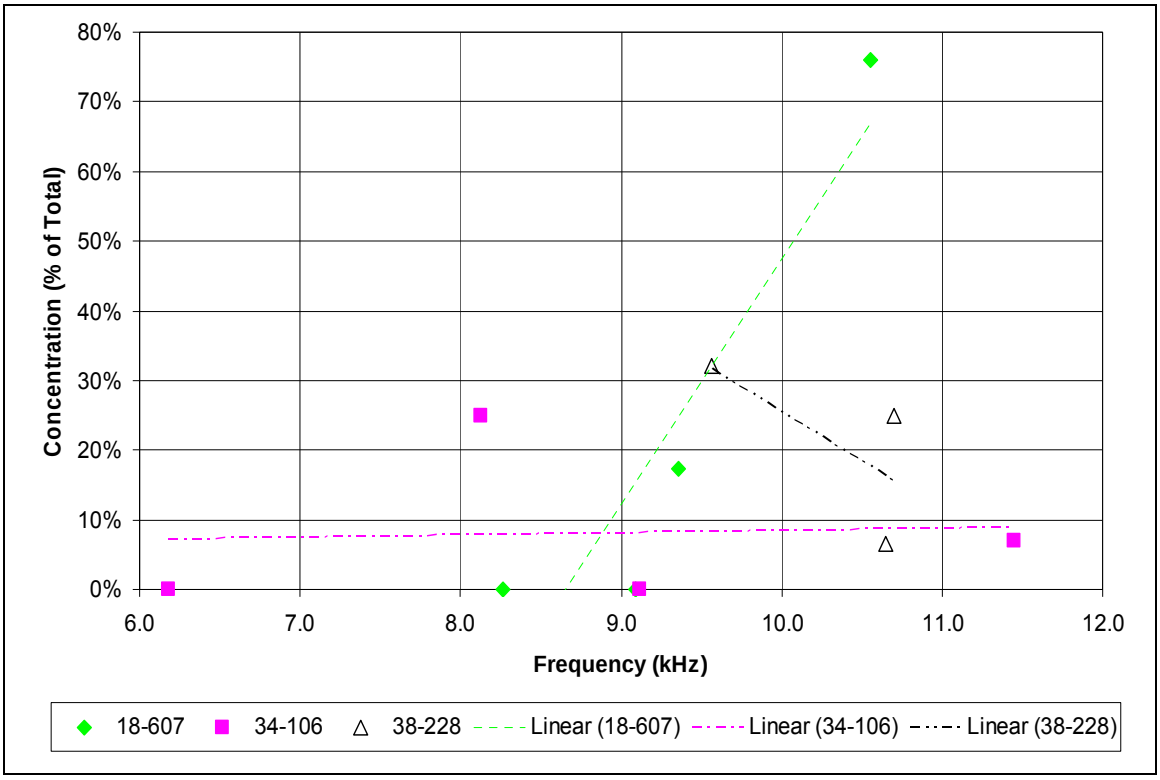

Figure 0-4 Concentration of Amorphous Calcite With Respect to First Resonant Frequency the Showing Regression Lines

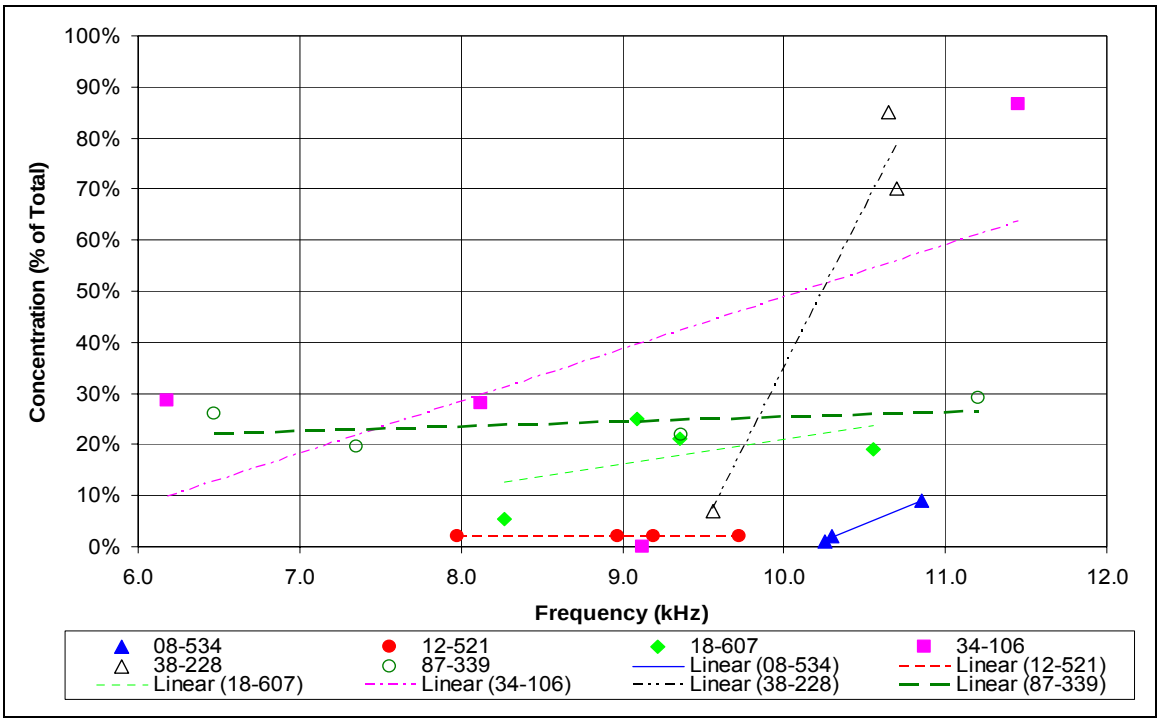

Figure 0-5 Concentration of Sparry Calcite With Respect to First Resonant Frequency Showing Regression Lines

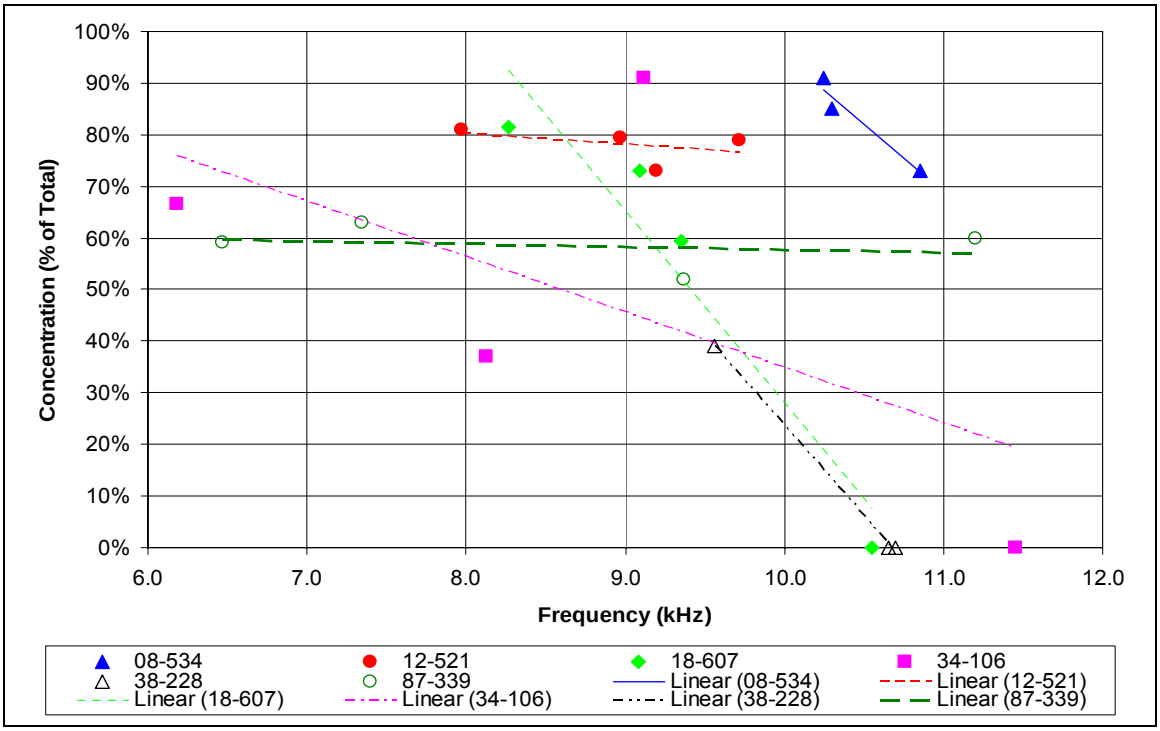

Figure 0-6 Concentration of Matrix With Respect to First Resonant Frequency Showing Regression Lines

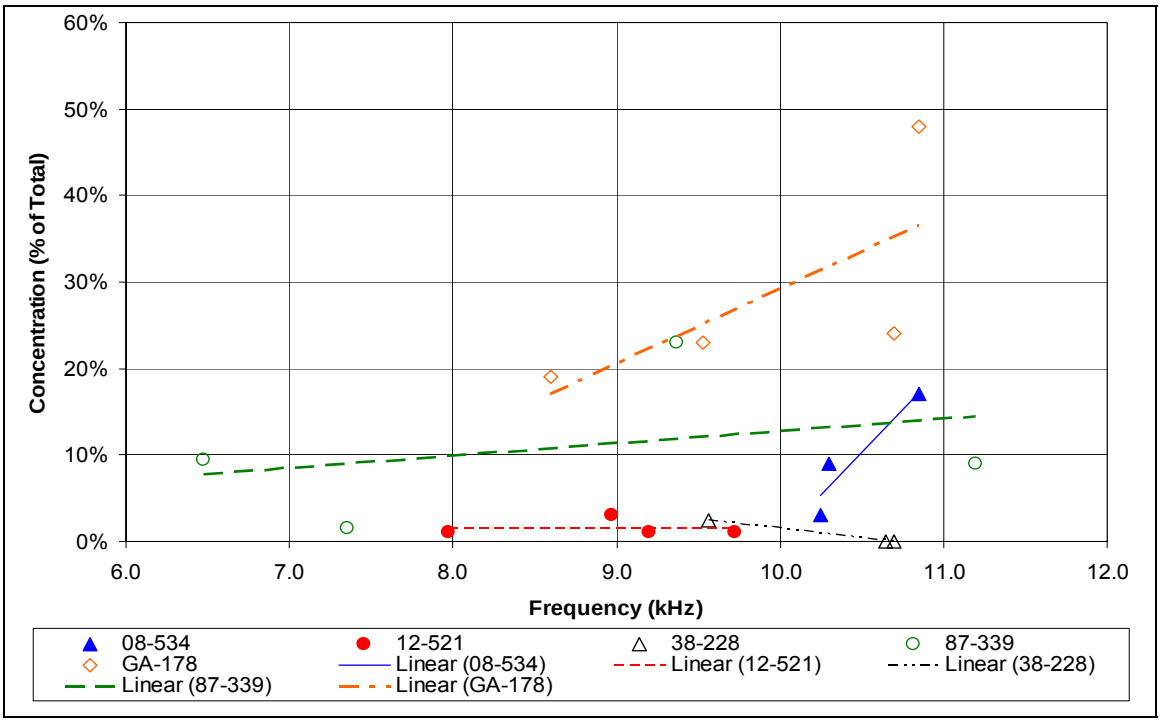

Figure 0-7 Concentration of Quartz With Respect to First Resonant Frequency Showing Regression Lines

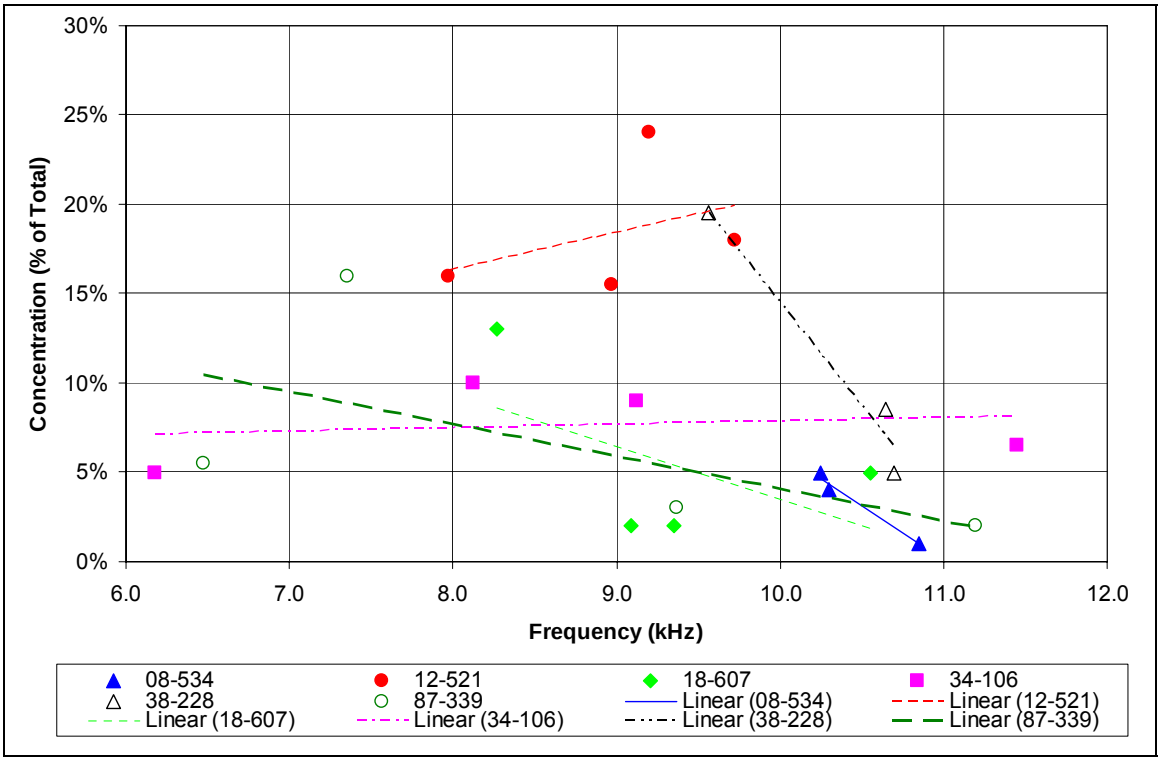

Figure 0-8 Concentration of Voids With Respect to First Resonant Frequency Showing Regression Lines

The regression lines for the data shown in the preceding figures are widely varied in their slopes. Of interest is whether the regression lines show positive or negative sloping trends for a particular property. The trend lines for the concentration of sparry calcite (Figure 0-5), matrix (Figure 0-6), and Quartz (Figure 0-7) (with the exception of the samples from 38-228) with respect to the first resonant frequency have consistent slopes within the petrographic property. Both the sparry calcite and quartz show positive trend lines, possibly indicating that higher concentrations of these properties contribute substantially to the aggregate's stiffness. The trend lines for the concentration of matrix with respect to the first resonant frequencies show negative slopes, possibly indicating that increased concentrations of matrix contribute more to the inertial effects within the sample than to its stiffness.

The presence of consistently sloped regression lines is important to the development of a quality test because it indicates a strong possibility of being able to identify relative concentrations of factors from one sample to another. For example, based on the data presented, it may be possible with additional testing to consistently identify the relative concentrations of sparry calcite and matrix. The data indicates that higher resonant frequencies for the first mode may correspond to samples with greater concentrations of sparry calcite and lower concentrations of matrix. Of course this assumption would have to be scaled relative to some average level common to the aggregates and verified with additional testing. Most importantly there is the possibility for future work to expand upon these results with the goal of developing an accurate

measure of petrographic properties which are related to aggregate quality without the need to analyze thin sections.

The remaining plots which do not show consistent trends in the concentration of the various properties with respect to frequency show that the contribution that these properties have on the measured response is not always the same. It is especially interesting that the concentration of porosity with respect to frequency in Figure 0-8 did not show consistent trend lines across all the sources. Sources 12-521 and 34-106 both had positive slopes while the other sources showed negative slopes. Theoretically, the addition of voids to a material should cause a decrease in the structure's stiffness and lower its resonant frequency assuming that all else in the sample remains constant. It is also important to understand that it may be possible to have a very stiff material with high porosity. In this case, the high stiffness to mass ratio would correspond to a high resonant frequency. Conversely, less stiff material may be paired with low porosity and yield the opposite result. The inconsistently sloped relationships shown in Figure 0-8 are an indication of this or possibly the result of using samples that are too small to normalize the effect of certain features. In Chapter 8 the effect of sample size was discussed in relation to Figure 0-10 which showed the relation ship between mass and resonant frequency. For the carbonate samples, an increase in mass also corresponded to an increase in frequency. Additional tests using larger prepared samples may provide more information to substantiate whether the regressions are dependent on the sample size.

Additionally, it is also important to consider the effect that porosity has on the geometry of the test structure. Samples that are composed of loosely conglomerated grains may be adversely altered by the coring process. Water flowing through the bit

may dislodge more material from the surface of the core thereby reducing either the sample's diameter, or the amount of material on the sample's surface, which could have a significant impact on stiffness. Equation 8-1 showed that the area moment of inertia plays an important roll in the structure's stiffness term in the numerator of the radicand. If material is shifted closer to the cross section's neutral axis, the stiffness of the member can be reduced. This point can be taken a step further in understanding that on a piecewise basis, along the core's length, larger voids may not always be distributed the same way throughout the sample. The location of those larger voids could also significantly impact the measured response and is perhaps one explanation for the low correlation between porosity and natural frequency across all the samples.

Inconsistent regression lines are important because they further substantiate the need for a better understanding of the interactions between the different petrographic features. Clearly, the presence of some strong relationships between the measured response of the impact FRF test and the aggregate's properties warrants further investigation. Cooperation with qualified geologists on future analysis of the data would be ideal in order to identify meaningful combinations of petrographic factors for comparison with resonant frequencies. If the challenges facing the test setup's effect on the damping estimates can be overcome, it would be interesting to see how similar correlations compare with the ones presented here.

While no additional conclusions can be made from looking at the regression coefficients obtained by comparing the petrographic properties identified by McClellan (2006) with the resonant frequencies of the corresponding samples, the data is provided in Table 0-6 in the interest of thoroughness.

Table 0-6 Regression Coefficients for Comparisons of Petrographic Properties with Resonant Frequencies for Data Provided by McClellan (2006)

Property Concentration	Regression Coefficient (Carbonates only)
Fossil Grains	0.5398
Non-Fossil Grains	0.3866
Moldic Porosity	0.0015
Interparticle Porosity	0.0324
Intragranular Porosity	0.0001
Micrite Cement	0.0381
Microspar & Sparite	0.1187
Dolomitic Grains	0.5304
Chert	0.0022
Quartz	0.4844
Opaques	0.0197
Total Porosity	0.0015
Total Cement/Matrix	0.0183
Petrographic Number	0.1114

In general, the global regression coefficients for total porosity and calcite features, i.e. total cement/matrix, in Table 0-6 are consistently low as were those in Table 0-5. The best relationships seem to be between fossil and non-fossil grains, dolomite and quartz with respect to the measured frequencies of the same samples analyzed. One exception this observation is that there is a strong relationship between the measured frequencies and the concentration of micrite cement if a second order regression is used as shown in Figure 0-9.

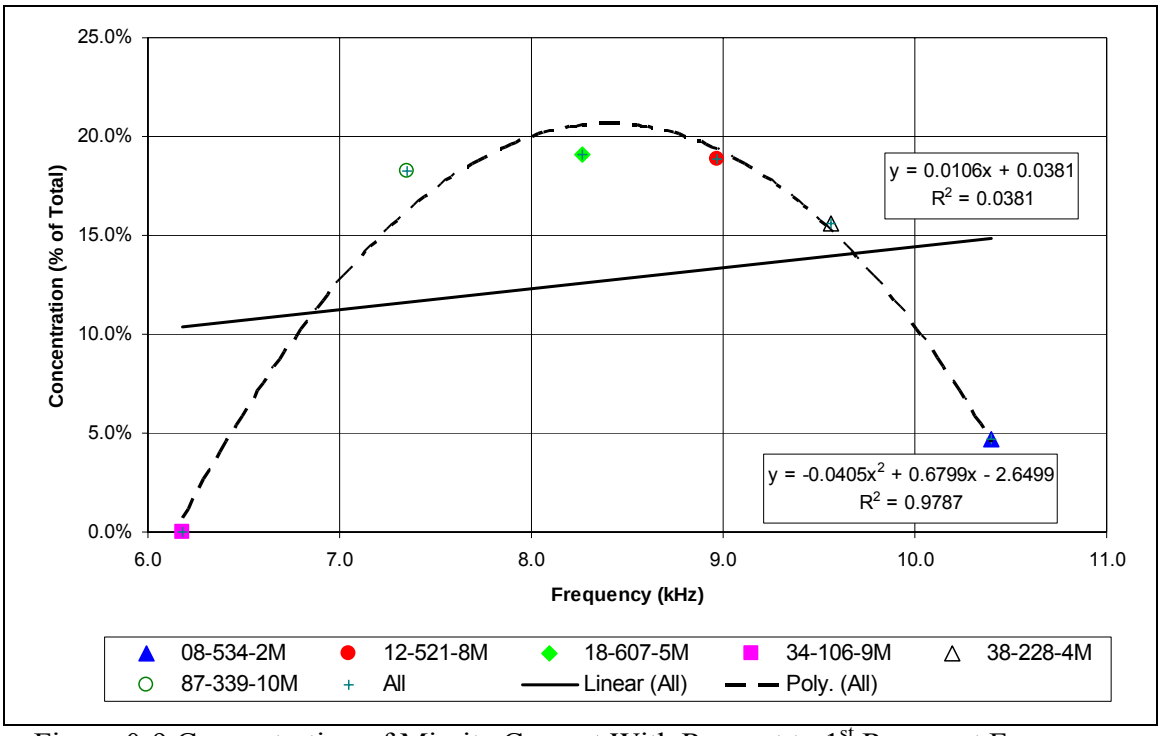

Figure 0-9 Concentration of Micrite Cement With Respect to 1st Resonant Frequency

Data from McClellan (2006) will be used more extensively in the next section where the current tests used by the FDOT are compared with the petrography of the aggregate samples. It is also important to keep in mind that the additional petrographic characteristics again only represent one data point for each of the aggregate sources studied compared against only one measured response from the corresponding sample. These global comparisons are interesting to examine but do not represent a statistically significant sample pool.

1.42 PETROGRAPHY VERSUS FDOT TEST RESULTS

In a similar fashion to the previous two tests the petrographic properties of the aggregates studied are compared with the tests currently used by the FDOT to certify the quality of these materials. The five primary petrographic characteristics examined in the

previous analyses are averaged by source and the trends are compared globally, i.e. across the various sources. The FDOT provided test data for the absorption, bulk specific gravity, L.A. Abrasion, and sodium sulfate soundness tests performed on aggregates from the seven sources used in this study. The resulting data was presented in Table 0-3 and is meant to represent average results for the aggregate studied, however the data only provides one data point for comparison with the petrography. Conversely, petrographic characteristics reported by McClellan (2006) represent only one or two samples from each of the corresponding sources, and where necessary it too has been averaged by source for comparison with the FDOT tests.

Comparisons of the reported results from the FDOT and the average petrographic characteristics from a particular source are compared graphically in the same manner as in the previous analyses. Regressions were performed considering all of the lithologies and also considering only the carbonate samples. The FDOT test results are compared globally with the five major petrographic features, i.e. amorphous calcite, sparry calcite, matrix, quartz, and voids, in Table 0-7.

Table 0-7 Regression Coefficients for Comparison Between Petrography and FDOT Quality Tests Across All Lithologies

Regression Coefficients For Concentration - ALL Lithologies					
	Absorption	Specific Gravity	L.A. Abrasion	Sodium Sulfate	Rating
Amorphous Calcite	0.0441	0.0536	0.0005	0.0863	0.1286
Sparry Calcite	0.0072	0.0001	0.3763	0.0056	0.0011
Matrix	0.4714	0.6508	0.0020	0.1828	0.1700
Quartz	0.3805	0.3788	0.2712	0.2019	0.1548
Voids	0.3985	0.4192	0.6076	0.3315	0.3633

Regression Coefficients For Median Grain Size - All Lithologies					
	Absorption	Specific Gravity	L.A. Abrasion	Sodium Sulfate	Rating
Amorphous Calcite	0.0004	0.0208	0.0572	0.0010	0.0022
Sparry Calcite	0.0021	0.0550	0.0560	0.0500	0.0580
Matrix	0.2987	0.2488	0.0085	0.1689	0.1125
Quartz	0.1472	0.1221	0.0217	0.0831	0.0408
Voids	0.4062	0.4876	0.3439	0.1490	0.1530

Additionally, the regression coefficients obtained when making the same comparisons as those in Table 0-7 across only the carbonate samples are given in Table 0-8.

Table 0-8 Regression Coefficients for Comparison Between Petrography and FDOT Quality Tests Across Carbonate Sources Only

Regression Coefficients For Concentration - Carbonates Only					
	Absorption	Specific Gravity	L.A. Abrasion	Sodium Sulfate	Rating
Amorphous Calcite	0.3397	0.5220	0.0364	0.2189	0.2659
Sparry Calcite	0.0936	0.2730	0.2687	0.0121	0.0180
Matrix	0.1797	0.3682	0.1691	0.0621	0.0722
Quartz	0.0018	0.0513	0.0956	0.0786	0.0568
Voids	0.1654	0.1596	0.5093	0.2242	0.2854

Regression Coefficients For Median Grain Size - Carbonates Only					
	Absorption	Specific Gravity	L.A. Abrasion	Sodium Sulfate	Rating
Amorphous Calcite	0.1284	0.4133	0.0094	0.0137	0.0345
Sparry Calcite	0.1456	0.0291	0.3066	0.2302	0.2177
Matrix	0.0379	0.0003	0.0933	0.0540	0.0269
Quartz	0.0508	0.2138	0.1026	0.0001	0.0057
Voids	0.1227	0.1650	0.1863	0.0377	0.0583

The ratings of each source were computed based on the number of passing tests as described in Chapter 0.

Comparisons between the FDOT tests and the petrographic characteristics are done across all the lithologies and across the carbonates separately to see how they compare. In the previous analyses better correlations were often achieved if the granite samples were excluded, not in every case, but in some. It doesn't always make sense to include those samples because the constituents are so different. In the case of the FDOT tests, all of the lithologies are subjected to the same requirements shown in Table 0-1 and so it is interesting to note that in some cases better regression coefficients were obtained when all of the sources were used in the comparison while in others this was not the case.

Perhaps the most important regression coefficients to examine from Table 0-7 and Table 0-8 are those comparing the porosity and those FDOT tests which would likely compare well with it, the absorption, specific gravity, and the sodium sulfate soundness tests. In the case where all the lithologies are considered, only the sodium sulfate test was most strongly correlated with porosity, though the other two tests were best correlated with porosity as their second best property when considering concentration. Median void sizes were best correlated with absorption and specific gravity overall when considering all lithologies. In the case where only the carbonate sources are considered, both absorption and specific gravity place porosity as their second or third best correlated feature. Sodium sulfate, L.A. Abrasion, and the rating of the aggregate based on the number of passed FDOT tests, are in both cases best correlated with the porosity.

While the results presented in Table 0-7 and Table 0-8 don't seem to make physical sense given that the abrasion test correlated better with porosity than tests that are intuitively direct measurements of porosity, there is a plausible explanation for this observation. The petrographic analysis examines thin sections of the aggregate extracted from the interior of the rock. It may be easy to identify voids this way, but not necessarily so easy to identify voids that are interconnected, or would otherwise allow water to flow into them. Both the absorption and specific gravity are submersion tests and rely on the water's ability to penetrate the material's voids. Just because a certain level of porosity exists does not necessarily mean that water will penetrate the material fully. It is for this reason that other researchers have begun to perform other types of porosity tests and question the results typically obtained from the FDOT's standard tests of this type as discussed in Chapter 0. In every case the sodium sulfate soundness tests is

better correlated with the aggregates porosity than either of the other intrusion based tests. This could be due in part because of the lengthy submersion cycles.

It is difficult to make conjectures about the effectiveness of the FDOT's tests based on the presented data. The reason for this is there so little test data provided by the FDOT. Overall, the regression coefficients suggest that low to moderate relationships exist between the FDOT's tests and the petrographic characteristics of the carbonate samples. To get a better sense of how the FDOT's tests compare with the other two tests examined in this chapter, the regression coefficients obtained by comparing the five petrographic features against the measured responses of all the tests, considering only the carbonate samples, are given in Table 0-9.

Table 0-9 Regression Coefficients Comparing Experimental Tests with Average Petrographic Properties by Source Across Carbonate Sources

Concentration - Carbonates Only

	Absorption	Specific Gravity	L.A. Abrasion	Sodium Sulfate	Rating (1-4)	Impact FRF	Windsor Pin
Amorphous Calcite	0.3397	0.5220	0.0364	0.2189	0.2659	0.0588	0.0895
Sparry Calcite	0.0936	0.2730	0.2687	0.0121	0.0180	0.0998	0.0154
Matrix	0.1797	0.3682	0.1691	0.0621	0.0722	0.1432	0.0066
Quartz	0.0018	0.0513	0.0956	0.0786	0.0568	0.0180	0.0004
Voids	0.1654	0.1596	0.5093	0.2242	0.2854	0.0700	0.0181

Median Grain Size - Carbonates Only

	Absorption	Specific Gravity	L.A. Abrasion	Sodium Sulfate	Rating (1-4)	Impact FRF	Windsor Pin
Amorphous Calcite	0.1284	0.4133	0.0094	0.0137	0.0345	0.1316	0.0053
Sparry Calcite	0.1456	0.0291	0.3066	0.2302	0.2177	0.0145	0.0002
Matrix	0.0379	0.0003	0.0933	0.0540	0.0269	0.1362	0.0028
Quartz	0.0508	0.2138	0.1026	0.0001	0.0057	0.0274	0.1735
Voids	0.1227	0.1650	0.1863	0.0377	0.0583	0.0306	0.0089

The highest regression coefficient for each test is boxed and highlighted in Table 0-9, and close examination of the table will reveal that for amorphous calcite, sparry

calcite, and the concentration of matrix, the FDOT's specific gravity test boasts the highest regression coefficient of any of the tests in the table. The Los Angeles abrasion test shows the highest regression coefficients for the concentration of quartz and voids. Because of the small amounts of data from current durability tests, and the use of weak regression coefficients from global analyses of the other test data, it is questionable if the data in Table 0-9 represents a meaningful comparison of the relative effectiveness of the tests examined.

In Chapter 0 many of the variables lowering the confidence in the accuracy of the FDOT's tests were discussed in detail, including significant variability arising from inconsistent procedures, dissolution of aggregates in solution, and whether the quantities measured by these tests are truly accurate. It is highly unlikely that the data provided by the FDOT is not representative of typical results for the aggregates studied, but it has only provided a very limited amount of information. Furthermore, examination of the petrographic characteristics of the samples that were cored and eventually tested using the Windsor Pin System® and impact FRF technique contained a fair amount of variability from one sample to the next. Without knowing the petrographic characteristics of the samples that were subject to the FDOT's tests and having more data points from the FDOT to show the consistency of their tests, little confidence can truly be placed in determining if the current tests surpass those applied in this study in terms of their dependence on the measured petrography.

If the FDOT's tests are compared with the petrographic characteristics identified in the analysis performed by McClellan (2006), the results are significantly different.

Table 0-10 shows the regression coefficients resulting from the comparison of the FDOT and impact FRF test with these petrographic properties.

Table 0-10 Regression Coefficients Comparing FDOT & Impact FRF Tests with Petrographic Properties Identified by McClellan (2006)

Carbonates Only						
Property Concentration	**Absorption**	**Specific Gravity**	**L.A. Abrasion**	**Sodium Sulfate**	**Rating**	**Impact FRF**
Fossil Grains	0.8579	0.6468	0.4968	0.8247	0.8473	0.5398
Non-Fossil Grains	0.9400	0.8144	0.2767	0.7977	0.8294	0.3866
Moldic Porosity	0.0923	0.1858	0.2530	0.0501	0.0838	0.0015
Interparticle Porosity	0.0711	0.2625	0.3407	0.0031	0.0010	0.0324
Intragranular Porosity	0.0268	0.0018	0.0499	0.0874	0.0662	0.0001
Micrite Cement	0.0000	0.0367	0.0047	0.0573	0.0361	0.0381
Microspar & Sparite	0.0382	0.0008	0.8384	0.1473	0.1621	0.1187
Dolomitic Grains	0.1598	0.0054	0.1635	0.4166	0.3379	0.5304
Chert	0.1174	0.0834	0.6877	0.2505	0.3005	0.0022
Quartz	0.0108	0.0166	0.1106	0.0250	0.0129	0.4844
Opaques	0.5080	0.7717	0.1142	0.2225	0.2909	0.0197
Total Porosity	0.0039	0.0009	0.2588	0.0034	0.0004	0.0015
Total Cement/Matrix	0.0279	0.0306	0.5126	0.0178	0.0354	0.0183
Petrographic Number	0.0655	0.1728	0.9509	0.3718	0.4071	0.1114
All Lithologies						
Petrographic Number	0.0195	0.0896	0.1905	0.0534	0.0831	N/A

Table 0-10 shows some very strong correlations between the FDOT's tests and the petrographic properties identified in McClellan's (2006) analysis. In fact, based on the regression coefficients in Table 0-10, the Los Angeles Abrasion test appears to be the best correlated of all the tests having the highest regression coefficients when compared with moldic porosity, interparticle porosity, microspar and sparite cement, chert, total porosity, total cement, and petrographic number. The impact FRF test did fare considerably better having had the highest correlations of all the tests for the concentration of dolomite and chert, both perhaps the least abundant of the petrographic properties identified by McClellan (2006) across all the samples analyzed by this method.

The results in Table 0-10 are not very surprising. The petrographic analyses were performed in order to develop the petrographic number. The petrographic technique developed by Oyen *et al.*(1998), which is based on that developed by Bayne *et al.* (1955), was developed to correlate with the L.A. abrasion and sodium soundness tests. The strong correlation is somewhat irrelevant if one considers the data itself. Figure 0-10 shows the petrographic number for the sources studied with respect to the percent loss from the L.A. abrasion test provided by the FDOT.

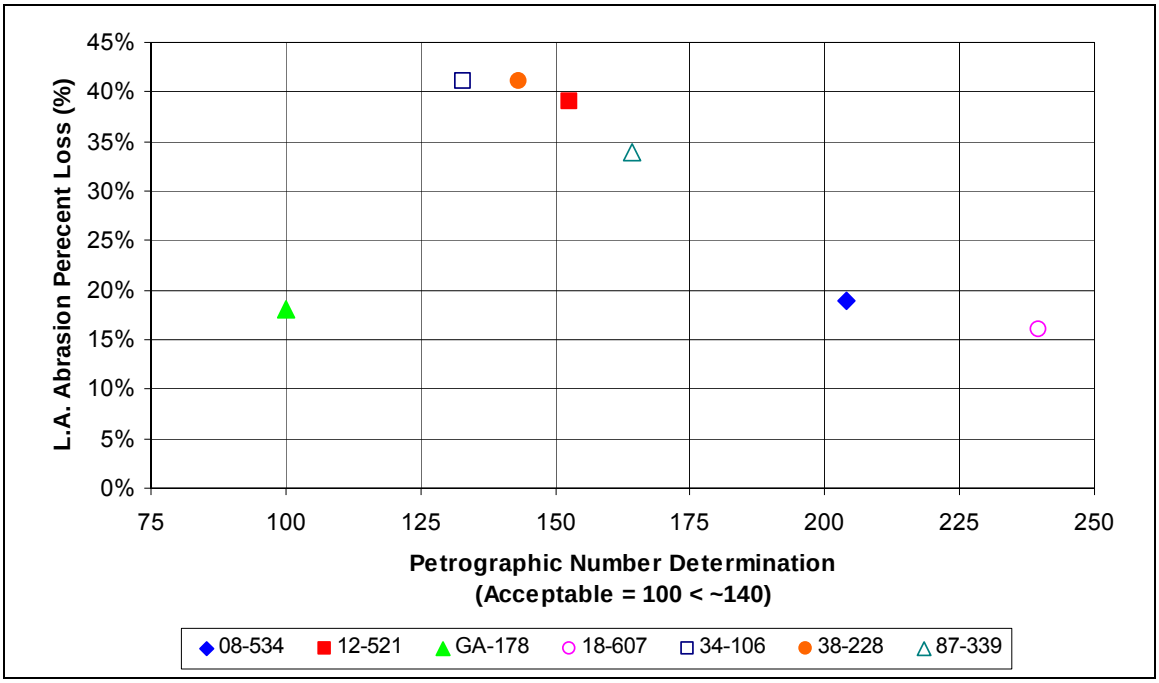

Figure 0-10 Petrographic Number With Respect to Los Angeles Abrasion Percent Loss Reported by FDOT

Based on the FDOT's requirements, listed in Table 0-1, aggregates showing a low percent loss are considered good quality. Conversely, the best aggregates have a petrographic number of 100, and are generally considered acceptable between 100 and 140. Petrographic numbers exceeding 140 are generally considered to have marginal to poor quality. Figure 0-10 shows that for the carbonate samples there is an excellent

correlation between the percent-loss from the abrasion test with the petrographic number, however the plot indicates that higher petrographic numbers result in lower percent loss, opposite of what is expected. Again, the data available from both techniques is too limited to pass substantial judgment on the validity of these results.

Plots showing the comparisons between the petrographic properties and the FDOT's tests are provided in Appendix G for further reference.

1.43 CONCLUDING REMARKS

Regression analyses resulting from the comparison of the measured responses from the applied test methods with the aggregate's petrographic properties have revealed an overwhelming amount of information. From this information there are several key things which stand out among the rest. In terms of both the Windsor Pin System® and the impact FRF test, strong relationships appear to exist for aggregates originating from the same source in many cases. The regression analyses for these tests showed many moderate to very strong relationships with several of the major petrographic characteristics examined. Conversely, neither test showed a strong global relationship between any of the petrographic properties examined and the applied tests. This result presents additional challenges to the development of a quality test using these test methods. Aggregate sources may have to be calibrated with the test in order to accurately discern concentrations of important geologic features. Global results may be improved if geologists, transportation authorities, and engineers can work together to better identify key characteristics or combinations of characteristics and investigate how well they can be measured with these techniques.

Comparing the FDOT's current line-up of tests against the Windsor Pin® and impact FRF test showed that the FDOT's tests produced better regression coefficients with the petrographic properties of interest, however there is such a limited amount of data that little confidence can truly be placed on these results. While initial findings suggest that in a global sense the FDOT's test are more effective at measuring aggregate properties, one cannot ignore the fact that correlations with some groups of samples for the other tests, the impact FRF tests in particular, were extremely strong showing regression coefficients greater than 0.95. One cannot also ignore the comparison of the petrographic number with the FDOT's L.A. Abrasion test which showed an unexpected relationship between high petrographic number and low percent loss.

To summarize the results, there is inconclusive evidence to support that the current FDOT quality tests are more effective than any of the methods applied in this study. There is clearly enough evidence to provide a foundation not only for future analysis of the data obtained in this study, but also to move forward with additional testing to expand on the results of the impact FRF test and perhaps also the Windsor Pin System®. The cooperation of members from the three fields of study will be essential in future work if an accurate quality test for these aggregates is to be developed.

SUMMARY, CONCLUSIONS, AND RECOMMENDATIONS

1.44 SUMMARY AND CONCLUSIONS

The development of a new method for evaluating the durability of aggregate material is truly multidisciplinary in nature. By examining previous research efforts and the history of aggregate quality testing, it is determined that there is a need for both accurate and efficient methods of assessing the properties of aggregates that affect its durability in various applications. Examination of the weathering mechanisms of rocks established a fundamental understanding of the basic properties that affect aggregate performance not only for carbonates, but across many classes of rock.

Mineral content, grain size, and porosity, the petrographic properties assumed to have a significant impact on aggregate performance, were identified through petrographic analysis by consultant geologists. These characteristics represent a collection of properties that describe a system, i.e. the aggregate samples. The applied test methods were used to measure these properties and were selected based on their simplicity, ease of implementation, and ability to perform at the quarry site.

Relationships between the applied methods and the system properties of interest must be established to properly develop any new testing protocol. To guide this process, the concept of a transfer function is applied to the analysis. Windsor Pin System®, acoustic impact-emission, and impact frequency response function testing were performed on the aggregate samples because it is assumed that the mechanical properties

of the samples' constituents will be strongly related to the measured responses. Linear regression analysis of the relationships between the petrographic properties of the samples and the measured responses of the applied methods was used to validate this assumption and establish the feasibility of the applied methods for use as an aggregate quality test. In the following paragraphs, the results of each test are summarized and their importance with respect to the development of a quality test is discussed.

Windsor Pin System® Tests

Windsor Pin System® tests, which indent the surface of the rock with a hardened steel pin, were performed on three or four rock samples from each of the seven aggregate sources. The measurements showed that in general the depth of penetration decreases with successive use of the pin. Several of the sources showed consistency in the average penetration depth, but several sources were also found to produce inconsistent average depth measurements. The variation in measurements is most likely attributed to factors such as, whether a grain or void is impacted, surface preparation, and the quality of the indentation left by the device. The observed variability could potentially be improved by more carefully preparing a flat surface on the test specimen and the collection of additional data.

Comparisons made between the petrographic features of interest and the depth of penetration measurements from the Windsor Pin System® showed several strong causal relationships when regression analysis was performed on samples originating from the same source. The relative levels of correlation between the measurements and the aggregate properties were shown to be similar across some sources. Comparisons of

depth measurements with respect to the petrographic characteristics across all of the sources did not reveal causal relationships that were as strong. The most immediate benefit that this test method poses for transportation officials is its potential as an initial screening tool; however, data supplied by the manufacturer, and the presence of some strong causal relationships indicate that the Windsor Pin System® has the potential to be used as an aggregate quality test with further study of the causal relationships observed.

Acoustic Impact-Emission Tests

Acoustic Impact-Emission tests were performed on three rocks samples from each aggregate source. The samples were excited with a steel ball suspended from a jig. Some samples were also excited using a hammer fitted with a force sensor. The acoustic response was measured with a microphone and examined in both the time and frequency domain. For some tests, an accelerometer was also affixed to the sample and its response examined in the frequency domain. The data indicated that the samples were not excited very well beyond 6 kHz. The measured responses were also found to be dependent on the orientation of the sample tested. There are significant similarities between the measured acoustic responses and the responses measured by the accelerometer. The level of background noise relative to the acoustic response, poor excitation at higher frequencies, poor coherence of measured acoustic response with respect to the input force, and the different and irregular geometries of the samples make it difficult to use this test to understand the true material differences of the samples. The non-contacting acoustic impact-emission test does not seem to be as effective at discerning material properties when performed on rough rock samples as contacting

measurements would be on uniformly prepared specimens. Further study of acoustic test methods is needed to understand how certain characteristics of the acoustic response may be related to material properties.

Impact Frequency Response Function Tests

Impact frequency response function measurements were conducted on core samples cut from the rocks subjected to petrographic analysis. The core samples were impacted using a lightweight force hammer and the response was measured with an accelerometer affixed to one end of the core. The acceleration with respect to force was measured several times for each core and the resonant frequencies, damping, and in some cases mode shapes were estimated from the data. It was found that the resonant frequencies could be estimated with much better consistency than damping from the collected measurements.

Considerable effort was made to investigate the factors contributing to inconsistencies in the damping estimates. It was found that environmental effects and the method of affixing the sensor to the core have a significant impact on the damping present in the response. The data showed that the measured frequencies were far less sensitive to the test setup than the damping estimates. The dependency of the damping estimates on the test set up was significant enough to omit them from analysis with the petrographic characteristics of the aggregates. Further study is needed to determine the most consistent method for measuring the response and estimating damping before it can be used to measure aggregate properties.

Regression analysis of resonant frequencies with respect to the petrographic characteristics of the samples showed many strong relationships when samples from a single source were analyzed. The relative level of correlation between the resonant frequencies and the petrographic characteristics were similar across several sources. Regression analysis of the data across all of the samples did not reveal relationships that were as meaningful as those for an individual source.

Analysis of the regression lines showed that certain constituents consistently affect the measured response, contributing to either mass or stiffness across all of the sources. Constituents that do not show consistent regression slopes indicate that combinations and distribution of petrographic characteristics within a particular sample are important to consider in future analysis and the development of a durability test. Sample geometry was also found to be important to the regression analyses.

While global analyses did not show strong causal relationships, the impact frequency response function test shows great potential as an aggregate durability test. This potential may be realized with further analyses of various combinations of petrographic characteristics with respect to the resonant frequencies. Such a study may be accomplished with the use of principle component analysis and other statistical methods. Damping estimates may reveal additional useful information if additional testing can improve the dependency of the damping estimates on the material properties of the tested structure.

Comparison of Test Methods

The current durability and soundness tests used by the Florida Department of Transportation were compared with the average petrographic characteristics of the rock sources examined. These global analyses showed slightly stronger relationships between the aggregate properties and the FDOT test data than was evident in global comparisons between the aggregate properties and the Windsor Pin® and impact FRF data. However, the relationships between any one of the FDOT's aggregate tests compared to the petrographic characteristics were not as strong as the strongest relationships between the impact FRF and Windsor Pin® data for a single source in many instances. The relationships between the current durability tests and the petrographic characteristics of the samples should be examined with additional test data from the four durability tests performed by the FDOT. This is necessary to better understand whether these tests are truly better related, in a global sense, to the petrographic characteristics than the physical tests used in this study. Examination of relationships between the several of the FDOT tests and the petrographic characteristics, as well as the petrographic number determination, revealed some unexpected results, and further supports the need to examine additional FDOT test data with respect to aggregate properties.

1.45 RECOMMENDATIONS

The presence of strong relationships between the measured responses and the system properties for some aggregate sources is a positive indicator that physical tests can be used to evaluate aggregate properties. While relationships on a global scale were not as telling of this, the strength of the local relationships cannot be ignored. The

applied methods warrant further study through additional analysis and testing. Recommendations for future work are summarized below.

1) It is recommend that engineers, geologists, and transportation officials continue to work closely to develop efficient and effective means of evaluating the durability of aggregate materials. A higher level of cooperation between the contributing disciplines is needed to better understand the factors affecting their performance and possible means of measuring them.
2) It is recommended that a standard method be devised to define and document aggregate quality and field performance. Bayne *et al.* (1955) based their petrographic number technique on an extensive study of aggregates with varying degrees of durability and serves as an excellent model for a modern system. The system should be comprehensive, yet qualitative so that once implemented assessments of field performance can be used to establish the relationship between field performance and quality tests. Duration of field service, on-site conditions, and source quarry are important pieces of information to record in such a system. This recommendation is inline with the recommendation of several past studies such as Eades *et al.* (1997).
3) It is recommended that future work should attempt to identify meaningful combinations of the petrographic characteristics that affect aggregate durability. Identification of the proper combinations of matrix, voids, and other granular material in Florida aggregates that relate to durability will provide a foundation for more thorough analysis of aggregate properties with respect to the measured

responses of applied test methods. As an example, a study performed by Tuğrul (1999) compared the ratio of quartz and feldspars (ratio of highly durable to considerably less durable constituents) in granite samples to engineering properties of interest. A similar pairing of mineralogical and textural components for carbonate samples may lead to very useful analyses of data in the future. The use of principle component analysis or other multivariate correlation techniques may be useful tools in determining the best relationships which exist between aggregate petrography and the physical tests applied in this study.

4) Additional impact FRF tests on core specimens with tighter tolerances on geometry should be performed to increase the statistical significance of the results presented in the thesis. These specimens should be larger than those used in this study to investigate the effect of sample size on the bulk properties and measured responses. Tests should also utilize more consistent methods of affixing sensors to the test structure especially if damping estimates are to be used in the analysis. Even though the frequencies were shown to be only marginally affected by the environmental conditions examined, this too should be further investigated to validate the results presented.
5) As an alternative to coring additional rock samples, the methods investigated in this study can be applied other materials such as concrete or asphalt mix designs. In many cases it may be possible to manufacture a large number of test specimens with specified ratios of constituents to establish causal relationships between physical nondestructive tests and the properties of the mix. This may be a very feasible approach to apply to concrete mix designs since there is an abundance of

data which relates the mix characteristics to engineering properties. The cooperation of transportation officials, geologists, and engineers would still be required for such a study to be successful. While this alternative does not relate directly to rip rap structures or other methods of bank and shore protection, it would continue to develop the necessary fundamentals of a durability test that are required for the task at hand.

6) Future Windsor Pin System® tests should be performed on rock samples with prepared surfaces to reduce the observed variability as much as possible. Additional analysis should be performed comparing the measured indentations with combinations of petrographic characteristics with the cooperation of geologists. The success of this device as a mildly nondestructive test of concrete compressive strength and the instances of strong relationships with petrographic properties suggests that the Windsor Pin System® has definite potential as an aggregate durability test.
7) If acoustic methods are to be pursued in future studies, the material and structural properties of the test article that affect the response characteristics needs to be studied. It needs to be determined if the characteristic sound of the impact can be paired with material properties with some consistency. Descriptions of audible responses must also be characterized through examination of the data in some definitive manner and not through subjective observation.

1.46 FINAL REMARKS

The results of analyzing the causal relationships between the measured responses and the system properties showed promise for the Windsor Pin System® and impact frequency response functions to eventually be developed into viable quality tests. The analyses will be more meaningful, and possibly yield better correlations, if geologists and engineers can continue to work together to establish meaningful combinations of petrographic properties that are important to the durability of the materials studied.

It is clear from the literature and the results of this study that the biggest problem facing the development of aggregate quality tests lies in understanding the aggregate's properties and how they are related to field performance. Acquiring a more rigorous understanding of aggregates' properties, and in what ways they affect durability, is critical for future analyses and the validation of new test methods. Once the properties of the system which drive durability are clearly understood, the input-output dependency on the system's properties with respect to the Windsor Pin System® and impact frequency response functions can be more easily described across many aggregate sources. In keeping with the transfer function model presented, the ability to demonstrate strong dependencies of aggregate properties with measurable responses must serve as the foundation for an accurate quality test. The results of this study indicate that such strong relationships do exit between aggregate petrography and physical test data. While enough information has not yet been compiled to develop a durability test, this study has taken an important first step to accomplishing this goal.

LITERATURE CITED

Construction Aggregates Manual, Published by FDOT, Date Issued: December 1, 2004.

AASHTO T 85-91 (2000), ASTM C 127-88 (1993), "Specific Gravity and Absorption of Coarse Aggregate."

Eades, James L., McClellan, Guerry H., Ruth, Byron E., Fountain, Kendall B., and Bennett, David; "Evaluation of Soundness Tests on Florida Aggregates," Department of Geology & Department of Civil Engineering, University of Florida. Sponsored by the Florida Department of Transportation, March 1997.

Florida Method of Test FM 1 T-085, "Specific Gravity and Absorption of Coarse Aggregate."

Florida Method of Test FM 3-C 535, "Resistance to Degradation of Large-Size Coarse Aggregates by Abrasion and Impact in the Los Angeles Machine."

ASTM C 535 – 01, "Standard Test Method for Resistance to Degradation of Large-Sise Coarse Aggregate by Abrasion and Impact in the Los Angeles Machine."

Wu, Yiping; Parker, Frazier; and Kandhal, Ken; "Aggregate Toughness/Abrasion Resistance and Durability/Soundness Tests Related To Asphalt Concrete Performance in Pavements." NCAT Report No. 98-4, January 1998.

Meininger, Richard C.; "Validity of the Sulfate Soundness Test." Rockproducts.com, ©2005 by Primedia Business Magazines & Media Inc., Aug 1, 2002.

Gregory, James Scott; "Testing Protocol Evaluation and Petrologic Characteristics of Florida Riprap Sources." Master's Thesis, Department of Geological Sciences, University of Florida, 2004.

Florida Method of Test, FM1-T104, "Sodium or Magnesium Sulfate Soundness Test for Riprap."

AASHTO T 104-99, "Soundness of Aggregate by Use of Sodium Sulfate or Magnesium Sulfate."

FDOT Standard Specifications for Road and Bridge Construction Section 530 – Riprap.

Federal Interagency Stream Corridor Restoration Handbook, Appendix A: Techniques. United Stated Department of Agriculture, Natural Resources Conservation Service. Accessed January 19th, 2006. http://www.nrcs.usda.gov/technical/stream_restoration/appendix0002.html

"Classification of NDT Methods" The American Society For Nondestructive Testing. http://www.asnt.org/ndt/primer4.htm read revision accessed 10/24/2006.

Doebling, Scott W.; Farrar, Charles R.; Prime, Michael B.; and Shevitz, Daniel W.; "Damage Identification & Health Monitoring of Structural & Mechanical Systems From Changes in Their Vibration Characteristics: A Literature Review" LA-13070-MS, Produced by Los Alamos National Laboratory, May 1996.

Johnson, Paul A., and Cate, James A Ten, "The New Wave in Acoustic Testing," Materials World, the Journal of the Institute of Materials for publication in the September 1999 issue pp. 544-546. See also http://www.ees11.lanl.gov/nonlinear/diagnostics.html, this paper also titled, "Non Destructive Testing of Materials By Nonlinear Elastic Wave Spectroscopy (NEWS)," Los Alamos Seismic Research Laboratory, Los Alamos National Laboratory.

Abeele, Koen E-A. Van Den; Sutin, Alexander; Carmeliet, Jan; and Johnson, Paul A., "Micro-damage diagnostics using nonlinear elastic wave spectroscopy. NDT & E International, 34, 2001, pp. 239-248.

Bodare, Anders G., "Non destructive test methods of stone and rock," Geo Texts & Publications, www.Geoforum.com. Last accessed October 6th, 2006. http://www.geoforum.com/knowledge/texts/bodare/index.asp?Lang=Eng

Essenreiter, Robert; Karrenbach, Martin; Treitel, Sven; "Multiple Reflection Attenuation in Seismic Data Using Backpropagation," IEEE Transactions on Signal Processing, v. 46, no. 7, July 1998.

Delsanto, P. P.; Johnson, P. A.; Scalerandi, M; and TenCate, J. A., "LISA simulations of time-reversed acoustic and elastic wave experiments," Journal of Physics D: Applied Physics, 35, 2002, pp. 3145-3152.

Guyer, Robert A., & Johnson, Paul A., "Nonlinear Mesoscopic Elasticity: Evidence for a New Class of Materials", Physics Today, April 1999, pp 30-36.

Guyer, Robert A., TenCate, James, & Johnson, Paul, "Hysteresis and the Dynamic Elasticity of Consolidated Granular Materials," Physical Review Letters, The American Physical Society, Vol. 82, No. 16, April 19, 1999.

Johnson, Paul A., Ten Cate, James A., Smith, Eric, Guyer, Robert A., & Shankland, Thomas J., "The Concept of Universality Class, Slow Dynamics and universality," Poster produced by EES-11 Geophysics Group, Los Alamos National Laboratory. Last Accessed on-line at: http://www.ees11.lanl.gov/EES11/Staff/Johnson/Poster1/UniversalityClass.PDF, or at: http://www.ees11.lanl.gov/EES11/Staff/Johnson/Poster1/index.html January, 2007.

Feldman, R. F., "Non Destructive Testing of Concrete," CBD-187. Canadian Building Digest. Originally published 1977. Accessed online 10/24/06 at: http://irc.nrc-cnrc.gc.ca/pubs/cbd/cbd187_e.html.

Pascale, Giovanni; Di Leo, Antonio; Carli, Roberto; "Evaluation of Actual Compressive Strength of High Strength Concrete by NDT," 15th World Conference on Nondestructive Testing, 2000 conference paper.

Saeed,, Athar; Hall, Jim W. Jr.; Barker, Walter; "Performance-Related Tests of Agggregates for use in Unbound Pavement Layers," NCHRP Report 453, National Academy Press, Washington, D.C., 2001.

Roy, Dr. Della M., "Relationships of Portland Cement Characteristics to Concrete Durability," Research Results Digest, No. 270, October 2002.

Folliard, Dr. Kevin J.; Smith, Kurt D.; "Aggregate Tests for Portland Cement Concrete Pavements: Review & Recommendations," Research Results Digest, No 281, September 2003.

McClellan, Guerry, H. Consultant Geologist, Final Report and Addenda for Petrographic Rock Studies submitted to the University of Massachusetts Lowell, June, 2006.

Nagel, Scott, Consultant Geologist (Scott Nagel Consultant Geologist Inc.), Final reports for petrographic studies of aggregate samples submitted to the University of Massachusetts Lowell, August, 2006.

Bayne, R. L., Brownridge, F. C., "Petrographic Analysis for Determining Quality of Coarse Aggregates," Proceedings of the convention – Canadian Good Roads Association, vol. 36, 1955, pp. 114-122.

McClellan, Guerry, H.; Eades, James L.; Gregory, James Scott; Fountain, Kendall B.; "Evaluation and Petrologic Characters of Florida Rip Rap Sources, Final Report," Department of Geological Sciences, College of Liberal Arts and Sciences, University of

Florida. Sponsored by the Florida Department of Transportation State Contract No. BC354, RPWO #33, 2002.

Skinner, Brian J., & Porter, Stephen C., "The Dynamic Earth, an introduction to physical geology," 2nd ed. Wiley, New York, 1992.

Kemp, James Furman. Ed. By Grout, Frank F. "A Handbook of Rocks," D. Van Nostrand Co. Inc., New York, 1926.

Tyrrell, G. W., "The principles of Petrology," Methuen & Co. LTD, London, 1926.

Chesterman, Charles W., and Lowe, Kurt E., "National Audubon Society Field Guide to Rocks and Minerals," Knopf, New York, 1979.

Allaby, Ailsa, Allaby, Michael, "Dictionary of the Earth Sciences," 2nd ed., Oxford University Press, New York, 2003.

Moorhouse, W.W., "The Study of Rocks in Thin Section," Harper & Row, New York, 1959.

Berubé, Marc-André, "The mineralogical and Petrographic Analysis of Concrete Aggregates," Journal of the Minerals, Metals & Materials Society, December, 2001, pp. 45-47.

Oyen, C.W., Fountain, K.B., McClellan, G.H., and J.L. Eades, "Thin-section petrography of concrete aggregates: An alternative approach for petrographic number evaluation of carbonate aggregate soundness," Transportation Research Record, No. 1619, 1998 pp. 18-25.

Tuğrul, A., Zarif, I.H., "Correlation of mineralogical and textural characteristics with engineering properties of selected granitic rocks from Turkey," Engineering Geology, No. 51, 1999, pp. 303-317.

NDT James Instruments, Inc. James Windsor Pin System Technical Manual and brochure. Can be found at www.ndtjames.com. Technical Manual last accessed 11/15/2006.

Callister, William D., Jr., "Materials Science and Engineering, An Introduction," 6th Ed., Wiley, 2003, pp. 134-140.

Harris, Cyril M., Piersol, Allan G., "Harris' Shock and Vibration Handbook," 5th Ed., McGraw-Hill, New York, 2002, p. 1.13.

Boggs, Sam Jr., "Principles of Sedimentology and Stratigraphy," 3rd Ed., Prentice Hall, New Jersey, 2001, pp. 2-9, 170-208.

EMPA, Materials Science & Technology, "Non-destructive testing methods," accessed online from http://empa.ch, Article can be found at http://www.empa.ch/plugin/template/empa/*/8938/---/l=2, last accessed online January 2007.

SOURCES REFERENCED BUT NOT CITED

United States Army Corps of Engineers, EM 1110-2-1601, Chapter 3: Riprap Protection, Change 1, June 30, 1994.

Lake, Donald W. Jr., Section 7B: Permanent Structural Measures for Erosion and Sediment Control. New York Standards and Specifications For Erosion and Sediment Control, March 2003.

6010 Specification for Stone Riprap at Bridges. Saskatchewan Highways and Transportation, January 1996.

Avitabile, Peter. "Mechanical Vibrations Overview of Experimental Modal Analysis." Department of Mechanical Engineering, University of Massachusetts Lowell. February, 2003.

Berner, Elizabeth Kay, Berner Robert A., "Global Environment, Water, Air, and Geochemical Cycles," Prentice Hall, New Jersey, 1996.

"Introduction to Nondestructive Testing" The American Society For Nondestructive Testing. http://www.asnt.org/ndt/primer1.htm read revision accessed 10/24/2006.

"Purpose of Nondestructive Testing" The American Society For Nondestructive Testing. http://www.asnt.org/ndt/primer2.htm read revision accessed 10/24/2006.

"Rapid Growth And Acceptance of Nondestructive Testing" The American Society For Nondestructive Testing. http://www.asnt.org/ndt/primer3.htm read revision accessed 9/29/2003.

Iddings, Frank A., "Vibration Analysis Sensors," Back to Basics, The American Society For Nondestructive Testing, 1997. http://www.asnt.org/publications/materialseval/basics/may97basics/may97basics.htm

Dijkstra, F. H., & Raad, J. A. de, "NDT Solution, Nondestructive Testing: Necessary Evil or Benefit?" The American Society For Nondestructive Testing, 2003. http://www.asnt.org/publications/materialseval/solution/aug02solution/aug02sol.htm

Bhardwaj, Mahesh C., "Non-Contact Ultrasound For Civil Infrastructure Diagnostics." Author is the director R&D, SecondWave Systems, 1020 Boal Avenue, Boalsburg, PA 16827, www.secondwavesystems.com.

Ehle, Austin & Sumali, Hartono (Advisor), "Exploring Dynamic Properties of Fruit, an Undergraduate Research Report," Agricultural and Biological Engineering Department, Purdue University, April 2002.

Tran, Ai Binh; Fines, Pamela; Miller, Stuart; Williams, David; Wilson, Ward; "Hydrological and Geotechnical Characterization of Two Full-Scale Waste Rock Piles, A Joint University/Industry Research Program Sponsored by INAP," Geotechnical News, volume 21, number 3, September 2003, pp. 36-42.

"A Summary of Operational Differences Between Nuclear And Non-Nuclear Density Measuring Instruments," Prepared by Sully-Miller Contracting Company Quality Control Department, October 2000.

APPENDIX A: NONDESTRUCTIVE TEST METHODS

There are many varieties of non-destructive tests. Many of these methods have been tabulated from the literature and are listed in Table A-1. The table may stretch across several pages.

Table A-1 Table of Non-Destructive Testing Techniques

Category	***Objectives***	***Typical Tests Performed***	***Description of Tests***
Mechanical	Detection of color, cracks, dimensions, film thickness, gauging, reflectivity, strain distribution & magnitude, surface finish, surface flaws, through-cracks	Modal Hamer	A force hammer is used in conjunction with a transducer or set of transducers (usually accelerometers) to acquire FRF's in an effort to determine M, C, & K for the structure
		Shaker	A mechanical shaker or vibrator is used to excite one or a bandwith of frequencies of a structure to acquire an FRF in an effort to determine M, C, & K for the structure
		Rebound Hammer	Typically use of a Schmidt Hammer
		Schmidt Hammer	Spring loaded impact test that measures the rebound of the impactor. Rebound number related to the amount of energy dissipated in the material. Non homogeneous materials (geotech) are difficult to test.
		Hammer Impact	Measures the force time history from a hammer impact. Length of impact varies for high and low quality material
Seismic Methods	Similar to the Mechanical Objectives	Seismic Transmission Method	Similar to Modal hamer or Shaker test. Primary and Secondary waves are measured from a pulse source or steady-state vibration. For this method transducers must be located on the face opposite the excitation. Calculation of average wave speed in the material is accomplished by using time differences between excitation and response. While using the steady-state method, the phase difference is measured in order to accquire the average wave speed in the material. Can be used to measure internal dissipation, damping, and attenuation. - Bodare
		Seismic Refraction Method	Excitation by detonation or large vibrator. Travel times and locations are measured. In principle this method works for a shallow homogeneous layer with Cp1 on top of another homogeneous layer with wave speed Cp2 of infinite depth. P-wave velocity must increase monotonically with depth. Only global damages can be detected.
		Seismic Reflection Method	Measures reflected waves from discontinuities or damages beneath the surface. Can detect local and global damages. Established method in geophysics. Similar to Seismic Refraction.

		Seismic Surface Wave Method	New method called SASW (Spectral Analysis of Surface Waves) and is developed from the Thompson-Haskell Method. Excitation by drop weight, vibrator, hammer, or other short mechanical pulse. R-waves, or surfave waves penetrate to a distance approximately 1 wavelength, thus different frequencies can be used to investigate the medium to different depths. Trial and error is an integral part of the data processing which may prove to be difficult and time consuming.
		Impact Echo Method	Hammer is used to introduce a stress pulse. Discontinuities reflect the pulse back to the surface and so forth. Frequency of surface motion from this excitation is measured. The movement is regarded as a resonance between the surface and the discontinuity. Both local and global damage can be detected, though this is not an established test method at the time Bodare wrote the article.
Optical	Detection of color, cracks, dimensions, film thickness, gaging, reflectivity, strain distribution & magnitude, surface finish, surface flaws, through-cracks	Photoelastic Stress Analysis	Involves creating a scale model out of transparent plastic such that stress induced birefringence is proportional to the stress in the part.
		Holographic Interferometry	The interference of the two coherent wavefronts is recorded on a photographic plate. To measure surface displacements, two such wave patterns are recorded when the object is in its original and deformed states, and these are combined to give an interference fringe pattern, called an interferogram, related to the movement that has taken place. The fringes actually represent contours of equal displacement, with each successive fringe representing a change in displacement of the object approximately one-half the wavelength of the light source used in the recording process.
		Moiré Method	Uses two gratings overlayed on an object. Displacements change the spacial frequency of the grating. The displaced image is compared with the original undisplaced one.
		Speckle Photography	Scattered light from an object is recorded on a photographic plate before and after deformation. The displacement is determined by illuminating the photographic plate and viewing the light in the Fourier Plane.
		Electronic Speckle Pattern Interferometry	Continuous speckle patterns from illuminating an object with laser light are compared. An interferogram is used to determine the displacement.
		Visual Inspection	Visual tools are perhaps still the most widely used form of NDT. A skill technitian or field expert can in many situations identify deficiencies in a structure. Much the way food can look burned, rocks are often examined by geologists using thin speciments (<50μm) or by examination of rock on a larger scale.
Penetrating Radiation	Detection of cracks, density & chemistry variations, elemental distribution, foreign objects, inclusions, microporosity, misalignment, missing parts, segregation, service degradation, shrinkage, thickness, voids	Ground Penetrating Radar (GPR)	Antenna transmits FM radio frequency pulses into the ground. Electric mediums in the ground reflect some of the signal and a subsurface profile can be create by measuring this reflection. Can only be performed on non-conducting materials.
		Nuclear Proctor Moisture Density Test	Standard compaction level tests performed using a nuclear source and detector. The source is driven into compacted subgrade and allowed to emit to the surface. The device is calibrated to display % compaction and moisture content when used in conjunction with compaction

			moisture curve.
Electromagnetic	Detection of alloy content, anisotropy, cavities, cold work, local strain, hardness, composition, contamination, corrosion, cracks, crack depth, crystal structure, electrical and thermal conductivities, flakes, heat treatment, hot tears, inclusions, ion concentrations, laps, lattice strain, layer thickness, moisture content, polarization, seams, segregation, shrinkage, state of cure, tensile strength, thickness, disbonds	Alternating Current Field Measurements	A uniform electric current is induced in the material. It produces a magnetic field which is disturbed by the presence of discontinuities.
		Electromagnetic induction of burried conductors	Buried coils are used to induce electromagnetic currents in conductive materials in the ground. Their electromagnetic field is then measured. Only local metal objects can be detected. Used to study clay deposits, salinity of ground water, weathering of rock, weak zones, etc.
Electronic	Detection of alloy content, anisotropy, cavities, cold work, local strain, hardness, composition, contamination, corrosion, cracks, crack depth, crystal structure, electrical and thermal conductivities, flakes, heat treatment, hot tears, inclusions, ion concentrations, laps, lattice strain, layer thickness, moisture content, polarization, seams, segregation, shrinkage, state of cure, tensile strength, thickness, disbonds	Ground Resistivity	Apparent resistivity is measured by introducing a current between two surface electrodes and measuring the resitance between two others. Factors that affect results include salinity content of moisture, porosity, etc. Different soil types and conditions can yeild the same results. Detects only Global damages
Sonic	Detection of crack initiation and propagation, cracks, voids, damping factor, degree of cure, degree of impregnation, degree of sintering, delaminations, density, dimensions, elastic moduli, grain size, inclusions, mechanical degradation, structure of composites, surface stress, tensile, shear & compressive strength, disbonds, wear	Local Interaction Simulation Approach (LISA) for Time Reversed-Acoustic (TRA) & Time Reversed Elastic (TRE) measurements	Uses a piezoelectric source to induce waves in a material. Through the use of computers and receiver transmitters, the time reversed signals can be used to locate scatering discontinuities in the material.
		Acoustic Emission Methods	Measures elastic wave propagation to surface. Using several transducers can help to locate the source. Counts, or events, are measured per unit time. Often frequency content, energy, and duration are also measured. Similar to measurements taken by seismologists. This method requires complicated procedures and equipment

Ultrasonic	Detection of crack initiation and propagation, cracks, voids, damping factor, degree of cure, degree of impregnation, degree of sintering, delaminations, density, dimensions, elastic moduli, grain size, inclusions, mechanical degradation, structure of composites, surface stress, tensile, shear & compressive strength, disbonds, wear	Ultrasonic Pulse Velocity (UPV)	Similar to Seismic Transmission Method but using ultrasonic waves f>20kHz
		Ultrasonic Pulse Echo (UPE)	Similar to Seismic Reflection Method
		Seismic Echo (SE)	Reflection method utilizing lower frequencies excited by a hammer. Provides force data in addition to time and location data
		Impulse Response (IR)	Dynamic Stiffness and distance to discontinuity acquired by measuring a transfer function between the acceleration and force excitation of the material.
		Quantitative Ultrasonics (QU)	Transmission or reflection. Used to measure distributed damages such as micro cracks and porosity variations.
		Acousto Ultrasonics (AU)	Originally developed for composite materials. Monitors changes of the element with time.
Thermal	Detection of bonding, composition, emissivity, heat contours, plating thickness, porosity, reflectivity, stress, thermal conductivity, thickness, voids		
Infrared	Detection of bonding, composition, emissivity, heat contours, plating thickness, porosity, reflectivity, stress, thermal conductivity, thickness, voids		
Chemical	Alloy identification, composition, cracks, elemental analysis & distribution, grain size, inclusions, mactrostructure, porosity, segregation, surface anomalies		
Analytical	Alloy identification, composition, cracks, elemental analysis & distribution, grain size, inclusions, mactrostructure, porosity, segregation, surface anomalies		
Image Generation	Detection of dimensional variations, dynamic performance, anomaly characterization and definition, anomaly distribution, anomaly propagation, magnetic field configurations		
Signal Image Analysis	Detection of data selection, processing & display, anomaly mapping, correlation & identification, image enhancement,		

	separation of multiple variables, signature analysis.		
Nuclear	Use of a radioactive source to detect penetrating properties of mediums. Rely on a variety of parameter ranging from particle detection to back scatter detection to attenuation.	Radon Detection	There are several different classes of radon detection techniques. These techniques are based on the detection of Alpha particles but in some cases may also include beta and gama emissions. The most common detection techniques as described by Andreas C. George are: Grab Sampling, Integrating techniques, and integrated Radon Progeny monitors.
		Borehole explorations	A combination of radioactive sources are contained in a pressure vessel and sunk into a fluid or mud filled borehole. Through this type of investigation Porosity, saturation, lithology and mineral content can often be detected.
		X-Ray Radiography	Image of sample is produced in the same manner as bone from a medical X-Ray. May allow detection of various properties including changes in density, composition, and the presense of internal flaws in the material
		Neutron Radiography	Requires radiating a sample in a chamber. The presnsence of decaying nuclear particles indicates the composition of the material. Contrastly from X-Rays, neutron radiography can detect both light and heavy elements. Often is used in conjunction with X-Rays. See http://mnrc.ucdavis.edu/radiography.html
		Neutron Tomography	Maps a 3D representation of the object using tomography and neutron radiology techniques. Some pictures have been printed from http://mnrc.ucdavis.edu/radiography.html.

APPENDIX B: PETROGRAPHIC DESCRIPTIONS

B.1 GENERAL REMARKS

Petrographic descriptions are furnished by two consultant geologists contracted independently for this project. Petrographic descriptions provided by SNCGI Incorporated of Boston, Massachusetts (Nagel, 2006) and by Dr. Guerry McClellan, Consultant Geologist, of Gainesville, Florida (McClellan, 2006). Petrographic samples are identified by FDOT aggregate source number and sample number with multiple descriptions for the same rock denoted by a letter following the sample number.

B.2 PETROGRAPHIC DESCRIPTIONS BY SNCGI

Petrographic slides were prepared during the coring process which created the test specimens for the impact frequency response function tests described in Chapter 8. Multiple core samples cut from a single rock are identified by a letter following the sample number. Petrographic slides for SNCGI's analyses (Nagel, 2006) are prepared from core samples used for impact FRF testing. Multiple slides from a single core are identified by a letter following the place holder value in the core identification scheme.

The results of each analysis are documented in a one-page report which includes percent concentrations of the observed features, a written description of the sample, and a color photograph of the magnified slide. The reports are organized by aggregate source. The results of the point-count analysis are tabulated in Table B-2 through Table B-7. The individual reports follow. Notes pertaining to the tabulated data for SNCGI's analyses (Nagel, 2006) are provided in Table B-1.

Table B-1 Notes With Respect to Point-Count Tables for Nagel's (2006) Data

Notes:	1) Median Sizes are Calculated based on the Max and Min size on the reports.
	2) If the percentage of a mineral is listed as <1%, it is entered into the sheet as 0.1%.
	3) If typical size is listed as <0.01mm it is entered as 0.001mm.
	4) Cells containing a "0%" have had that zero placed there to assure that the reduced data's percentages add up to 100%. Excel would otherwise neglect the empty cells in the average.

Table B-2 Results of Point-Count Analysis for 08-534 and 12-521

Source			08-534			12-521				
Feature/slide No.			1	2B	7	1B	6	8AA	8BB	9
Calcite, Sparry	Percentage (%)		9%	1%	2%	2%	2%	2%	2%	2%
	Size (mm)	Min	0.12	0.04	0.12	0.02	0.08	0.03	0.03	0.03
		Median	1.01	0.17	0.25	0.03	0.18	0.06	0.05	0.11
		Max	1.90	0.30	0.38	0.04	0.28	0.08	0.07	0.18
Matrix	Percentage (%)		73%	91%	85%	73%	81%	84%	75%	79%
	Size (mm)	Min	0.00	0.00	0.00	0.00	0.00	0.00	0.00	0.00
		Median	0.01	0.01	0.01	0.01	0.01	0.02	0.02	0.01
		Max	0.01	0.01	0.01	0.01	0.01	0.03	0.03	0.01
Quartz	Percentage (%)		17%	3%	9%	1%	1%	3%	3%	1%
	Size (mm)	Min	0.07	0.03	0.04	0.05	0.04	0.08	0.05	0.05
		Median	0.11	0.07	0.10	0.14	0.11	0.13	0.18	0.20
		Max	0.15	0.10	0.15	0.23	0.17	0.18	0.30	0.35
Void	Percentage (%)		1%	5%	4%	24%	16%	11%	20%	18%
	Size (mm)	Min	0.03	0.10	0.07	0.07	0.02	0.05	0.02	0.12
		Median	0.42	0.49	0.28	1.25	1.61	1.14	4.19	2.60
		Max	0.80	0.87	0.48	2.42	3.20	2.23	8.35	5.07

Table B-3 Results of Point-Count Analysis for 18-607

Source			18-607								
Feature/slide No.			5AA	5BB	8AA	8BB	9	10A	10B	10D	10E
Calcite, Amorphous	Percentage (%)				72%	80%		69%			
	Size (mm)	Min			0.00	0.00		0.00			
		Median			0.02	0.02		0.02			
		Max			0.03	0.03		0.03			
Calcite, Sparry	Percentage (%)		3%	8%	24%	14%	25%	28%	22%	17%	18%
	Size (mm)	Min	0.03	0.03	0.03	0.03	0.03	0.03	0.03	0.03	0.03
		Median	0.07	0.24	0.14	0.12	0.11	0.14	0.08	0.09	0.08
		Max	0.10	0.45	0.25	0.20	0.18	0.25	0.12	0.15	0.13
Matrix	Percentage (%)		93%	70%			73%	0%	78%	81%	79%
	Size (mm)	Min	0.00	0.00			0.00		0.00	0.00	0.00
		Median	0.02	0.02			0.02		0.02	0.02	0.02
		Max	0.03	0.03			0.03		0.03	0.03	0.03
Void	Percentage (%)		4%	22%	4%	6%	2%	3%	0%	2%	3%
	Size (mm)	Min	0.03	2.55	0.11	0.03	0.10	0.02	0.20	0.05	0.12
		Median	0.68	6.40	1.10	2.45	1.18	0.76	0.26	1.33	0.51
		Max	1.32	10.25	2.08	4.87	2.25	1.50	0.32	2.60	0.90

Table B-4 Results of Point-Count Analysis for 34-106

Source			34-106							
Feature/slide No.			2AA	2BB	6AA	6B	9A	9B	10AA	10B
Calcite, Amorphous	Percentage (%)					50%			14%	
	Size (mm)	Min				0.00			0.00	
		Median				0.02			0.02	
		Max				0.03			0.03	
Calcite, Sparry	Percentage (%)		0%	0%	16%	40%	57%		80%	93%
	Size (mm)	Min	0.03	0.03	0.03	0.03	0.04		0.03	0.02
		Median	0.04	0.07	0.27	0.08	0.14		0.07	0.06
		Max	0.04	0.10	0.50	0.12	0.23		0.10	0.10
Matrix	Percentage (%)		90%	92%	74%		37%	96%		
	Size (mm)	Min	0.00	0.00	0.00		0.00	0.00		
		Median	0.02	0.02	0.02		0.01	0.01		
		Max	0.03	0.03	0.03		0.01	0.01		
Pyrite	Percentage (%)							0%		
	Size (mm)	Min						0.01		
		Median						0.03		
		Max						0.04		
Void	Percentage (%)		10%	8%	10%	10%	6%	4%	6%	7%
	Size (mm)	Min	0.02	0.03	0.06	0.07	0.02	0.02	0.00	0.07
		Median	0.48	1.06	3.51	2.29	0.15	0.40	0.04	0.23
		Max	0.93	2.08	6.95	4.50	0.28	0.78	0.07	0.38

Table B-5 Results of Point-Count Analysis for 38-228

Source			38-228				
Feature/slide No.			1B	1C	3	4AA	4BB
Calcite, Amorphous	Percentage (%)		6%	7%	25%	64%	
	Size (mm)	Min	0.00	0.00	0.00	0.00	
		Median	0.02	0.02	0.02	0.02	
		Max	0.03	0.03	0.03	0.03	
Calcite, Sparry	Percentage (%)		88%	82%	70%	6%	8%
	Size (mm)	Min	0.03	0.03	0.03	0.03	0.02
		Median	0.08	0.06	0.17	0.14	0.16
		Max	0.13	0.08	0.30	0.25	0.30
Matrix	Percentage (%)						78%
	Size (mm)	Min					0.00
		Median					0.01
		Max					0.01
Quartz	Percentage (%)					2%	3%
	Size (mm)	Min				0.07	0.07
		Median				0.14	0.12
		Max				0.20	0.17
Void	Percentage (%)		6%	11%	5%	28%	11%
	Size (mm)	Min	0.15	0.17	0.15	0.05	0.25
		Median	0.37	0.74	1.17	4.91	2.09
		Max	0.58	1.30	2.18	9.77	3.92

Table B-6 Results of Point-Count Analysis for 87-339

Source			87-339					
Feature/slide No.			5AA	5BB	6	8	10	10B
Calcite, Sparry	Percentage (%)		21%	31%	22%	29%	19%	20%
	Size (mm)	Min	0.04	0.10	0.08	0.04	0.05	0.10
		Median	0.16	0.30	0.19	0.14	0.24	0.28
		Max	0.27	0.50	0.30	0.23	0.43	0.45
Matrix	Percentage (%)		59%	59%	52%	60%	54%	72%
	Size (mm)	Min	0.00	0.00	0.00	0.00	0.00	0.00
		Median	0.01	0.01	0.01	0.01	0.01	0.01
		Max	0.01	0.01	0.01	0.01	0.01	0.01
Quartz	Percentage (%)		12%	7%	23%	9%	1%	2%
	Size (mm)	Min	0.10	0.09	0.13	0.12	0.15	0.08
		Median	0.28	0.22	0.24	0.25	0.27	0.26
		Max	0.45	0.35	0.35	0.37	0.38	0.43
Void	Percentage (%)		8%	3%	3%	2%	26%	6%
	Size (mm)	Min	0.55	0.22	1.07	0.10	0.07	0.15
		Median	2.10	0.57	2.54	3.00	4.49	0.36
		Max	3.65	0.92	4.00	5.90	8.90	0.57

Table B-7 Results of Point-Count Analysis for GA-178

Source			GA-178			
Feature/slide No.			4A	4B	6	9
Biotite	Percentage (%)		3%	4%	33%	16%
	Size (mm)	Min	0.05	0.20	0.07	0.28
		Median	0.16	0.43	0.35	0.43
		Max	0.27	0.65	0.63	0.58
Calcite	Percentage (%)		0%	1%	0%	0%
	Size (mm)	Min		0.08		
		Median		0.17		
		Max		0.25		
Carbonate	Percentage (%)				1%	8%
	Size (mm)	Min			0.20	0.18
		Median			1.26	0.75
		Max			2.32	1.32
Hornblende	Percentage (%)				5%	16%
	Size (mm)	Min			0.13	0.70
		Median			0.37	0.93
		Max			0.60	1.15
Microline	Percentage (%)		14%	7%		0%
	Size (mm)	Min	1.08	0.50		1.08
		Median	3.12	1.00		1.30
		Max	5.15	1.50		1.52
Muscovite	Percentage (%)			1%		
	Size (mm)	Min		0.20		
		Median		0.29		
		Max		0.37		
Orthoclase	Percentage (%)		39%	27%	12%	21%
	Size (mm)	Min	0.30	0.53	0.50	0.55
		Median	1.38	1.73	1.45	1.35
		Max	2.45	2.92	2.40	2.15
Plagioclase	Percentage (%)		20%	12%	24%	20%
	Size (mm)	Min	0.67	0.52	0.25	0.33
		Median	1.11	0.94	1.00	0.92
		Max	1.55	1.35	1.75	1.50
Pyrite	Percentage (%)			0%		0%
	Size (mm)	Min		0.02		0.10
		Median		0.16		0.16
		Max		0.30		0.22
Pyroxene	Percentage (%)				2%	
	Size (mm)	Min			0.32	
		Median			0.44	
		Max			0.55	
Quartz	Percentage (%)		24%	48%	23%	19%
	Size (mm)	Min	0.10	0.10	0.18	0.12
		Median	0.44	0.25	0.29	0.49
		Max	0.78	0.40	0.40	0.85

B.2.1 REPORTS FOR SOURCE 08-534, BROOKSVILLE, FLORIDA

SNCGI PETROGRAPHIC ANALYSIS

Sample ID: 08-534-1

Date Analyzed: 6/15/06

Analyzed By: SN

Project: RipRap Study
Location: Florida
Client: University of Massachusetts, Lowell

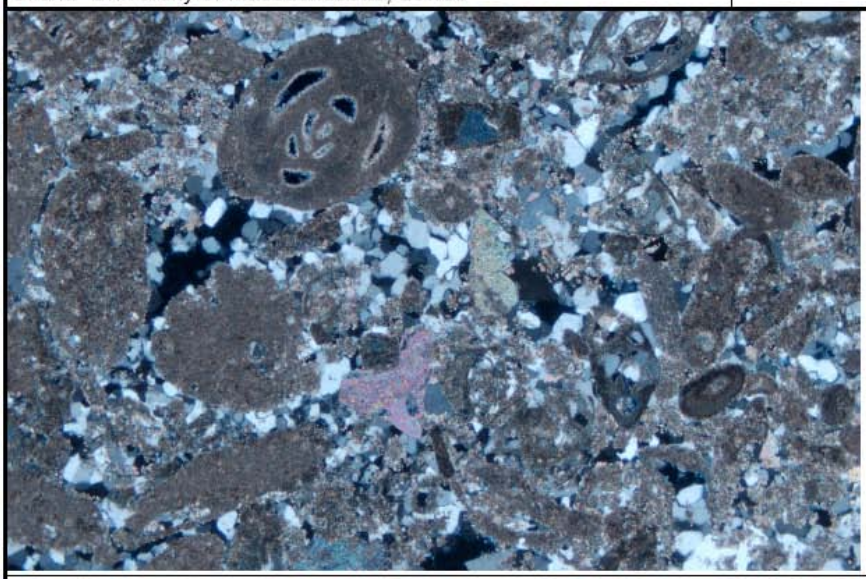

MICROSCOPIC VIEW
Magnification 40x
Field of View
3.25mm x 2.15mm

COMPOSITION

Mineral	Percentage	Typical Size Range (mm)
MATRIX	73	<0.01 - 0.01
QUARTZ	17	0.07 - 0.15
SPARRY CALCITE	9	0.12 - 1.90
VOID	1	0.03 - 0.80

REMARKS

SANDY LIMESTONE - Fine detrital quartz sand comprises nearly 20 percent of this sample. It is seen as fine, angular grains that are clotted together in the matrix. The majority of the calcite is fine matrix material. Coarse calcite is less than 10 percent of the total mineral assemblage. Voids are rare and typically present where replacement of bioclasts is incomplete. Bioclasts (primarily ostracods) are abundant and well distributed.

SNCGI PETROGRAPHIC ANALYSIS

Sample ID: 08-534-2B

Date Analyzed: 6/16/06

Analyzed By: SN

Project: RipRap Study
Location: Florida
Client: University of Massachusetts, Lowell

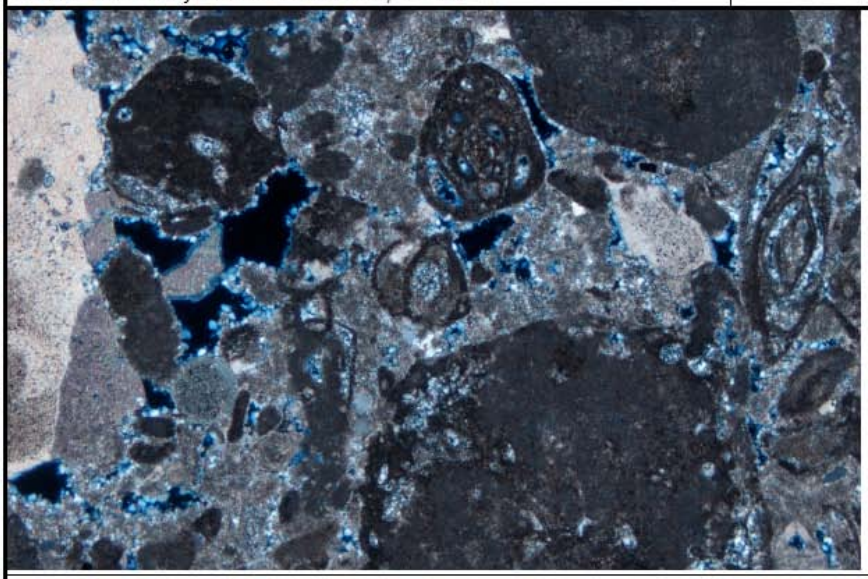

MICROSCOPIC VIEW
Magnification 40x
Field of View
3.25mm x 2.15mm

COMPOSITION

Mineral	Percentage	Typical Size Range (mm)
MATRIX	91	<0.01 - 0.01
VOID	5	0.10 - 0.87
QUARTZ	3	0.03 - 0.10
SPARRY CALCITE	1	0.04 - 0.30

REMARKS

LIMESTONE - Nearly all of this sample is matrix composed of a microcrystalline mixture of calcite and clay. Bioclasts are abundant and consist chiefly of ostracods. These have been replaced with matrix material. Voids are minor. They occur as open patches in the matrix and often contain a small amount of quartz. There is a trace of quartz that in addition to that found in the voids, is also present as well scattered detrital grains in the matrix.

SNCGI PETROGRAPHIC ANALYSIS

Sample ID: 08-534-7

Date Analyzed: 6/16/06

Analyzed By: SN

Project: RipRap Study
Location: Florida
Client: University of Massachusetts, Lowell

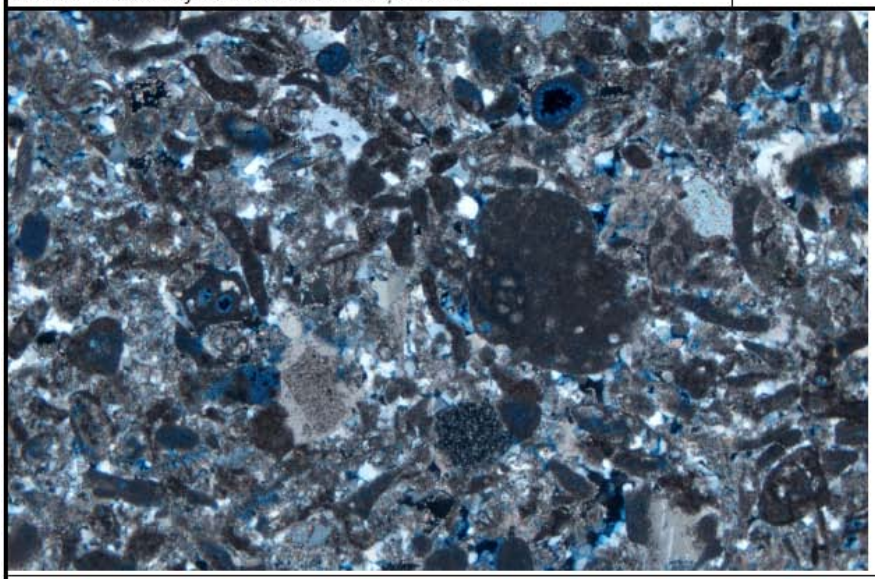

MICROSCOPIC VIEW
Magnification 40x
Field of View
3.25mm x 2.15mm

COMPOSITION

Mineral	Percentage	Typical Size Range (mm)
MATRIX	85	<0.01 - 0.01
QUARTZ	9	0.04 - 0.15
VOID	4	0.07 - 0.48
SPARRY CALCITE	2	0.12 - 0.38

REMARKS

LIMESTONE - The majority of this sample is matrix consisting of a microcrystalline mixture of calcite and clay. This material is also present as replacement for the abundant bioclasts that consist primarily of ostracods. There is a trace of coarser or sparry calcite. There is a minor amount of fine, detrital quartz that is well distributed. Voids are relatively rare. They typically appear as open patches in the matrix as well as in the bioclasts where replacement with matrix material is incomplete.

B.2.2 REPORTS FOR SOURCE 12-521, BONITA SPRINGS, FL

SNCGI PETROGRAPHIC ANALYSIS

Sample ID: 12-521-1B

Date Analyzed: 6/16/06

Analyzed By: SN

Project: RipRap Study
Location: Florida
Client: University of Massachusetts, Lowell

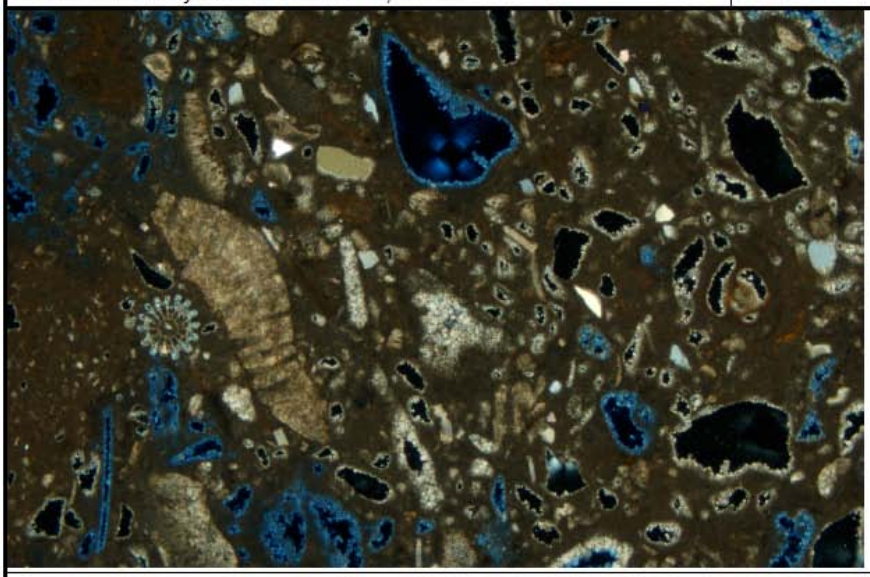

MICROSCOPIC VIEW
Magnification 40x
Field of View
3.25mm x 2.15mm

COMPOSITION

Mineral	Percentage	Typical Size Range (mm)
MATRIX	73	<0.01 - 0.01
VOID	24	0.07 - 2.42
SPARRY CALCITE	2	0.02 - 0.04
QUARTZ	1	0.05 - 0.23

REMARKS

LIMESTONE - Nearly a quarter of this sample is void space that is seen as irregulary open patches in the matrix. These are often rimmed by coarser calcite than seen in the matrix. Bioclasts and fragments are present and have been replaced by matrix material. This matrix material consists of a microcrystalline mixture of calcite and clay. The majority of this sample is comprised of matrix that consists of micro-crystalline calcite and clay. There are traces of detrital quartz and sparry calcite.

SNCGI PETROGRAPHIC ANALYSIS

Sample ID: 12-521-6

Date Analyzed: 6/17/06

Project: RipRap Study
Location: Florida
Client: University of Massachusetts, Lowell

Analyzed By: SN

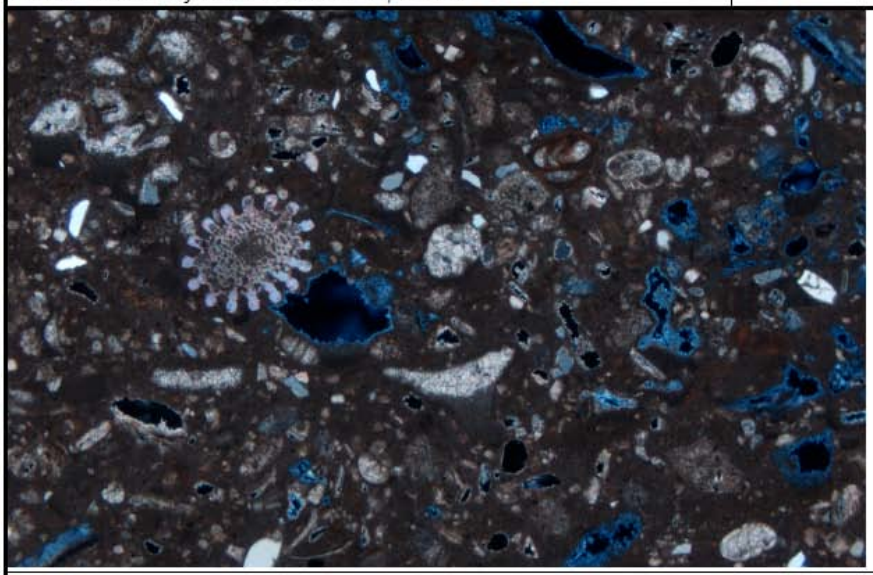

MICROSCOPIC VIEW
Magnification 40x
Field of View
3.25mm x 2.15mm

COMPOSITION

Mineral	Percentage	Typical Size Range (mm)
MATRIX	81	<0.01 - 0.01
VOID	16	0.02 - 3.20
SPARRY CALCITE	2	0.08 - 0.28
QUARTZ	1	0.04 - 0.17

REMARKS

LIMESTONE - The majority of this sample is matrix that is composed of an aphanitic mixture of calcite and clay. This material is also present as replacement of the bioclasts. Coarser calcite is rare and is most often seen in the interior chambers of the bioclasts and as rims on the voids. Coarser calcite is also present as rounded aggregates in the matrix. Voids are relatively common and are seen as open, irregular patches in the matrix. Bioclasts and bioclast fragments are not common.

SNCGI PETROGRAPHIC ANALYSIS

Sample ID: 12-521-8AA

Date Analyzed: 8/14/06

Analyzed By: SN

Project: RipRap Study
Location: Florida
Client: University of Massachusetts, Lowell

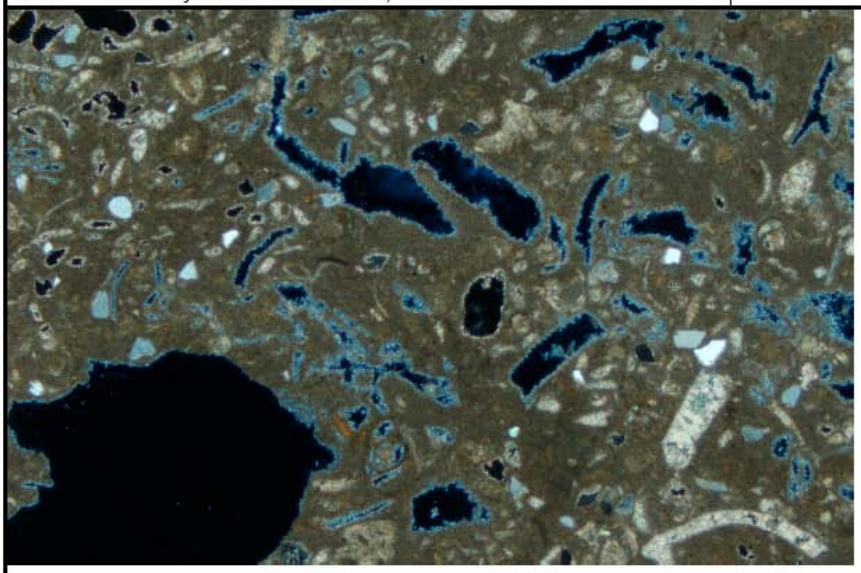

MICROSCOPIC VIEW
Magnification 40x
Field of View
3.25mm x 2.15mm

COMPOSITION

Mineral	Percentage	Typical Size Range (mm)
MATRIX	84	<0.01 - 0.03
VOID	11	0.05 - 2.23
SPARRY CALCITE	2	0.03 - 0.08
QUARTZ	3	0.08 - 0.18

REMARKS

LIMESTONE - The bulk of this sample is composed of an amorphous paste of calcite and clay. Suspended in this matrix are fine angular detrital grains of quartz. Bioclasts in the form of foraminifera are common. Voids are typically vuggy but mouldic voids are present where infilling of the bioclasts is incomplete.

SNCGI PETROGRAPHIC ANALYSIS

Sample ID: 12-521-8BB

Date Analyzed: 8/14/06

Analyzed By: SN

Project: RipRap Study
Location: Florida
Client: University of Massachusetts, Lowell

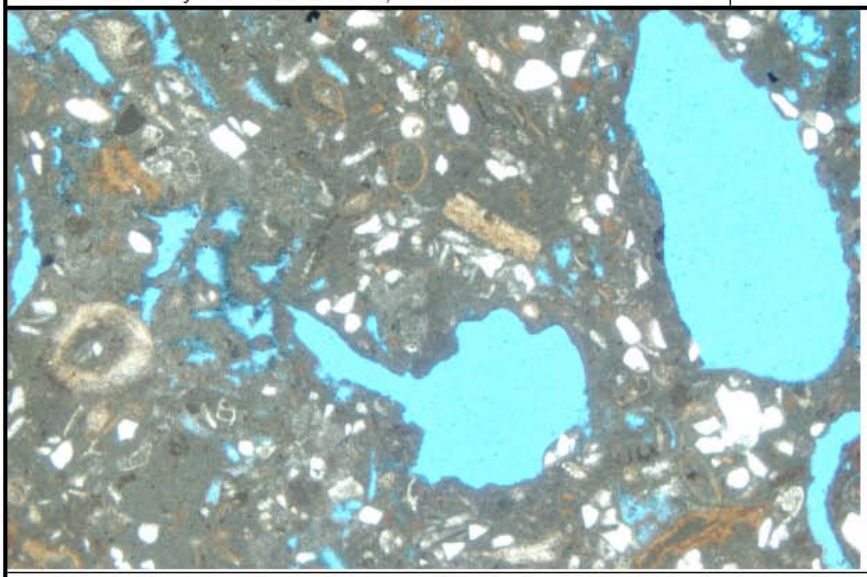

MICROSCOPIC VIEW
Magnification 40x
Field of View
3.25mm x 2.15mm

COMPOSITION

Mineral	Percentage	Typical Size Range (mm)
MATRIX	75	<0.01 - 0.03
VOID	20	0.02 - 8.35
SPARRY CALCITE	2	0.03 - 0.07
QUARTZ	3	0.05 - 0.30

REMARKS

LIMETSTONE - The bulk of this sample is an amorphous paste matrix composed of calcite and clay. Suspended in the matrix is a trace amount of very fine, angular, detrital quartz. Bioclasts are common and are chiefly foraminifera. Some of the bioclasts have been replaced with sparry calcite and others remain as mouldic voids. The majority of the voids are vugs. The photo of this sample was taken under plane polarized light due to the general opacity of the sample.

SNCGI PETROGRAPHIC ANALYSIS

Sample ID: 12-521-9

Date Analyzed: 6/17/06

Analyzed By: SN

Project: RipRap Study
Location: Florida
Client: University of Massachusetts, Lowell

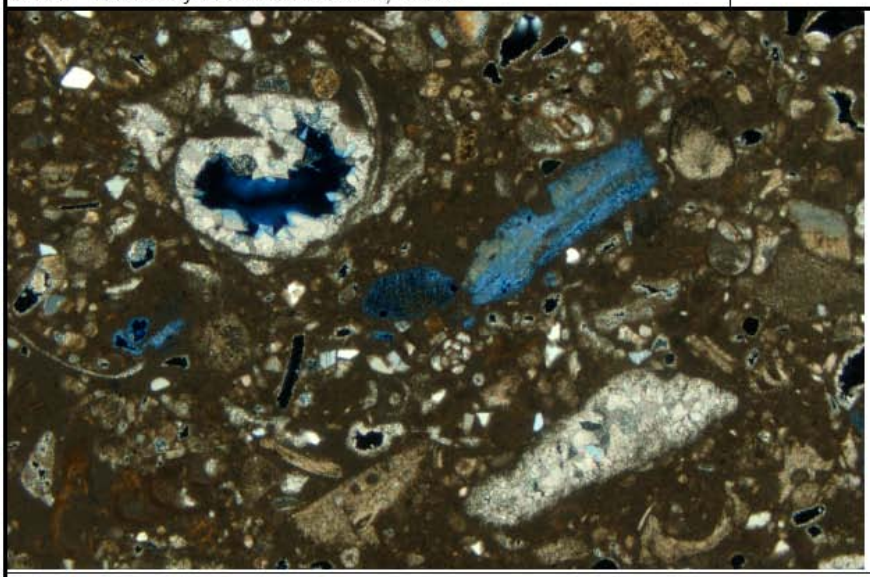

MICROSCOPIC VIEW
Magnification 40x
Field of View
3.25mm x 2.15mm

COMPOSITION

Mineral	Percentage	Typical Size Range (mm)
MATRIX	79	<0.01 - 0.01
VOID	18	0.12 - 5.07
SPARRY CALCITE	2	0.03 - 0.18
QUARTZ	1	0.05 - 0.35

REMARKS

LIMESTONE - Most of this sample is matrix consisting of a microcrystalline mixture of calcite and clay. Within the matrix material are very small rounded areas where there is no clay present. Well distributed throughout the matrix are voids that are irregularly shaped. The larger voids are often rimmed with coarse or sparry calcite. Bioclasts are present but not common. There is a trace of angular, detrital quartz.

B.2.3 REPORTS FOR SOURCE 18-607, CENTER HILL, FL

SNCGI PETROGRAPHIC ANALYSIS

Sample ID: 18-607-5AA

Date Analyzed: 8/14/06

Analyzed By: SN

Project: RipRap Study
Location: Florida
Client: University of Massachusetts, Lowell

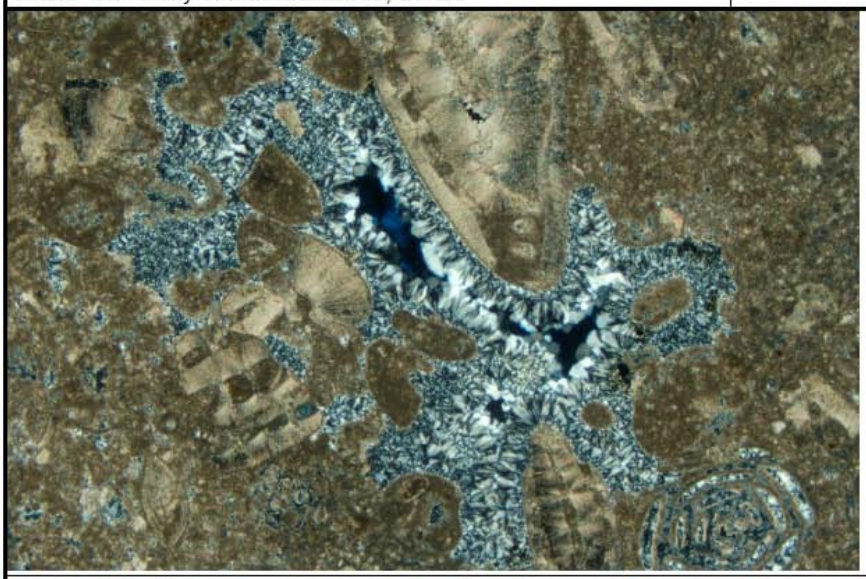

MICROSCOPIC VIEW
Magnification 40x
Field of View
3.25mm x 2.15mm

COMPOSITION

Mineral	Percentage	Typical Size Range (mm)
MATRIX	93	<0.01 - 0.03
VOID	4	0.03 - 1.32
SPARRY CALCITE	3	0.03 - 0.10

REMARKS

LIMESTONE - Bioclasts are very abundant in this sample and are chiefly nummulites. They have been replaced with very fine to amorphous calcite. There is a matrix and it is composed of amorphous calcite. Within the matrix are voids that are principally vuggy. Some of these voids exceed 1mm in size. In most cases the voids have been partially infilled with sparry calcite.

SNCGI PETROGRAPHIC ANALYSIS

Sample ID: 18-607-5BB

Date Analyzed: 8/14/06

Analyzed By: SN

Project: RipRap Study
Location: Florida
Client: University of Massachusetts, Lowell

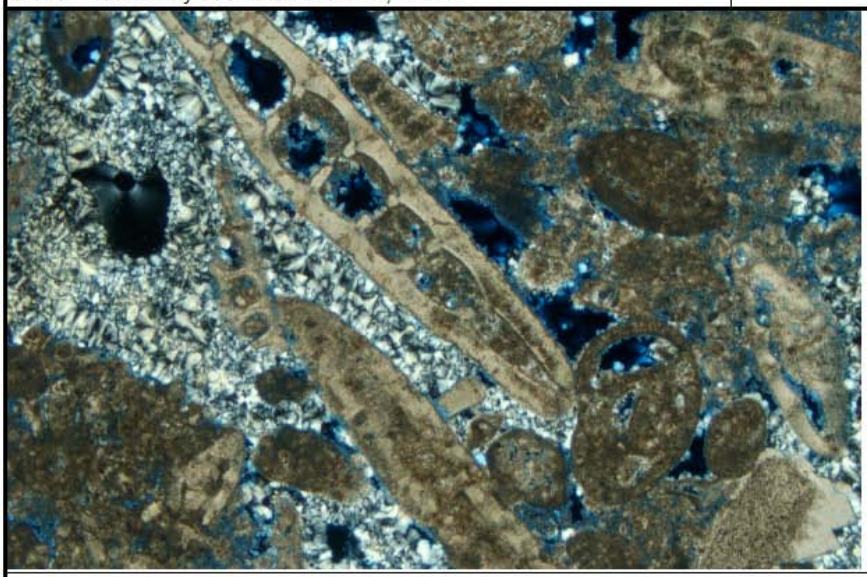

MICROSCOPIC VIEW
Magnification 40x
Field of View
3.25mm x 2.15mm

COMPOSITION

Mineral	Percentage	Typical Size Range (mm)
MATRIX	70	<0.01 - 0.03
VOID	22	2.55 - 10.25
SPARRY CALCITE	8	0.03 - 0.45

REMARKS

LIMESTONE - Bioclasts are abundant in this sample and are chiefly nummulites. They have been replaced with a mixture of amorphous calcite. The sample is quite porous with voids that are both mouldic and vuggy. The voids constitute nearly a quarter of the sample. There is a minor amount of sparry calcite that is present as void infilling.

SNCGI PETROGRAPHIC ANALYSIS

Sample ID: 18-607-8AA

Date Analyzed: 8/16/06

Project: RipRap Study
Location: Florida
Client: University of Massachusetts, Lowell

Analyzed By: SN

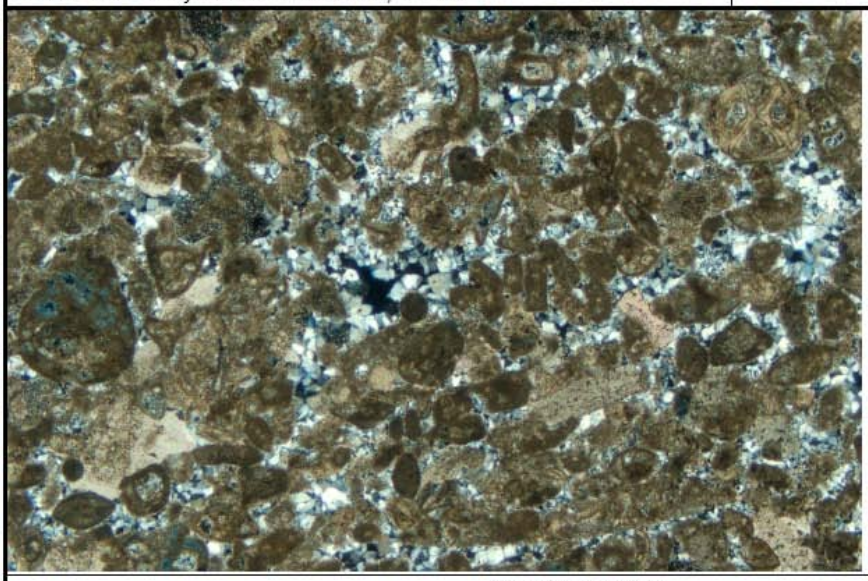

MICROSCOPIC VIEW
Magnification 40x
Field of View
3.25mm x 2.15mm

COMPOSITION

Mineral	Percentage	Typical Size Range (mm)
AMORPHOUS CALCITE	72	<0.01 - 0.03
SPARRY CALCITE	24	0.03 - 0.25
VOID	4	0.11 - 2.08

REMARKS

LIMESTONE - Abundant peloids and lesser foraminifera make up the bulk of this sample. They are composed of amorphous calcite but contain micritic calcite in the internal voids that occur where infilling is incomplete. The structure is relatively open with the space between the bioclasts filled with sparry calcite. Voids occur as both open vugs and as open areas within the bioclasts. The vugs are frequently rimmed with micritic calcite.

SNCGI PETROGRAPHIC ANALYSIS

Sample ID: 18-607-8BB

Date Analyzed: 8/16/06

Analyzed By: SN

Project: RipRap Study
Location: Florida
Client: University of Massachusetts, Lowell

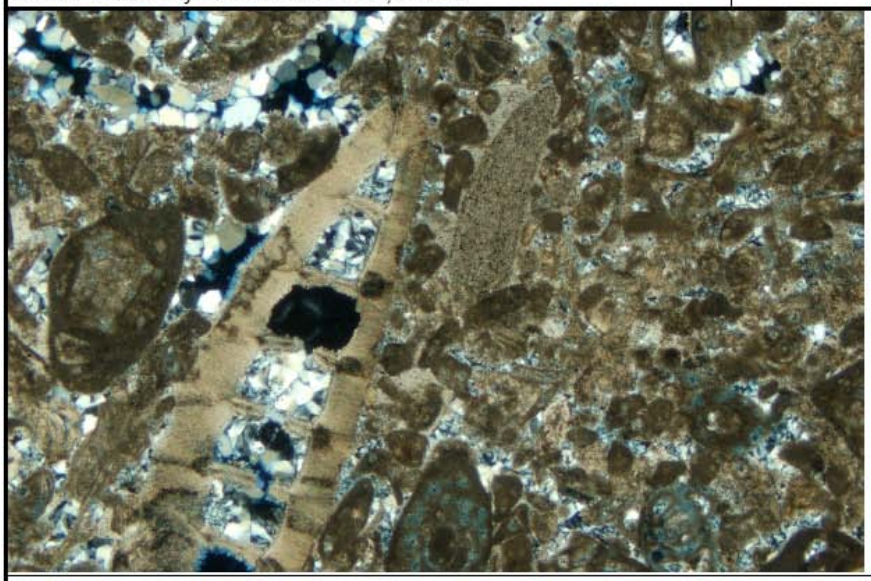

MICROSCOPIC VIEW
Magnification 40x
Field of View
3.25mm x 2.15mm

COMPOSITION

Mineral	Percentage	Typical Size Range (mm)
AMORPHOUS CALCITE	80	<0.01 - 0.03
SPARRY CALCITE	14	0.03 - 0.20
VOID	6	0.03 - 4.87

REMARKS

LIMESTONE - Abundant peloids for the majority of this sample. Bioclasts are common and include foraminifera such as nummulites. These have been replaced with amorphous calcite. The cement is sparry calcite. The voids are primarily vuggy but some mouldic voids are present in the larger bioclasts.

SNCGI PETROGRAPHIC ANALYSIS

Sample ID: 18-607-9

Date Analyzed: 8/16/06

Analyzed By: SN

Project: RipRap Study
Location: Florida
Client: University of Massachusetts, Lowell

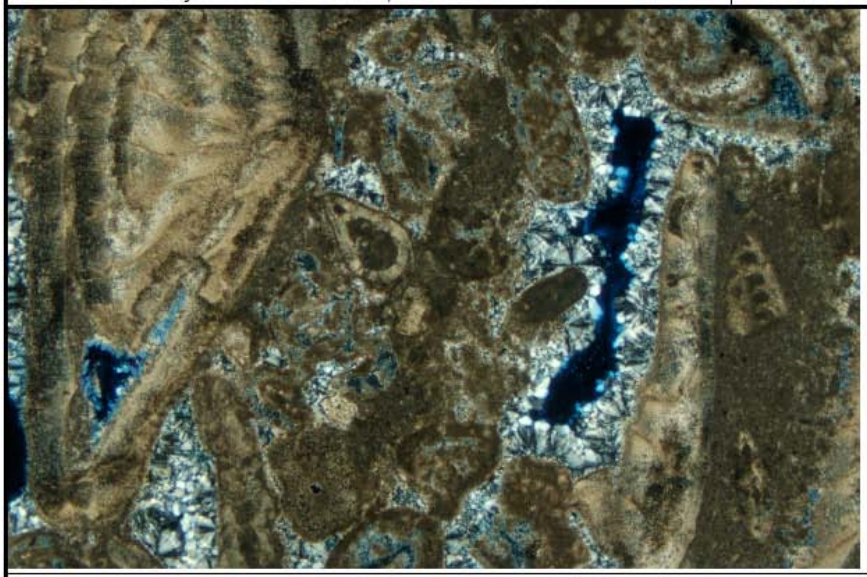

MICROSCOPIC VIEW
Magnification 40x
Field of View
3.25mm x 2.15mm

COMPOSITION

Mineral	Percentage	Typical Size Range (mm)
MATRIX	73	<0.01 - 0.03
SPARRY CALCITE	25	0.03 - 0.18
VOID	2	0.10 - 2.25

REMARKS

LIMESTONE - This sample is characterized by abundant bioclasts that form a loose framework. These bioclasts have been replaced by amorphous calcite. The space between the bioclasts is filled with sparry calcite. Voids are rare but can exceed 2mm in size. They typically occur within the bioclasts where infilling and replacement is incomplete.

SNCGI PETROGRAPHIC ANALYSIS

Sample ID: 18-607-10A

Date Analyzed: 8/16/06

Project: RipRap Study
Location: Florida
Client: University of Massachusetts, Lowell

Analyzed By: SN

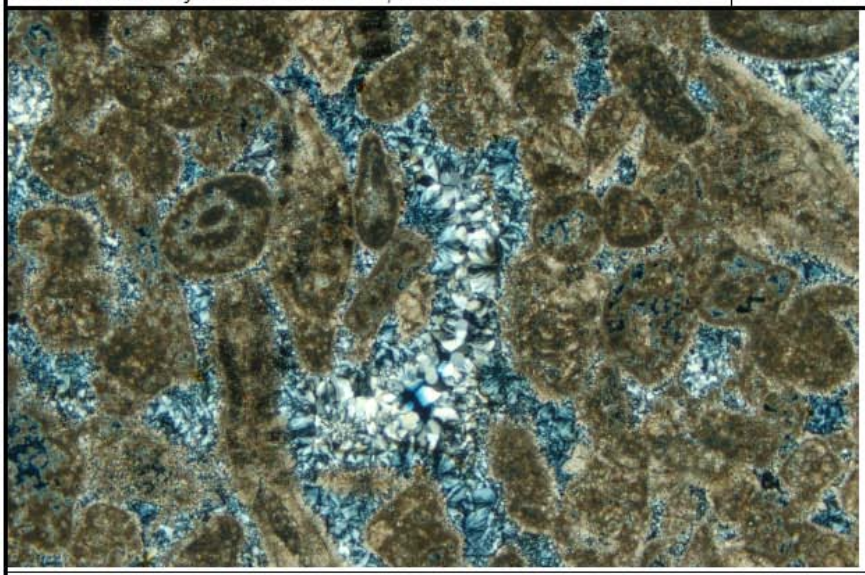

MICROSCOPIC VIEW
Magnification 40x
Field of View
3.25mm x 2.15mm

COMPOSITION

Mineral	Percentage	Typical Size Range (mm)
AMORPHOUS CALCITE	69	<0.01 - 0.03
SPARRY CALCITE	28	0.03 - 0.25
VOID	3	0.02 - 1.50

REMARKS

LIMESTONE - This sample contains abundant bioclasts that are primarily nummulites and foraminifera. The bioclasts have been replaced with microcrystalline calcite. There is some cement between the bioclasts and it is mostly calcite. The voids are both mouldic and vuggy.

SNCGI PETROGRAPHIC ANALYSIS

Sample ID: 18-607-10D

Date Analyzed: 8/15/06

Project: RipRap Study
Location: Florida
Client: University of Massachusetts, Lowell

Analyzed By: SN

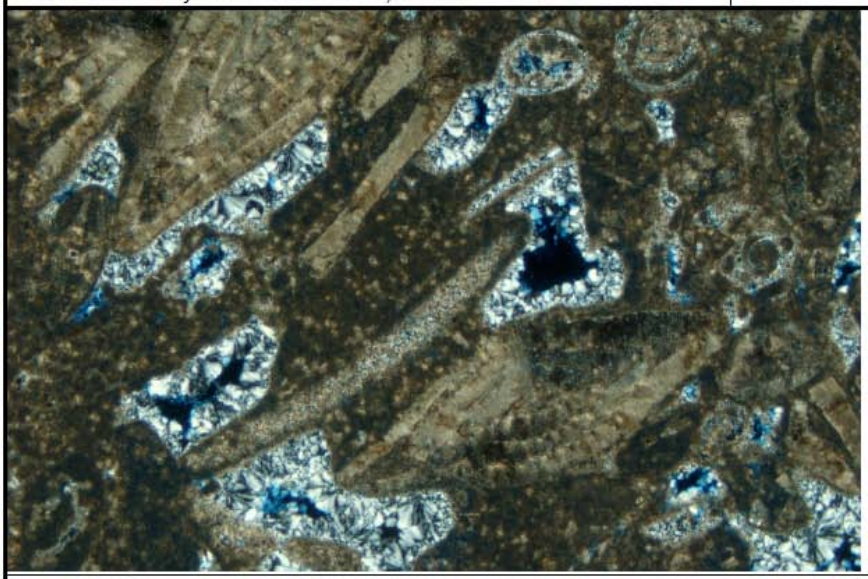

MICROSCOPIC VIEW
Magnification 40x
Field of View
3.25mm x 2.15mm

COMPOSITION

Mineral	Percentage	Typical Size Range (mm)
MATRIX	81	<0.01 - 0.03
SPARRY CALCITE	17	0.03 - 0.15
VOID	2	0.05 - 2.60

REMARKS

LIMESTONE - Bioclasts including primarily nummulites are common in this sample. They have been replaced by amorphous calcite. The sample is relatively open in structure with the space between bioclasts filled with amorphous calcite in some instances and sparry calcite in others. Voids appear to be more common than the point count suggest and are estimated to be closer to 10 percent in some areas. These voids are chiefly where infilling between the bioclasts is incomplete.

SNCGI PETROGRAPHIC ANALYSIS

Sample ID: 18-607-10E

Date Analyzed: 8/15/06

Project: RipRap Study
Location: Florida
Client: University of Massachusetts, Lowell

Analyzed By: SN

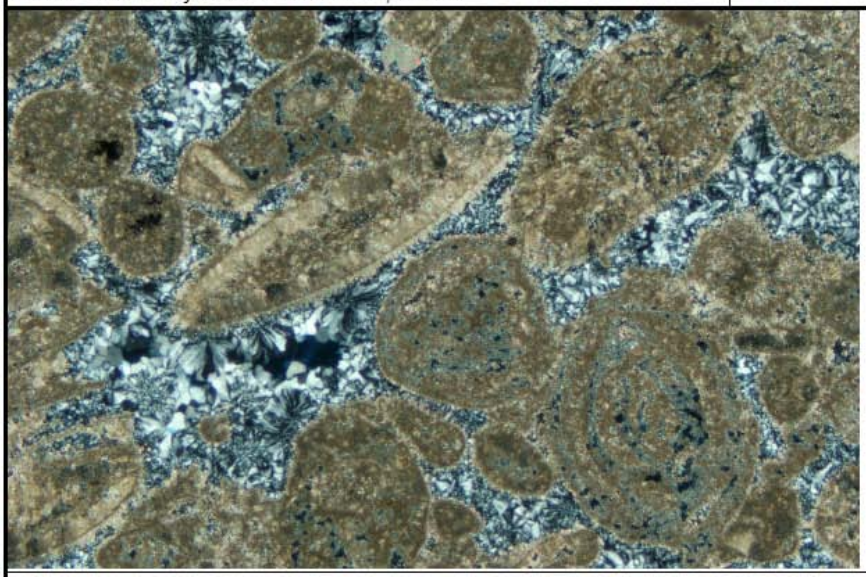

MICROSCOPIC VIEW
Magnification 40x
Field of View
3.25mm x 2.15mm

COMPOSITION

Mineral	Percentage	Typical Size Range (mm)
MATRIX	79	<0.01 - 0.03
SPARRY CALCITE	18	0.03 - 0.13
VOID	3	0.12 - 0.90

REMARKS

LIMESTONE - Bioclasts are common in this sample and include nummulites and peloids. The structure is relatively open and the space between bioclasts is filled primarily with mcrocrystalline to amorphous calcite. The bioclasts themselves have been replaced with amorphous calcite. Voids are both mouldic and vuggy. These voids are frequently rimmed with sparry calcite. In many cases the void has been completely filled with this mineral.

B.2.4 REPORTS FOR SOURCE 34-106, GULF HAMMOCK, FL

SNCGI PETROGRAPHIC ANALYSIS

Sample ID: 34-106-2AA

Date Analyzed: 8/16/06

Analyzed By: SN

Project: RipRap Study
Location: Florida
Client: University of Massachusetts, Lowell

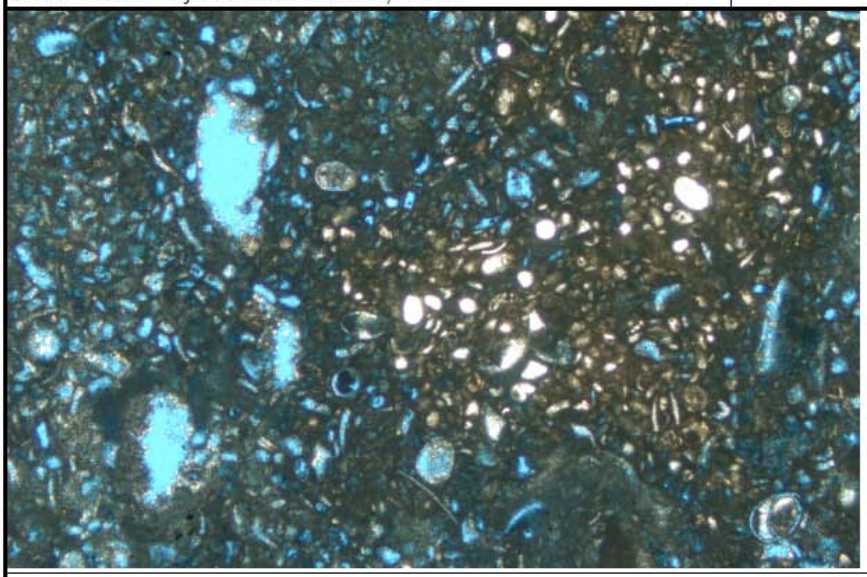

MICROSCOPIC VIEW
Magnification 40x
Field of View
3.25mm x 2.15mm

COMPOSITION

Mineral	Percentage	Typical Size Range (mm)
MATRIX	90	<0.01 - 0.03
VOID	10	0.02 - 0.93
SPARRY CALCITE	<1	0.03 - 0.04

REMARKS

LIMESTONE - This sample is comprised almost entirely of an amorphous paste matrix that is primarily calcite but has some clay and or iron oxide present. There is a trace of sparry or micritic calcite this is seen as rims to the larger voids. Voids are vuggy, open patches in the matrix. Bioclasts are rare and are primarily foraminifera. The photo of thisi slide was taken in plane polarized light due to the general opacity of the sample.

SNCGI PETROGRAPHIC ANALYSIS

Sample ID: 34-106-2BB

Date Analyzed: 8/15/06

Analyzed By: SN

Project: RipRap Study
Location: Florida
Client: University of Massachusetts, Lowell

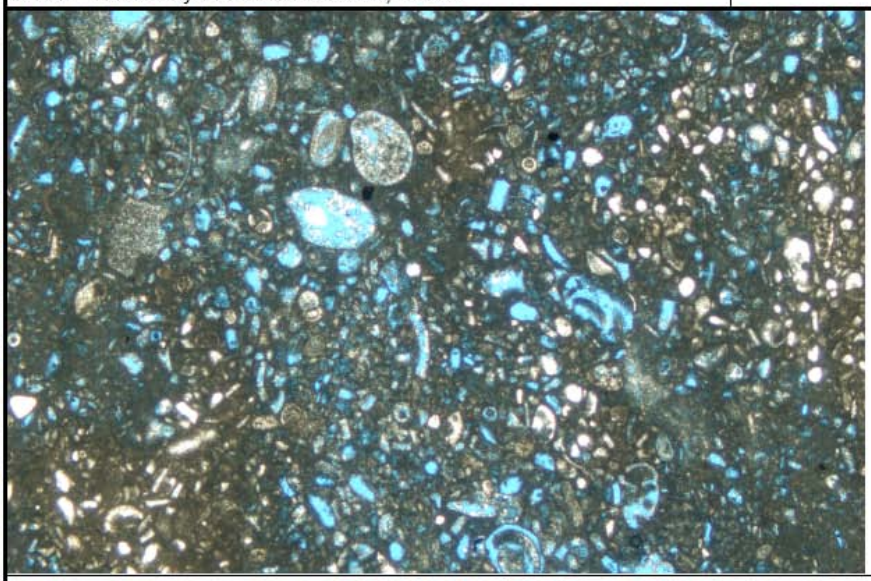

MICROSCOPIC VIEW
Magnification 40x
Field of View
3.25mm x 2.15mm

COMPOSITION

Mineral	Percentage	Typical Size Range (mm)
MATRIX	92	<0.01 - 0.03
VOID	8	0.03 - 2.08
SPARRY CALCITE	<1	0.03 - 0.10

REMARKS

LIMESTONE - The majority of this sample is matrix composed of an amorphous paste of calcite possibly mixed with clay. Well dispersed throughout is a small amount of fine foraminifera. Voids are minor but well dispersed. They are vugs that are primarily very fine but can exceed 2mm in size. The photo of this sample was taken in plane polarized light due to the opacity of the sample.

SNCGI PETROGRAPHIC ANALYSIS

Sample ID: 34-106-6AA

Date Analyzed: 8/16/06

Project: RipRap Study
Location: Florida
Client: University of Massachusetts, Lowell

Analyzed By: SN

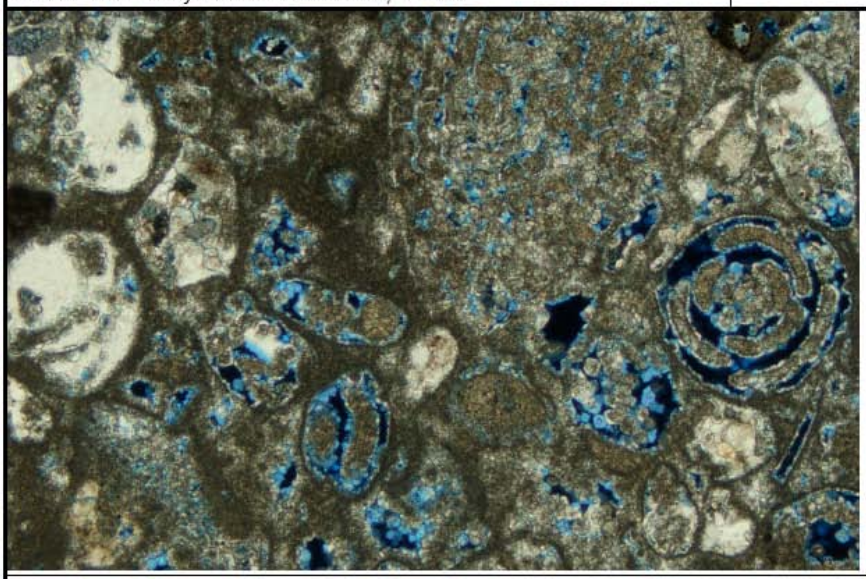

MICROSCOPIC VIEW
Magnification 40x
Field of View
3.25mm x 2.15mm

COMPOSITION

Mineral	Percentage	Typical Size Range (mm)
MATRIX	74	<0.01 - 0.03
SPARRY CALCITE	16	0.03 - 0.50
VOID	10	0.06 - 6.95

REMARKS

LIMESTONE - Much of this sample is amorphous calcite that is present as bioclast replacement and as irregular patches. Scattered throughout the sample are small zones of sparry calcite. These represent the internal area of bioclasts that are no longer present. Voids are present both as vuggs and as mouldic openings where replacement and infilling of bioclasts is incomplete.

SNCGI PETROGRAPHIC ANALYSIS

Sample ID: 34-106-6B

Date Analyzed: 8/16/06

Project: RipRap Study
Location: Florida
Client: University of Massachusetts, Lowell

Analyzed By: SN

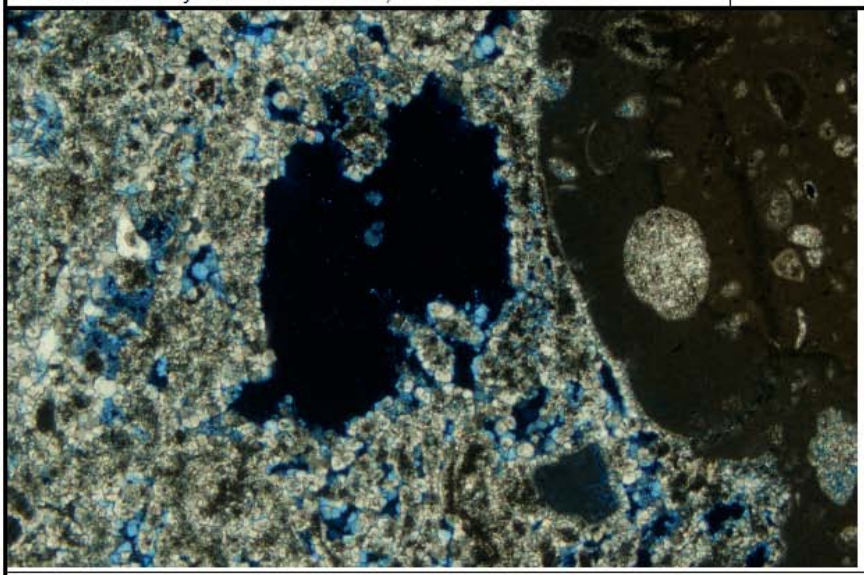

MICROSCOPIC VIEW
Magnification 40x
Field of View
3.25mm x 2.15mm

COMPOSITION

Mineral	Percentage	Typical Size Range (mm)
AMORPHOUS CALCITE	50	<0.01 - 0.03
SPARRY CALCITE	40	0.03 - 0.12
VOID	10	0.07 - 4.50

REMARKS

LIMESTONE - This sample is characterized by fine crystalline calcite that is tightly interlocked. Scattered throughout are small zones of amorphous calcite. Bioclasts are abundant and have been replaced with a combination of micritic and amorphous calcite. Voids appear to be more abundant than the point count suggests and are estimated to be closer to 15 percent. They occur as vugs and as mouldic voids where replacement and infilling of the bioclasts is incomplete.

SNCGI PETROGRAPHIC ANALYSIS

Sample ID: 34-106-9A

Date Analyzed: 5/09/06

Project: RipRap Study
Location: Florida
Client: University of Massachusetts, Lowell

Analyzed By: SN

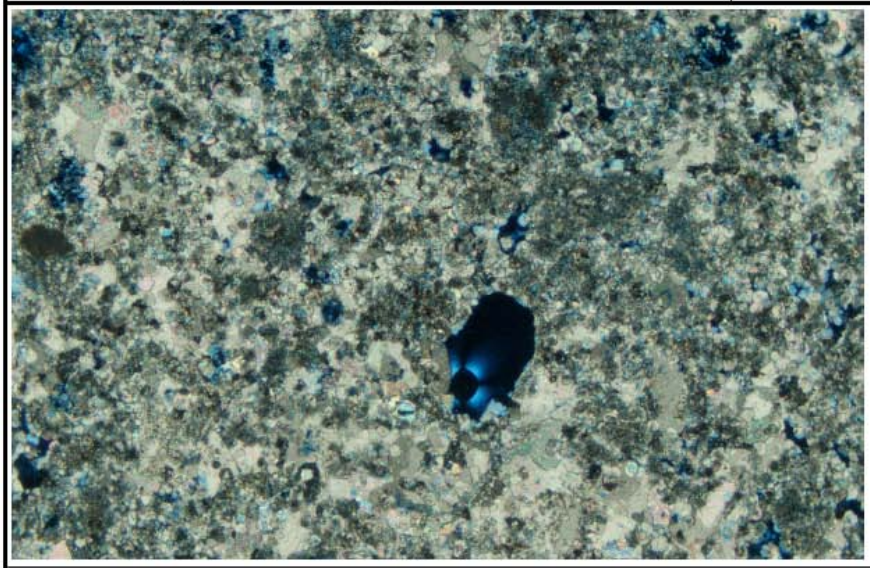

MICROSCOPIC VIEW
Magnification 40x
Field of View
3.25mm x 2.15mm

COMPOSITION

Mineral	Percentage	Typical Size Range (mm)
SPARRY CALCITE	57	0.04 - 0.23
MATRIX	37	<0.01 - 0.01
VOID	6	0.02 - 0.28

REMARKS

LIMESTONE - Over half of this sample is made of uniformly fine-grained crystalline calcite that is tightly interlocked. Within this mass is well dispersed amorphous calcite matrix mixed with clay. The sample appears to be more porous than the point count suggests and it is estimated that voids make up nearly 10 percent of the sample. The voids occur as open patches in the rock fabric.

SNCGI PETROGRAPHIC ANALYSIS

Sample ID: 34-106-9B

Date Analyzed: 6/02/06

Analyzed By: SN

Project: RipRap Study
Location: Florida
Client: University of Massachusetts, Lowell

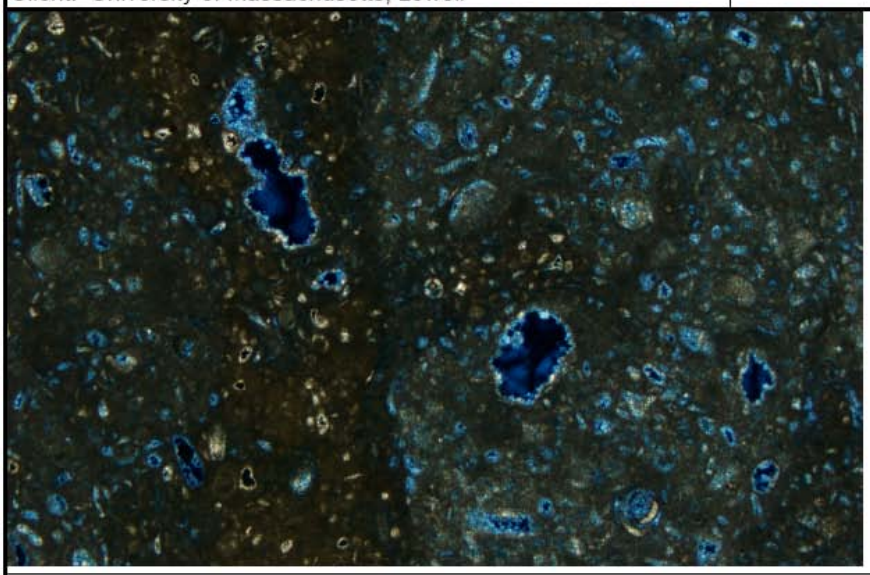

MICROSCOPIC VIEW
Magnification 40x
Field of View
3.25mm x 2.15mm

COMPOSITION

Mineral	Percentage	Typical Size Range (mm)
MATRIX	96	<0.01 - 0.01
VOID	4	0.02 - 0.78
PYRITE	<1	0.01 - 0.04

REMARKS

LIMESTONE - The majority of this sample is an amorphous matrix consisting of calcite and clay. The sample is porous based on the presence of blue epoxy impregnating material in the matrix. However, These voids are very small and difficult to measure. Accordingly, the percentage of voids listed here may be slightly larger but not exceeding 10 percent. Within the matrix are angular fragments roughly 6mm in size that are similar in composition but less porous based on the absence of impregnating epoxy except in the larger voids.

SNCGI PETROGRAPHIC ANALYSIS

Sample ID: 34-106-10AA

Date Analyzed: 8/16/06

Analyzed By: SN

Project: RipRap Study
Location: Florida
Client: University of Massachusetts, Lowell

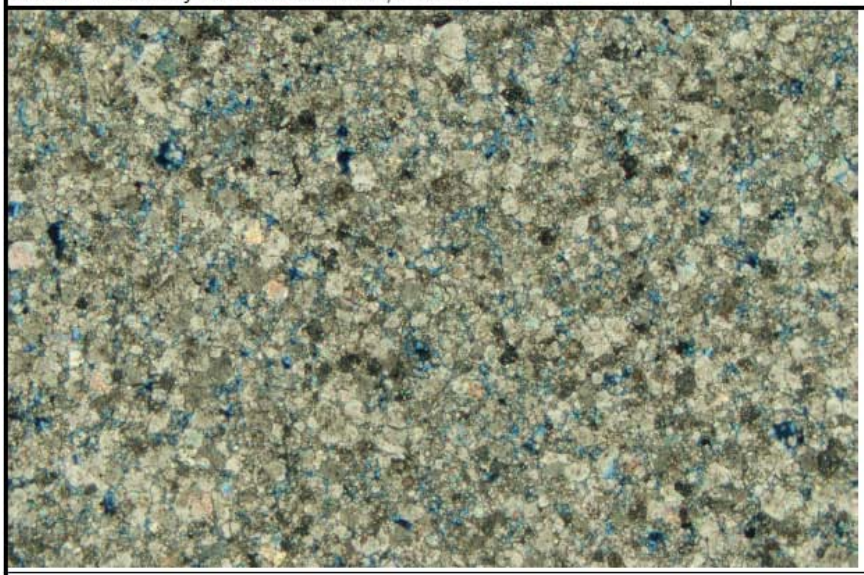

MICROSCOPIC VIEW
Magnification 40x
Field of View
3.25mm x 2.15mm

COMPOSITION

Mineral	Percentage	Typical Size Range (mm)
SPARRY CALCITE	80	0.03 - 0.10
AMORPHOUS CALCITE	14	<0.01 - 0.03
VOID	6	<0.01 - 0.07

REMARKS

LIMESTONE - This is a uniformly equigranular sample composed of fine-grained calcite crystals. They are tightly compact. Mixed in with the calcite crystals is a minor amount of amorphous or very fine-grained calcite that is seen as small zones or patches in the crystalline mass. Voids are intercrystalline and also very fine. No shells or other bioclasts were observed.

SNCGI PETROGRAPHIC ANALYSIS

Sample ID: 34-106-10BB

Date Analyzed: 6/03/06

Project: RipRap Study
Location: Florida
Client: University of Massachusetts, Lowell

Analyzed By: SN

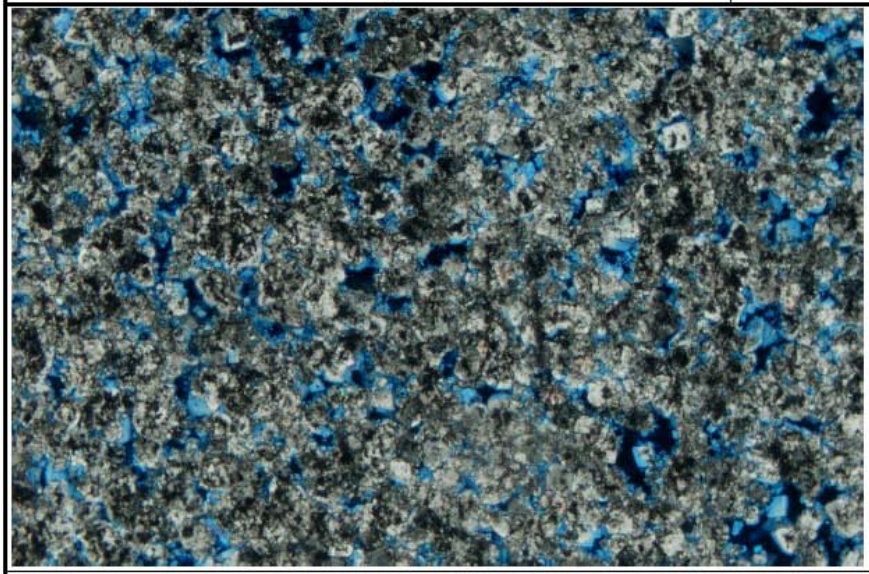

MICROSCOPIC VIEW
Magnification 40x
Field of View
3.25mm x 2.15mm

COMPOSITION

Mineral	Percentage	Typical Size Range (mm)
SPARRY CALCITE	93	0.02 - 0.10
VOID	7	0.07 - 0.38

REMARKS

LIMESTONE - The bulk of this sample is composed of equigranular, finely crystalline calcite with minor clay present. Voids occupy approximately 7 percent of the sample and are well distributed.

B.2.5 REPORTS FOR SOURCE 38-228, PERRY, FL

SNCGI PETROGRAPHIC ANALYSIS

Sample ID: 38-228-1B

Date Analyzed: 8/15/06

Analyzed By: SN

Project: RipRap Study
Location: Florida
Client: University of Massachusetts, Lowell

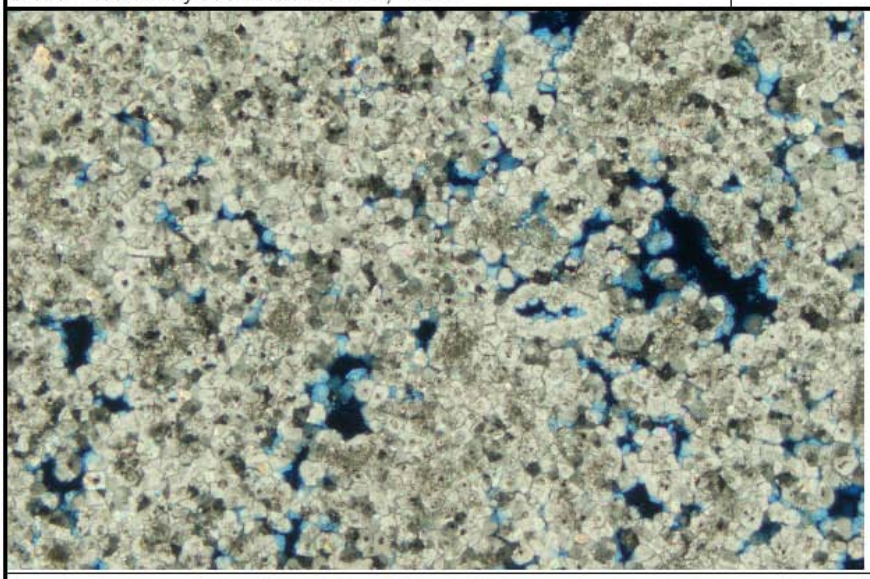

MICROSCOPIC VIEW
Magnification 40x
Field of View
3.25mm x 2.15mm

COMPOSITION

Mineral	Percentage	Typical Size Range (mm)
SPARRY CALCITE	88	0.03 - 0.13
AMORPHOUS CALCITE	6	<0.01 - 0.03
VOID	6	0.15 - 0.58

REMARKS

LIMESTONE - This sample consists of equigranular, tightly packed, finely crystalline calcite. Within this mass of crystals are minor zones of amorphous calcite. Voids are relatively minor and are intergranular. They are well dispersed and not interconnected.

SNCGI PETROGRAPHIC ANALYSIS

Sample ID: 38-228-1C

Date Analyzed: 8/16/06

Project: RipRap Study
Location: Florida
Client: University of Massachusetts, Lowell

Analyzed By: SN

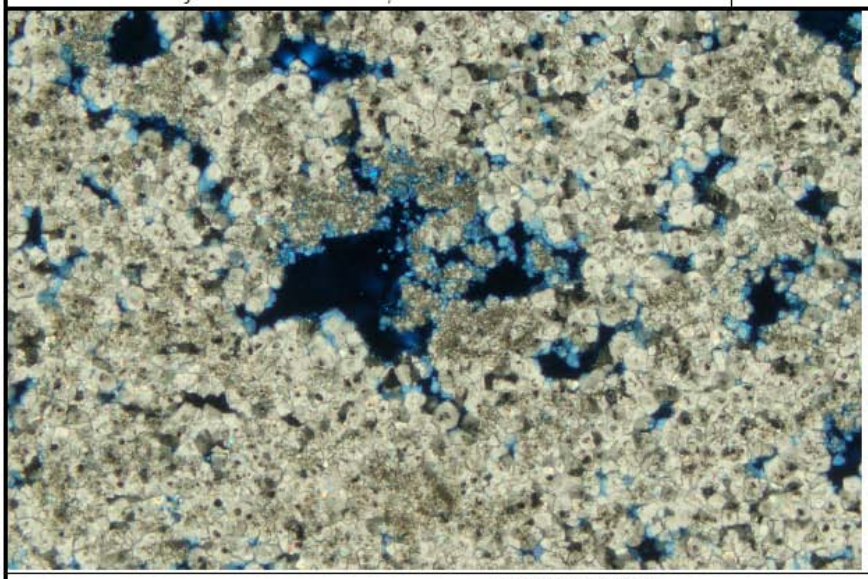

MICROSCOPIC VIEW
Magnification 40x
Field of View
3.25mm x 2.15mm

COMPOSITION

Mineral	Percentage	Typical Size Range (mm)
SPARRY CALCITE	82	0.03 - 0.08
VOID	11	0.17 - 1.30
AMORPHOUS CALCITE	7	<0.01 - 0.03

REMARKS

LIMESTONE - This sample is composed of finely-crystalline calcite that is tightly interlocked. It has well distributed zones that are rich in amorphous calcite. There are no bioclasts evident. Voids are typically vuggy but are also intercrystalline. This is a very uniformly crystalline sample.

SNCGI PETROGRAPHIC ANALYSIS

Sample ID: 38-228-3

Date Analyzed: 8/16/06

Project: RipRap Study
Location: Florida
Client: University of Massachusetts, Lowell

Analyzed By: SN

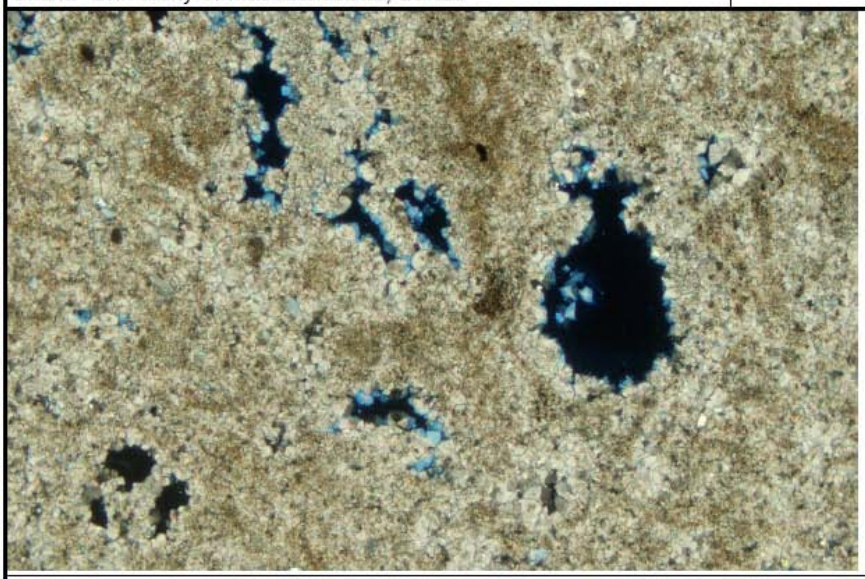

MICROSCOPIC VIEW
Magnification 40x
Field of View
3.25mm x 2.15mm

COMPOSITION

Mineral	Percentage	Typical Size Range (mm)
SPARRY CALCITE	70	0.03 - 0.30
AMORPHOUS CALCITE	25	<0.01 - 0.03
VOID	5	0.15 - 2.18

REMARKS

LIMESTONE - This sample is a mixture of sparry calcite crystals that are intermixed with zones of microcrystalline to amorphous calcite. Some clay may be present in these zones as well that make them opaque. There is a trace of bioclasts present and these are chiefly foraminifera. The sample is tightly compact but there are voids present. These are typically vuggy and contain rims of micritic calcite.

SNCGI PETROGRAPHIC ANALYSIS

Sample ID: 38-228-4AA

Date Analyzed: 8/16/06

Project: RipRap Study
Location: Florida
Client: University of Massachusetts, Lowell

Analyzed By: SN

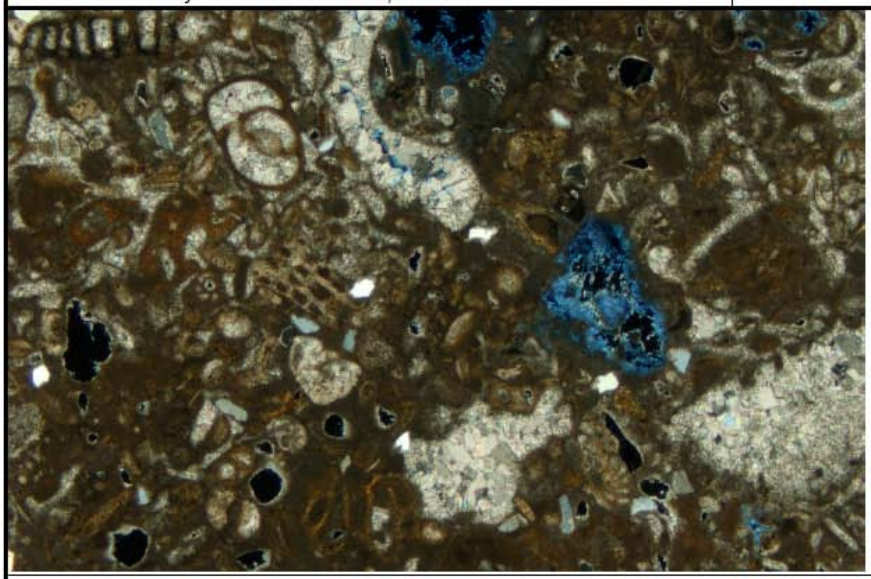

MICROSCOPIC VIEW
Magnification 40x
Field of View
3.25mm x 2.15mm

COMPOSITION

Mineral	Percentage	Typical Size Range (mm)
AMORPHOUS CALCITE	64	<0.01 - 0.03
VOID	28	0.05 - 9.77
SPARRY CALCITE	6	0.03 - 0.25
QUARTZ	2	0.07 - 0.20

REMARKS

LIMESTONE - This sample is rich in bioclasts that include foraminifera as well as peloids. Many of these have been replaced with very fine micritic calcite and others have been replaced with sparry calcite. Voids are common. They are typically rimmed with sparry calcite. There is a trace of detrital quartz that is present as widely distributed, angular grains. The voids are typically vuggy.

SNCGI PETROGRAPHIC ANALYSIS

Sample ID: 38-228-4BB

Date Analyzed: 6/02/06

Project: RipRap Study
Location: Florida
Client: University of Massachusetts, Lowell

Analyzed By: SN

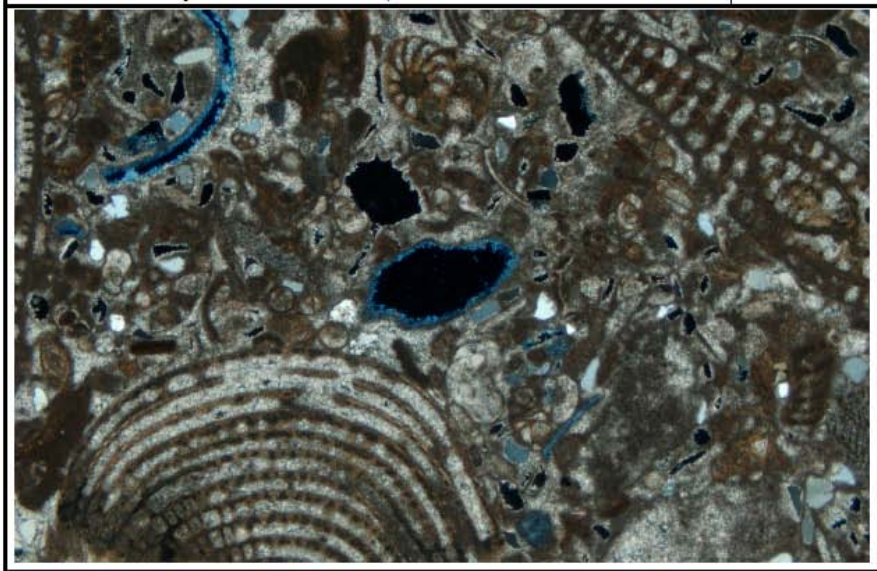

MICROSCOPIC VIEW
Magnification 40x
Field of View
3.25mm x 2.15mm

COMPOSITION

Mineral	Percentage	Typical Size Range (mm)
MATRIX	78	<0.01 - 0.01
VOID	11	0.25 - 3.92
SPARRY CALCITE	8	0.02 - 0.30
QUARTZ	3	0.07 - 0.17

REMARKS

LIMESTONE - Nearly 80 percent of this sample is matrix made up of an intimate mixture of calcite and clay. Embedded in the matrix are abundant bioclasts including ostracods and foraminifera. Some of these have been replaced with coarse, sparry calcite but the majority have been replaced with matrix material. Voids are minor and consist of open patches in the matrix typically ranging in size from 0.07mm to 0.95mm. There is a trace of detrital quartz.

B.2.6 REPORTS FOR SOURCE 87-339, HIALEAH, FL

SNCGI PETROGRAPHIC ANALYSIS

Sample ID: 87-339-5A

Date Analyzed: 6/04/06

Project: RipRap Study
Location: Florida
Client: University of Massachusetts, Lowell

Analyzed By: SN

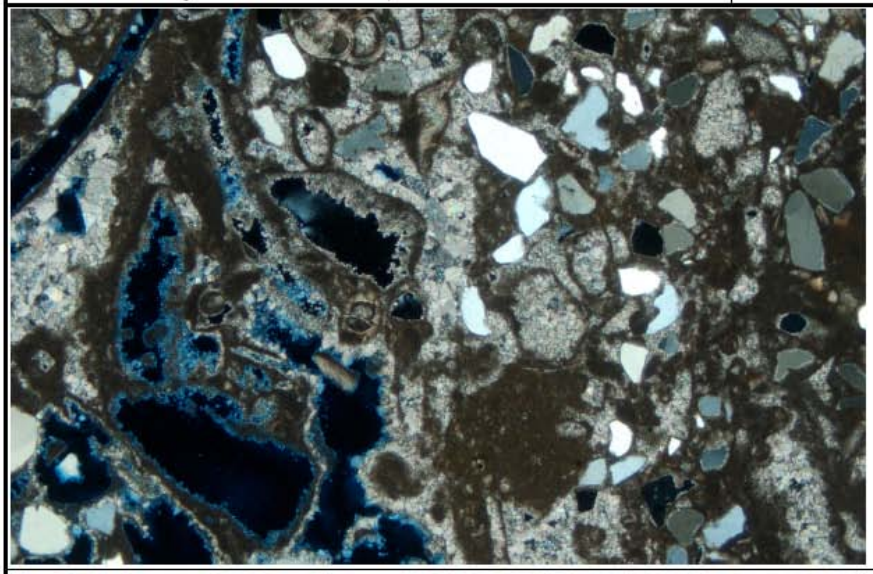

MICROSCOPIC VIEW
Magnification 40x
Field of View
3.25mm x 2.15mm

COMPOSITION

Mineral	Percentage	Typical Size Range (mm)
MATRIX	59	<0.01 - 0.01
SPARRY CALCITE	21	0.04 - 0.27
QUARTZ	12	0.10 - 0.45
VOID	8	0.55 - 3.65

REMARKS

LIMESTONE - The fine matrix consists of an amorphous mixture of calcite and clay. Embedded in the matrix are fine to coarse bioclast fragments (primarily ostracods but also bryozoans) that have been nearly completely replaced with sparry calcite. Also present is a minor amount of detrital quartz that is angular to to subangular in shape. Voids are present and constitute less than 10 percent of the sample. They occur where replacement of the bioclasts with calcite is incomplete.

SNCGI PETROGRAPHIC ANALYSIS

Sample ID: 87-339-5BB

Date Analyzed: 6/05/06

Project: RipRap Study
Location: Florida
Client: University of Massachusetts, Lowell

Analyzed By: SN

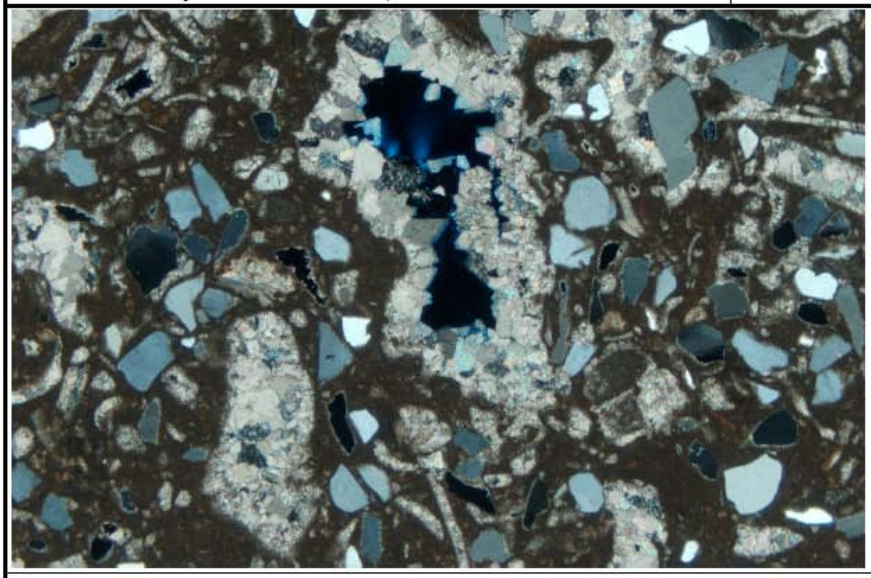

MICROSCOPIC VIEW
Magnification 40x
Field of View
3.25mm x 2.15mm

COMPOSITION

Mineral	Percentage	Typical Size Range (mm)
MATRIX	59	<0.01 - 0.01
SPARRY CALCITE	31	0.10 - 0.50
QUARTZ	7	0.09 - 0.35
VOID	3	0.22 - 0.92

REMARKS

LIMESTONE - Matrix consisting of a microcrystalline mixture of calcite and clay make up nearly 60 percent of this sample. Embedded in the matrix are abundant bioclast fragments that have been almost completely replaced with coars, sparry calcite. Some of the replacement is incomplete leaving voids. There is a minor amount of detrital quartz present that is subangular to subrounded in shape grains that are well distributed.

SNCGI PETROGRAPHIC ANALYSIS

Sample ID: 87-339-6

Date Analyzed: 6/05/06

Analyzed By: SN

Project: RipRap Study
Location: Florida
Client: University of Massachusetts, Lowell

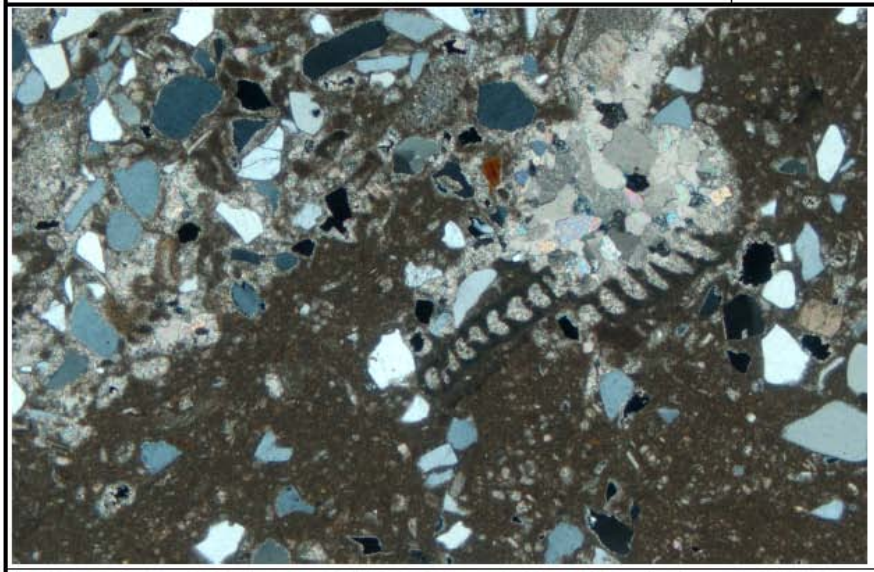

MICROSCOPIC VIEW
Magnification 40x
Field of View
3.25mm x 2.15mm

COMPOSITION

Mineral	Percentage	Typical Size Range (mm)
MATRIX	52	<0.01 - 0.01
QUARTZ	23	0.13 - 0.35
SPARRY CALCITE	22	0.08 - 0.30
VOID	3	1.07 - 4.00

REMARKS

LIMESTONE - The microcrystalline matrix consists of an intimate mixture of calcite and clay and forms half the mineral content of this sample. Coarser calcite is seen as replacement of bioclasts and as rims on voids. Detrital quartz makes up nearly a quarter of the sample and is subrounded to subangular in shape. Voids are minor and are frequently found where calcite replacement of bioclasts is incomplete.

SNCGI PETROGRAPHIC ANALYSIS

Sample ID: 87-339-8

Date Analyzed: 6/02/06

Project: RipRap Study
Location: Florida
Client: University of Massachusetts, Lowell

Analyzed By: SN

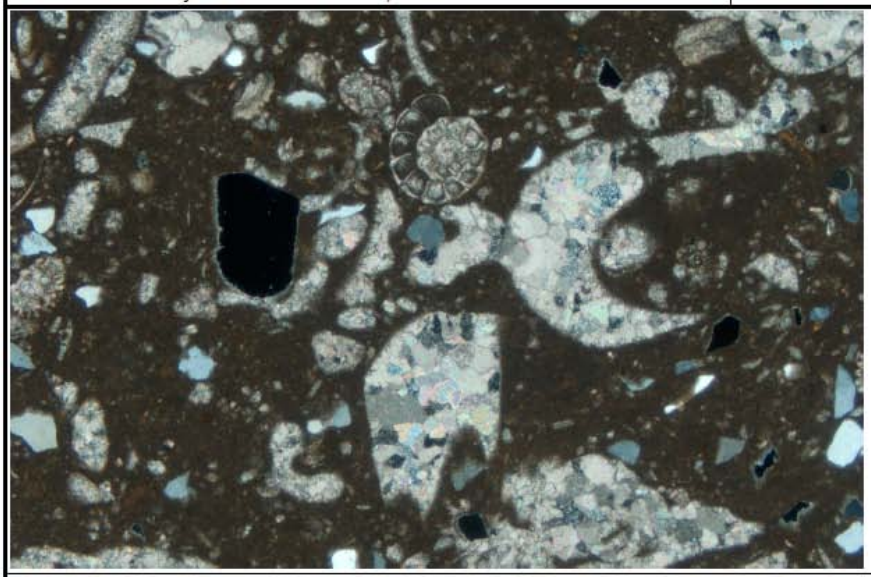

MICROSCOPIC VIEW
Magnification 40x
Field of View
3.25mm x 2.15mm

COMPOSITION

Mineral	Percentage	Typical Size Range (mm)
MATRIX	60	<0.01 - 0.01
SPARRY CALCITE	29	0.04 - 0.23
QUARTZ	9	0.12 - 0.37
VOID	2	0.10 - 5.90

REMARKS

LIMESTONE - Clay-rich microcrystalline matrix is most abundant. It consists of a mixture of calcite and clay. It contains bioclasts (primarily ostracods) that have been replaced with sparry calcite. Detrital quartz is angular and well distributed. Voids represent only 2 percent and therefore, the sample is only slightly porous.

SNCGI PETROGRAPHIC ANALYSIS

Sample ID: 87-339-10

Date Analyzed: 5/08/06

Project: RipRap Study
Location: Florida
Client: University of Massachusetts, Lowell

Analyzed By: SN

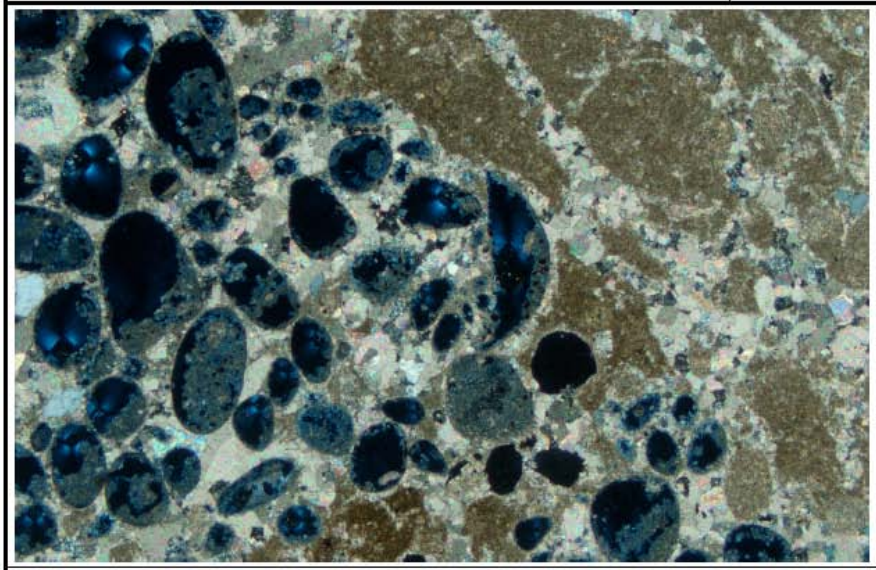

MICROSCOPIC VIEW
Magnification 40x
Field of View
3.25mm x 2.15mm

COMPOSITION

Mineral	Percentage	Typical Size Range (mm)
MATRIX	54	<0.01 - 0.01
VOID	26	0.07 - 8.90
SPARRY CALCITE	19	0.05 - 0.43
QUARTZ	1	0.15 - 0.38

REMARKS

LIMESTONE - Slightly more than half of this sample is matrix composed of a microcrystalline to amorphous mixture of calcite and clay. The sample contains abundant bioclasts in the form of ostracods and algae. Sparry or coarse calcite is present in zones and as infilling or replacement of the bioclasts. There is a trace of detrital quartz that is fine-grained and rounded to subrounded in shape. Many of the bioclasts have not been completely filled with replacement calcite leaving abundant voids throughout the sample.

SNCGI PETROGRAPHIC ANALYSIS

Sample ID: 87-339-10B

Date Analyzed: 6/05/06

Project: RipRap Study
Location: Florida
Client: University of Massachusetts, Lowell

Analyzed By: SN

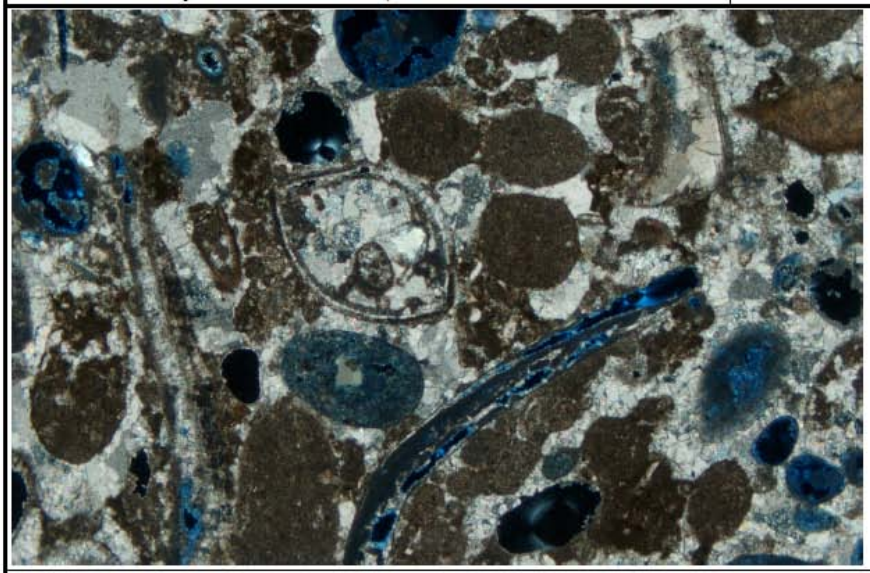

MICROSCOPIC VIEW
Magnification 40x
Field of View
3.25mm x 2.15mm

COMPOSITION

Mineral	Percentage	Typical Size Range (mm)
MATRIX	72	<0.01 - 0.01
SPARRY CALCITE	20	0.10 - 0.45
VOID	6	0.15 - 0.57
QUARTZ	2	0.08 - 0.43

REMARKS

LIMESTONE - Matrix consisting of calcite, iron oxide and clay comprises nearly two thirds of the sample. The matrix has an amorphous appearance due to the intimate mixing of its components. Within the matrix are areas of coarser calcite. Often these occur where bioclasts have been replaced but coarser calcite is also present in irregular, discontinuous zones. There is a trace of detrital quartz that is sub-angular to rounded in shape. Voids appear to be more abundant than the point count suggests. They are estimated to be closer to 10 percent. In some cases, they represent incomplete replacement of bioclasts with calcite. In other areas they are open patches in the matrix.

B.2.7 REPORTS FOR SOURCE GA-178, MACON, GA

SNCGI PETROGRAPHIC ANALYSIS

Sample ID: GA-178-4A

Date Analyzed: 6/06/06

Analyzed By: SN

Project: RipRap Study
Location: Florida
Client: University of Massachusetts, Lowell

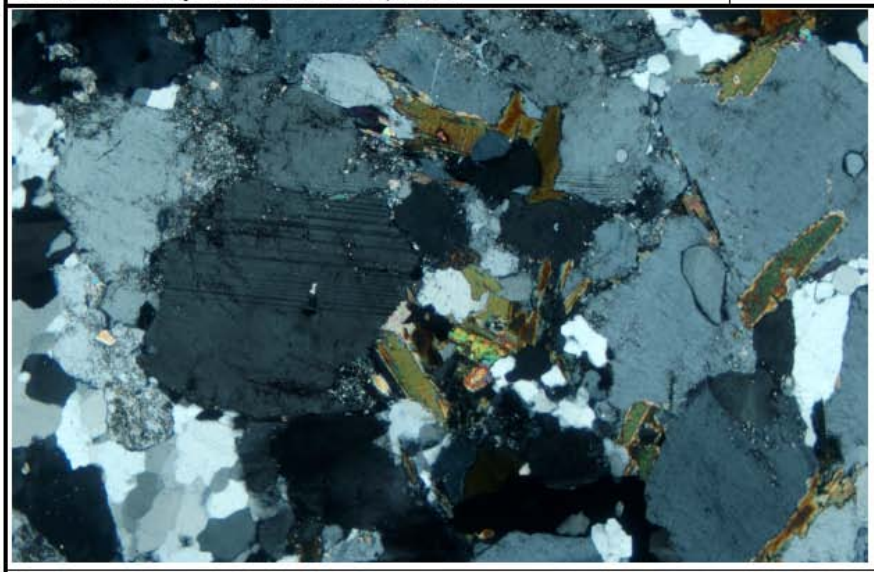

MICROSCOPIC VIEW
Magnification 40x
Field of View
3.25mm x 2.15mm

COMPOSITION

Mineral	Percentage	Typical Size Range (mm)
ORTHOCLASE	39	0.30 - 2.45
QUARTZ	24	0.10 - 0.78
PLAGIOCLASE	20	0.67 - 1.55
MICROCLINE	14	1.08 - 5.15
BIOTITE	3	0.05 - 0.27

REMARKS

GRANITIC GNEISS - This is a coarsely crystalline sample in which the feldspars orthoclase and microcline are dominant over plagioclase. These minerals are seen as relatively equant crystals. While the orthoclase and plagioclase have varying degrees of chemical alteration to white mica (sericite) and calcite, the microcline is virtually unaltered. Biotite is present as a trace and is often associated with pyrite that is an alteration product of the biotite. The boundaries of the feldspar crystals are particularly altered.

SNCGI PETROGRAPHIC ANALYSIS

Sample ID: GA-178-4B

Date Analyzed: 6/06/06

Project: RipRap Study
Location: Florida
Client: University of Massachusetts, Lowell

Analyzed By: SN

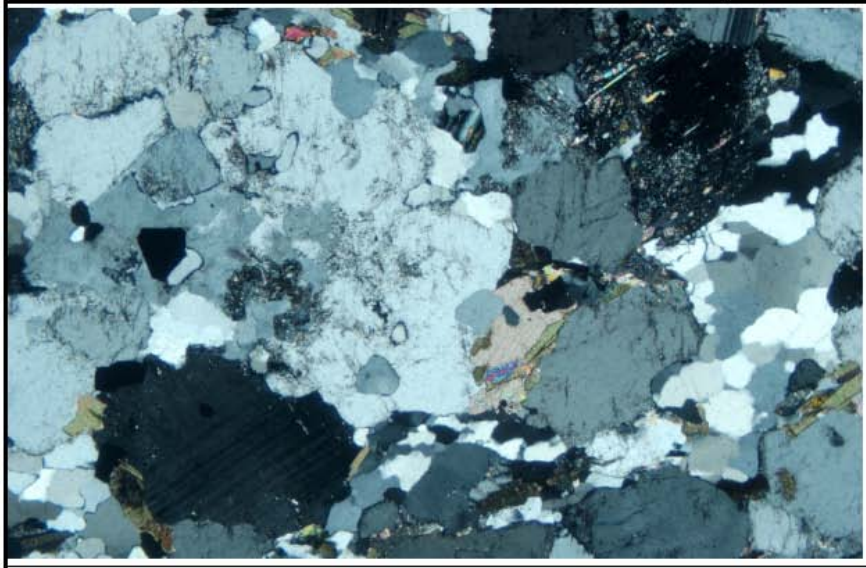

MICROSCOPIC VIEW
Magnification 40x
Field of View
3.25mm x 2.15mm

COMPOSITION

Mineral	Percentage	Typical Size Range (mm)
QUARTZ	48	0.10 - 0.40
ORTHOCLASE	27	0.53 - 2.92
PLAGIOCLASE	12	0.52 - 1.35
MICROCLINE	7	0.50 - 1.50
BIOTITE	4	0.20 - 0.65
CALCITE	1	0.08 - 0.25
MUSCOVITE	1	0.20 - 0.37
PYRITE	<1	0.02 - 0.30

REMARKS

GRANITIC GNEISS - Quartz constitutes nearly half the mineral content of this sample. It is seen as relatively fine crytals that are segregated together in zones. The orthoclase and plagioclase have undergone varying degrees of chemical alteration to white mica and calcite. The maximum degree of alteration in any one crystal is estimated at 65 percent however, the majority of crystals are rarely more than half this amount. The microcline is essentially unaltered. The biotite has undergone partial alteration to pyrite.

SNCGI PETROGRAPHIC ANALYSIS

Sample ID: GA-178-6

Date Analyzed: 6/06/06

Project: RipRap Study
Location: Florida
Client: University of Massachusetts, Lowell

Analyzed By: SN

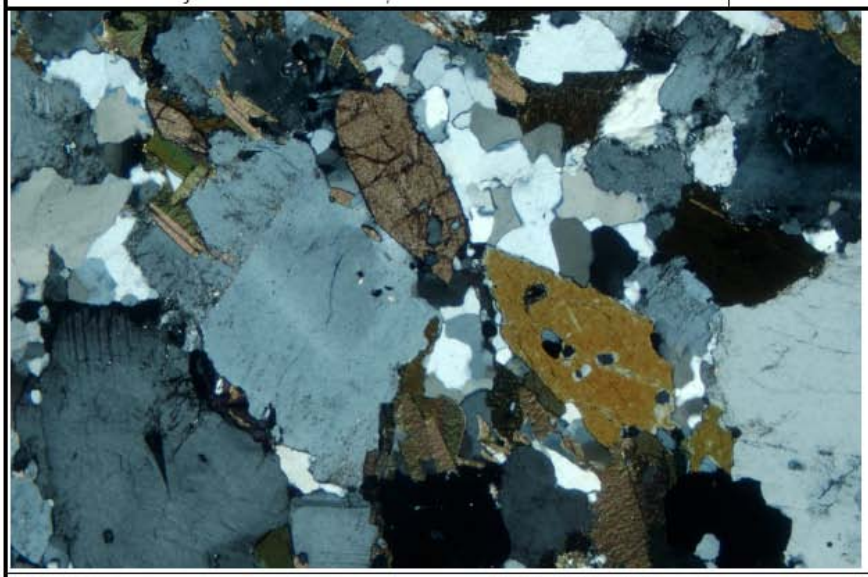

MICROSCOPIC VIEW
Magnification 40x
Field of View
3.25mm x 2.15mm

COMPOSITION

Mineral	Percentage	Typical Size Range (mm)
BIOTITE	33	0.07 - 0.63
PLAGIOCLASE	24	0.25 - 1.75
QUARTZ	23	0.18 - 0.40
ORTHOCLASE	12	0.50 - 2.40
HORNBLENDE	5	0.13 - 0.60
PYROXENE	2	0.32 - 0.55
CARBONATE	1	0.20 - 2.32

REMARKS

BIOTITE GNEISS - Biotite is most abundant in this sample consituting a third of the mineral content. It is seen as thin to coarse blades that show moderate parallel orientation. Some of the biotite has been partially altered to pyrite. Plagioclase and orthoclase are relatively unaltered and are typically coarse grained. Quartz is fine-grained and is most often seen clotted together between the feldspar grains. There are traces of hornblende, pyroxene and carbonate. The carbonate while only present as a trace, is seen as large, well developed euhedral crystals.

SNCGI PETROGRAPHIC ANALYSIS

Sample ID: GA-178-9

Date Analyzed: 6/06/06

Project: RipRap Study
Location: Florida
Client: University of Massachusetts, Lowell

Analyzed By: SN

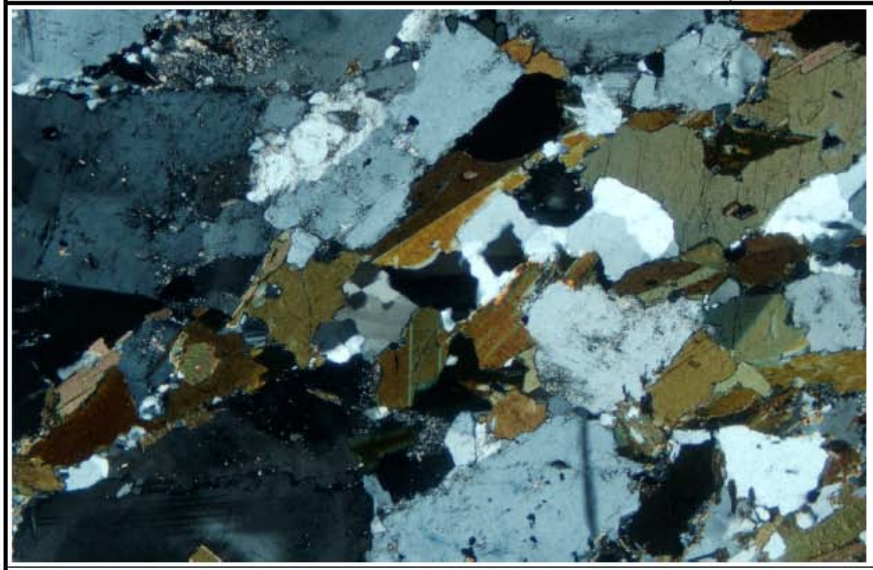

MICROSCOPIC VIEW
Magnification 40x
Field of View
3.25mm x 2.15mm

COMPOSITION

Mineral	Percentage	Typical Size Range (mm)
ORTHOCLASE	21	0.55 - 2.15
PLAGIOCLASE	20	0.33 - 1.50
QUARTZ	19	0.12 - 0.85
BIOTITE	16	0.28 - 0.58
HORNBLENDE	16	0.70 - 1.15
CARBONATE	8	0.18 - 1.32
MICROCLINE	<1	1.08 - 1.52
PYRITE	<1	0.10 - 0.22

REMARKS

BIOTITE HORNBLENDE SCHIST - The feldspars plagioclase and orthoclase for the major portion of this sample. They are slightly to moderately altered to sericite, typically in the cores of the crystals. The estimated maximum alteration in any one crystal is estimated at 40 percent. There is a trace of microcline and it is unaltered. Quartz is found as clots of small grains in between the larger feldspar crystals and the biotite. Biotite and hornblende are present in equal amounts and have undergone very little chemical alteration, primarily to magnetite. There is a minor amount of free carbonate present that occurs as well developed euhedral crystals.

B.3 PETROGRAPHIC DESCRIPTIONS BY G. MCCLELLAN

The full text of Dr. McClellan's (2006) report is reproduced here including all addenda.

* * *

To: Dr. Christopher Niezrecki
Principal Investigator

From: Guerry McClellan
Professional Geologist

Date: June 1, 2006

Subject: Petrographic Rock Studies

As part of the preparation for the petrographic studies, I have examined the specimens provided by the University of Massachusetts -Lowell staff to confirm the rock types and develop a macro-description. This has been done to determine similarities and differences in rocks used in this study and materials used in previous characterization studies for the Materials Office of the Florida Department of Transportation.

Following the macro-textural characterization representative portions were selected and slabs were sawn from the macro-samples for thin section study. These slabs were sent to a commercial lab for section preparation. Sample numbers were randomly drawn for the order of investigation to increase objectivity in the petrographic analysis. The mechanical stage was arbitrarily moved after each study to assure that the starting point on the next study began and ended at a random location. A minimum of 100 points were counted on each slide, and the data were recorded following the examples previously reported for textural types.

The same procedure was followed for the granite thin section, but the textural types for this stone did not fit the protocol used for the sedimentary rocks. The mineralogy of the granite was recorded and local texture was described. The results for this stone were recorded to have a petrographic number of 100 in keeping with previous work and values recorded in the literature.

The descriptions of the stones follow:

08-534 from Goodwin Brothers Construction, Brooksville, Florida. The sample provided is a partially silicified, partially recrystallized portion of the fossiliferous, calcareous Suwannee Limestone. Literature descriptions of the Suwannee LS from this area often call it "case hardened," referring to the dense texture of the stone and the upper 10-25 feet of the underlying Ocala LS. Most of the previously studied materials were from the former Florida Crushed Stone (now operated by Rinker Materials) quarries.

Table B-8 Count Table for 08-534-02

Sample ID	***8534***			
Location	***Brooksville***			
Description	**Count Number**	**Percent of Total**	**Factor**	**Weighted Value**
Fossil Grains	38	36.1	1.3	46.93
Non-fossil Grains	8	7.6	1	7.6
Moldic porosity	5	4.7	3	14.1
Interparticle porosity	2	1.9	3	5.7
Intragranular porosity	4	3.8	2	7.6
TOTAL POROSITY	11	10.4		
Micrite cement	5	4.7	1.5	7.05
Microspar & sparite cement	13	12.3	1	12.3
TOTAL CEMENT/MATRIX	18	17		
Dolomitic cement/grains	0	0	1.5	0
Chert	6	5.7	6	34.2
Quartz	24	22.8	3	68.4
Opaques	0	0	6	0
Total	**105**	**99.6**		**203.88**

This sample is not typical of limestones we have previously examined from the Brooksville area because of its high chert content. Rocks with chert contents in excess of 3% have their factor value raised to 6 in anticipation of potential problems with alkali silica reactivity (ASR) and a resultant increase in their petrographic numbers, indicating a decline in performance expectations.

GA-178 from Rinker, Macon, Georgia. This is a sample of one of the Precambrian metamorphosed granites in the Macon area. Gneissic banding is very common in the specimens provided as are other textural inhomgeneities. This results in the alternating light and dark bands which are easily seen in had specimens. Gneissic banding causes the rock properties to be anisotropic (different if measured parallel or perpendicular to the banding). . Previous studies have used the Tyrone granite from the Florida Rock Industries quarry in the Atlanta area. The petrographic number assigned to

this rock is arbitrarily set at 100 based on previous studies and literature reports on granites used as aggregates.

12-521 from Bonita Sand and Gravel, Bonita Springs, Florida. These specimens are from the very fossiliferous Tamiami Limestone. This rock is very porous at the macroscale (moldic and other secondary porosity is obvious) and consists of a mixture of tan colored fragments in a grey limestone matrix.

Table B-9 Count Table for 12-521-08

Sample ID ***125218***

Location ***Bonita Springs - Tamiami***

Description	Count Number	Percent of Total	Factor	Weighted Value
Fossil Grains	7	6.3	1.3	8.19
Non-fossil Grains	41	36.9	1	36.9
Moldic porosity	5	4.5	3	13.5
Interparticle porosity	1	0.9	3	2.7
Intragranular porosity	1	0.9	2	1.8
TOTAL POROSITY	7	1.8		
Micrite cement	21	18.9	1.5	28.35
Microspar & sparite cement	20	18	1	18
TOTAL CEMENT/MATRIX	41	36.9		
Dolomitic cement/grains	0	0	1.5	0
Chert	0	0	3	0
Quartz	14	12.6	3	37.8
Opaques	1	0.9	6	5.4
Total	**111**	**99.9**		**152.64**

This is a typical example of the Tamiami LS (PN=149.1) except for the higher than expected content of quartz. The latter observation combines with an unidentified opaque mineral to give a slightly higher than expected petrographic number. This stone would be expected to have fair to poor field performance.

38-228 from Martin Marietta, Lamont, Madison County, Florida. This sample consists of a mixture of soft tan calcareous limestone and a hard, dense, grey limestone in nearly equal proportions. The material in the tan portions is somewhat more friable than the grey rock and weathering has decreased the overall induration of the stone. These textures are typical of Suwannee Limestone found in western Taylor County and parts of Madison County.

Table B-10 Count Table for 38-228-04

Sample ID	***38228***			
Location	***Lamont, Suwannee LS***			
Description	**Count Number**	**Percent of Total**	**Factor**	**Weighted Value**
Fossil Grains	33	28.6	1.3	37.18
Non-fossil Grains	12	10.4	1	10.4
Moldic porosity	5	4.3	3	12.9
Interparticle porosity	5	4.3	3	12.9
Intragranular porosity	6	5.2	2	10.4
TOTAL POROSITY	16	13.8		
Micrite cement	18	15.6	1.5	23.4
Microspar & sparite cement	33	28.6	1	28.6
TOTAL CEMENT/MATRIX	51	44.2		
Dolomitic cement/grains	0	0	1.5	0
Chert	1	0.8	3	2.4
Quartz	2	1.7	3	5.1
Opaques	0	0	6	0
Total	**115**	**99.5**		**143.28**

The Suwannee Limestone is regarded as one of the best construction materials in Florida (reported PN=129.6). The relatively low PN determined for this stone indicates this material should have good performance characteristics in a wide range of applications.

18-607 from Statewide Aggregates, Center Hill, Florida. This sample is chert that formed at the top of the Ocala Limestone. It is fossiliferous, dense and very hard.

Table B-11 Count Table for 18-607-05

Sample ID	***18607***			
Location	***Center Hill Ocala LS***			
Description	**Count Number**	**Percent of Total**	**Factor**	**Weighted Value**
Fossil Grains	37	32.1	1.3	41.73
Non-fossil Grains	19	16.5	1	16.5
Moldic porosity	1	0.8	3	2.4
Interparticle porosity	1	0.8	3	2.4
Intragranular porosity	1	0.8	2	1.6
TOTAL POROSITY	3	2.4		
Micrite cement	22	19.1	1.5	28.65
Microspar & sparite cement	7	6	1	6
TOTAL CEMENT/MATRIX	29	25.1		
Dolomitic cement/grains	0	0	1.5	0
Chert	27	23.4	6	140.4
Quartz	0	0	3	0
Opaques	0	0	6	0
Total	**115**	**99.5**		**239.68**

The high content of chert in this sample is very atypical of the Ocala Limestone. This formation is characterized by stones that contain 99% $CaCO_3$. Samples with high silica contents usually occur at the very top of the formation where silicification from weathering of the overlying clay bearing Hawthorn Group sediments has taken place. This is somewhat similar to 08-534 (Ocala-Suwannee material from Brooksville area).

87-339 from White Rock Aggregate, West Palm Beach, Florida. This sample is an oolitic limestone typical of the Miami Limestone. Many of the macropores are mud-filled and part of the calcite recrystallized in areas. These pieces are rather inhomogeneous and one portion shows traces of manganese staining. This rock is slightly friable, but is well enough indurated that sawing is not a problem.

Table B-12 Count Table for 87-339-10A

Sample ID	***87339A***			
Location	***Miami Oolite***			
Description	**Count Number**	**Percent of Total**	**Factor**	**Weighted Value**
Fossil Grains	6	5.3	1.3	6.89
Non-fossil Grains	28	25	1	25
Moldic porosity	13	11.6	3	34.8
Interparticle porosity	0	0	3	0
Intragranular porosity	11	9.8	2	19.6
TOTAL POROSITY	24	21.4		
Micrite cement	19	16.9	1.5	25.35
Microspar & sparite cement	29	25.8	1	25.8
TOTAL CEMENT/MATRIX	48	42.7		
Dolomitic cement/grains	0	0	1	0
Chert	0	0	1.5	0
Quartz	4	3.5	3	10.5
Opaques	2	1.7	6	10.2
Total	**112**	**99.6**		**158.14**

Table B-13 Count Table for 87-339-10B

Sample ID	***87339B***			
Location	***Miami oolite***			
Description	**Count Number**	**Percent of Total**	**Factor**	**Weighted Value**
Fossil Grains	6	5.8	1.3	7.54
Non-fossil Grains	35	34.3	1	34.3
Moldic porosity	1	0.9	3	2.7
Interparticle porosity	3	2.9	3	8.7
Intragranular porosity	5	4.9	2	9.8
TOTAL POROSITY	9	8.7		
Micrite cement	20	19.6	1.5	29.4
Microspar & sparite cement	20	19.6	1	19.6
TOTAL CEMENT/MATRIX	40	39.2		
Dolomitic cement/grains	0	0	1.5	0
Chert	8	7.8	6	46.8
Quartz	4	3.9	3	11.7
Opaques	0	0	6	
Total	**102**	**99.7**		**170.54**

The PN values for this sample are similar to those previously reported (148.8). In this case we are reporting two PN values, determined by measuring the same slide twice, first and last in our study to minimize any learning effect from measuring the other slides. The difference in the PN values is largely the result of encountering a significant number of chert grains in the second series of measurements resulting in an increased PN. The values determined for other components are more or less the same between samples.

34-106 from Florida Rock Industries at Gulf Hammock, Florida. This rock is a mixture of tan and grey dolomite with no indication of particle boundaries between the various colored stone. Stone from this site has been extensively studied, and these specimens submitted here are rather atypical in appearance. Previous work in the mid- to late 1990s showed the Avon Park at the Gulf Hammock Mine is a mixture of dark grey and nearly white dolomitic stone. The Gulf Hammock mine has moved south and east into a tan dolomite similar to that seen in the past at the Cemex mine (formerly

Independent Aggregate) located several miles to the south. The material in this study is from a transitional area between the 1990 type ore and that which is currently being mined.

Because of the heterogeneity of this stone, two thin sections were made at right angles to each other, and a PN was determined for each thin section. The results obtained for the two measurements are the same within statistical variation and are in good agreement with previous measurements (129.8).

Table B-14 Count Table for 34-106-09A

Sample ID	***341069A***			
Location	***Gulf Hammock, Avon Park***			
Description	**Count Number**	**Percent of Total**	**Factor**	**Weighted Value**
Fossil Grains	5	4.5	1.3	5.85
Non-fossil Grains	33	30.2	1	30.2
Moldic porosity	0	0	3	0
Interparticle porosity	8	7.3	3	21.9
Intragranular porosity	5	4.5	2	9
TOTAL POROSITY	13	11.8		
Micrite cement	0	0	1.5	0
Microspar & sparite cement	23	21.1	1	21.1
TOTAL CEMENT/MATRIX	58	21.1		
Dolomitic cement/grains	35	32.1	1.5	48.15
Chert	0	0	3	0
Quartz	0	0	3	0
opaques	0	0	6	0
Total	**109**	**99.7**		**136.2**

Table B-15 Count Table for 34-106-09B

Sample ID	***34106B***			
Location	***Gulf Hammock, Avon Park***			
Description	**Count Number**	**Percent of Total**	**Factor**	**Weighted Value**
Fossil Grains	3	2.8	1.3	3.64
Non-fossil Grains	29	27.6	1	27.6
Moldic porosity	8	7.6	3	22.8
Interparticle porosity	1	0.9	3	2.7
Intragranular porosity	0	0	2	0
TOTAL POROSITY	9	8.5		
Micrite cement	0	0	1.5	0
Microspar & sparite cement	35	33.3	1	33.3
TOTAL CEMENT/MATRIX	63	33.3		
Dolomitic cement/grains	28	26.6	1.5	39.9
Chert	0	0	3	0
Quartz	0	0	3	0
opaques	1		6	0
Total	**105**	**98.8**		**129.94**

Conclusions:

Based on the results of these studies, previous work done by this author and his colleagues, and professional experience, these seven materials can be divided into two types of stones from the producing areas.

Results similar to those obtained in previous studies of samples from the same or similar sites: 15-521 (Tamiami LS), 38-228 (Suwannee LS), 87-339 (Miami Oolite), and 34-106 (Avon Park).

Results that differ significantly from previous studies of samples from the same site or have not been studied in the past: 08-534 (Suwannee-Ocala LS), GA-178 (gneissic granite), and 18-607 (Ocala LS).

In previous work on stones studied for the FDOT none had been assigned a PN value of 160 or greater (= poor performance expected). Three of the stones reported here have PN values greater than 160.

B.3.1 ADDENDUM TO FINAL REPORT:

* * *

To: Dr. Christopher Niezrecki
Principal Investigator

From: Guerry McClellan
Professional Geologist

Date: June 14, 2006

Subject: Petrographic Rock Studies-Addendum

As part of the preparation for the petrographic studies, I have examined the specimens provided by the University of Massachusetts -Lowell staff to confirm the rock types and develop a macro-description and quantify the petrographic textures using the petrographic number method developed at UF. This has been done to determine similarities and differences in rocks used in this study and materials used in previous characterization studies for the Materials Office of the Florida Department of Transportation.

Following the macro-textural characterization representative portions were selected and slabs were sawn from the macro-samples for thin section study. These slabs were sent to a commercial lab for section preparation. Sample numbers were randomly drawn for the order of investigation to increase objectivity in the petrographic analysis. The mechanical stage was arbitrarily moved after each study to assure that the starting point on the next study began and ended at a random location. A minimum of 100 points were counted on each slide, and the data were recorded following the examples previously reported for textural types.

The same procedure was followed for the granite thin section, but the textural types for this stone did not fit the protocol used for the sedimentary rocks. The mineralogy of the granite was recorded and local texture was described.

The descriptions of this stone follow:

GA-178 from Rinker, Macon, Georgia. This is a sample of one of the Precambrian metamorphosed igneous rocks in the Macon area. Gneissic banding is very common in the specimens provided as are other textural inhomgeneities. These result in the alternating light and dark bands which are easily seen in had specimens. Gneissic banding causes the rock properties to be anisotropic (different if measured parallel or perpendicular to the banding).

As requested, the mineralogical data collected from GA-178 have been tabulated as an addendum to the earlier report. The results of this study are tabulated below:

Table B-16 Count Table for GA-178-03

Sample ID	***GA-178***	
Location	***Macon, Georgia- Rinker***	
Description	**Count Number**	**Percent of Total**
K-spar (othoclase/microcline)	3	2.7
Plagioclase	19	17.4
Quartz	41	37.6
Opaques	4	3.7
Biotite	42	38.5
Total	109	100.0

These data indicate that this rock is not a granite, but rather is a granodiorite based on IUGS classification using total silica and quartz contents as criteria. The ratio of K-spar to plagioclase is low and high content of biotite (and the absence of muscovite)

confirm a granodiorite. The gneissic texture derives from pronounced concentration and interlayering of biotite with quartz and plagioclase. The quartz shows undulatory extinction common in strained igneous rocks and occurs as large clear grains and fragmented pieces. Opaque grains are common in biotite and much less frequent in plagioclase. The opaque grains were not identified, but are likely magnetite and/or ilmentite.

No factor values for the determination of petrographic numbers have been reported for the components of igneous rocks. In keeping with literature practice, a PN of 100 has been empirically assigned to this rock.

APPENDIX C: ADDITIONAL EXPERIMENTAL DATA FROM WINDSOR PIN SYSTEM® TESTING

This appendix contains figures showing the trend in penetration depth with respect to measurement number. The figures presented are in similar to those shown in Figure 0-6 and Figure 0-7. The micrometer readings are subtracted from 1.0 inches to obtain the depth of penetration.

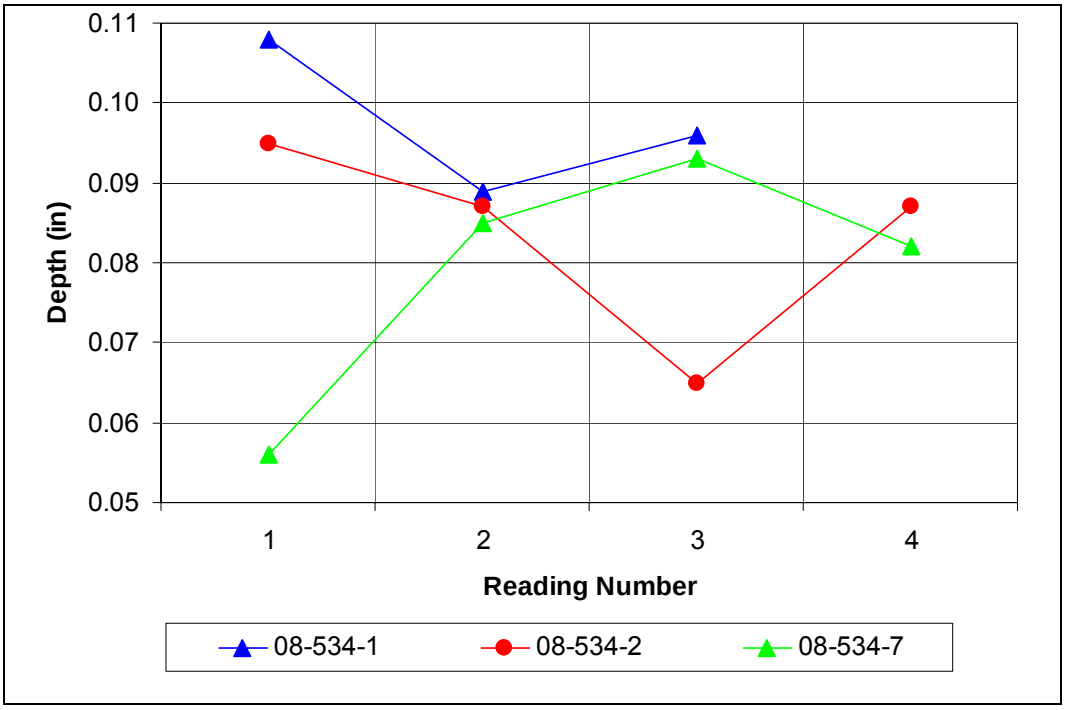

Figure C-1 Depth of Penetration With Respect to Measurement Number for 08-534

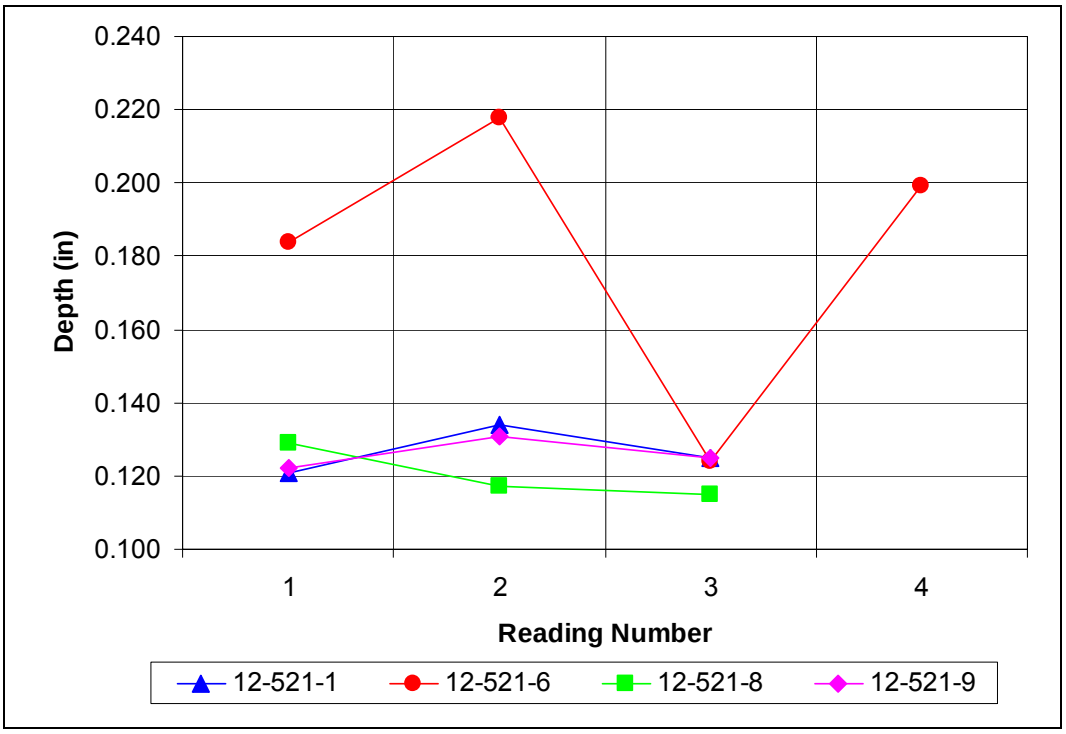

Figure C-2 Depth of Penetration With Respect to Measurement Number for 12-521

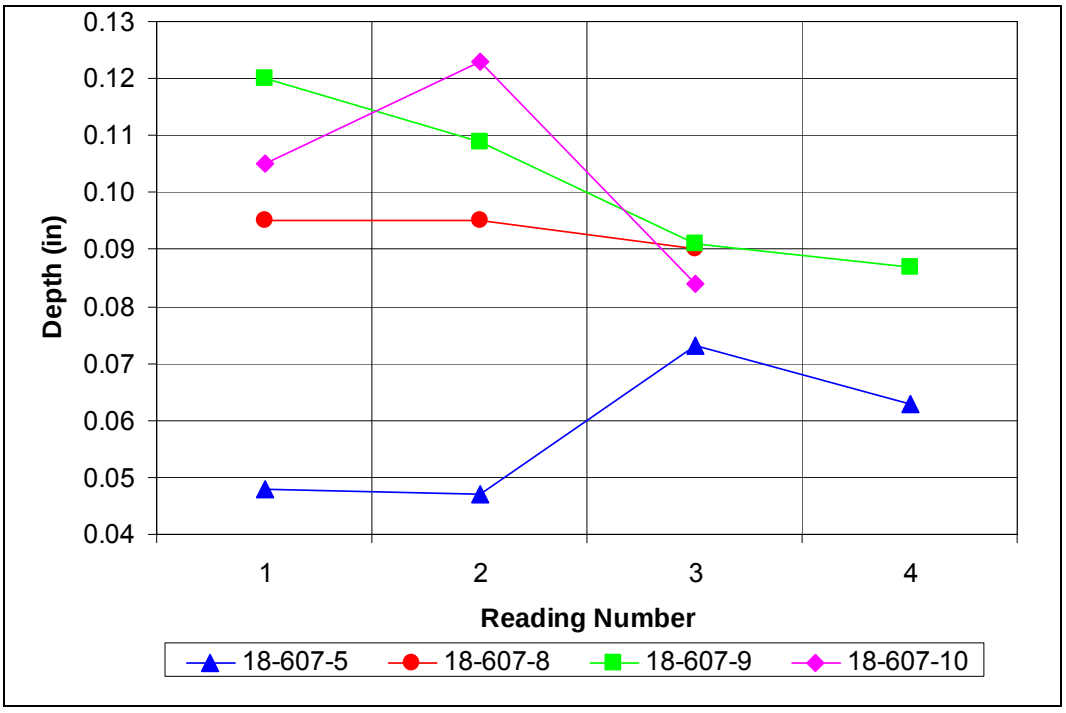

Figure C-3 Depth of Penetration With Respect to Measurement Number for 18-607

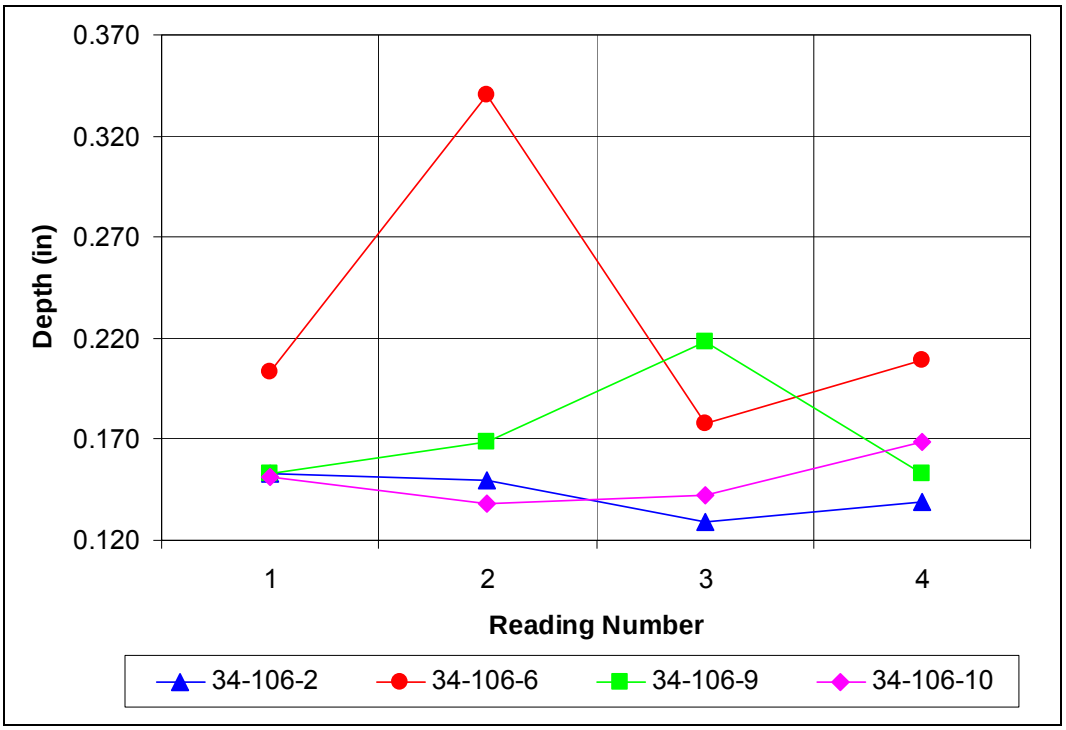

Figure C-4 Depth of Penetration With Respect to Measurement Number for 34-106

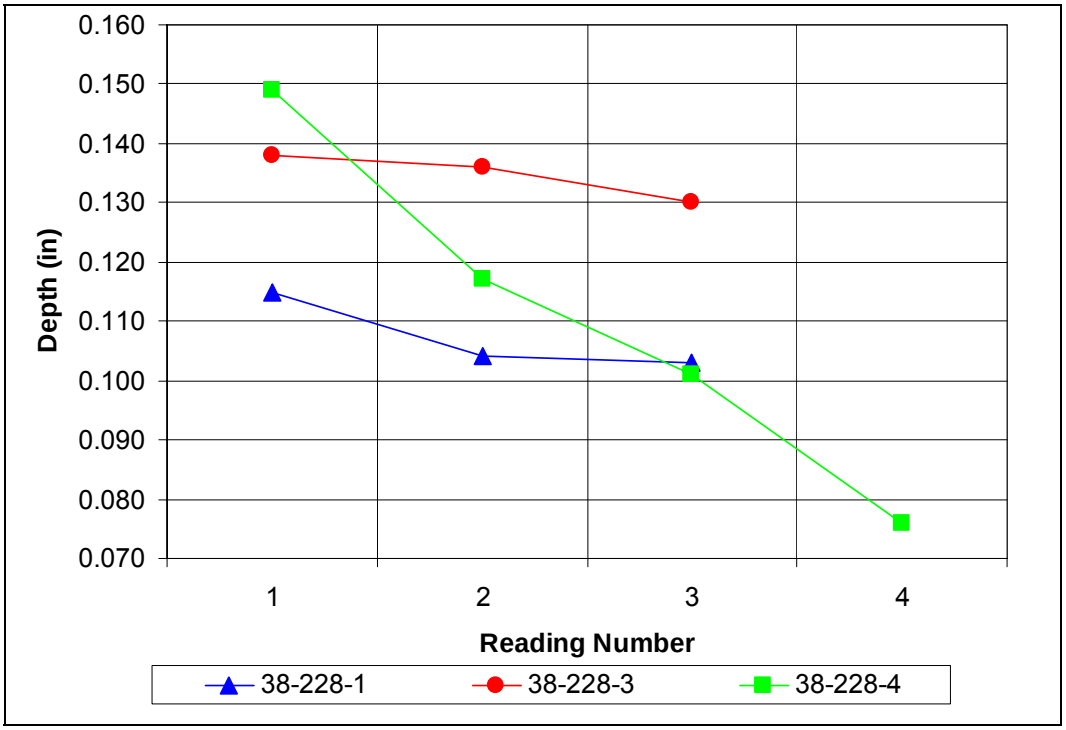

Figure C-5 Depth of Penetration With Respect to Measurement Number for 38-228

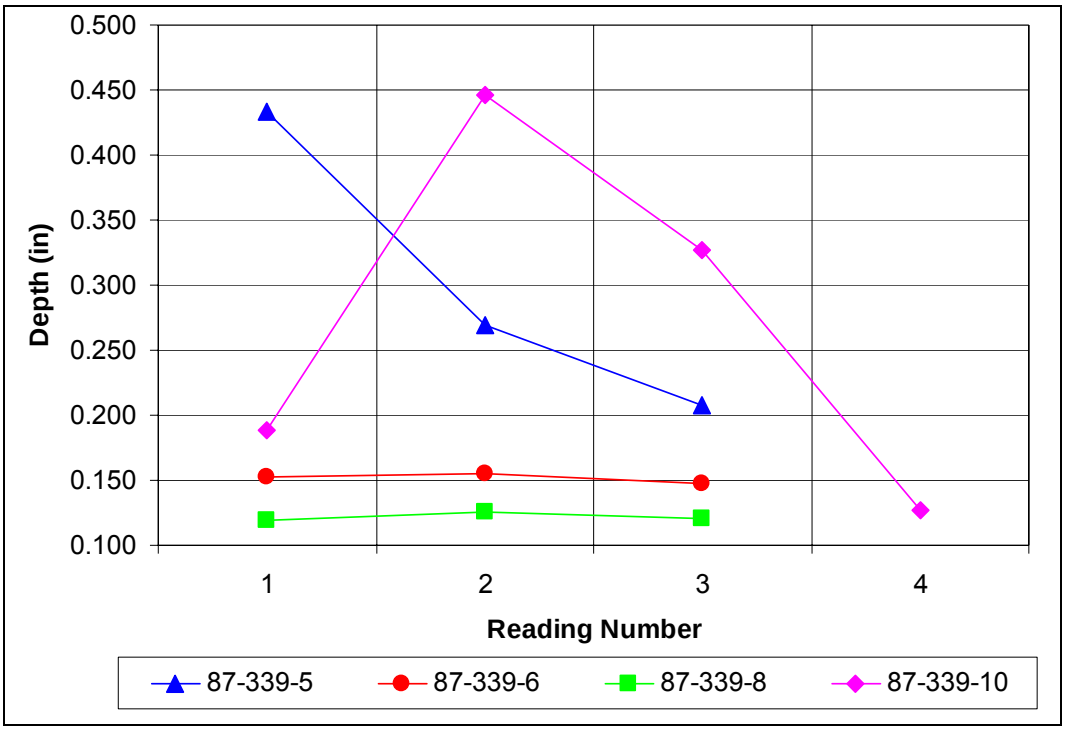

Figure C-6 Depth of Penetration With Respect to Measurement Number for 87-339

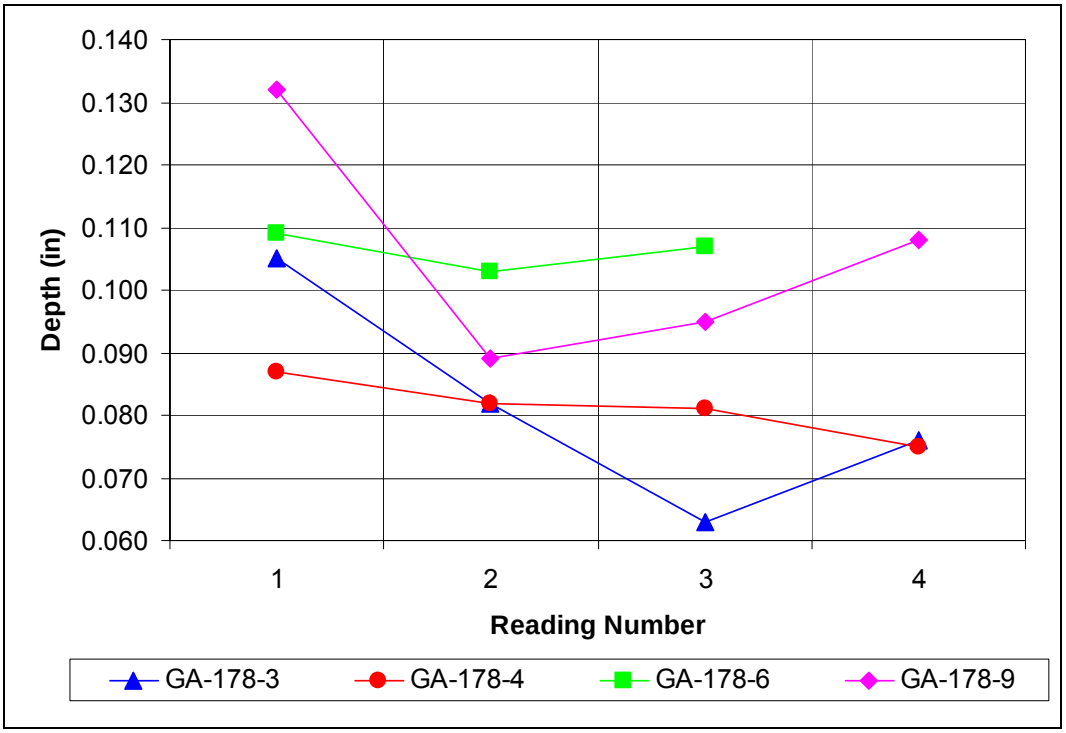

Figure C-7 Depth of Penetrations With Respect to Measurement Number for GA-178

APPENDIX D: EXPERIMENTAL RESULTS FOR ACOUSTIC IMPACT-EMISSION TESTS

Time and frequency domain plots of the acoustic impact-emission tests are provided in this appendix.

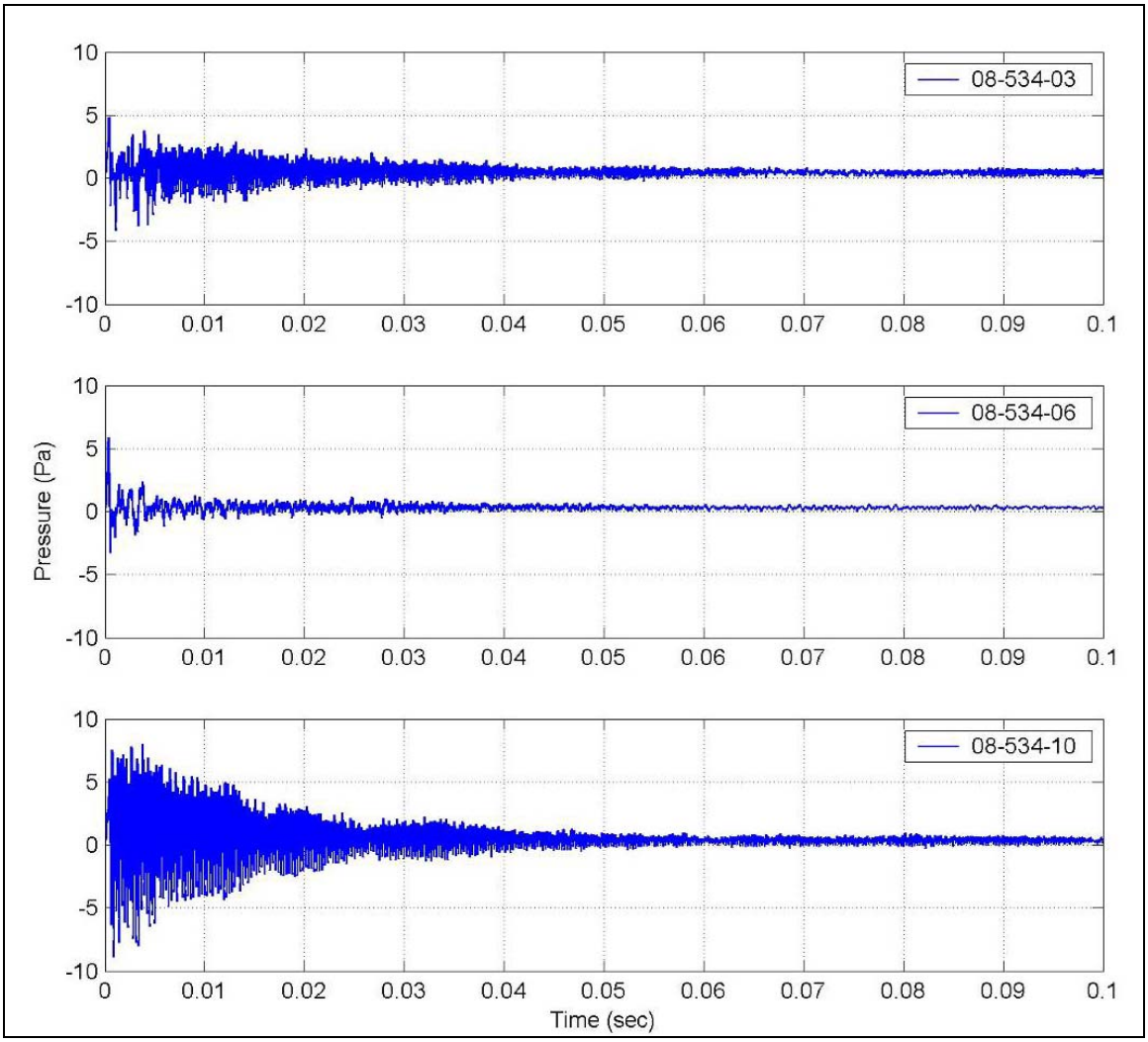

Figure D-1 Acoustic Pressure With Respect to Time for Source 08-534, Brooksville, FL

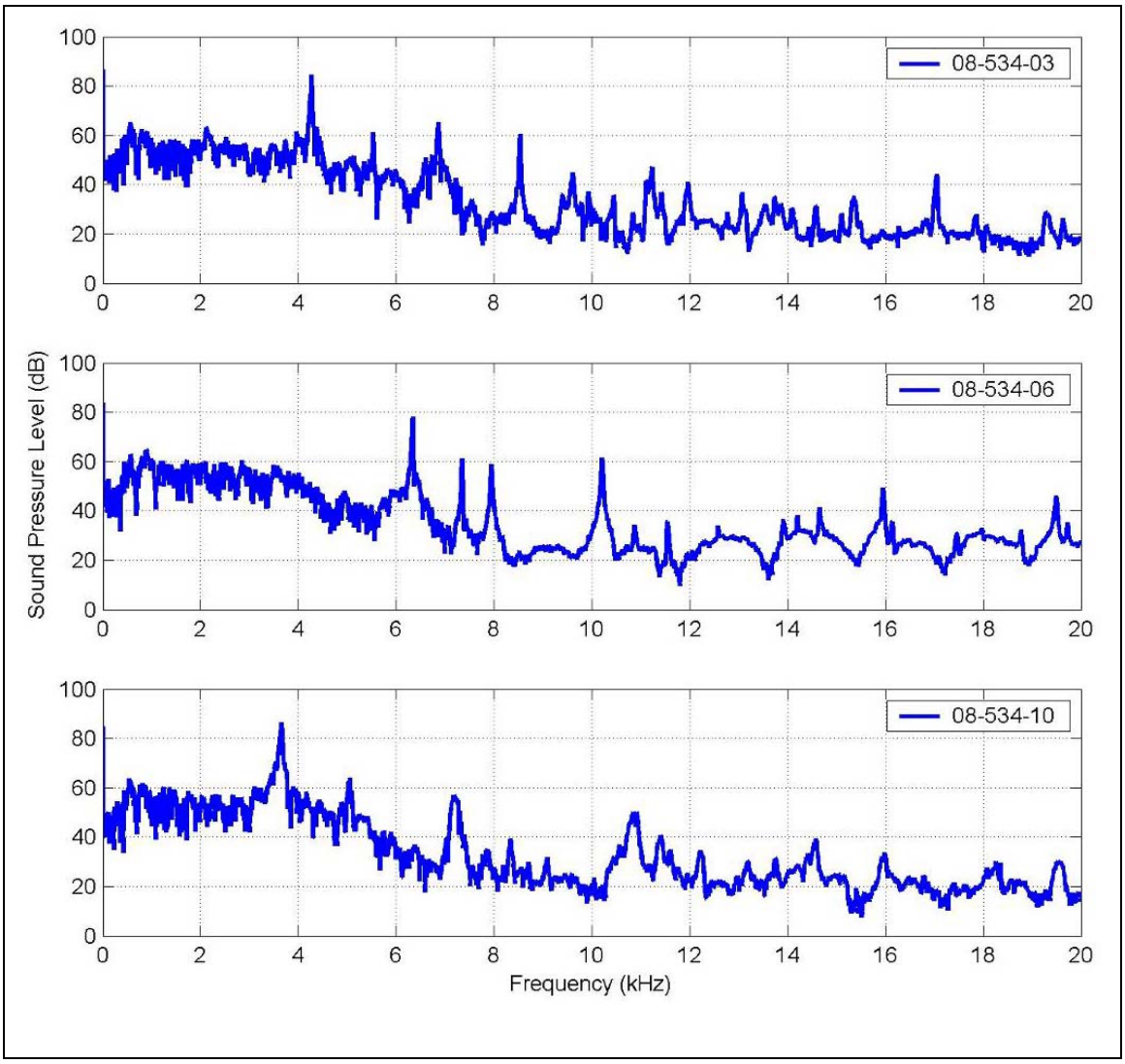

Figure D-2 Sound Pressure Level With Respect to Frequency for Source 08-534, Brooksville, FL

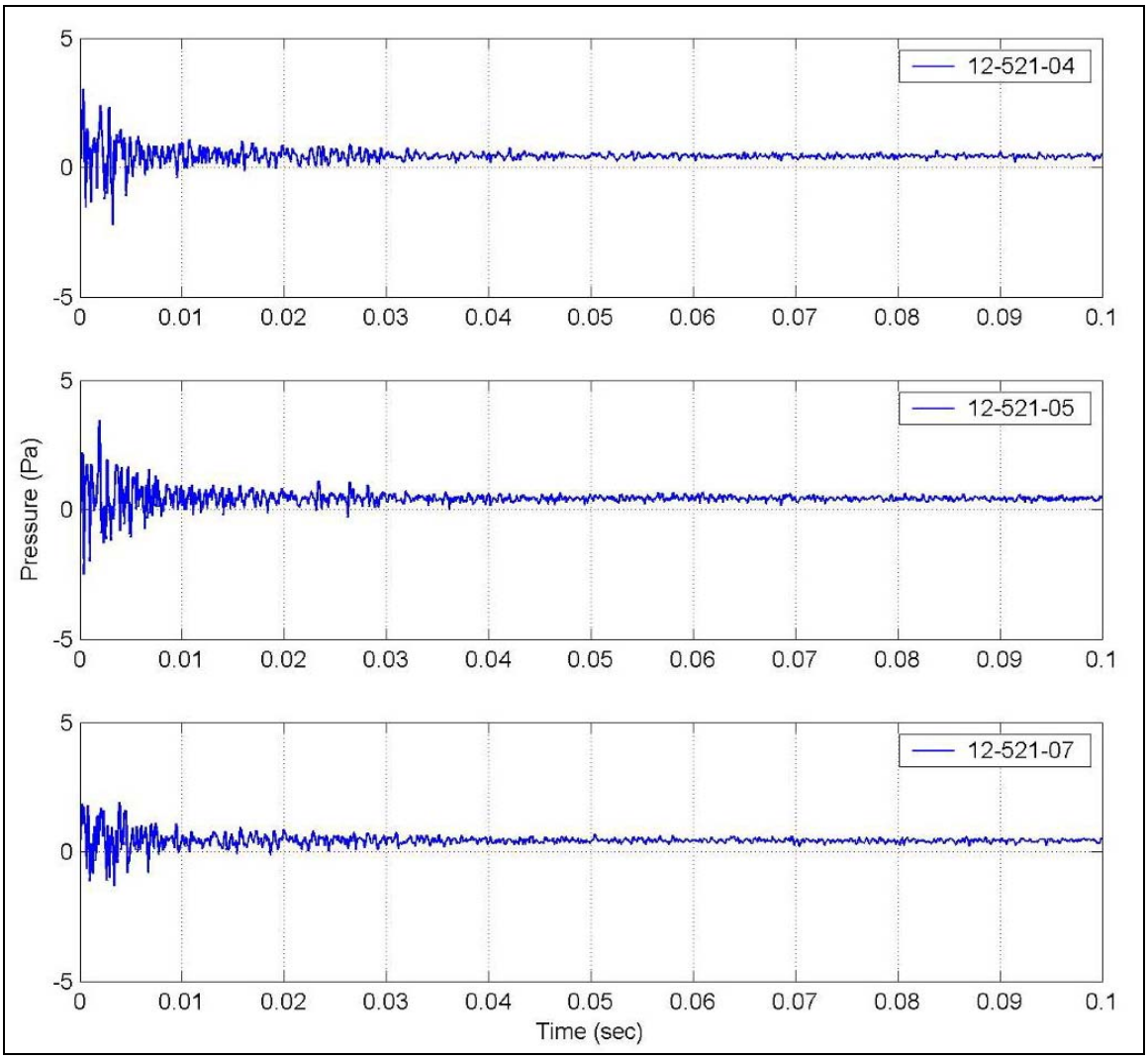

Figure D-3 Acoustic Pressure With Respect to Time for Source 12-521, Bonita Springs, FL

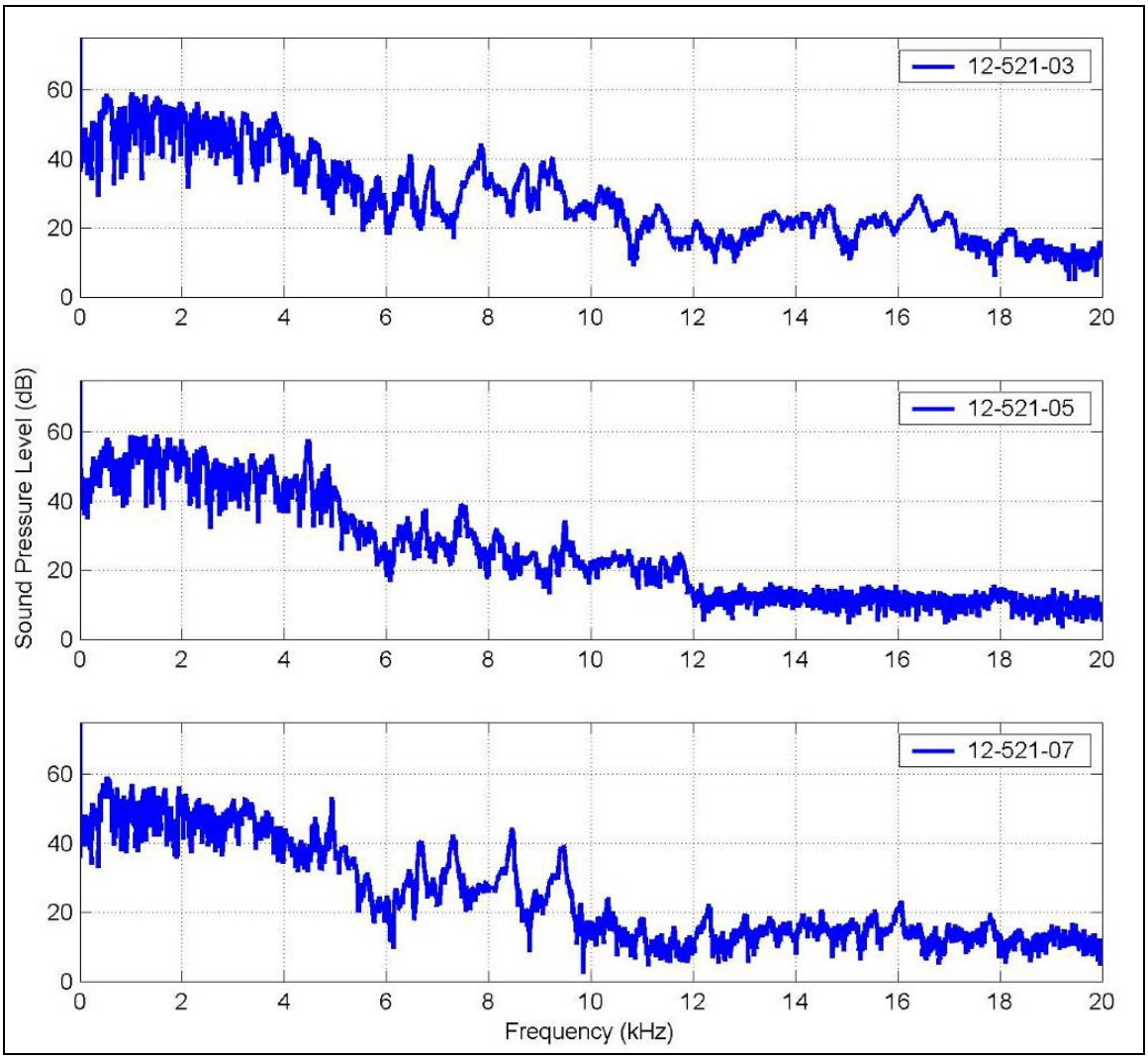

Figure D-4 Sound Pressure Level With Respect to Frequency for Source 12-521, Bonita Springs, FL

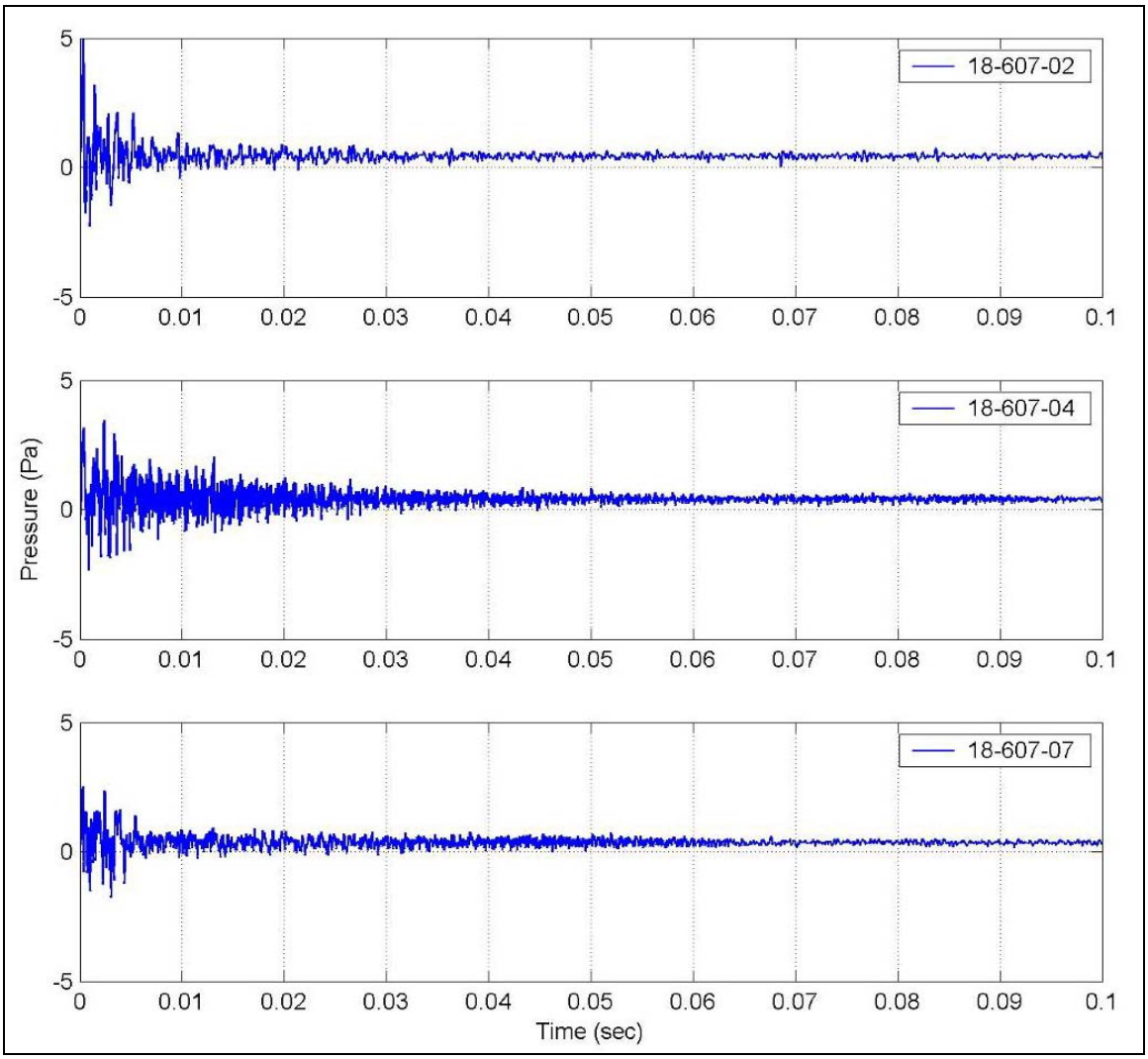

Figure D-5 Acoustic Pressure With Respect to Time for Source 18-607, Center Hill, FL

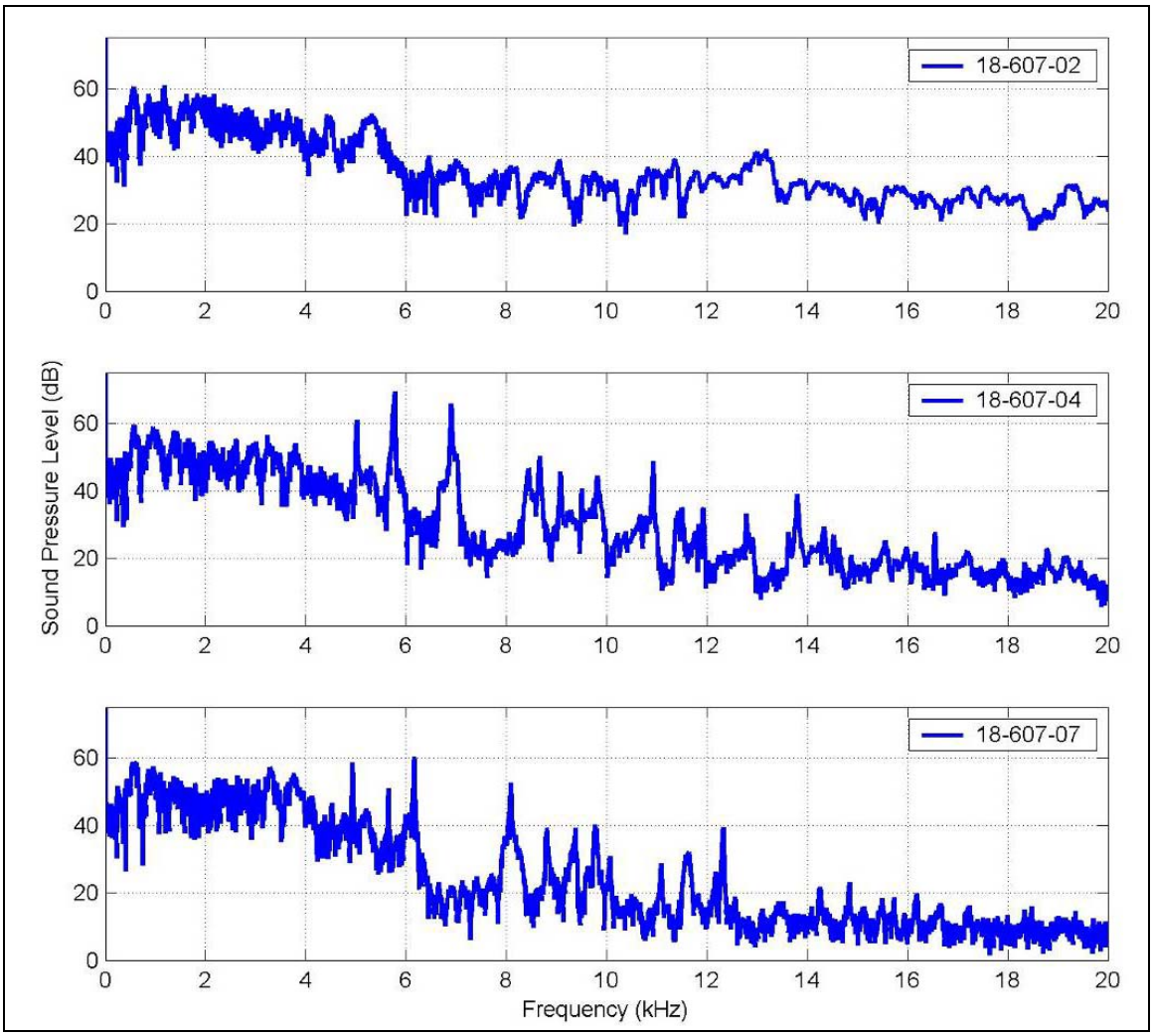

Figure D-6 Sound Pressure Level With Respect to Frequency for Source 18-607, Center Hill, FL

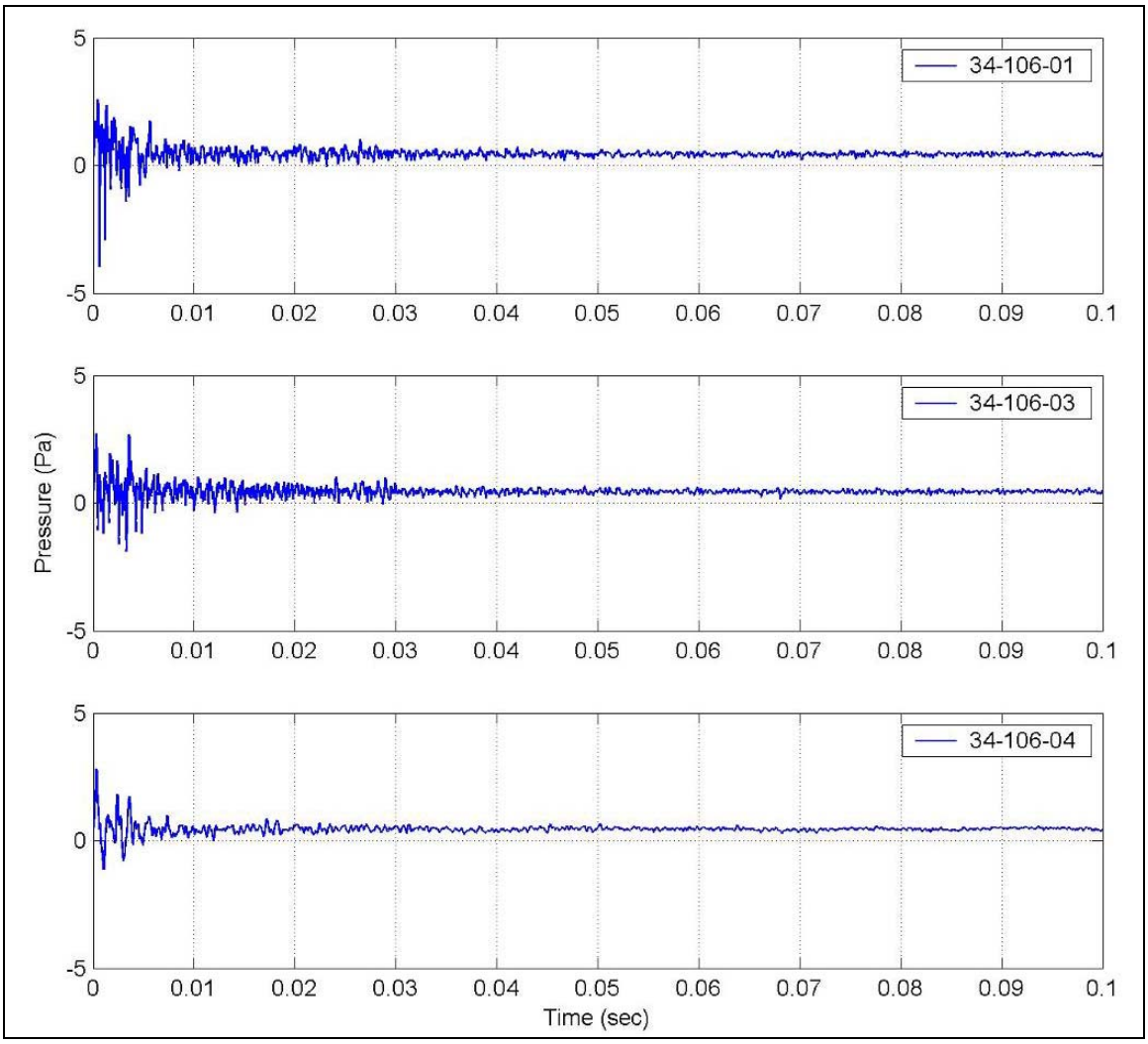

Figure D-7 Acoustic Pressure With Respect to Time for Source 34-106, Gulf Hammock, FL

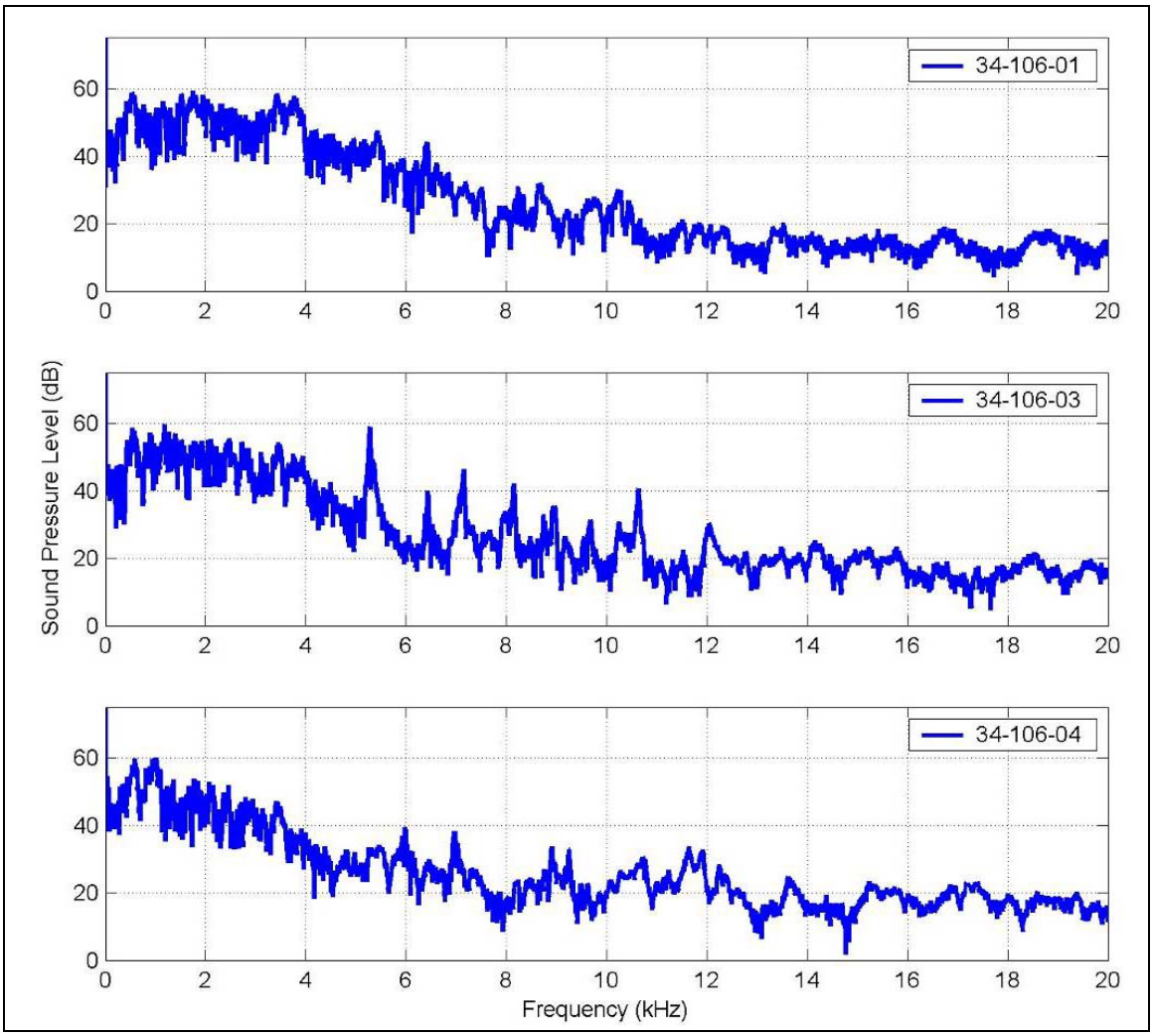

Figure D-8 Sound Pressure Level With Respect to Frequency For Source 34-106, Gulf Hammock, FL

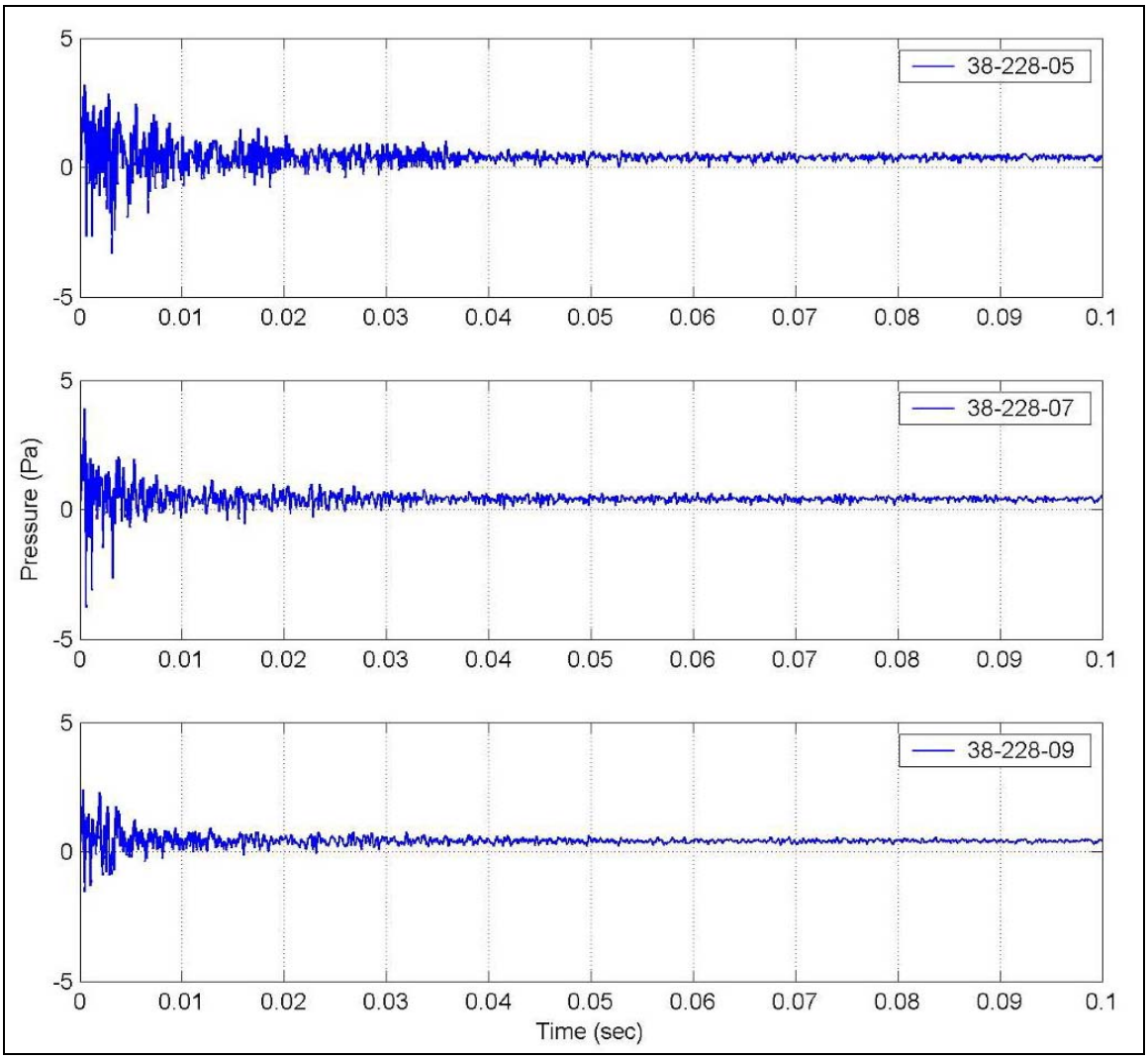

Figure D-9 Acoustic Pressure With Respect to Frequency for Source 38-228, Perry, FL

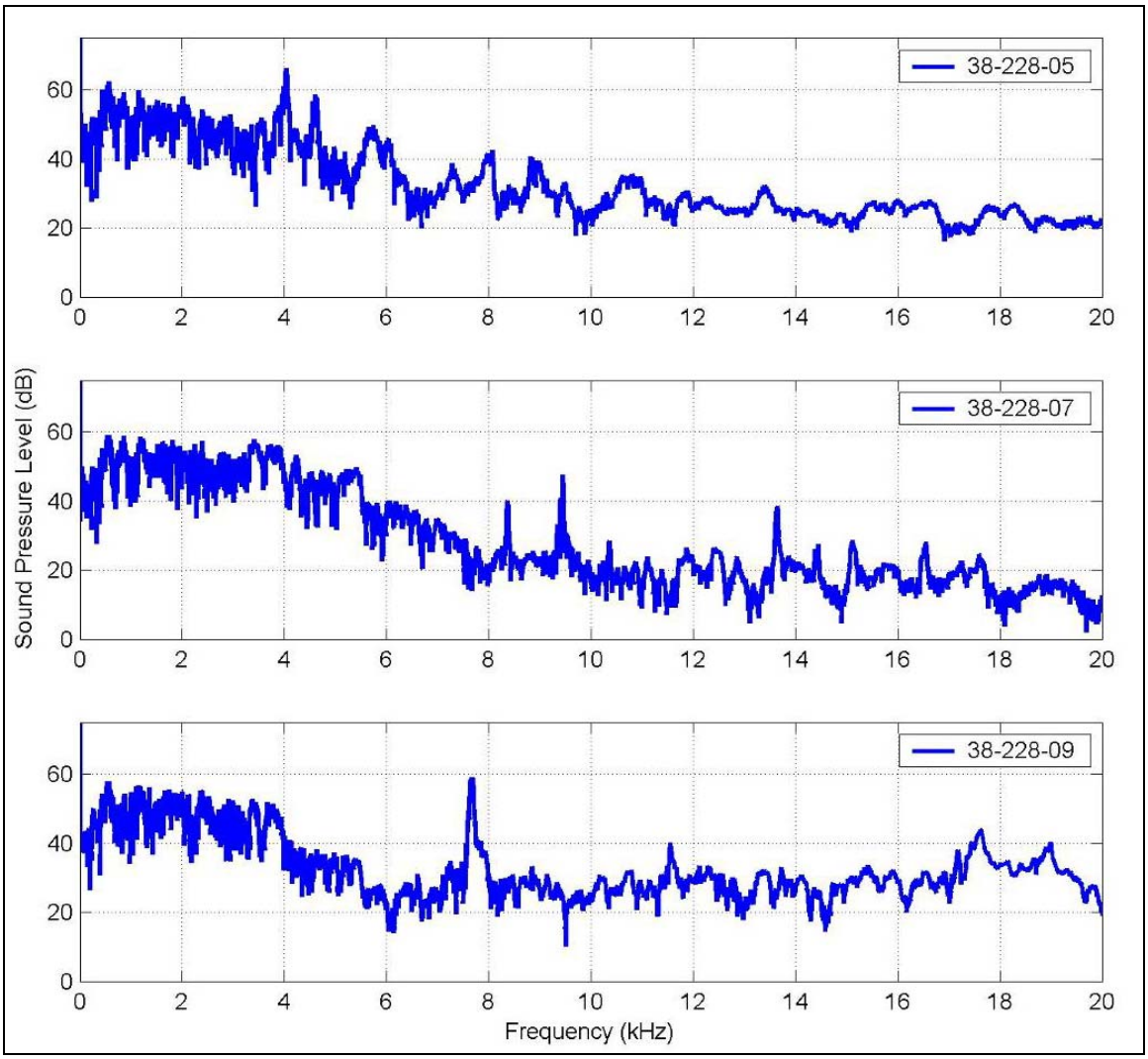

Figure D-10 Sound Pressure Level With Respect to Frequency for Source 38-228, Perry, FL

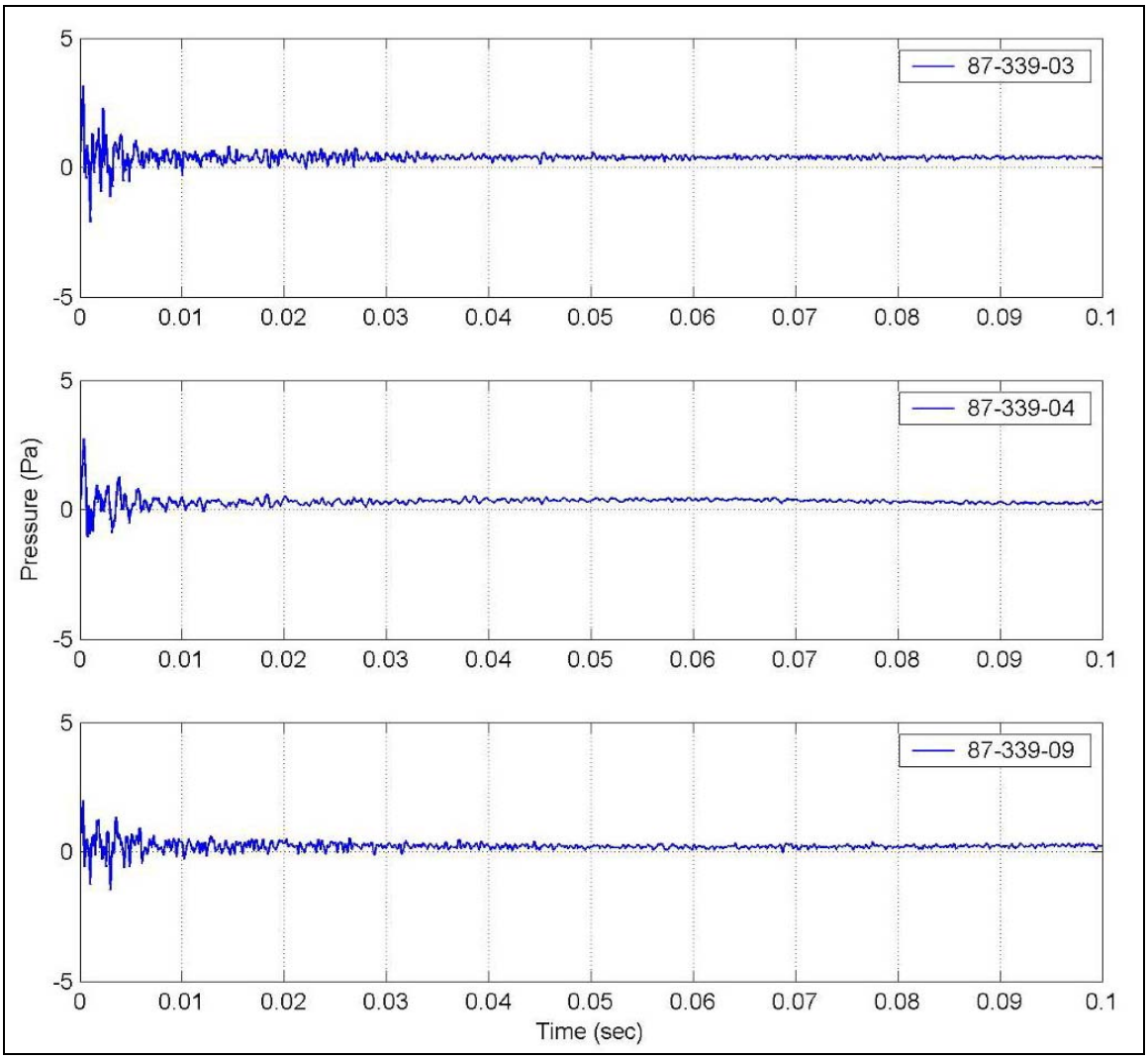

Figure D-11 Acoustic Pressure With Respect to Time for Source 87-339, Hialeah, FL

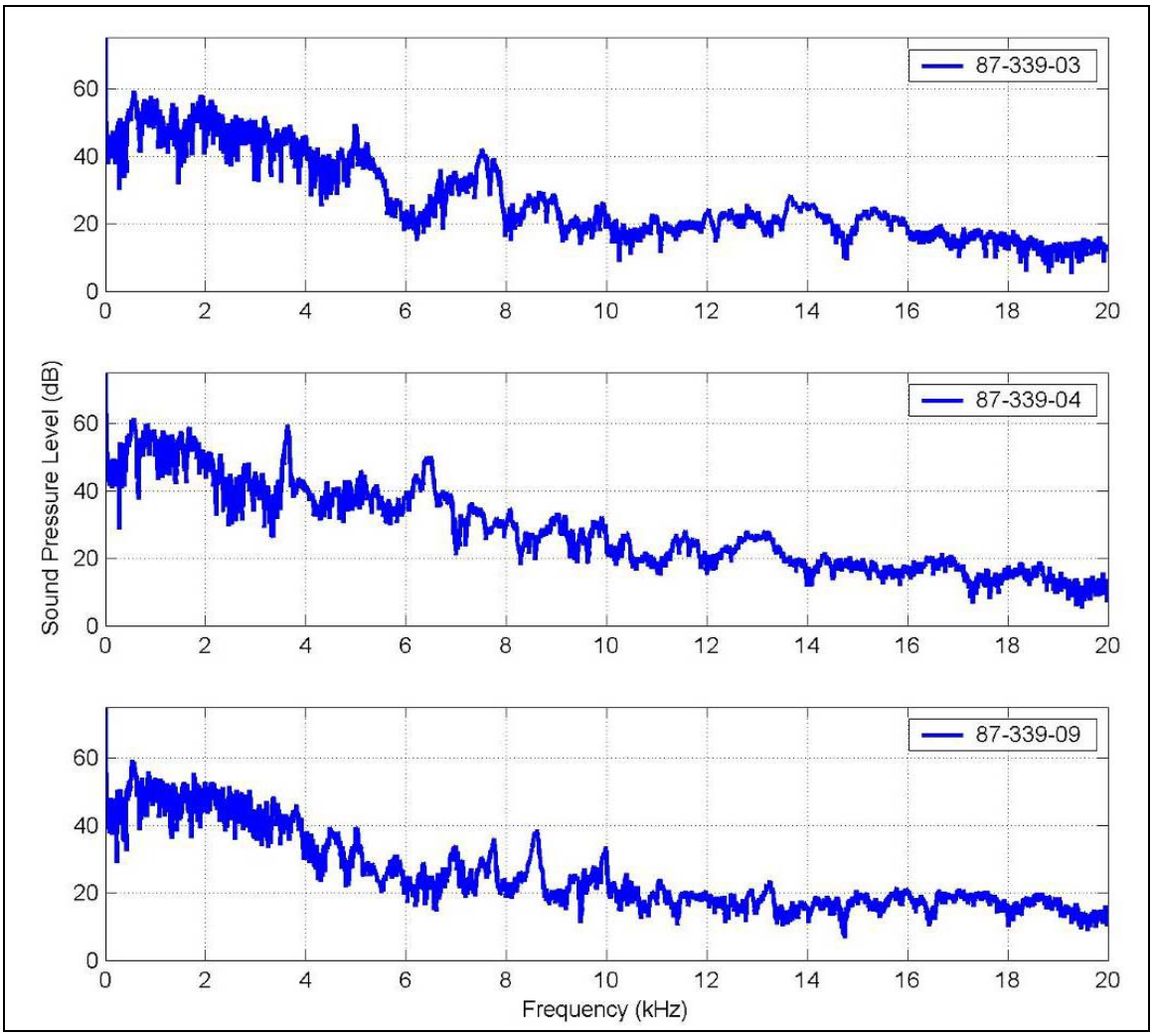

Figure D-12 Sound Pressure Level With Respect to Frequency for Source 87-339, Hialeah, FL

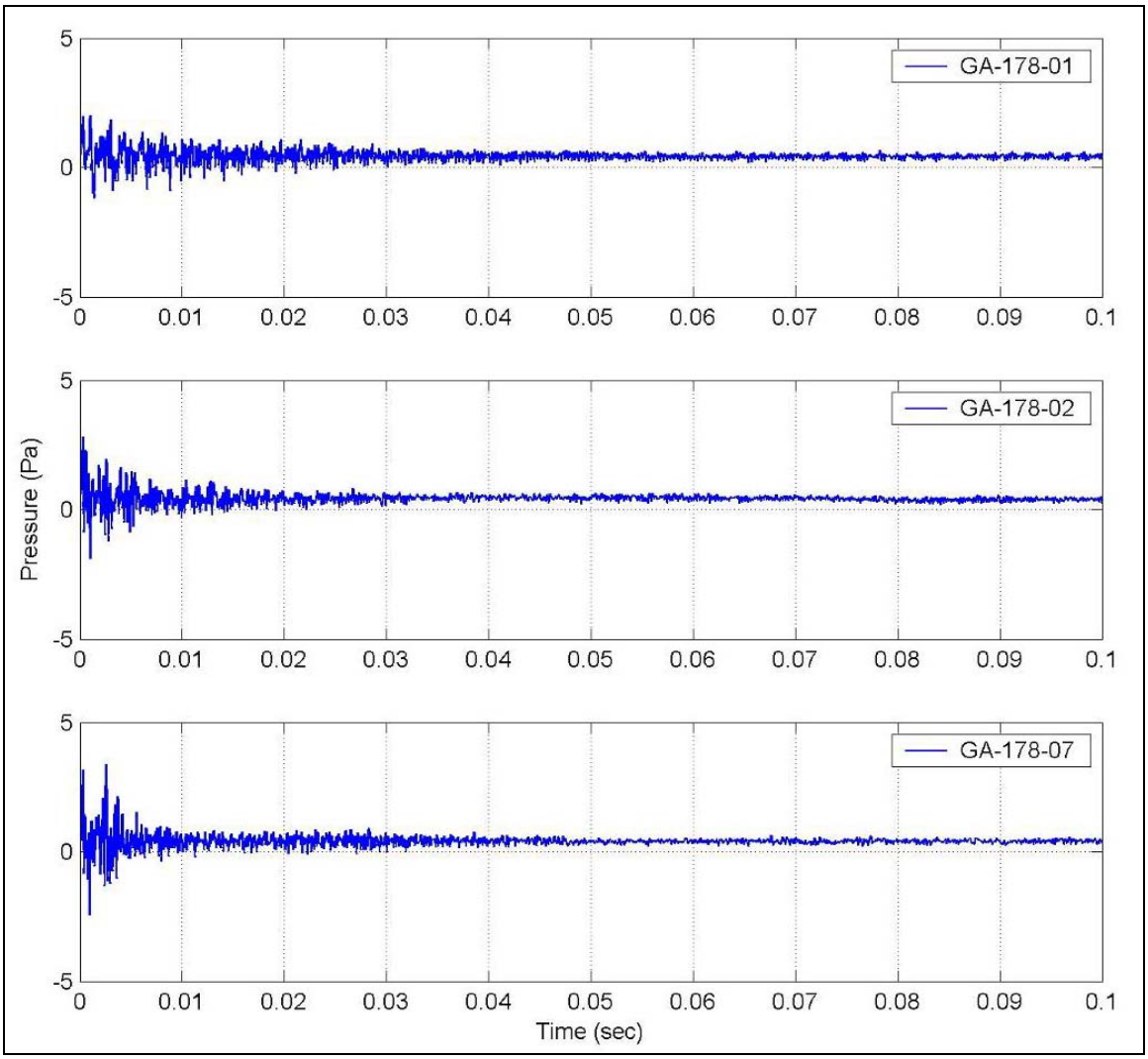

Figure D-13 Acoustic Pressure With Respect to Time for Source GA-178, Macon, GA

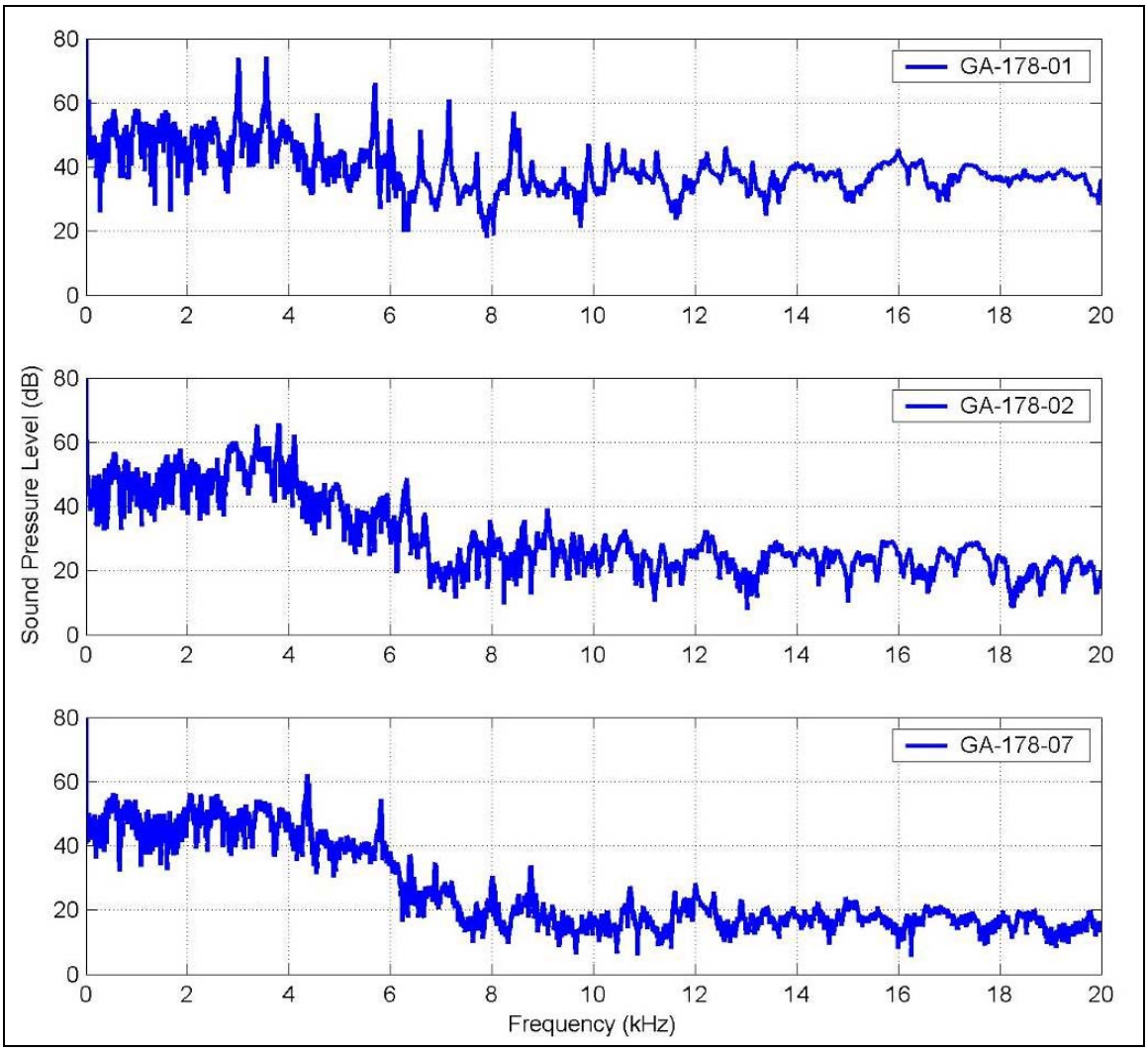

Figure D-14 Sound Pressure Level With Respect to Frequency for Source GA-178, Macon, GA

APPENDIX E: EXPERIMENTAL RESULTS FOR IMPACT FREQUENCY RESPONSE FUNCTION TESTS

E.1 GENERAL REMARKS

Frequency response function curves and data pertaining to the parameter estimation process are provided in this appendix. Response curves are shown for end-to-end measurements in one orientation only. Refer to Chapter 0 for the experimental description and important information with respect to these measurements.

Notes:

Peaks have been fit using data from only one direction at a time, and only using one end-to-end and one drive-point measurement to extract the frequencies and damping of the system unless other measurements for that direction are available. In this case, all the measurements are used. The data represents the nominal frequencies and damping for each sample. Damping estimates are formulated by selectively curve fitting the response curves for a particular resonant frequency from both directions for a particular sample. The damping estimates are scrutinized by the investigator during the process to assure that the best estimate of the damping is recorded. Details of the modal parameters estimated for each measurement and the formulation of the reported data are kept on file in the lab. The method of estimating damping is not very robust, especially since

damping estimates vary significantly from one measurement to the next for the same sample and resonant peak further reducing any confidence in the estimated damping of the sample. The frequencies represent the average for each mode only if the percent difference from one direction to the other is less than 5%. If the percent difference exceeds five percent, each measurement is examined and the frequencies are paired appropriately so that the reported frequency is the average of the response for a particular core at a particular frequency. Such estimates were not necessary very often.

Damping Estimates are shown here for informational purposes only and should be used with extreme caution since they are highly dependent on the boundary conditions and transducer mounting of the test setup.

E.2 DATA FOR SOURCE 08-534, BROOKSVILLE, FL

Table E-1 Frequency & Damping Estimates For All Core Samples From Source 08-534

Modal Parameter Estimation Data - REDUCED DATA								
	Mode 1		**Mode 2**		**Mode 3**		**Mode 4**	
Sample	**Freq (kHz)**	**Damp (%crit)**	**Freq (kHz)**	**Damp (%crit)**	**Freq (kHz)**	**Damp (%crit)**	**Freq (kHz)**	**Damp (%crit)**
08-534-01	10.9	1.41%	11.0	0.79%	25.1	0.23%	25.2	0.34%
08-534-02B	10.3	2.22%	10.3	0.57%	23.4	0.53%	23.5	0.18%
08-534-07	10.3	1.16%	10.4	1.08%	24.1	0.22%	24.1	0.15%
08-534-01p	11.2	0.88%	11.3	0.87%	25.7	0.21%	0.0	0.0
08-534-02Bp	10.4	2.11%	10.6	0.88%	23.9	0.44%	24.3	0.29%
08-534-07p	10.6	0.45%	24.4	0.32%	24.6	0.16%	0.0	0.0

Damping Estimates are shown for informational purposes only and should be used with extreme caution since they are highly dependent on the boundary conditions and transducer mounting of the test setup.

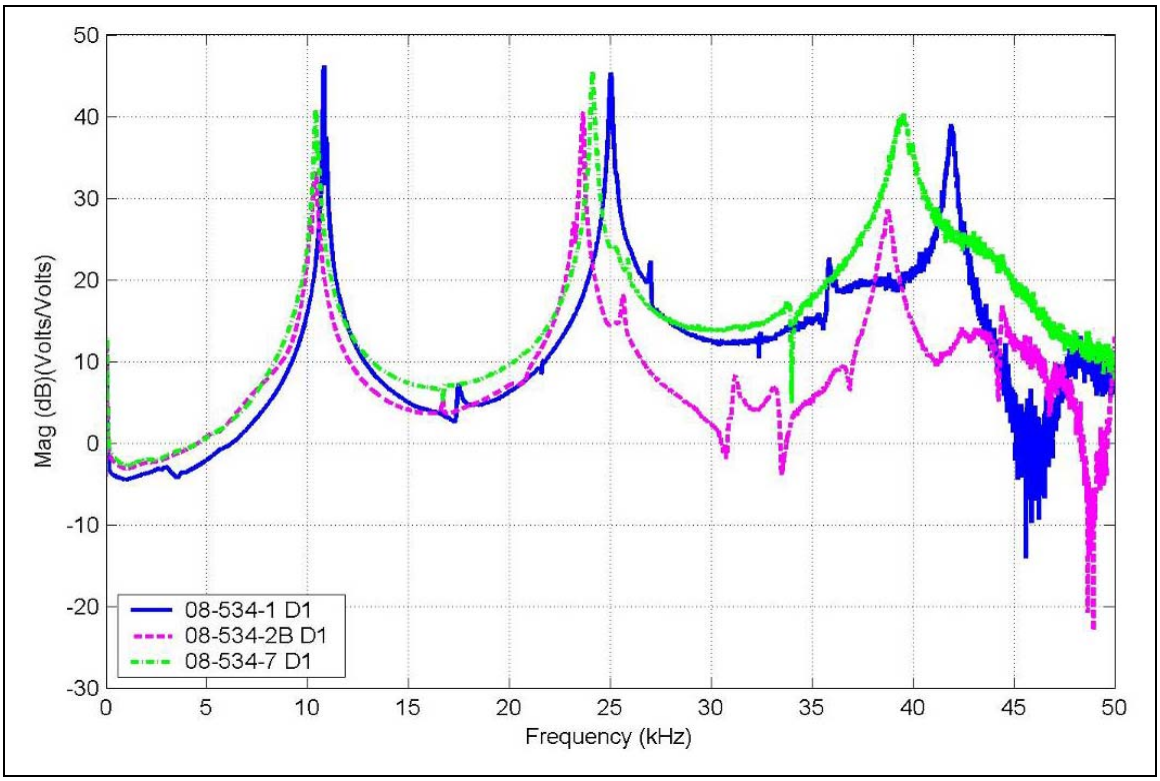

Figure E-1 Impact FRF's For End-to-End Measurements on Samples from Source 08-534

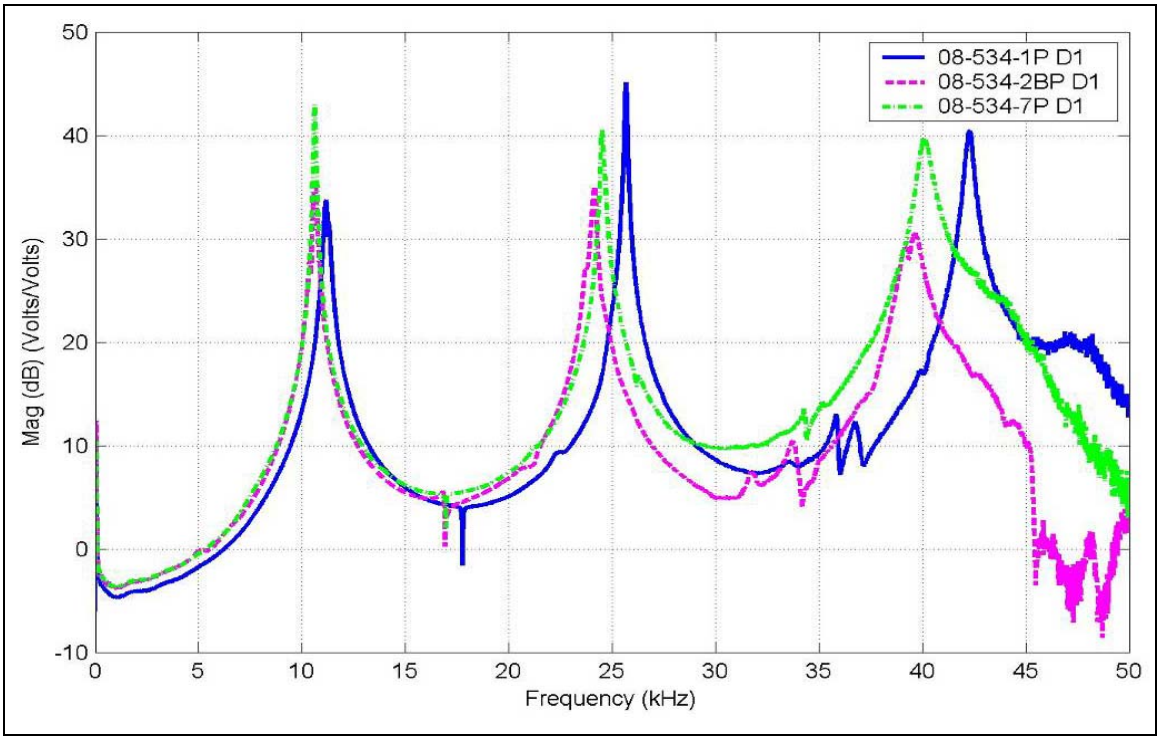

Figure E-2 Impact FRF's For End-to-End Measurements on Precision-Cut Core Samples from Source 08-534

E.3 DATA FOR SOURCE 12-521, BONITA SPRINGS, FL

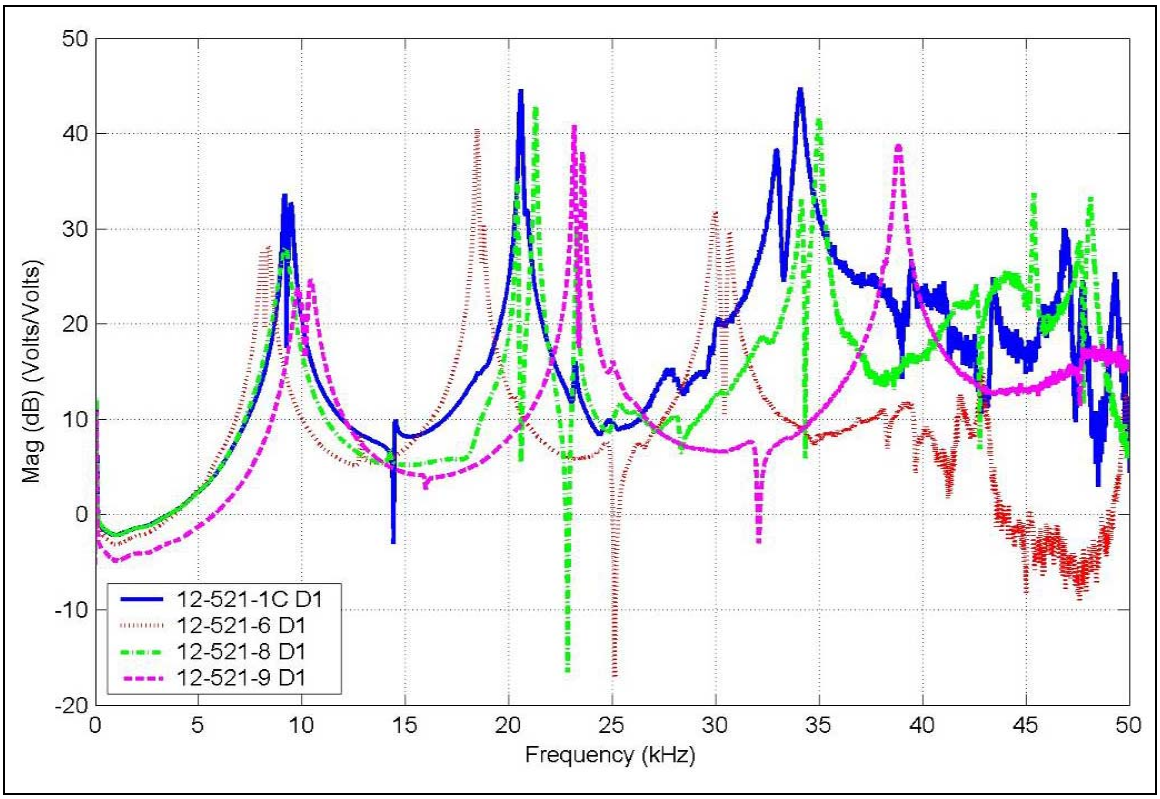

Figure E-3 Impact FRF's For End-to-End Measurements on Core Samples From Source 12-521

Table E-2 Frequency & Damping Estimates for All Core Samples From Source 12-521

Modal Parameter Estimation Data - REDUCED DATA								
	Mode 1		**Mode 2**		**Mode 3**		**Mode 4**	
Sample	**Freq (kHz)**	**Damp (%crit)**	**Freq (kHz)**	**Damp (%crit)**	**Freq (kHz)**	**Damp (%crit)**	**Freq (kHz)**	**Damp (%crit)**
12-521-1C	9.2	0.50%	9.4	1.14%	20.6	0.32%	20.8	0.24%
12-521-6	8.0	2.54%	8.3	1.53%	18.5	0.24%	18.8	0.27%
12-521-8	9.0	1.49%	20.4	0.23%	21.3	0.23%	23.3	0.18%
12-521-9	9.7	1.78%	10.4	1.30%	23.2	0.17%	23.6	0.18%

Damping Estimates are shown for informational purposes only and should be used with extreme caution since they are highly dependent on the boundary conditions and transducer mounting of the test setup.

E.4 DATA FOR SORUCE 18-607, CENTER HILL, FL

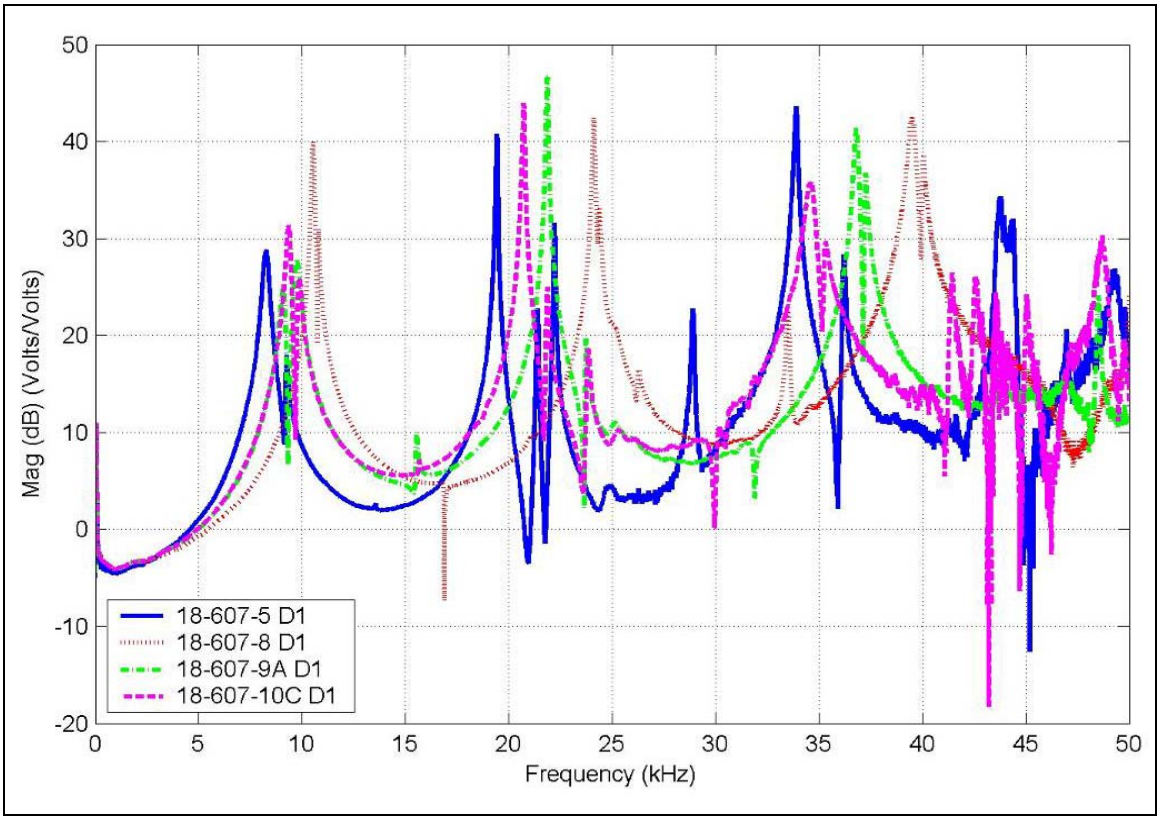

Figure E-4 Impact FRF's For End-to-End Measurements on Core Samples From Source 18-607

Table E-3 Frequency & Damping Estimates for All Core Samples From Source 18-607

Modal Parameter Estimation Data - REDUCED DATA								
	Mode 1		**Mode 2**		**Mode 3**		**Mode 4**	
Sample	**Freq (kHz)**	**Damp (%crit)**	**Freq (kHz)**	**Damp (%crit)**	**Freq (kHz)**	**Damp (%crit)**	**Freq (kHz)**	**Damp (%crit)**
18-607-5	8.3	1.79%	**9.1**	2.09%	19.5	0.18%	21.4	0.14%
18-607-8	10.6	0.47%	10.8	0.64%	24.1	0.17%	24.4	0.27%
18-607-9A	9.1	0.55%	9.7	1.61%	22.0	0.13%	23.7	0.39%
18-607-10C	9.4	1.10%	9.8	0.73%	20.8	0.20%	21.9	0.21%

Damping Estimates are shown for informational purposes only and should be used with extreme caution since they are highly dependent on the boundary conditions and transducer mounting of the test setup.

E.5 DATA FOR SOURCE 34-106, GULF HAMMOCK, FL

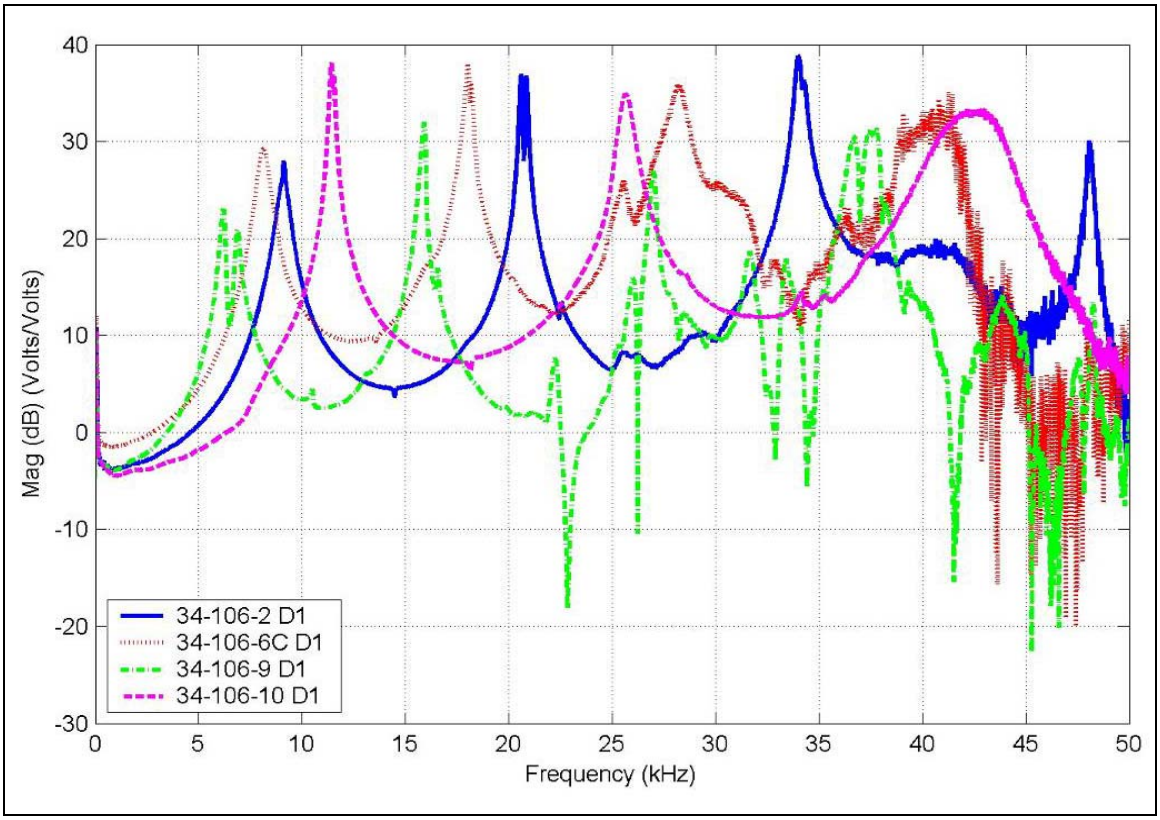

Figure E-5 Impact FRF's For End-to-End Measurements on Core Samples From Source 34-106

Table E-4 Frequency & Damping Estimates for All Core Samples From Source 34-106

Modal Parameter Estimation Data - REDUCED DATA								
	Mode 1		**Mode 2**		**Mode 3**		**Mode 4**	
Sample	**Freq (kHz)**	**Damp (%crit)**	**Freq (kHz)**	**Damp (%crit)**	**Freq (kHz)**	**Damp (%crit)**	**Freq (kHz)**	**Damp (%crit)**
34-106-2	9.1	2.32%	20.6	0.29%	20.8	0.25%	0.0	0.00%
34-106-6C	8.1	1.89%	**18.0**	**0.55%**	18.0	0.50%	0.0	0.00%
34-106-9	6.2	1.48%	6.8	2.65%	**15.1**	**0.74%**	**15.9**	0.60%
34-106-10	11.5	0.92%	25.8	0.92%	0.0	0.00%	0.0	0.00%

Damping Estimates are shown for informational purposes only and should be used with extreme caution since they are highly dependent on the boundary conditions and transducer mounting of the test setup.

Notes for sample 34-106-06C:

This sample had vastly different frequencies for mode 2 for direction 1 vs. direction 2. Mode 2 on this sheet is the average of D1, Modes 2 & 3, and D2 Mode 3. The damping is taken from average of the same modes. Mode 3 is the average of the

mode three frequencies and damping. On 9/6/06 the data was refit using all the measurements for this core available (4 response curves). The frequencies in the table are representative of this fit.

E.6 DATA FOR SOURCE 38-228, PERRY, FL

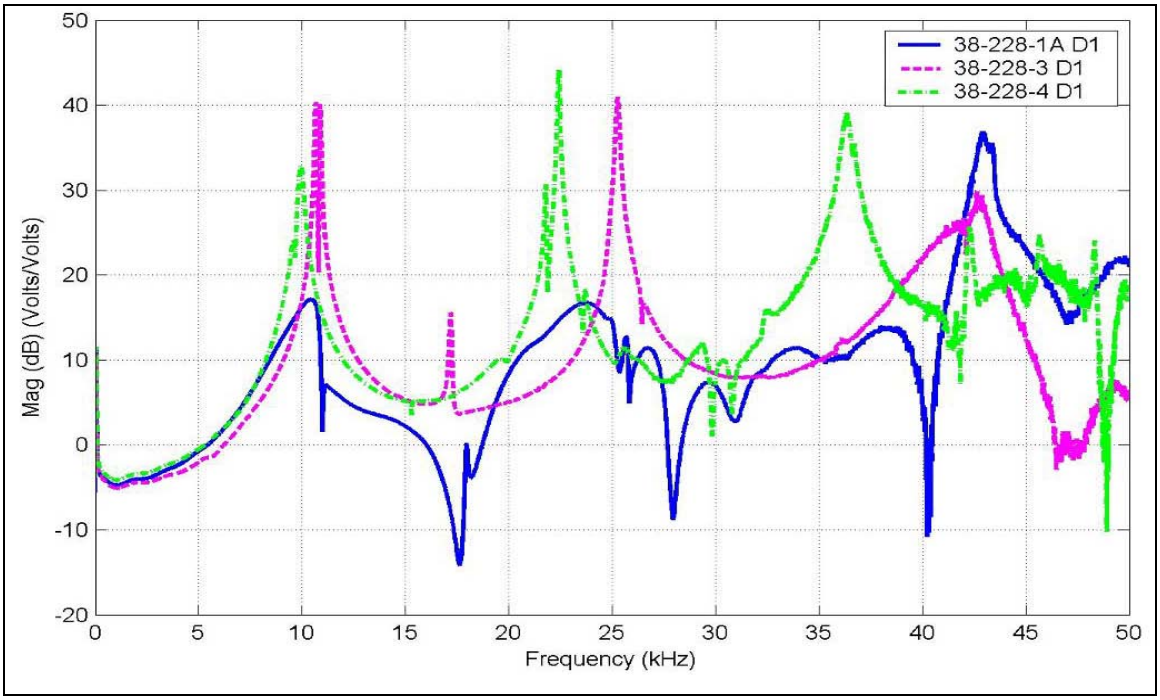

Figure E-6 Impact FRF's For End-to-End Measurements on Core Samples From Source 38-228

Table E-5 Frequency & Damping Estimates for All Core Samples From Source 38-228

Modal Parameter Estimation Data - REDUCED DATA								
	Mode 1		**Mode 2**		**Mode 3**		**Mode 4**	
Sample	**Freq (kHz)**	**Damp (%crit)**	**Freq (kHz)**	**Damp (%crit)**	**Freq (kHz)**	**Damp (%crit)**	**Freq (kHz)**	**Damp (%crit)**
38-228-1A	10.7	5.12%	25.3	1.35%	0.0	0.00%	0.0	0.00%
38-228-3	10.7	0.37%	11.0	0.66%	**25.3**	0.25%	0.0	0.00%
38-228-4	**9.6**	0.67%	**9.9**	0.21%	**21.7**	0.19%	22.4	0.00%

Damping Estimates are shown for informational purposes only and should be used with extreme caution since they are highly dependent on the boundary conditions and transducer mounting of the test setup.

E.7 DATA FOR SOURCE 87-339, HIALEAH, FL

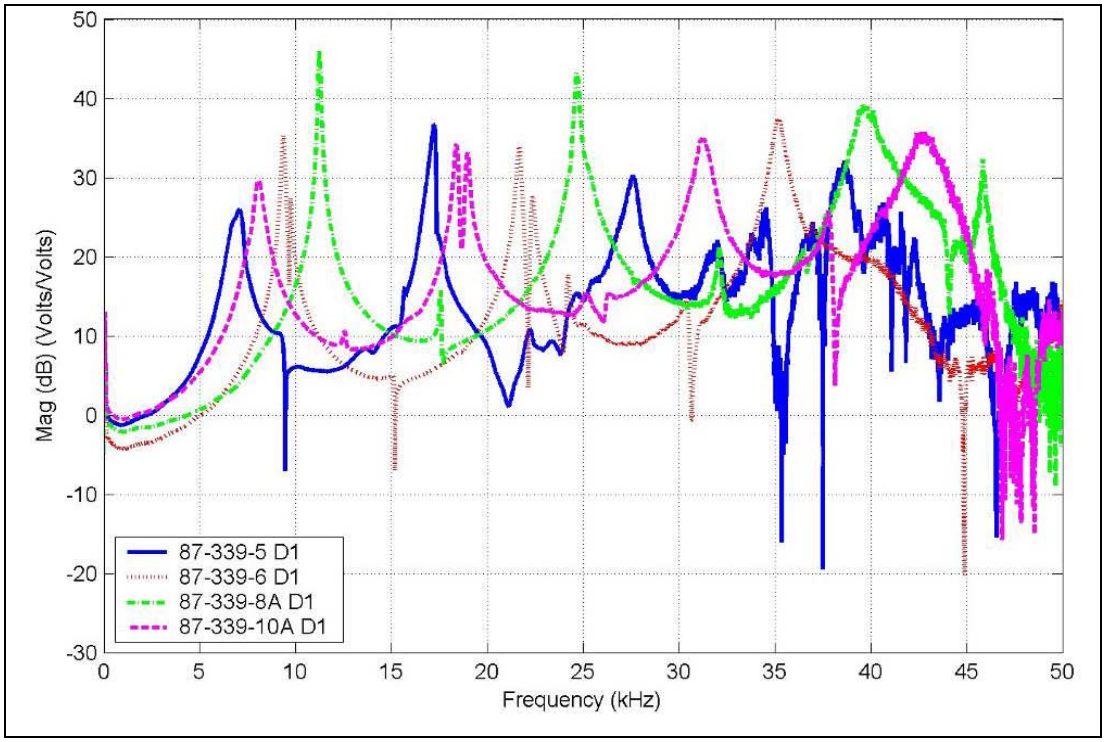

Figure E-7 Impact FRF's For End-to-End Measurements on Core Samples From Source 87-339

Table E-6 Frequency & Damping Estimates for All Core Samples From Source 87-339

Modal Parameter Estimation Data - REDUCED DATA								
	Mode 1		**Mode 2**		**Mode 3**		**Mode 4**	
Sample	**Freq (kHz)**	**Damp (%crit)**	**Freq (kHz)**	**Damp (%crit)**	**Freq (kHz)**	**Damp (%crit)**	**Freq (kHz)**	**Damp (%crit)**
87-339-05	**6.5**	3.16%	**7.1**	0.88%	**15.4**	1.54%	**17.2**	1.33%
87-339-06	9.4	0.75%	9.7	0.69%	21.7	0.47%	22.3	0.27%
87-339-08A	11.2	0.62%	**24.2**	0.41%	**24.8**	3.89%	0.0	0.00%
87-339-10A	**7.4**	2.51%	8.1	0.65%	18.4	0.47%	18.9	0.00%

Damping Estimates are shown for informational purposes only and should be used with extreme caution since they are highly dependent on the boundary conditions and transducer mounting of the test setup.

E.8 DATA FOR SOURCE GA-178, MACON, GA

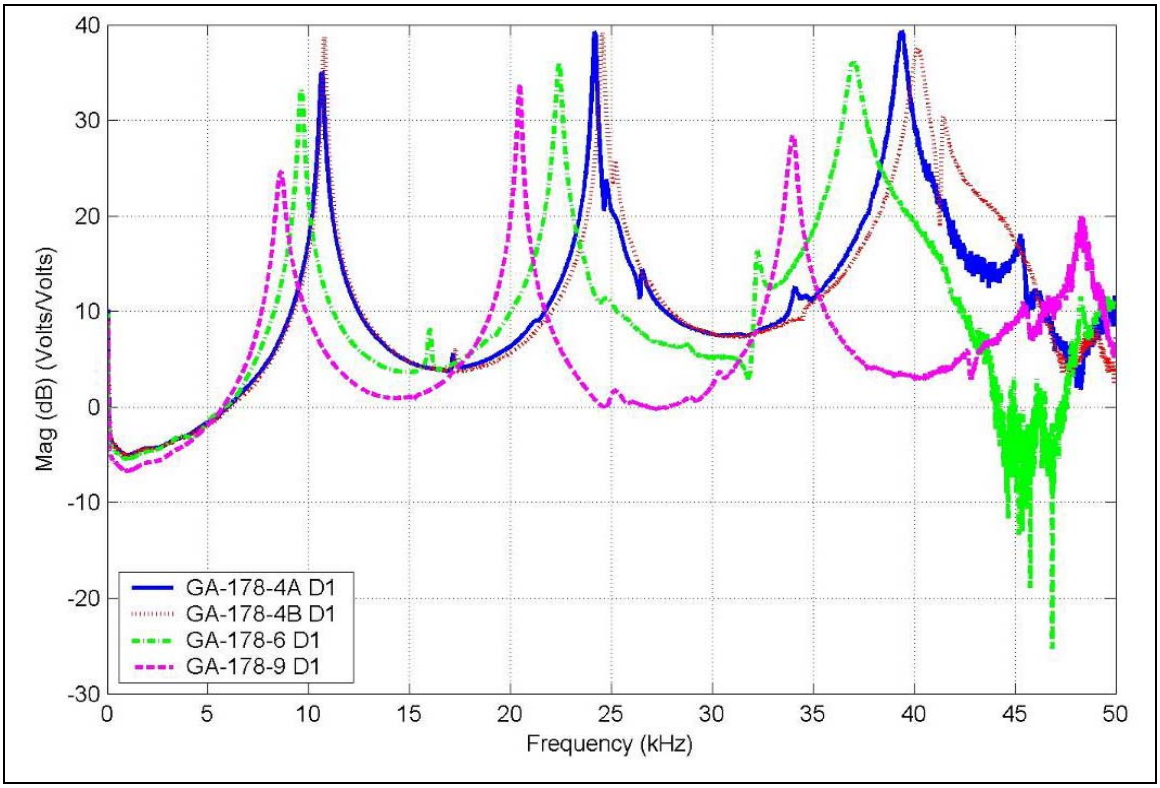

Figure E-8 Impact FRF's For End-to-End Measurements on Core Samples From Source GA-178

Table E-7 Frequency & Damping Estimates for All Core Samples from Source GA-178

Modal Parameter Estimation Data - REDUCED DATA								
	Mode 1		**Mode 2**		**Mode 3**		**Mode 4**	
Sample	**Freq (kHz)**	**Damp (%crit)**	**Freq (kHz)**	**Damp (%crit)**	**Freq (kHz)**	**Damp (%crit)**	**Freq (kHz)**	**Damp (%crit)**
GA-178-4A	10.7	0.79%	**24.2**	0.26%	24.7	0.28%	0.0	0.00%
GA-178-4B	10.9	1.18%	**24.5**	0.31%	**25.1**	0.28%	0.0	0.00%
GA-178-6	9.5	1.18%	22.5	0.45%	0.0	0.00%	0.0	0.00%
GA-178-9	8.6	2.14%	20.4	0.41%	0.0	0.00%	0.0	0.00%

Damping Estimates are shown for informational purposes only and should be used with extreme caution since they are highly dependent on the boundary conditions and transducer mounting of the test setup.

APPENDIX F: COMPARISONS OF PETROGRAPHY AND WINDSOR PIN SYSTEM MEASUREMENTS

F.1 GENERAL REMARKS

The analysis of the petrographic properties of the carbonate samples with the Windsor Pin System® measurements is presented in Section 1.40. The plots from which the regression coefficients are formulated are presented here. The regression equations and regression coefficients (R^2 values) have been omitted from the plots to show the data clearly. The plot styles for each source may be different from one plot to the next. The "linear (XX-XXX)" series correspond to the regression lines for the source indicated.

F.2 PLOTS: CONCENTRATIONS VS. WINDSOR PIN®

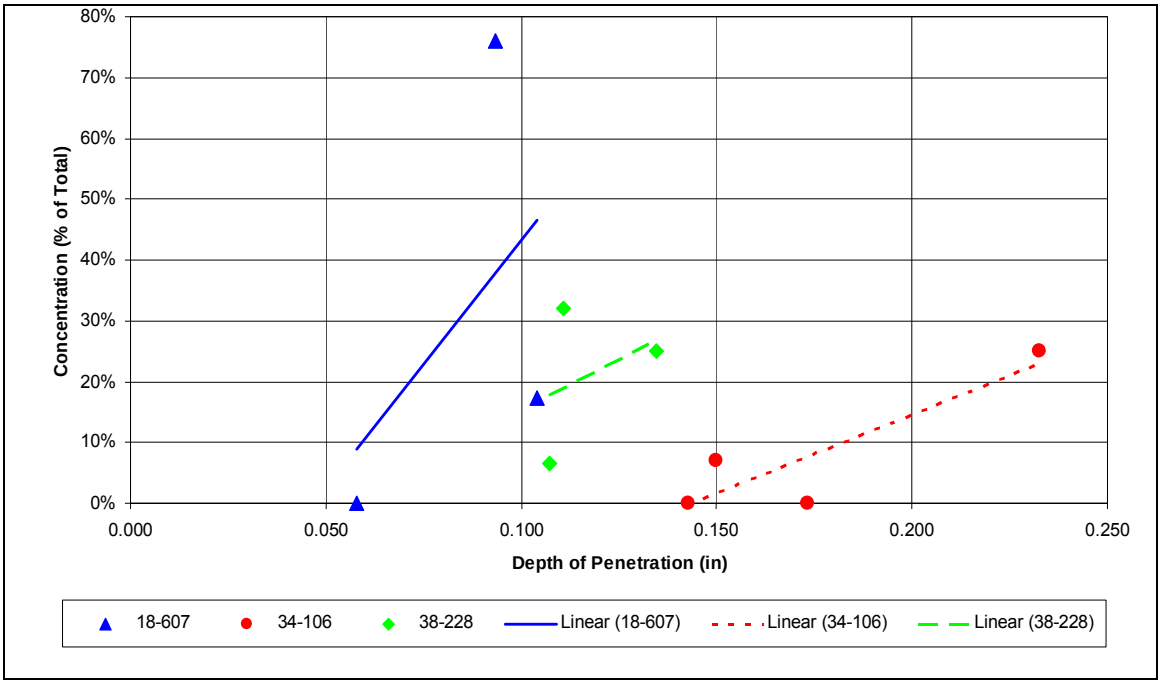

Figure F-1 Concentration of Amorphous Calcite With Respect to Penetration of Windsor Pin®

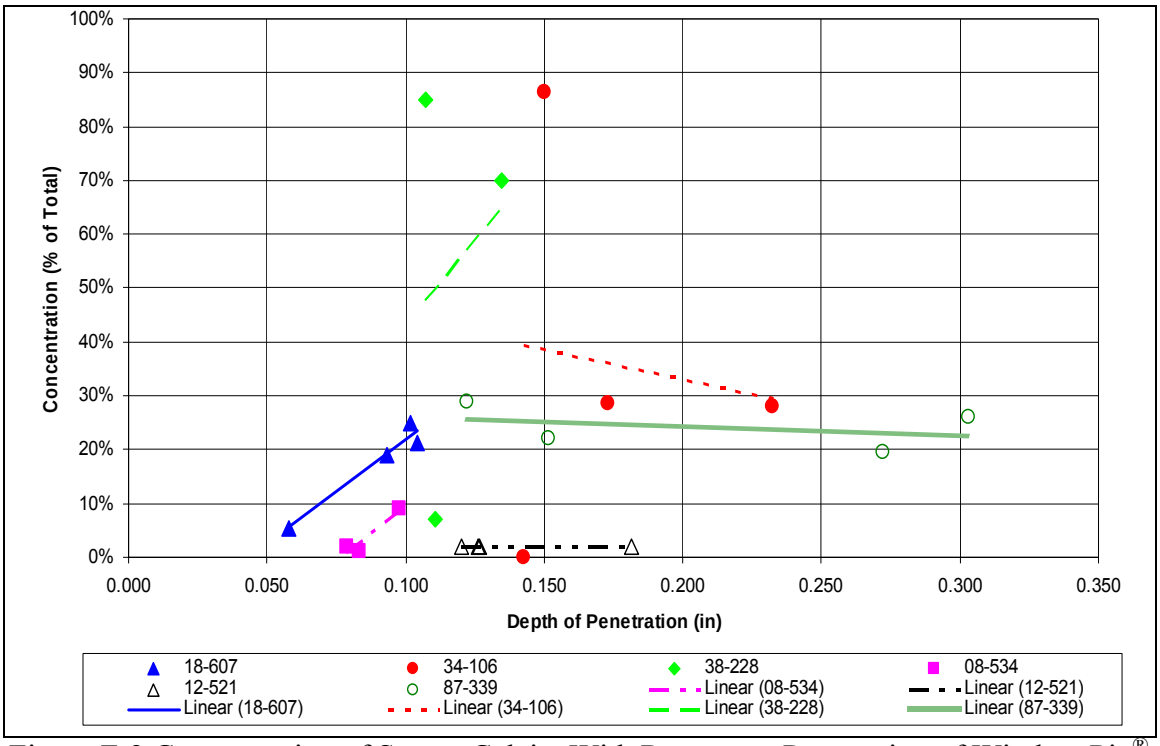

Figure F-2 Concentration of Sparry Calcite With Respect to Penetration of Windsor Pin®

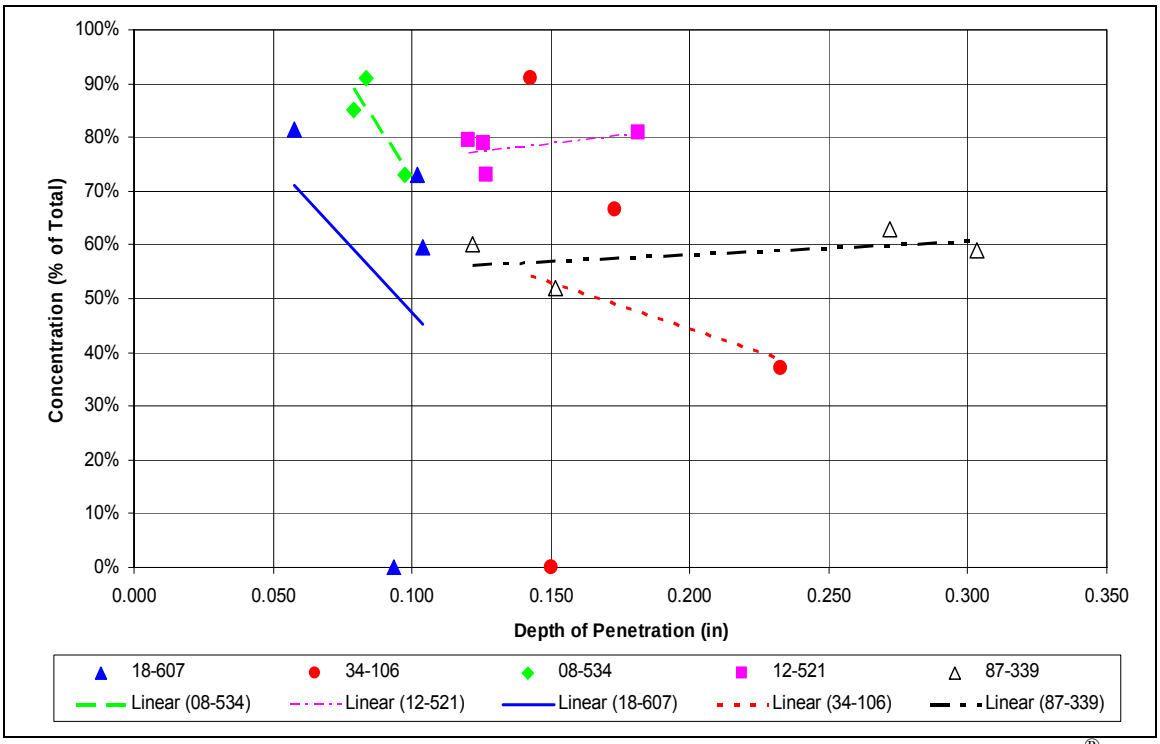

Figure F-3 Concentration of Matrix With Respect to Penetration of Windsor Pin®

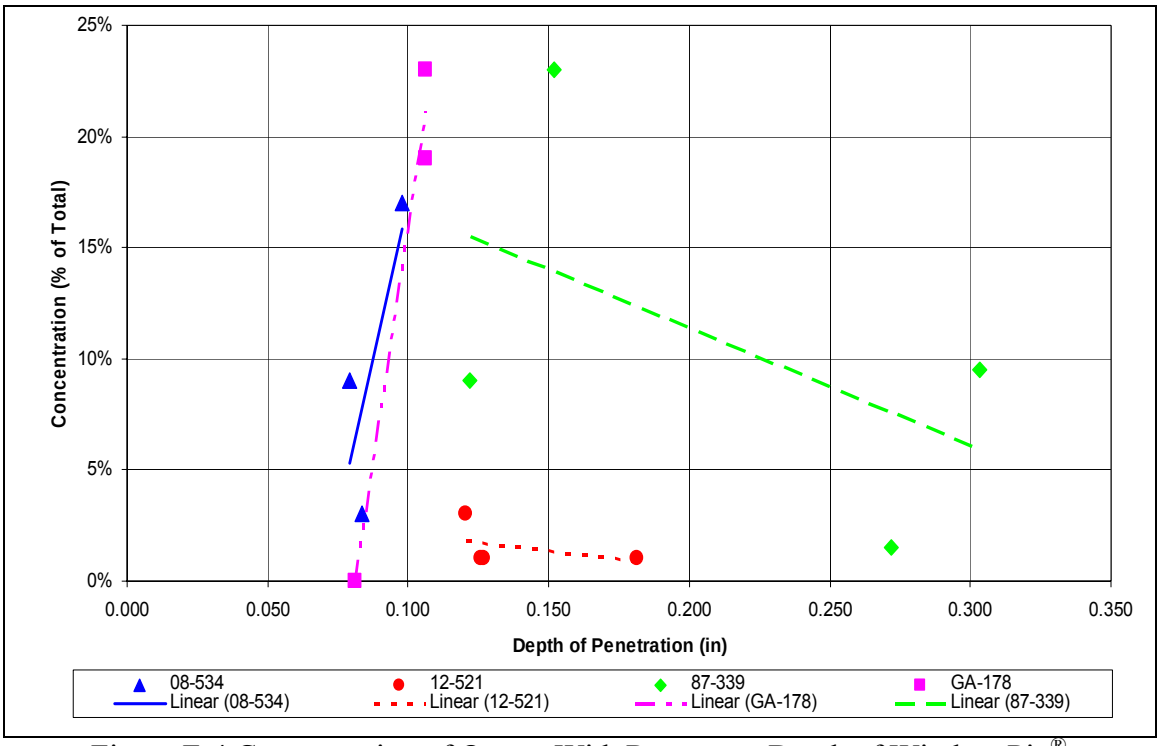

Figure F-4 Concentration of Quartz With Respect to Depth of Windsor Pin®

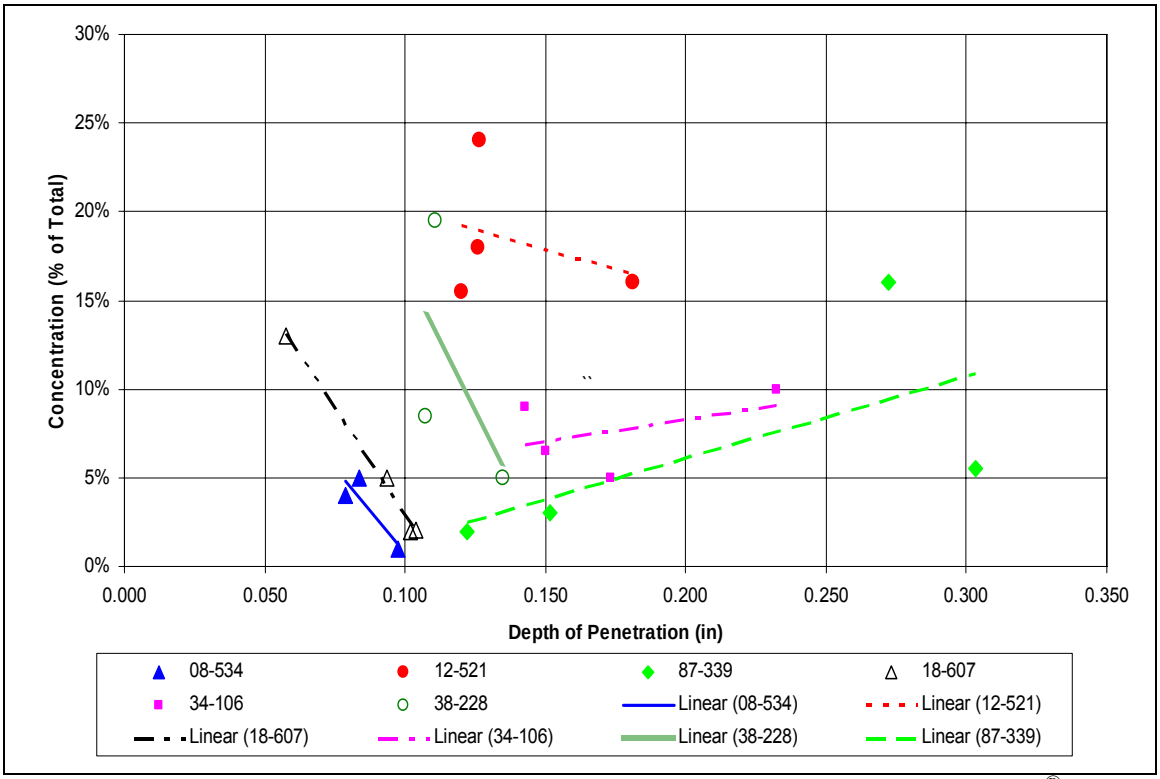

Figure F-5 Concentration of Voids With Respect to Depth of Windsor Pin®

F.3 PLOTS: GRAIN SIZE VS. WINDSOR PIN®

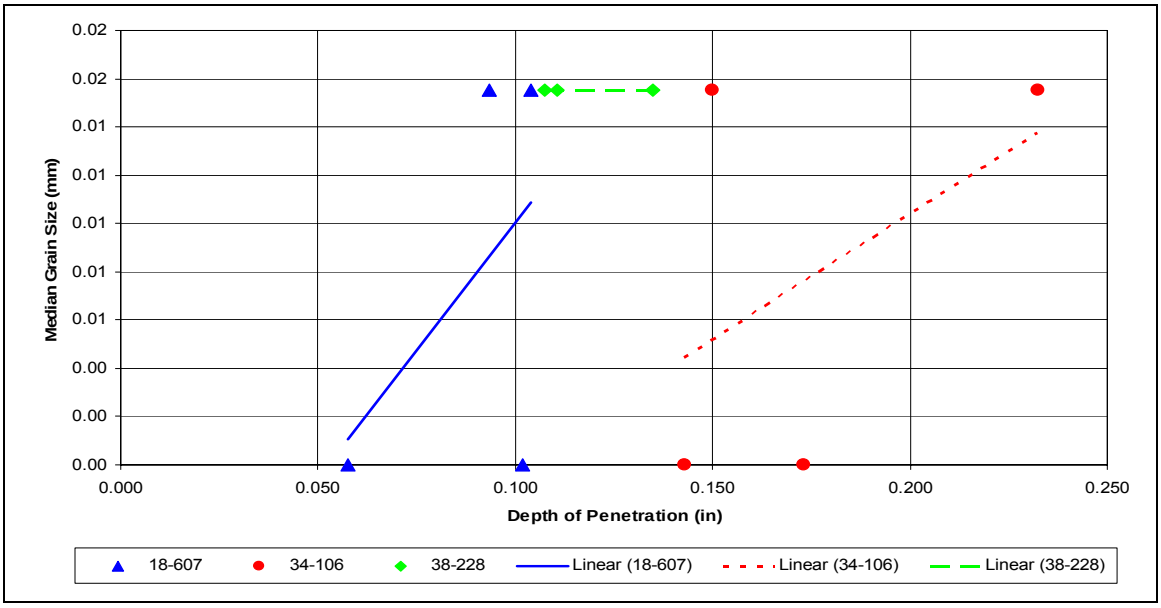

Figure F-6 Median Grain Size of Amorphous Calcite With Respect to Depth of Windsor Pin®

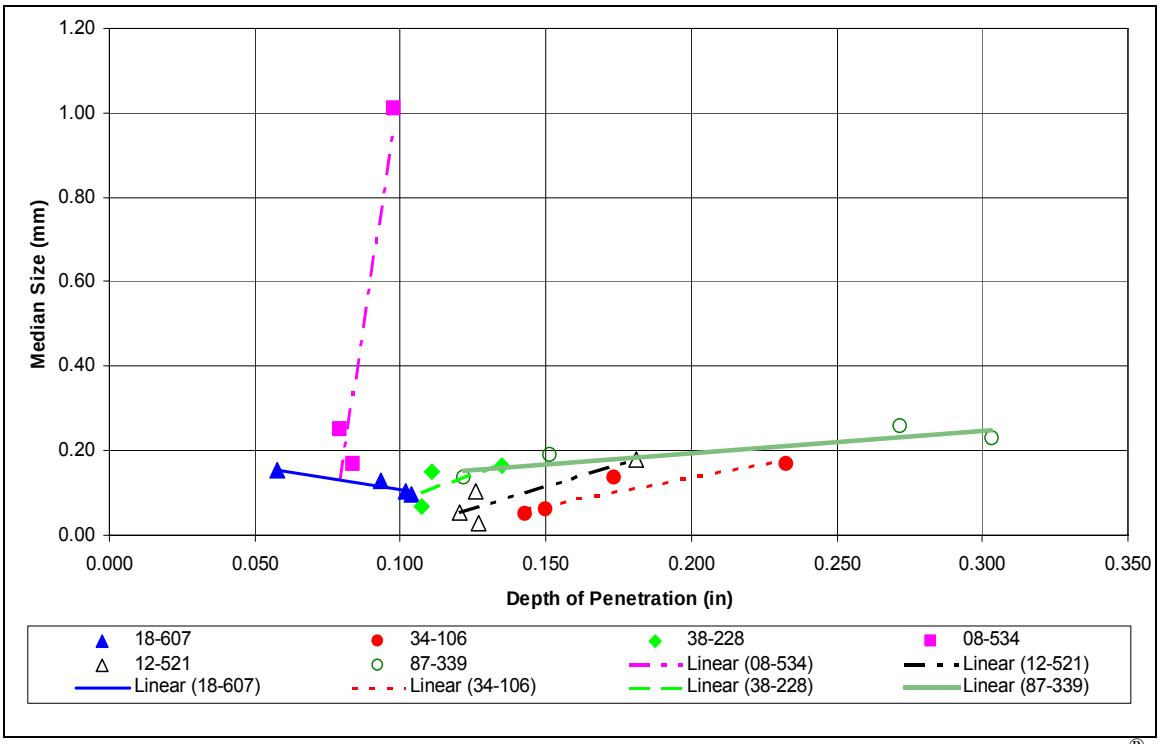

Figure F-7 Median Grain Size of Sparry Calcite With Respect to Depth of Windsor Pin®

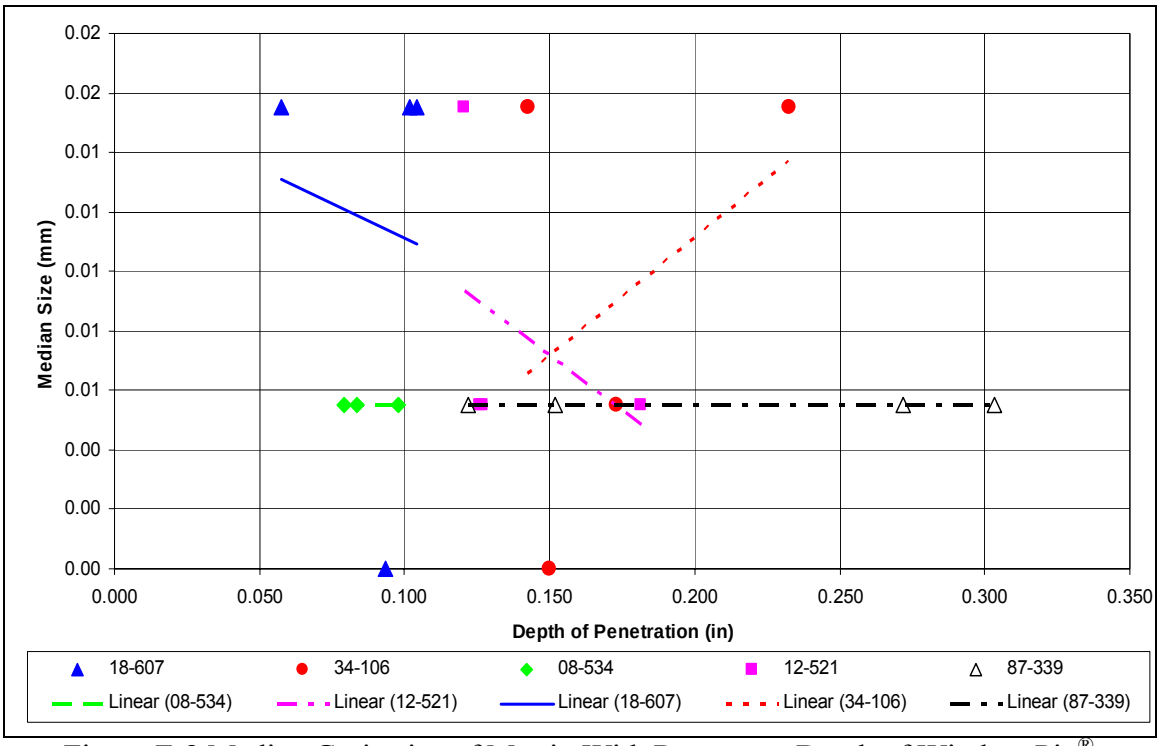

Figure F-8 Median Grain size of Matrix With Respect to Depth of Windsor Pin®

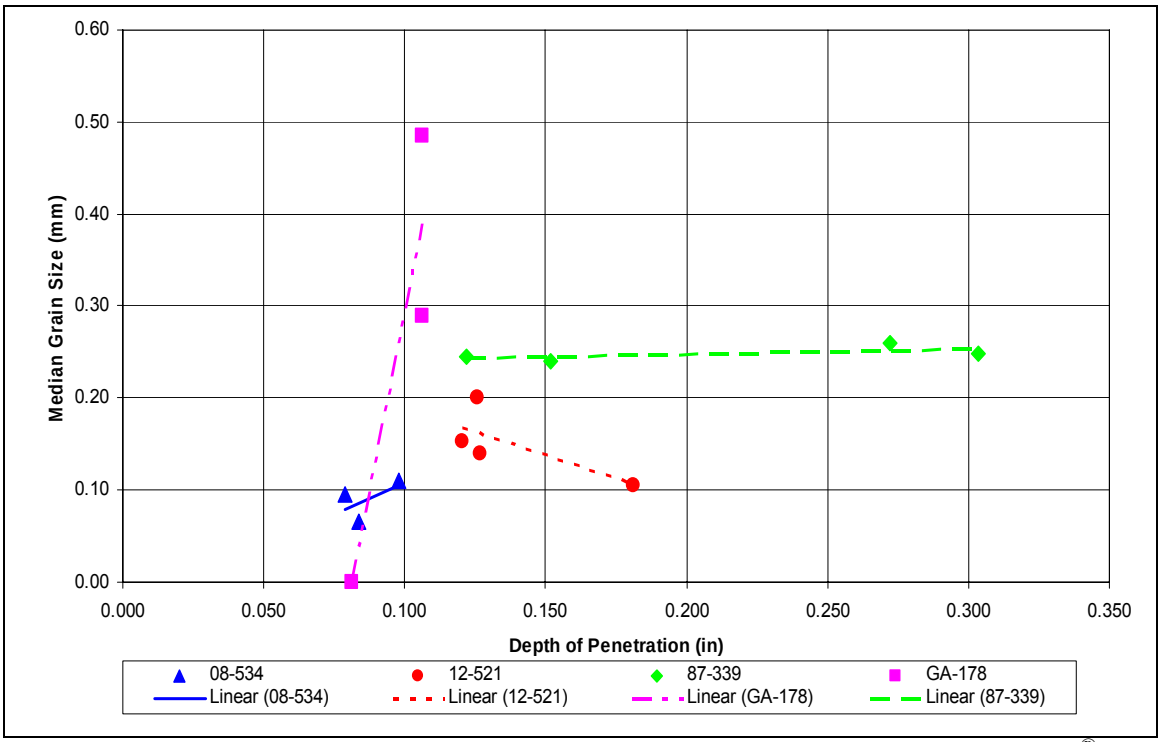

Figure F-9 Median Grain Size of Quartz With Respect to Depth of Windsor Pin®

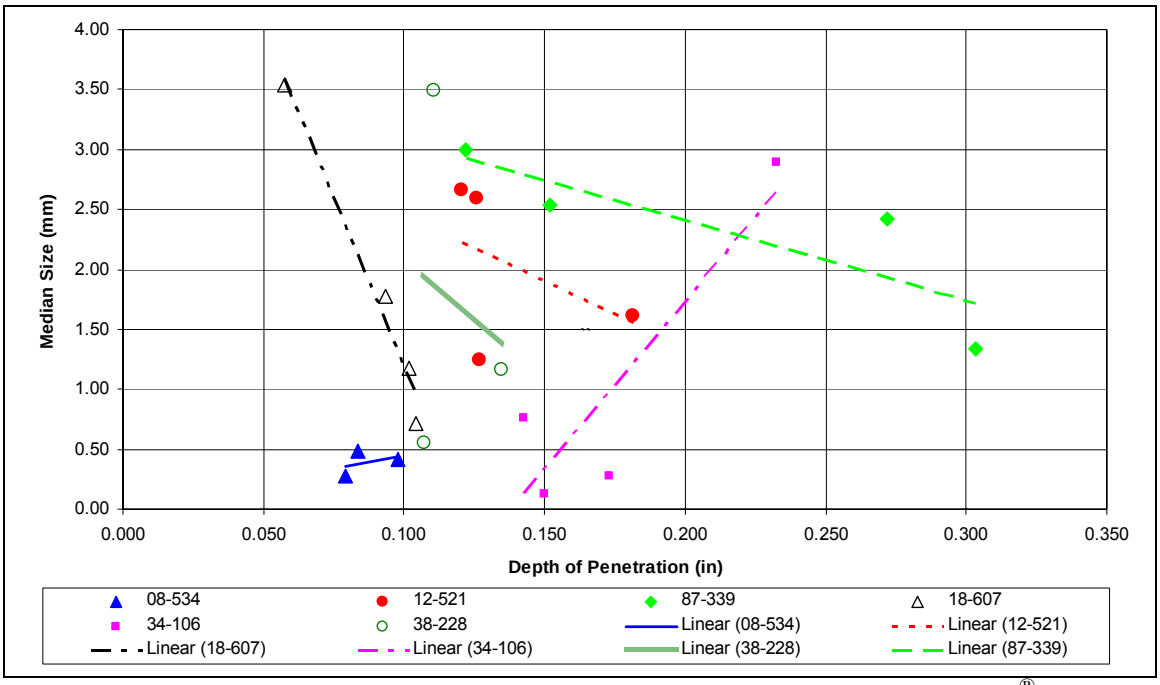

Figure F-10 Median Void Size With Respect to Depth of Windsor Pin®

APPENDIX G: COMPARISONS OF PETROGRAPHY AND FDOT PROVIDED TEST RESULTS

G.1 GENERAL REMARKS

Comparisons between the petrographic properties identified by each geologist and the data provided by the FDOT are discussed in Section 1.42. This appendix contains the plots from which the regression coefficients are obtained. The regression information has been omitted to clearly show the data. The series' symbols may not be consistent throughout all of the plots.

G.2 COMPARISON OF DATA FROM FDOT AND SNCGI

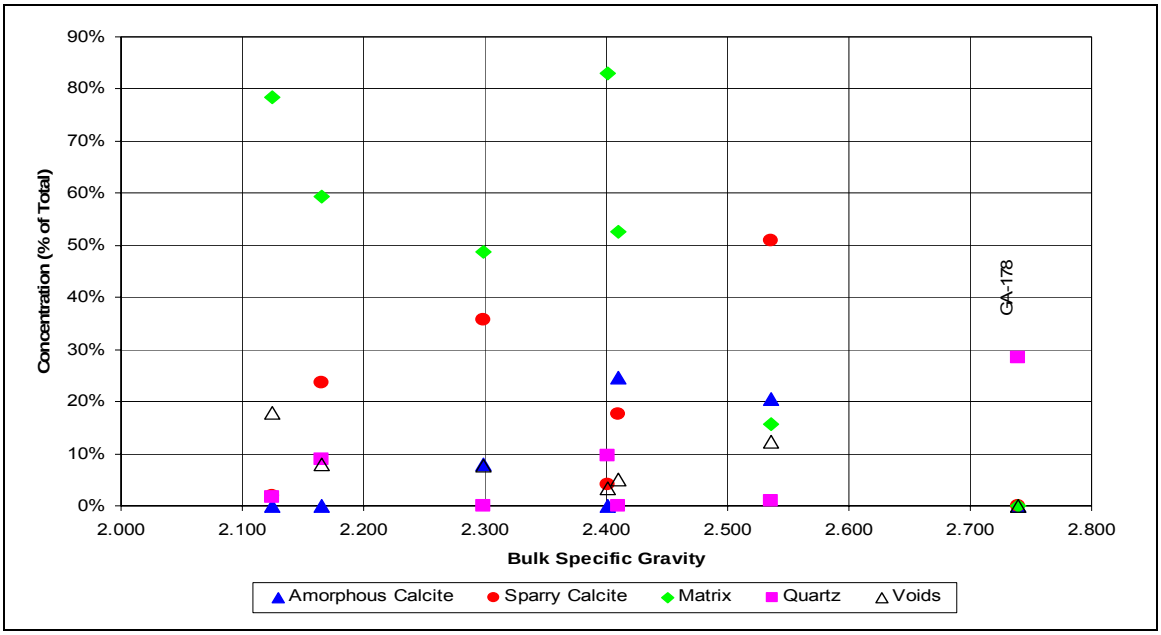

Figure G-1 Concentration of Petrographic Properties With Respect to Bulk Specific Gravity

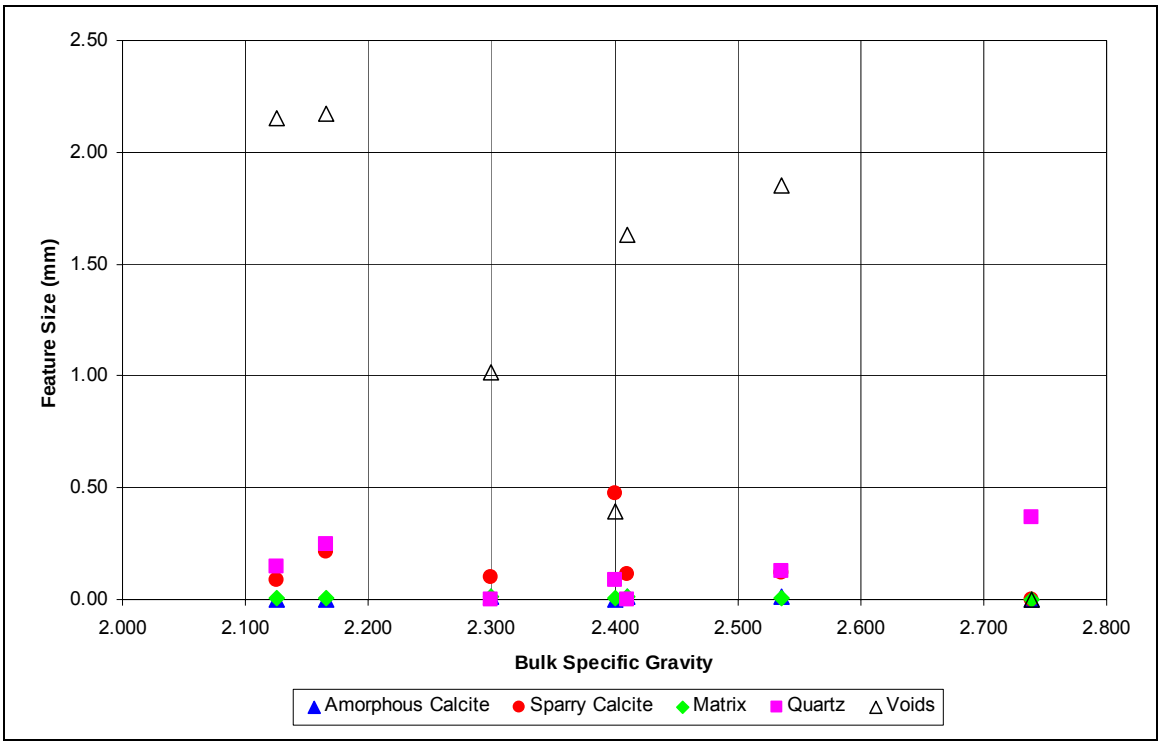

Figure G-2 Median Size of Petrographic Properties With Respect to Bulk Specific Gravity

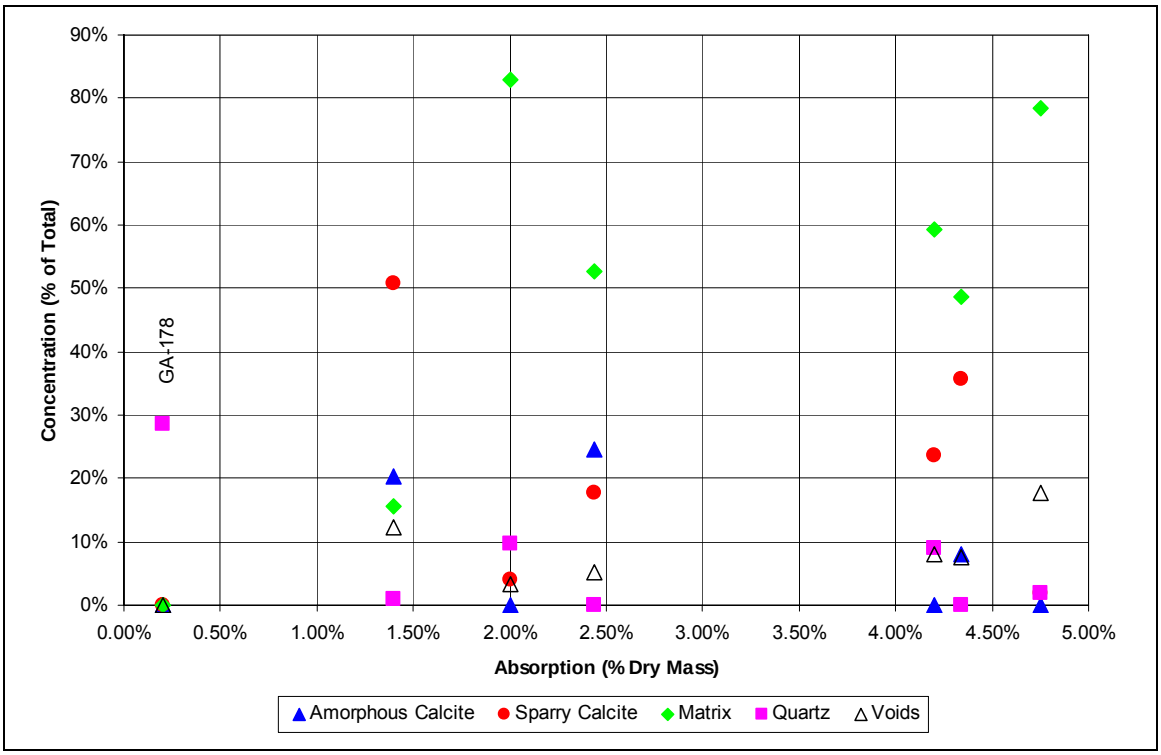

Figure G-3 Concentration of Petrographic Properties With Respect to Absorption

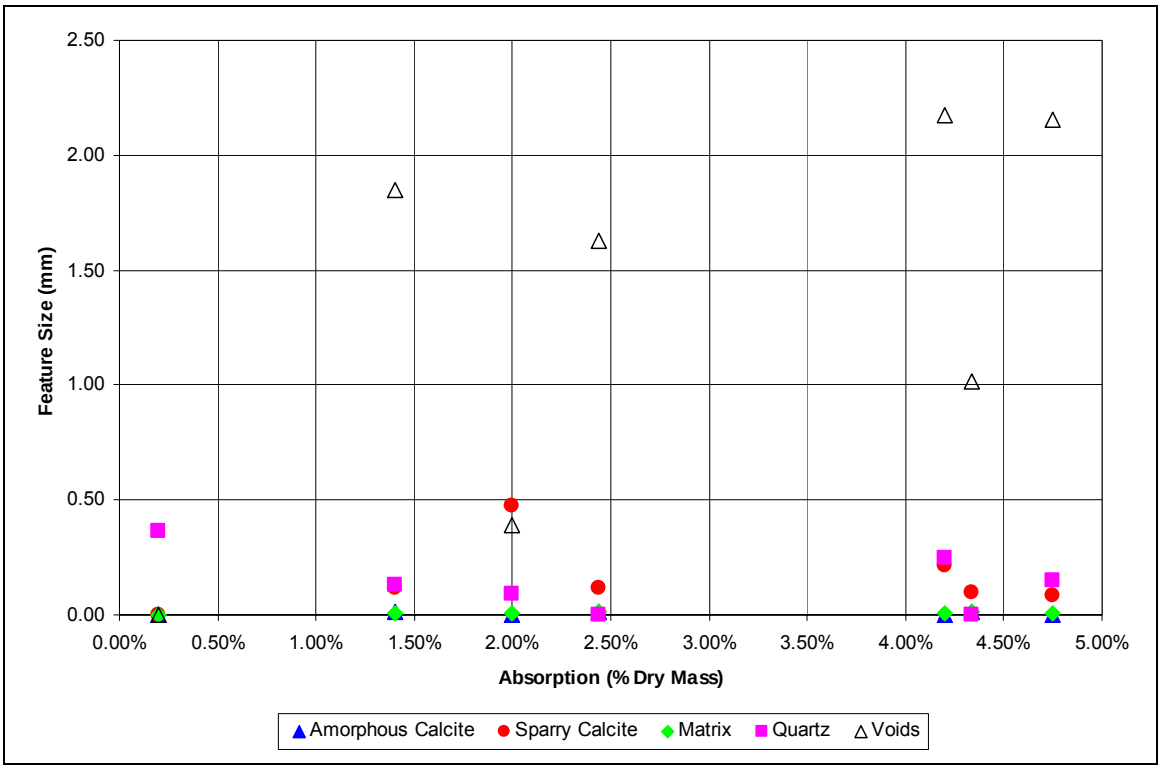

Figure G-4 Median Size of Petrographic Properties With Respect to Absorption

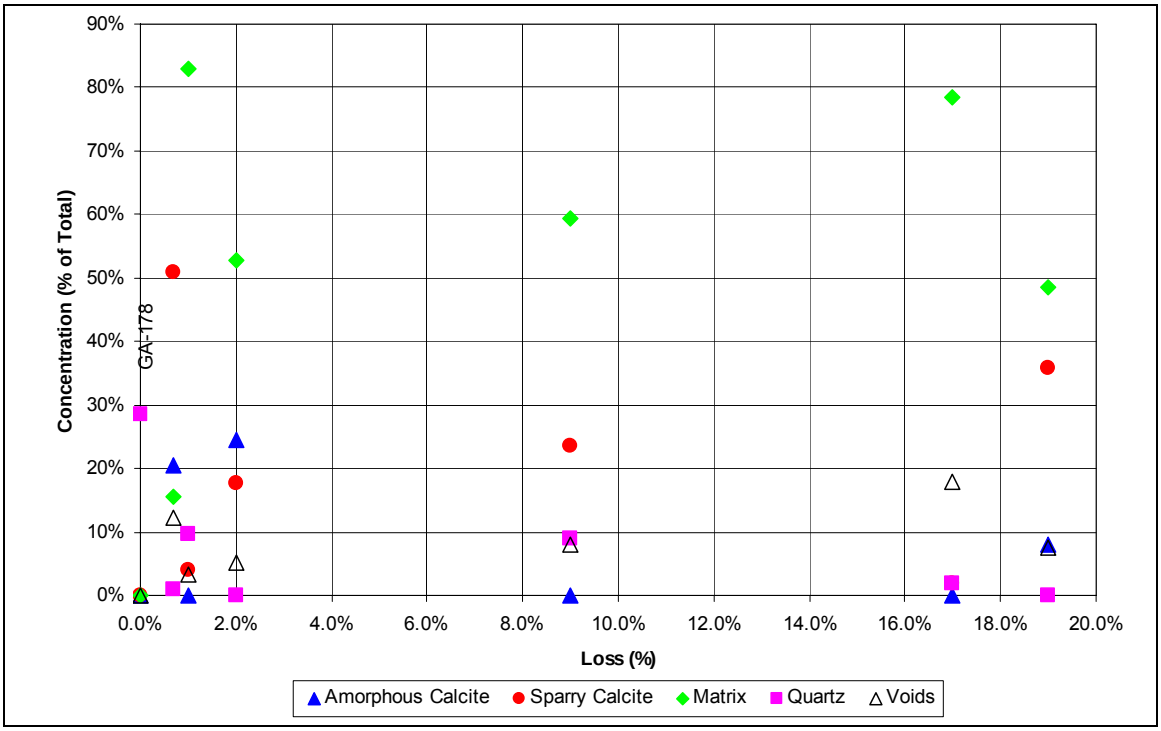

Figure G-5 Concentration of Petrographic Properties With Respect to Sodium Sulfate Percent Loss

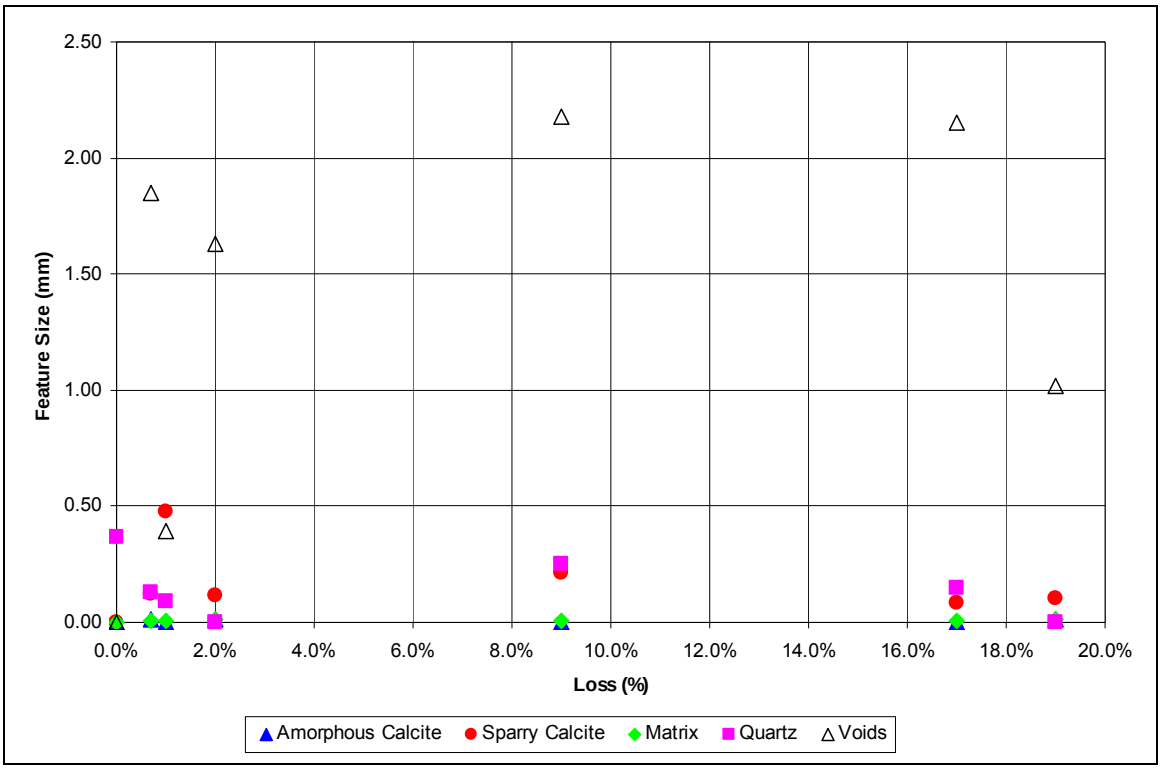

Figure G-6 Median Size of Petrographic Properties With Respect to Sodium Sulfate Percent Loss

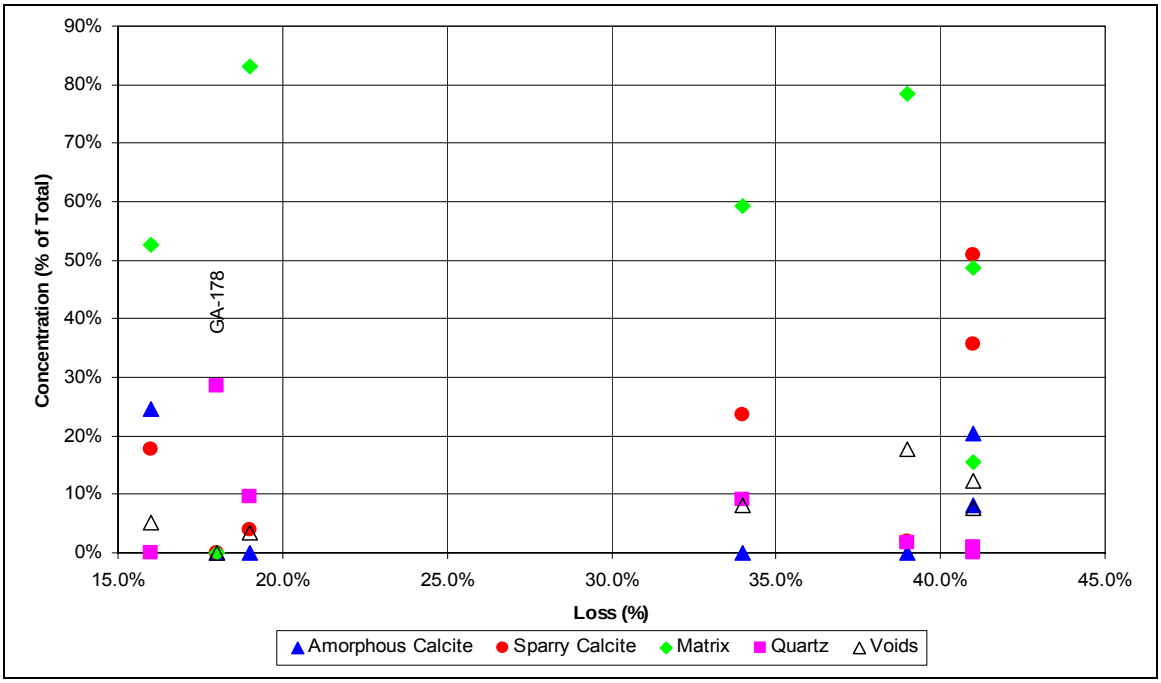

Figure G-7 Concentration of Petrographic Properties With Respect to Los Angeles Abrasion Percent Loss

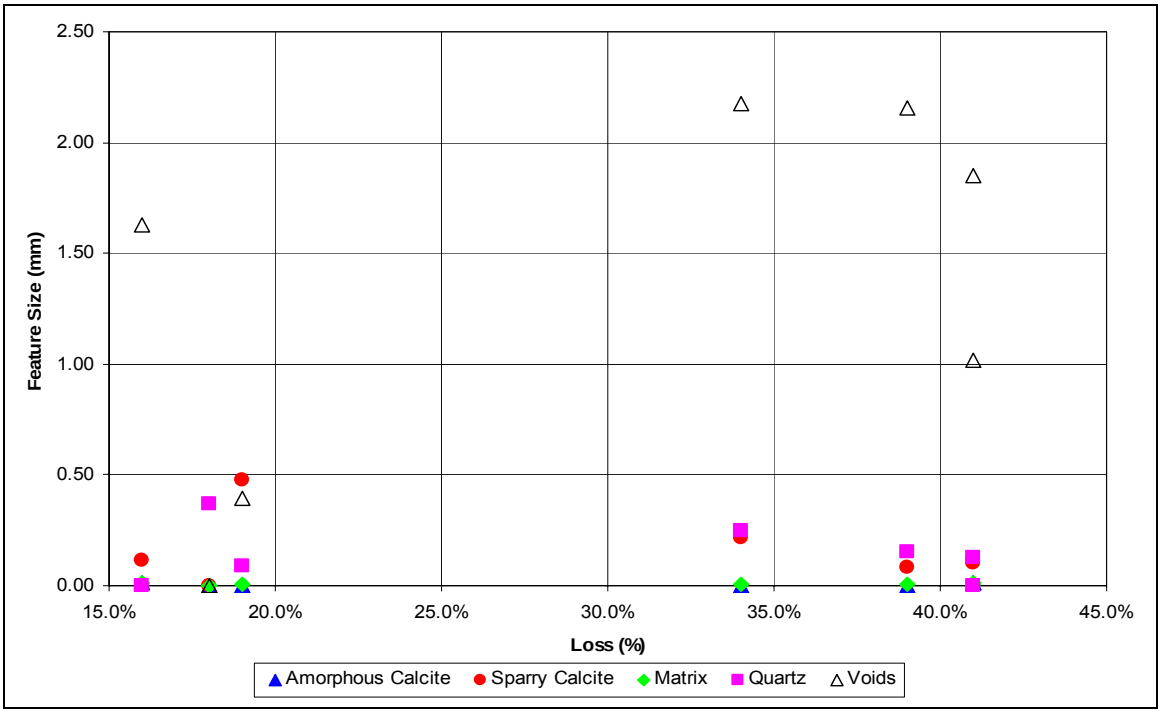

Figure G-8 Median Size of Petrographic Properties With Respect to Los Angeles Abrasion Percent Loss

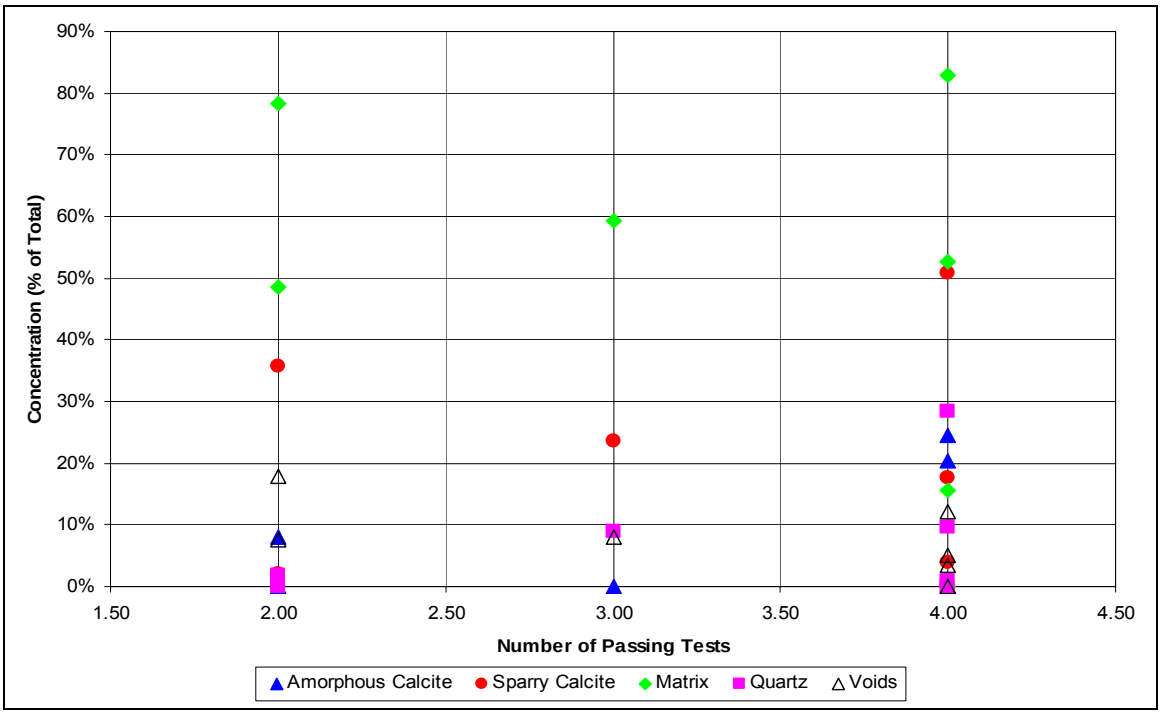

Figure G-9 Concentration of Petrographic Properties With Respect to the Number of Passed FDOT Tests

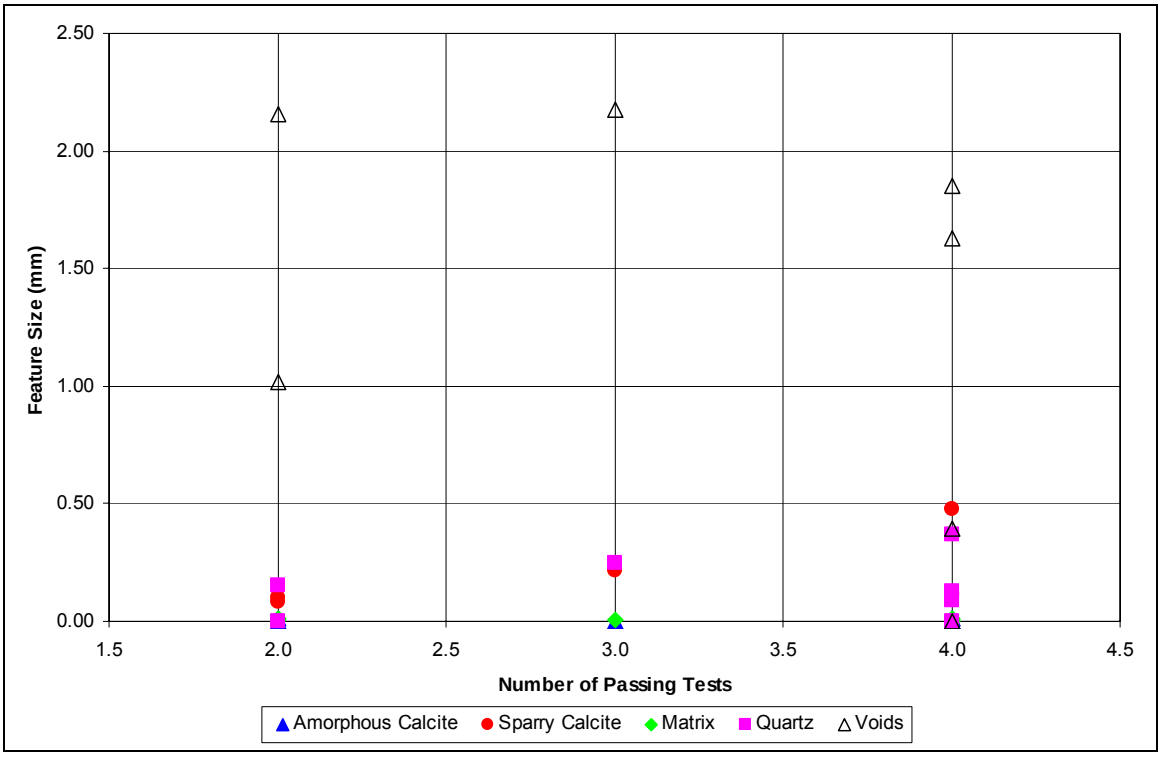

Figure G-10 Median Size of Petrographic Properties With Respect to the Number of Passed FDOT Tests

G.3 COMPARISON OF DATA FROM FDOT AND G. MCCLELLAN

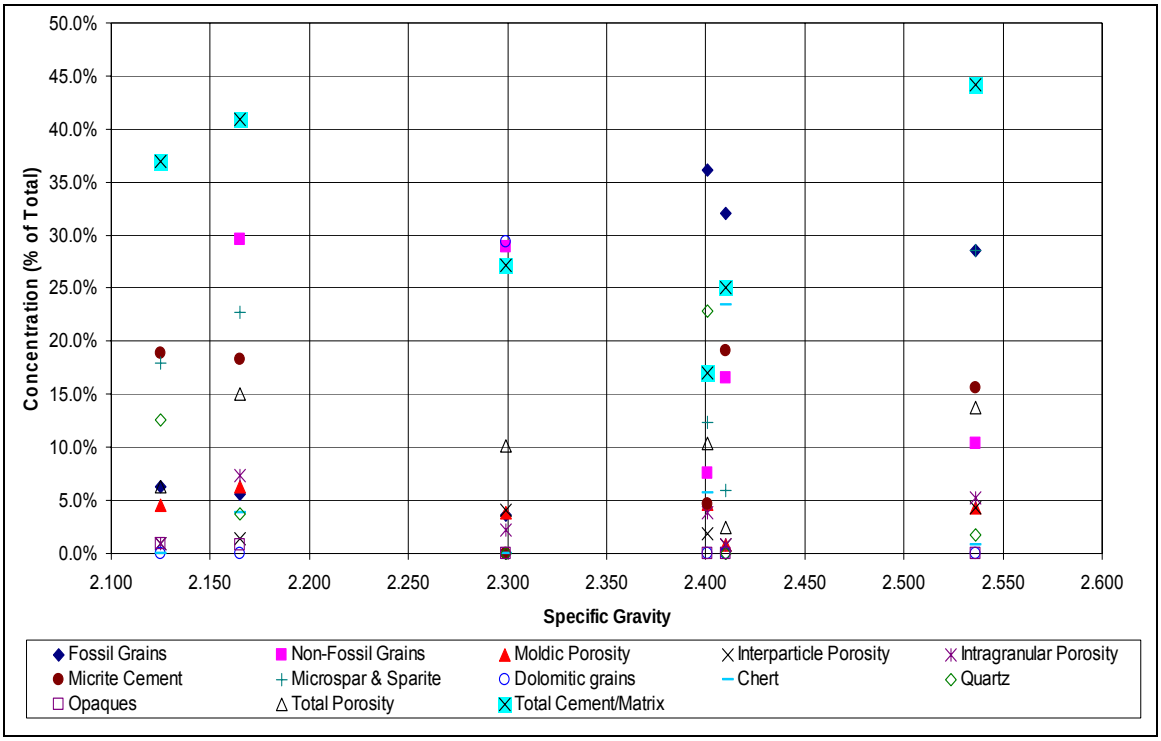

Figure G-11 Concentration of Petrographic Features With Respect to Bulk Specific Gravity (McClellan, 2006)

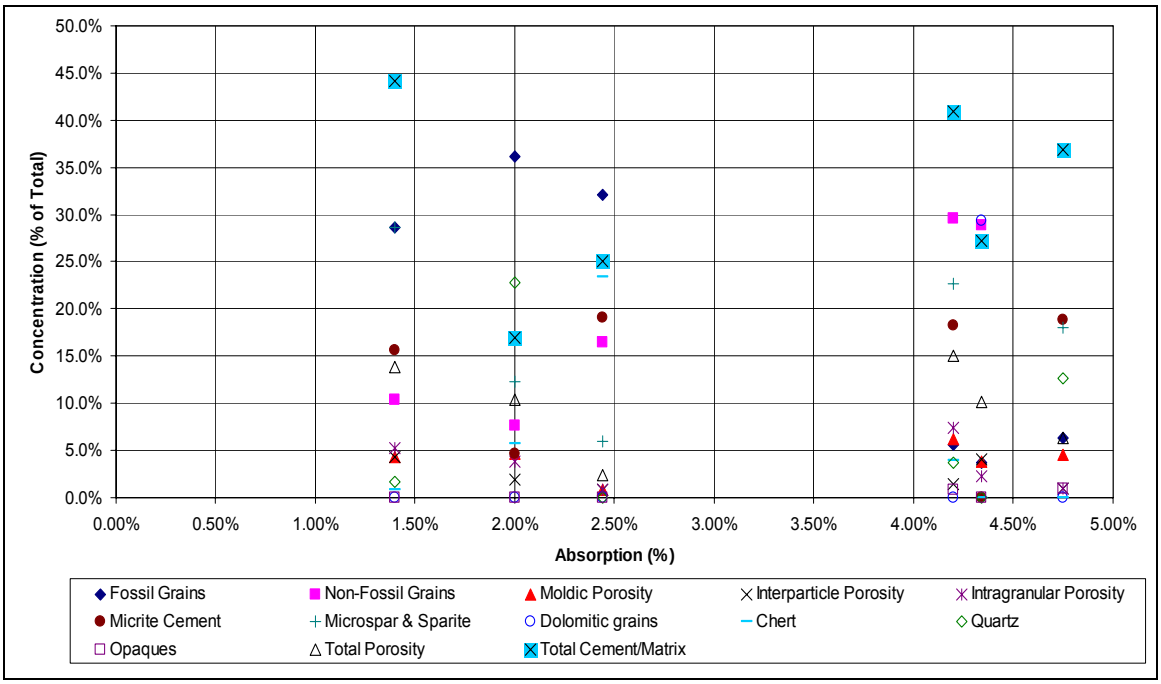

Figure G-12 Concentration of Petrographic Features With Respect to Absorption (McClellan, 2006)

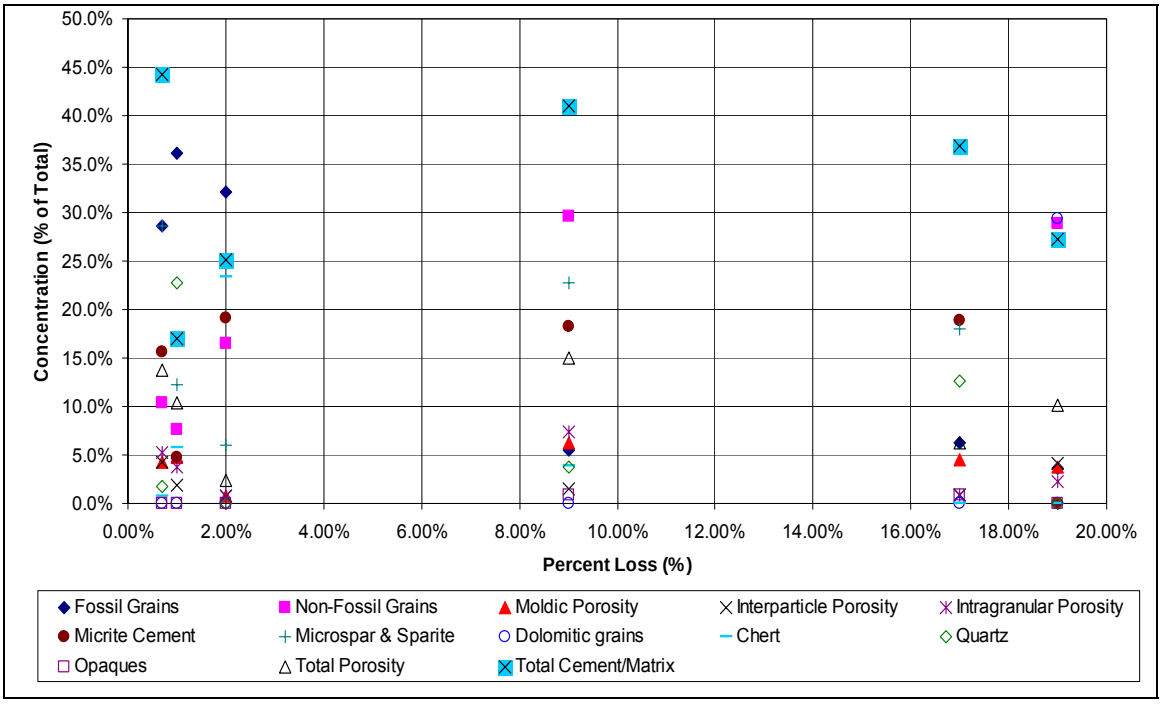

Figure G-13 Concentrations of Petrographic Properties With Respect to Sodium Sulfate Percent Loss (McClellan, 2006)

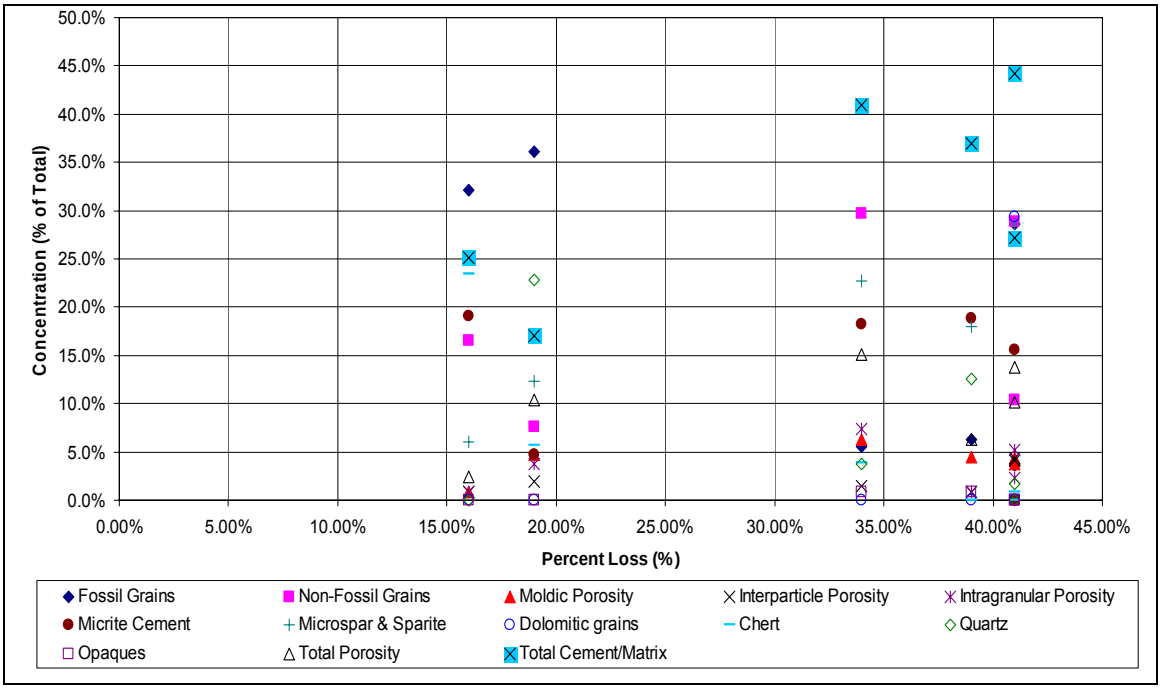

Figure G-14 Concentrations of Petrographic Properties With Respect to Los Angeles Abrasion Percent Loss (McClellan, 2006)

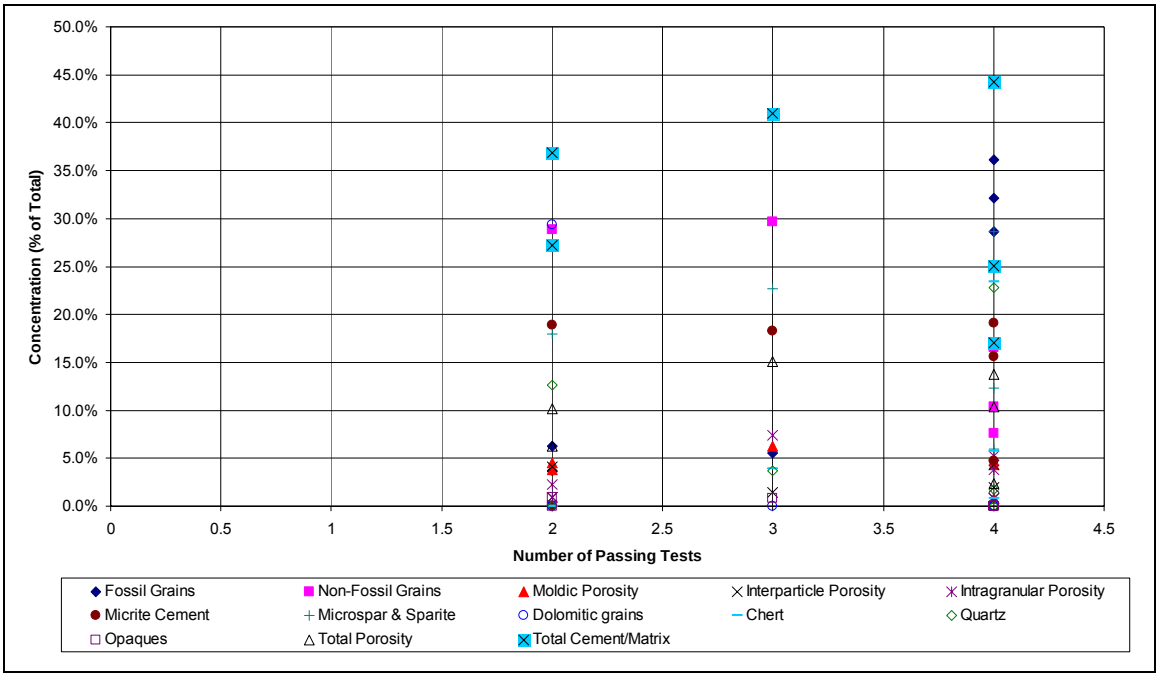

Figure G-15 Concentrations of Petrographic Properties With Respect to the Number of Passed FDOT Tests (McClellan, 2006)

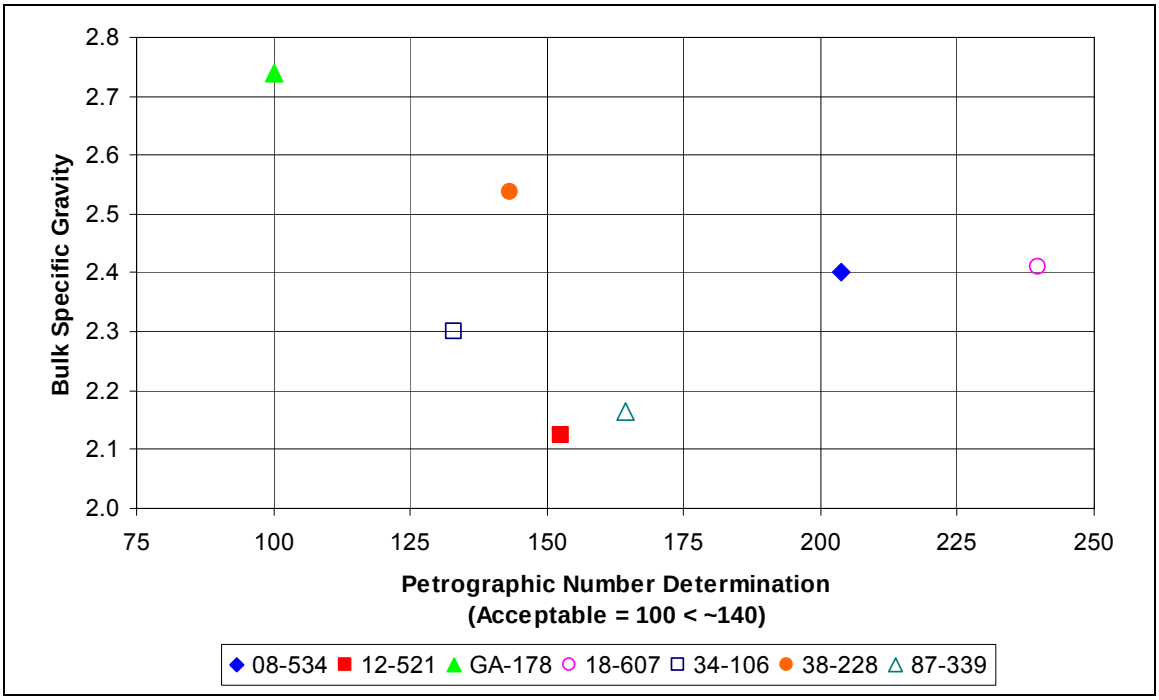

Figure G-16 Bulk Specific Gravity With Respect to Petrographic Number (McClellan, 2006)

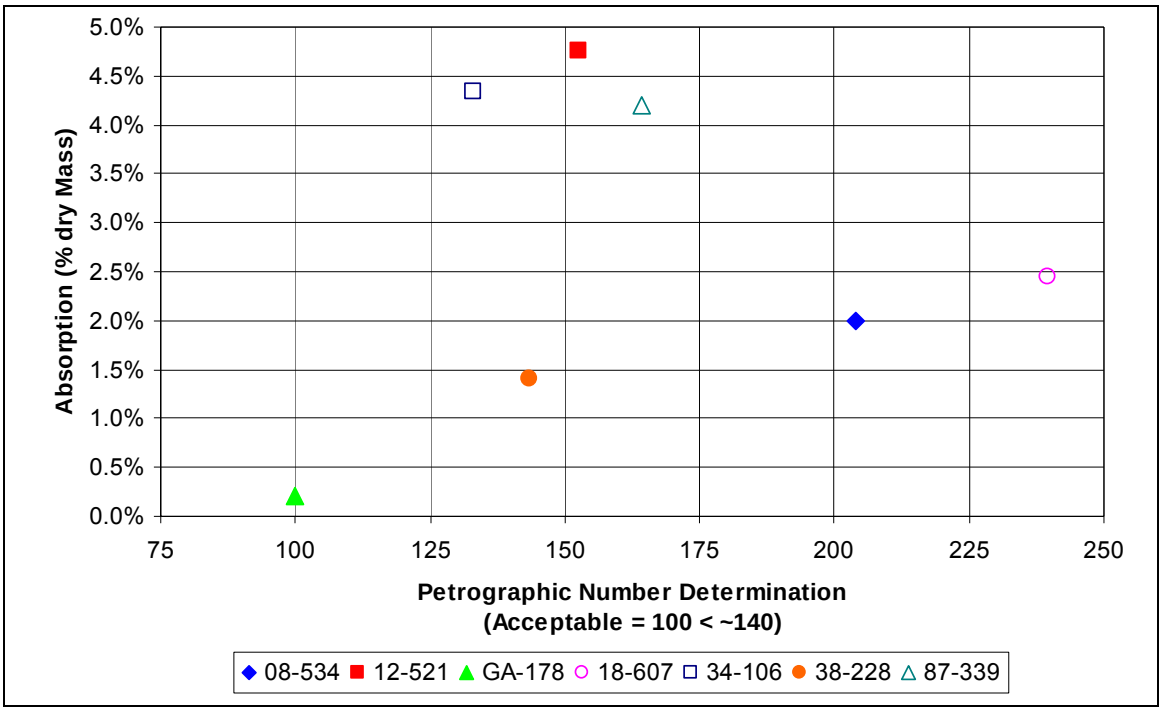

Figure G-17 Absorption With Respect to Petrographic Number (McClellan, 2006)

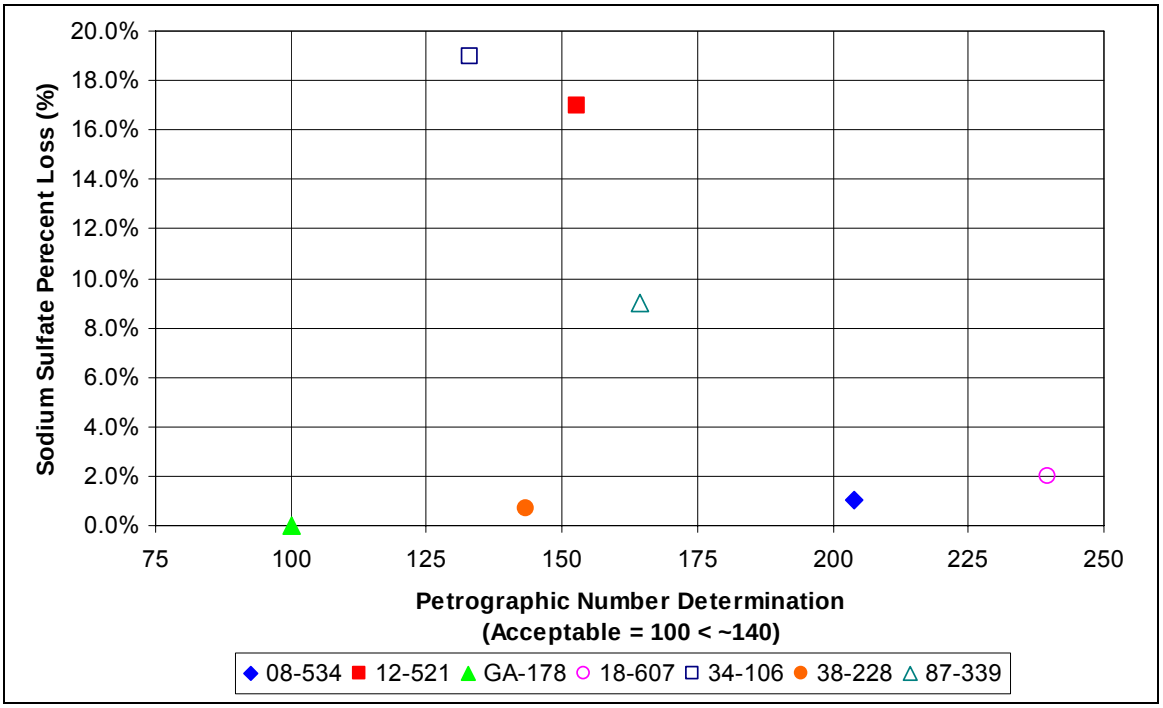

Figure G-18 Sodium Sulfate Percent Loss With Respect to Petrographic Number (McClellan, 2006)

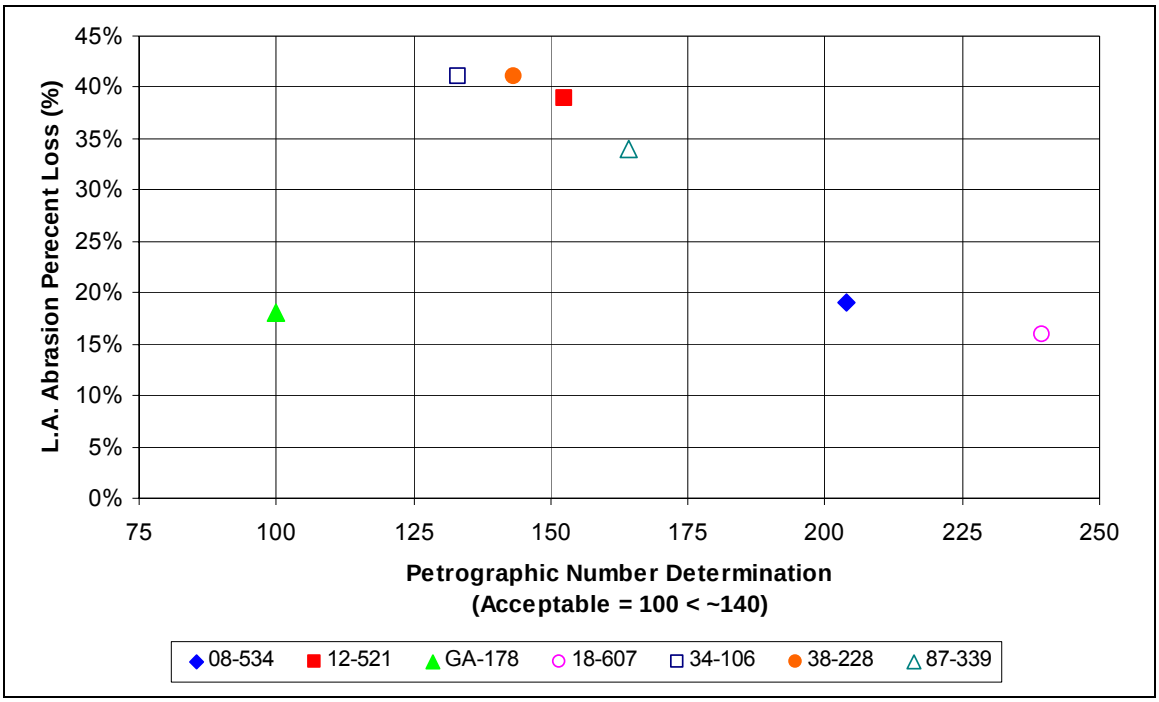

Figure G-19 Los Angeles Abrasion Percent Loss With Respect to Petrographic Number (McClellan, 2006)

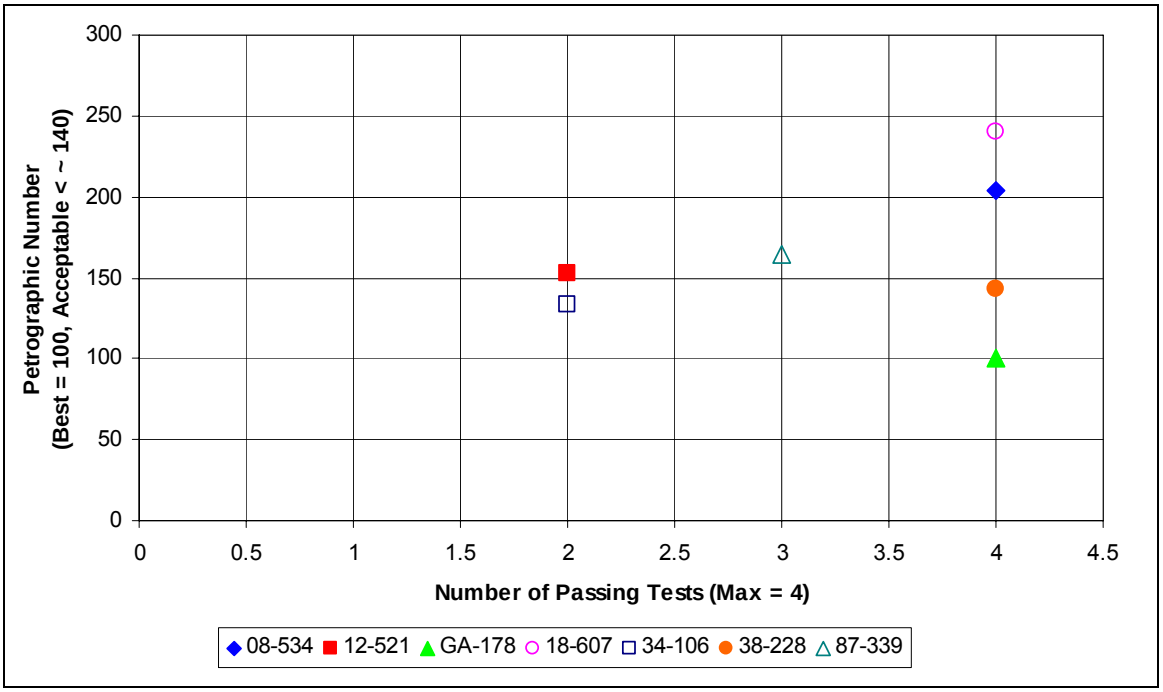

Figure G-20 Petrographic Number (McClellan, 2006) With Respect to the Number of Passed FDOT Tests

THIS PAGE LEFT BLANK